TU Delft
Faculty of Civil Engineering and Geosciences

Airtightness in the Retrofit of Historic Buildings

Master's Thesis in Building Engineering

Yara Ibrahim

Airtightness in the Retrofit of Historic Buildings

Investigation of a retrofit strategy for historic traditional buildings, optimizing their energy-efficiency, indoor environment quality, and heritage preservation

In fulfillment of the requirements for the degree of

Master of Science
in Civil Enineering

at the Delft University of Technology
to be defended publicly on 18th of December 2023

Master Thesis Report. Airtightness in the Retrofit of Historic Buildings.
December, 2023

Author

Name	Yara Ibrahim
Student Number	5603056
University	Delft University of Technology
Faculty	Civil Engineering and Geosciences
Department	Building Engineering
Specialization	Building Physics and Technology

Graduation Committee

Dr. ir. H.R. Schipper	Materials, Mechanics, Management & Design, TU Delft
Dr. ir. Z. Huijbregts	Architectural Engineering and Technology, TU Delft
Dr. ir. R.J. Labeur	Hydraurlic Engineering, TU Delft
Ing. A. van der Aa	Building Physics, ABT

Preface

This thesis – titled "Airtightness in the Retrofit of Historic Buildings" – is the final product of the research I have conducted for the last 12 months. It was written to fulfill the graduation requirements of the MSc degree in Civil Engineering, Building Engineering track, with Building Physics and Technology specialization at Delft University of Technology, faculty of Civil Engineering and Geosciences.

Embarking into this master's program, my interests were clear and my goals consistent: advocate for the conservation of existing structures, accentuating their value by enhancing their intrinsic qualities and honoring their essence.
This research investigates an innovative approach to the retrofit of historic traditional buildings. Going against the tides and questioning assumptions, the aim was to break the preconceived belief that good building performance and good building airtightness necessarily go hand in hand.
This research satisfied my appeal for the unconventional and gratified me with a challenge.

I acknowledge that the work I present in this thesis would not have been possible without the help of many people.
On this note, I would like to express my gratitude to the members of my committee. I would like to thank Dr. ir. H.R. Schipper for guiding me throughout this journey, from the start of my master studies up to the finalization of my thesis research. Thank you for patiently answering my deluge of questions and keeping me on track. I would also like to thank Dr. ir. Z. Huijbregts for her support in in my research and, particularly, for her contribution to the measurements that I could have not done without her. And to Dr. ir. R.J. Labeur for stepping up when needed.
I would like to send my special thanks to Ing. A. van der Aa – without whom this thesis would not be – for proposing the first premise to this research and for providing the advice, support and encouragement I needed to go through the many ups and downs of this work.
Besides my committee, I would also like to extend my gratitude to Dr. ir. W.H. van der Spoel for always being ready to help in the face of the many challenges I had to overcome in the development of my model.

Finally, I would like to thank my friends and family for their unwavering support and understanding throughout this process, and their inspiring belief in me and my capabilities. Special thanks to my parents, the shoulder I can always lean on, and to my sister, my first advisor and patient supporter.

Abstract

Despite being a critical aspect in improving the building stock's environmental performance and achieving the global environmental goals, the retrofit of traditional historic buildings is hindered by a lack of comprehensive guidelines tailored to their complex building physics and heritage preservation requirements.

The conventional retrofit approach – relying on the combined airtightness and insulation improvements – fail to address two decisive aspects of traditional historic buildings: First, the air leakage is a core contributor to their bioclimatic systems and building physics balance, making its sealing detrimental to their construction durability and their Indoor Environment Quality (IEQ). Second, their heritage protection requirements restrict the conventional retrofit interventions, and particularly hinder the implementation of the mechanical systems needed to mitigate their associated risks on the building and its occupants.

Accordingly, there arose an interest in challenging the conventional depiction of the air leakage as an overhead to be eliminated, and in developing a retrofit approach that preserves breathable buildings' inherent operations by exploiting their air leakage into achieving their optimal post-retrofit performance, accounting for both energy-efficiency and IEQ.

A potential solution to the feasibility of such strategy considered a natural phenomenon characteristic of the diffuse leakage through breathable envelopes – the infiltration heat recovery (IHR) – that is conventionally neglected in building performance assessments. The intentional and efficient exploitation of this effect results in construction elements, referred to as Dynamic Insulations (DI), in which air leakage could act as a heat exchanger, diffuse ventilation source, airborne contaminant filter, and diffusion barrier. Although their original design and operations were not tailored to efficiently harvest the IHR effect, the existing breathable constructions reveal similarities with DI systems. This suggests the potential of retrofitting them to act as an efficient DI system, thus exploiting the air leakage into the building performance improvements.

The present research aimed at identifying the envelope and ventilation retrofit variants that would optimize the IHR utilization through the construction, as to provide for performance improvements comparable to (or better than) the conventional approach while preserving the breathability of the construction and minimizing the heritage disruptions.

The study proposes a comprehensive framework for the assessment of the building's post-retrofit performance, in terms of its energy-efficiency and IEQ, and investigates the relevant retrofit variants to make performance-based decisions in the retrofit design for traditional breathable buildings. This performance was evaluated using a comprehensive building performance simulation (BPS) model.

For a reliable representation of the complex building physics and air leakage dynamics of breathable constructions, the BPS integrates three sub-models: the building energy simulation (BES) model, the air leakage model, and the dynamic insulation (DI) model. Due to a lack of BES tools simulating dynamic construction properties, the well-established analytical Taylor model was adopted and adapted to the dynamic simulation tool.

The analysis was implemented in EnergyPlus, for its integral Airflow Network (AFN) and advanced Energy Management System (EMS) capabilities. The model's validation process revealed significant limitations and highlighted a need for BPS tools capable of more efficiently incorporating the dynamic behavior of building materials and their interaction with dynamic flows, particularly when seeking the tailored, efficient and non-intrusive retrofit of historic traditional buildings.

The investigation of the retrofit strategy variants considered two main phases – a Morris sensitivity analysis for the selection of the conditioned zone boundary, and a NSGA II evolutionary optimization with a TOPSIS multi-criteria decision analysis for the evaluation of the ventilation strategy variants, and the definition of the retrofit recommendation and application framework.

One outcome of the analysis confirms the significance of incorporating the dynamicity of breathable constructions into their building performance assessment and the design of their retrofit strategies. With a focus on solid wall constructions, the retrofit recommendation highlights the reliance of the optimal performance of buildings with dynamic constructions on an inherently well-insulating construction and an exhaust fan-assisted building depressurization, under flowrates exceeding the minimum ventilation requirements for an efficient IHR exploitation. For such purpose, the exhaust fan is provided with heat recovery on the exhaust air and operated on a year round basis.
The developed retrofit approach outperforms the conventional strategy with no need for airtightness of either the walls or the pitched roof. Adapted to both buildings with heritage-protected and non-protected interiors, the only variation is in the added insulation that enhances the met energy-savings.

Further research avenues could consider improving the accessibility of such analysis for regular use through the development of the necessary comprehensive building simulation tools and analysis framework to reduce its computational costs. Other potential research aspects could address the further optimization of the proposed retrofit strategy by investigating the potential of wind-driven exhaust fans, or the validation of its demonstrated potential through its monitored implementation on real-life case study buildings. Following a similar approach, guidelines could also be developed for traditional historic buildings of varying functions and heritage-protection – e.g. offices, museums, etc.

Table of Contents

List of Tables

List of Figures

List of Abbreviations

ACH	Air Change Rate
AF	Attic Floor
AFN	Air Flow Network
BC	Base Case
BDT	Blower Door Test
BEP	Building Energy Performance
BES	Building Energy Simulation
BPS	Building Performance Simulation
BRC	Base Retrofit Case
BW	Breathing Wall
CMOO	Constrained Multi-Objective Optimization
CO_2	Carbon Dioxide
CondFD	Conduction Finite Difference
CRC	Conventional Retrofit Case
CZB	Conditioned Zone Boundary
DHW	Domestic Hot Water
DI	Dynamic Insulation
E.Opt	Evolutionary Optimization
EE	Elementary Effect
EMS	Energy Management System
Erl	EnergyPlus Runtime Language
EV	Exhaust Ventilation
FR	Flat Roof
GSA	Global Sensitivity Analysis
GUI	Graphical User Interface
IAQ	Indoor Air Quality
IEQ	Indoor Environment Quality
IHR	Infiltration Heat Recovery
IR	Infra-Red
LSA	Local Sensitivity Analysis
MCDA	Multi-Criteria Decision Analysis
MCDM	Multi-Criteria Decision-Making
MOEA	Multi-Objective Evolutionary Algorithm
MOO	Multi-Objective Optimization
MVHR	Mechanical Ventilation with Heat Recovery
NCRC	Non-Insulated Conventional Retrofit Case
NV	Natural Ventilation
PMV	Predicted Mean Vote
PPD	Predicted Percentage Dissatisfied
PR	Pitched Roof
RH	Relative Humidity
RQG	Research Question Group
RV	Reversible Fan Ventilation
SA	Sensitivity Analysis
SoA	State-of-the-Art
W	Walls
WE	Winter Exhaust Ventilation

1. Introduction

This Chapter presents an overview of the research. It first addresses the study's general background (Chapter 1.1) and problem statement (Chapter 1.2). The research objectives, questions, and structure are then described (Chapter 1.3, 1.4, 1.5 respectively).

1.1. General Background

1.1.1. Building Renovations: a main climate strategy

The building sector is the single largest contributor to the energy consumption and GHG emissions, accounting for around 40% of the EU's total primary energy use and 36% of its associated GHG emissions (*Energy Performance of Buildings Directive*, n.d.; *Factsheet - Energy Performance of Buildings*, 2021).

Although the improved new-built standards pursue the climate goals set in the Paris Agreement (*Paris Agreement*, n.d.) and European Climate Law (*European Climate Law*, n.d.), the performance of the built environment remains strongly dependent on the existing building stock. The latter constitutes an urgent concern and offers extensive potential to meet the current climate horizons (Blázquez et al., 2023; Ortiz & Bluyssen, 2022).
Indeed, it is estimated that 85-95% of the current EU buildings will remain in 2050, 75% of which are not energy-efficient (*Factsheet - Energy Performance of Buildings*, 2021).

With recorded renovation rates as low as 1% per year (*Energy Performance of Buildings Directive*, n.d.), building retrofits have become a strategic focus of the European agenda, in general, and Dutch national climate policies, in particular, (Blázquez et al., 2023; Camarasa et al., 2018) with a focus on the worst-performing section of the building stock (Renovation Wave, n.d.).

1.1.2. Target Building Stock

Attributed around 30% of the country's energy consumption and dominating its building stock (62%), residential buildings are currently the focus of renovations in the Netherlands (Camarasa et al., 2018; Ortiz & Bluyssen, 2022).

The introduction of Dutch thermal regulations in the 1980s translated into 80% of the residential buildings of poor energy performance (energy-label G) being constructed prior to 1946, with the remaining 20% being built within 1946-1980 (Camarasa et al., 2018). This established the retrofit of older residential buildings (pre-1945) as a priority.

Two aspects of pre-1945 buildings raise potential challenges to their effective renovation:

Traditional Buildings

The end of WWII (1945) marks a shift from traditional to modern constructions, addressing the needed reconstruction and the rising housing demand and quality of life standards (Hafez, 2016).
Traditional building construction in Central and Northern Europe takes the form of mass solid wall construction from a range of local and natural materials (Whitear & Duxbury, n.d.). These are characterized by bioclimatic systems, relying on breathable building fabrics.

Historic Buildings

Pre-1945 buildings are referred to as historic buildings and are often of heritage standing (Cabeza et al., 2018). The preservation of their monumental value is then protected by law (RVO, n.d.).

These two characteristics are of particular significance for the pre-1850 building stock, preceding the industrialization of building materials (Stenvert, 2012).

Brick construction has been predominantly practiced in the Dutch architecture and constitutes the foundation of the traditional Dutch domestic style (Hafez, 2016; Jones, 1988). Such buildings still prevail and account for the typical Dutch row houses (Jones, 1988).
Up to the early-19th century, brick construction followed a virtually-unaltered traditional and artisanal practice in the brick-making and construction techniques: Buildings exhibited load-bearing solid masonry walls with traditionally-baked bricks and lime mortars, and seldom presented any insulation (Braam, n.d.; *Historisch Metselwerk (URL 4003)*, n.d.). Historic and monumental buildings also presented elements of Timber construction, in the roof, doors, and window frames (*Historisch Timmerwerk (URL 4001)*, n.d.).

1.1.3. Conventional Retrofit Strategy and its Limitations

Due to the variety of climates, building typologies, construction systems and materials characterizing the building stock, building renovations constitute a main challenge (D'Agostino et al., 2017).

"Renovation", by definition, is "the process of repairing and improving" an existing building or group of buildings ("Renovation," n.d.). Different renovation levels may be distinguished, depending of the **nature of the interventions** and **obtained improvements**.

Nature of Interventions

- A predominant reliance on the same retrofit strategies is detected for virtually all buildings, despite the contrasting climates and building characteristics (Alev et al., 2014; Blázquez et al., 2019; Cabeza et al., 2018; Doran et al., 2014; Martínez-Molina et al., 2016; Zagorskas et al., 2013).
- Renovation programs focus on the improvement of the **building envelope's insulation and airtightness** as fundamental strategies to increase the buildings' energy-efficiency, followed by the implementation of **advanced low-energy HVAC systems** as popular methods to improve health and comfort (Ortiz & Bluyssen, 2022).

Target Improvements

- Standard and emerging retrofit strategies are often assessed based on their **energy-saving** and **winter thermal comfort** implications.
- Their unintended consequences on the **Indoor Environment Quality (IEQ)** are seldom used as performance indicators, despite wide evidence proving them critical to the occupants' health and comfort, as well as the construction's quality and durability (Ortiz & Bluyssen, 2022).

The above-mentioned trends identified in the literature are reflected in the Dutch industry practice. There is a somewhat general acceptance that a building's airtightness and insulation must both be improved to achieve higher sustainability standards (*Zesdelig Stappenplan Verduurzaming*, n.d.), which is put forward in virtually all available industry-guidelines and tools (*Monumenten Verduurzamen*, n.d.; *Toolkit Duurzaam Erfgoed*, n.d.; *Zesdelig Stappenplan Verduurzaming*, n.d.).

However, the scientific literature recognizes a distinction between traditional monumental and modern buildings, emphasizing that a standardization of the measures might ensue more harm than good if not compatible with the building's specific properties and requirements.

Besides the resulting energy-savings, the higher insulation and airtightness of the envelope reveal counter-productive trends (Blázquez et al., 2023; Doran et al., 2014; Fawaier & Bokor, 2022; Ortiz & Bluyssen, 2022), namely a degradation of the Indoor Environment Quality (IEQ).

- Build-up of indoor air contaminants and decrease in the Indoor Air Quality (IAQ)
- Build-up of humidity and an increased risk of moisture, condensation, and mold growth.
- Reduced heat removal in summer, causing an accumulation of internal and solar heat loads, and an increased risk of summer overheating and discomfort.

Although these unintended consequences may occur in any conventionally-retrofitted building, they are of particular importance in traditional and monumental constructions (Doran et al., 2014; Whitear & Duxbury, n.d.) for their two particular aspects, as detailed below:

Traditional Construction

Traditional historic buildings with solid wall masonry constructions exhibit **breathable and permeable building fabrics.**
They are complex bioclimatic systems with an intricate equilibrium between their thermal mass, air leakage, envelope properties, and heating regime. Their interaction regulates the heat loss and manages the moisture (Doran et al., 2014).
Their fundamentally different building physics call for fundamentally distinct retrofit approaches (Doran et al., 2014).

An important aspect of traditional constructions attributes many of their amplified retrofit-induced risks to **insufficient ventilation and air permeability**, disrupting their equilibrium (Bone et al., 2010).

Monumental Standing

Monumental historic buildings are subject to **heritage regulations**, imposing restrictions on the nature and extent of their allowable retrofit measures (RVO, n.d.).

They exhibit significant challenges to the implementation of many conventional retrofit interventions, particularly the active ventilation and air conditioning systems that are often needed to fix the building's post-retrofit IEQ (Bakowski, 2013; Becchio et al., 2017).

Due to the regulatory constraints and the challenges in their installation in historic buildings, all-air HVAC systems tend to be excluded. This was the case in Alongi *et al.* (2015), where water systems and natural ventilation are often found to be more adequate.

A need for tailored strategies for monumental retrofits is raised, integrating the buildings' characteristic building properties with the preservation of their monumental value. No clear general recommendation has, however, been defined for their construction type.

1.1.4. Airtightness Debate & Air Leakage Limit in Traditional Buildings

In view of the importance of sufficient ventilation in the building performance, a divide in the airtightness strategy is detected between modern and traditional buildings (Stephen, 1998):

Modern Buildings

Referred to as the "build tight-ventilate right" concept, proposed in the late 1900s (Stephen, 1998), the modern construction practice aims at making buildings as airtight as possible and providing adequate controlled ventilation.
All ventilation is ideally designed through purpose-provided systems; the envelope's air leakage is seen as an overhead to be eliminated.

Modern airtightness strategies are associated with simple building physics and are often standardized under different climates.

Traditional Buildings

Traditional construction practices rely on breathable and permeable envelopes. They are ventilated through a combination of purpose-provided openings and uncontrolled envelope air leakage (Salehi et al., 2017; Stephen, 1998). Considering traditional UK dwellings, for instance, Stephen (1998) asserts that air leakage plays the primary ventilation role in the wide majority of dwellings.

As per their bioclimatic properties, such buildings are rooted in their specific climatic and environmental context.

This divide raises a debate as to the airtightness strategy to adopt in the retrofit of historic traditional buildings; debate that is clearly translated in the literature. The two considered strategies are:

Conventional Modern Strategy

- Increase the envelope's airtightness and replace the air leakage's contribution by controlled ventilation systems, to ensure adequate ventilation and satisfactory IEQ.
  - Zagorskas *et al.* (2013) suggest combining added insulation with mechanically-balanced ventilation to avoid the retrofit-associated risks.

Alternative Strategy

- Preserve the breathability and permeability of the construction, and exploit the air leakage's contribution to the indoor environment.
  - Doran *et al.* (2014) promote measures that avoid reducing the air permeability of solid walls, by ensuring that 'breathable' materials are used and that no sealing impedes the air flow.
  - Examining the wetting and drying characteristics of historic masonry walls, Cassar *et al.* (2007) support the importance of maintaining traditional constructions' operation scheme.

Doran *et al.* (Doran et al., 2014) thus highlights the importance of establishing an optimal, effective, and realistic minimum air leakage for the retrofit of historic buildings.
Failure to do so would result in:

- Potential loss in energy-savings, if the air leakage is too high
- Decay of the building fabric and the IEQ, if it is too low
- High overheating risks and added cooling loads, possibly negating the heating-energy savings, if high airtightness and insulation are combined

1.2. Problem Statement

Despite being a critical aspect in the improvement of the building stock's environmental performance and achieving the climate goals, the retrofit of traditional historic buildings is hindered by the lack of overarching retrofit guidelines tailored to their characteristic building properties and heritage preservation requirements.

Conventional retrofit approaches, relying on the combined increase of the envelope's airtightness and insulation as practically possible, fail to address two decisive facets to traditional historic buildings, specifically the ones constructed prior to 1850.
On the one hand, their breathable fabric and complex bioclimatic systems rely heavily on the air leakage's contribution to their building physics balance, detrimental to both the durability of the construction and the Indoor Environment Quality (IEQ).
One the other hand, their heritage protection requirements restrict the nature and extent of permissible interventions, often impeding the implementation of the conventional measures.

The generally high appreciation of airtightness has been strongly influenced by the current building standards, catering for stricter energy performances.

Obstacles to the development of such solution-strategy have thus been the neglection of two factors in the relationship of between the building's air leakage and its overall performance:

- The Infiltration Heat Recovery (IHR) effect, which reduces the air infiltration's thermal load.
  - Although addressed in many studies (Buchanan & Sherman, 2000; Fawaier & Bokor, 2022; Qiu & Haghighat, 2007; Solupe & Krarti, 2014), it is typically **not accounted for in research and industry**.
  - The leakage's contribution to the **building's energy demand has often been overestimated**, possibly distorting the perceived performance of retrofits and misinforming retrofit decisions (Jokisalo et al., 2009; Solupe & Krarti, 2014).
  - The limited investigation of the IHR effect may, partly, be attributed to its absence in common building energy simulation tools (e.g. DesignBuilder, EnergyPlus, TRNSYS, and ESP-r).
    Design guidelines for the integration of the IHR effect as an applicable solution are thus not well developed.
- The Indoor Environment Quality (IEQ) performance indicators, which highlight the air leakage's importance in the building performance.
  - Airtightness strategies must not be valued solely based on their energy-saving potential, as customary, and must address the **trade-off between energy-savings and satisfactory IEQ levels**, to define an adequate ventilation regime (Gillott et al., 2016; Stephen, 1998).
  - Most **conventional retrofit's unintended consequences** are often attributed to an **excessive airtightness** (Doran et al., 2014; Gillott et al., 2016), and its reduction in the building's ventilation and construction breathability. Such consequences include:
    stale-air accumulation and poor IAQ, increased indoor relative humidity (RH), and moisture build-up, along with the resulting degradation of the construction (Younes et al., 2012) and the health and comfort implications on the occupants (d'Ambrosio Alfano et al., 2016; Gillott et al., 2016; Salehi et al., 2017).

Changes in the envelope's behavior may entail changes in the whole building's behavior and performance; i.e. the building physics balance, the indoor environmental quality, and overall construction quality. Retrofit work on historic buildings, specifically, must then aspire towards a balance of their different aspect (Doran et al., 2014).

1.3. Research Objectives

As per the state-of-the art on the energy retrofit of historic heritage buildings, particularly their approach to airtightness, the research objectives and ensuing research questions are defined.

1.3.1. Main Objective

The present research aims to: **contribute with a recommendation for the retrofit of traditional historic monuments, by investigating an applicable airtightness and ventilation strategy that optimizes the building's overall performance with regard to the trade-off between energy-efficiency and indoor environment quality (IEQ), and accounts for their characteristic building physics principles and heritage requirements.**

It is not the research's objective to develop a rigid comprehensive retrofit strategy to be standardly applied to all historic traditional buildings. Instead, the research is to present a flexible recommendation for historic buildings of varying levels of heritage protection. It is to highlight various possible airtightness and ventilation retrofit pathways along with their respective performances, limitations, and potential application framework.

The resulting recommendation should help in the design of optimal retrofit strategies tailored to the historic building's needs and restrictions. It is thus important to note that all following results are focused on buildings with solid wall constructions.

1.3.2. Sub-Objectives

The research's main objective is divided into four sub-objective groups, based on their relation to the main objective.

- The first group addresses the research's theoretical framework, assisting the main objective:
  - To define air leakage, and its impacts on the building's overall performance.
  - To ascertain a way to address the trade-off in the air-leakage's relationship with the building's performance.
  - To identify the state-of-the-art of airtightness and ventilation retrofit strategies, and particularly their application in monumental traditional buildings.
- The second group addresses the relevant airtightness and ventilation retrofit approaches for historic traditional buildings, defining the search space and comparative references for the resolution of the main objective:
  - To define the retrofit variants that could potentially present as a solution to the retrofit of traditional historic buildings.
  - To define the baseline properties and performance of traditional single-family dwellings, with reference to a case study in the Netherlands, and the properties and performance associated with the conventional retrofit approach.
- The third group addresses the evaluation framework and building model, providing for the resolution of the main objective:
  - To define the building performance evaluation framework, including the parameters and criteria, that identifies the retrofit strategies optimizing the performance trade-off between energy-efficiency and Indoor Environment Quality (IEQ).
  - To develop an integrated dynamic Building Performance Simulation (BPS) model, calibrated and validated to represent the existing building's characteristics and building physics.
- The fourth group addresses the optimal retrofit strategies and their respective recommended frameworks, and is thus directly attendant to the main objective.
  - To develop a flexible recommendation as to the retrofit strategy and associated application framework for the airtightness and ventilation of traditional historic buildings of varying levels of performance and heritage restrictions, with reference to a case study building in the Netherlands.

1.4. Research Questions

1.4.1. Main Question

The research's main question is: **What airtightness and ventilation retrofit approach optimizes the energy-efficiency and Indoor Environment Quality (IEQ) performance of traditional historic buildings, while accounting for their characteristic building physics principles and heritage preservation requirements?**

1.4.2. Sub-Questions

The main question is divided into four sub-question groups, in line with the research objectives defined in Chapter 1.3.

- The first group addresses the research's theoretical framework (Chapter 2), assisting the main objective:
  - What are: (1) the characteristics of building air leakage? (2) its different types? (3) their relationships with the building's performance, in terms of energy-efficiency and Indoor Environment Quality (IEQ)?
  - How could the trade-off identified in the air leakage's relationship with the building's performance be reduced?
  - With a particular focus on historic traditional buildings, what are: (1) the state-of-the-art airtightness and ventilation retrofit strategies? (2) their limitations? (3) the measures that have been conventionally used to address these limitations?
- The second group addresses the relevant airtightness and ventilation retrofit approaches for historic traditional buildings (Chapters 4 and 5), defining the search space and comparative references for the resolution of the main objective:
  - What are the airtightness and ventilation retrofit strategies that could present as potential solutions for traditional historic buildings?
  - What are the comparative references to the investigated strategies, namely: (1) the baseline properties and performance of a traditional historic buildings with reference to a case study in the Netherlands, and (2) their estimated properties and performance under a conventional retrofit approach?
- The third group addresses the evaluation framework and building model (Chapter 6 and 7), providing the framework for the resolution of the main objective:
  - What performance parameters and associated criteria are indicative of the building's overall post-retrofit performance, and could be used to evaluate a retrofit strategy's effectiveness?
  - How can the dynamic overall building performance be reliably evaluated, in relation to the building's characteristic air leakage behavior and envelope properties?
- The fourth group addresses the optimal retrofit strategies and their respective recommended frameworks (Chapters 8 and 9), and is thus directly attendant to the main objective.
  - What is the recommended: (1) building loft insulation configuration and (2) ventilation regime, for the exploitation of traditional historic building's air leakage into their optimal building operations?
  - What are the airtightness, insulation thickness, and fan flow rates associated to the successful application of the recommended retrofit approaches, for traditional historic buildings of varying levels of performance and heritage restrictions?

1.5. Research Structure

The research structure is in 12 Chapters.

Chapter 1 presents the context and motivation behind this work, and the arising questions it tackles.

Chapter 2 defines the theoretical background of air leakage in buildings, its properties and relation to the building's performance, and the current retrofit strategies' approach to it.

Chapter 3 establishes the overall methodology adopted to address the research questions, and presents a comprehensive scheme of the research workflow.

Chapter 4 defines the evaluated retrofit variants as potential solutions to the retrofit of traditional historic buildings, against the comparative baseline and conventional retrofit cases. In support of the latter, Chapter 5 addresses the characterization of the building's baseline characteristics and air leakage properties, covering its detailed methodology and results.

Chapters 6 and 7 develop the building performance evaluation framework and tool, respectively addressing the building performance parameters and criteria, and the constituting components of a validated and calibrated comprehensive BES model.

Chapters 8 and 9 address the detailed methodology, results, and discussion respective to the two main phases of the research, namely: the adopted conditioned zone boundary, and the optimal ventilation & airtightness strategies.

Chapter 10 develops the recommendations regarding the optimal retrofit strategies and associated application framework for the airtightness and ventilation of traditional historic buildings of varying levels of performance and heritage restrictions, with reference to the case study building in the Netherlands.

Chapter 11 summarizes this research's contribution, addressing the answers to all research questions.

Finally, Chapter 12 concludes this research, outlining its key findings and highlighting its relevance and recommendations for practice and research.

2. Literature Concepts

This Chapter presents a thorough review of the research's theoretical framework. It addresses the building air leakage properties (Chapter 2.1) and types (Chapter 2.2), along with its influence on the building's overall performance. A potential solution to its exploitation in favor of this performance is presented as a concept (Chapter 2.3). Its state-of-the-art retrofit strategies, their limitations and design considerations, are then described (Chapter 2.4), setting the foundation for this research.

2.1. Air Leakage Theory

2.1.1. Definition

Air Leakage vs. Ventilation

The movement of air in buildings relates to either controlled or uncontrolled air flows.
Ventilation typically refers to the controlled flow of air into and out of the building, designed for the purpose of providing the necessary indoor air change and quality (IAQ). Ventilation may be (Younes et al., 2012):

- Natural – through purpose-designed openings in the envelope.
- Mechanical – through purpose-designed mechanical fans and HVAC systems.

Air leakage, in contrast, refers to the uncontrolled component of this air movement.
It is a physical phenomenon, driven by the pressure gradient across the building envelope. It is thus dynamic and dependent on the surrounding environmental conditions (Gillott et al., 2016; Younes et al., 2012).

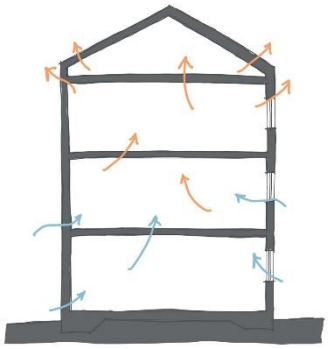

Figure 1: Air Leakage, a Physical Phenomenon (*Airtightness*, n.d.)

Air leakage is distinguished between **Air infiltration** and **Air exfiltration**, which are respectively the inward and outward leakages across the building envelope. Building codes and standards, however, often use air infiltration and air leakage interchangeably (Gillott et al., 2016; Younes et al., 2012).

Air Leakage vs. Airtightness

A building's air leakage behavior is often characterized by its **Airtightness**.
Referring to the resistance of the building envelope to leakage, it is the main building property impacting air leakage: The tighter the building is, the fewer leak pathways in its envelope, and the less air seeps through it (Berge, 2011; Gillott et al., 2016; Guillén-Lambea et al., 2019).

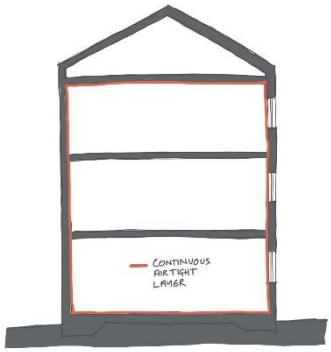

Figure 2: Airtightness, a Building Property (*Airtightness*, n.d.)

It is, however, important to emphasize that airtightness is the opposite of air permeability, not air leakage.
Airtightness is expressed as the leakage airflow at a specific pressure difference, typically 10Pa or 50Pa (10Pa in The Netherlands). Unlike air leakage, the building's airtightness is then independent of the dynamic environmental variations (Prignon & Van Moeseke, 2017).

It may be expressed as one of three quantities, in which the leakage flow rate (Q) is normalized by, respectively, the building's conditioned volume (V), the envelope's area (A_{env}), and the building's floor area (A_g) (Thamban, 2020).

- Air Change Rate [hr^{-1}] $n_{50} = \frac{Q}{V}$; $ACH = \frac{3600Q}{V}$
- Air Permeability [$m^3/m^2.s$] $q_{i,50} = \frac{Q}{A_{env}}$
- Specific Air Leakage [$m^3/m^2.s$] $q_{v,50} = \frac{Q}{A_g}$

2.1.2. Influencing Factors

A building's air permeability is intricately linked to a plethora of influencing factors. These factors may be categorized into four main groups, as shown below (Prignon & Van Moeseke, 2017).

Table 1: Air permeability' Influencing Factors

Geometry	Technology & Materials	Guidance & Supervision	External
· Volume · Number of Stories · Envelope Area · Floor Area · Envelope Openings · Frame Length	· Envelope Construction · Envelope Material · Construction Method · Ventilation System · Dwelling Type · Foundation & Roof Structures · Window Material · Heating System · Insulation Type & Position	· Supervision & Workmanship · Design Targets · Feedback & Guidance	· Climate Zone · Construction Year

Many of these factors exhibit inter-relations and variable correlations with building airtightness at regional, national, or even individual building levels.

Beyond spatial variability, building airtightness is not static over time. Influencing factors, such as the construction type and initial airtightness level, contribute to significant time-dependent fluctuations for several years post-construction. Verbeke & Audenarert's (2020) findings underscore the limited and variable reliability of airtightness measures over time, as they record decreases of 11-200% in a majority of low-energy buildings monitored for up to 12 years after construction.

Reliance on statistical models for airtightness characterization, without direct in-situ measurements, may yield unreliable and non-representative outcomes. Fan-pressurization and IR thermography tests are then employed to quantify a building's air leakage and pinpoint its primary pathways.

2.1.3. Driving Forces

Besides the influence of the building's airtightness, a building's leakage is driven by the pressure gradient across its envelope. The latter is influenced by three driving mechanisms operating in combination (Prignon & Van Moeseke, 2017; Thamban, 2020; Younes et al., 2012):

› Wind Effect › Stack Effect › Fan Effect *(in case of mechanical ventilation)*

The total pressure gradient may be expressed as the sum of the 3 pressure components, with positive differences denoting higher outdoor pressure compared to the indoor (Berge, 2011):

$$\Delta P_{tot} = \Delta P_s + \Delta P_w + \Delta P_v$$

ΔP_{tot} – total pressure difference [Pa]
ΔP_s – stack pressure difference [Pa]
ΔP_w – wind pressure difference [Pa]
ΔP_v – ventilation pressure difference [Pa]

The two primary components are naturally-driven and detailed below (Berge, 2011; Thamban, 2020).

The **wind pressure** is caused by the flow of air around the building, referred to as the **wind effect**, that results in over-pressures on the building's windward side and under-pressures on its leeward sides.
The wind pressure is given by:

$$\Delta P_w = \frac{1}{2}\rho_{air}\, C_p\, v^2$$

P_w – wind pressure [Pa]
ρ_{air} – outdoor air density [kg/m^3]
v – wind speed [m/s]
C_p- wind pressure coefficient [-]

The **wind pressure coefficient** ($\mathbf{C_p}$) is a non-dimensional coefficient describing the distribution of the wind pressure over the building surface.
The pressure profile depends on various factors, including the **wind velocity & direction**, the **air density**, the **local terrain & topography**, the **sheltering conditions**, and the **building shape**. Typically calculated based on experimental testing data for various building heights and shapes, it is defined as:

$$C_p = \frac{P - P_o}{\frac{1}{2}\rho_{air}\, v^2}$$

P – static pressure at building surface [Pa]
P_o – static pressure in free-stream region [Pa]

Despite the variability of the coefficients over the envelope, surface-averaged coefficients are conventionally considered due to the paucity of information regarding the leakage pathways' exact location.

The **stack pressure** is rooted in the temperature differences between the building's external and internal environments. As per the ideal gas law, temperature differences entail density differences that, in turn, cause buoyancy differences.
The **stack effect** (or **buoyancy effect**) thus refers to the pressure gradients over the building's height resulting from these buoyancy differences.
The stack pressure is thus calculated as a function of the building height and the indoor and outdoor ambient air temperatures. It is given by (Thamban, 2020; Walker & Wilson, 1998):

$$\Delta P_s = \rho_{air} g h \frac{|\Delta T|}{T_{in}}$$

P_s – stack pressure [Pa]
g – gravitational acceleration [m/s^2]
h – height difference between leakage points [m]
ΔT – air temperature difference between indoor and outdoor [^{o}C]
T_{in} – indoor air temperature [^{o}C]

Both the **wind** and **stack pressure** components present a highly dynamic nature, as per their dependency on the wind pressure coefficients and air temperature gradients, that vary with the surrounding weather conditions. The air leakage may thus only be accurately studied dynamically (Thamban, 2020).

In case the building is provided with mechanical ventilation, an additional **fan effect** further contributes to the pressure gradient across the envelope. Such ventilation may be delivered in one of four modes (Berge, 2011; Younes et al., 2012):

Natural Ventilation	Mechanical Supply	Mechanical Exhaust	Balanced Ventilation
With both natural supply and exhaust	*With natural exhaust*	*With natural supply*	*Often with a heat recovery system*

The fan pressures induced in any of the above-listed mechanical systems alters the total pressure gradient, consequently influencing the extent of the leakage (Berge, 2011; Younes et al., 2012).

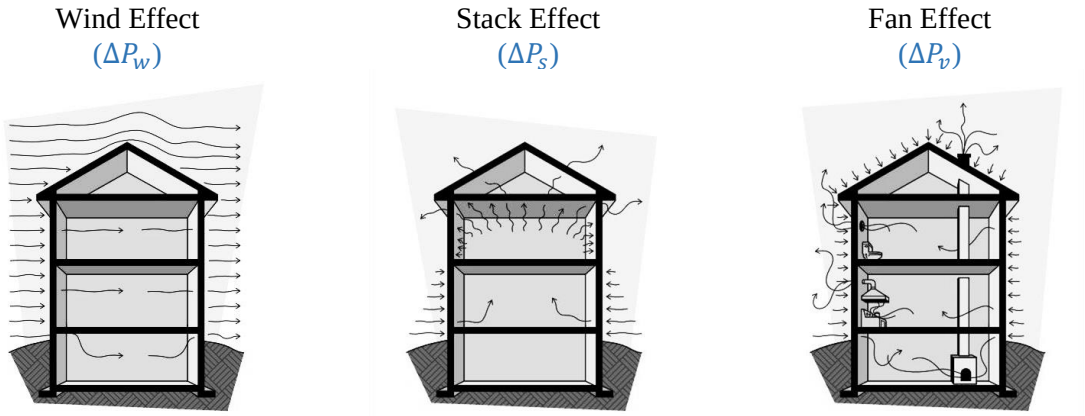

Figure 3: Air Leakage-driving Pressure Components (NAIMA Canada, n.d.)

Combining all pressure components results in a complex and variable pressure gradient distribution over the building surface. The air leakage is dependent on the interplay between the distribution of these pressure gradients and the air leakage pathways over the envelope (Refer to Figure 3).

2.2. Types of Air Leakage

2.2.1. Leakage Pathways

By definition, a building's air leakage owes to a wide network of joints, gaps, and cracks in its envelope. Although highly variable, both in space and time (Refer to Chapter 2.1.2), their distribution is associated with a number of typical pathways.

Reductive sealing measurements conducted over a set of BRE dwellings builds up a picture of this potential distribution (Stephen, 1998). High accuracy of these results must, however, not be expected. On the one hand, the buildings studied are pre-1988 buildings in the UK. Some discrepancies are expected with the Dutch context. However, empirical reporting on the leakage in over 300 Dutch dwellings using thermal IR imaging helps support most of these deductions.
On the other hand, reductive sealing measurements push the fan-pressurization equipment's resolution to its limit and may, thus, present inaccuracies (Stephen, 1998).

The following observations may, nonetheless, be raised (Stephen, 1998):

- The air leaking through the envelope provides the greater part of a dwelling's ventilation (with closed windows), while purpose-provided ventilation systems only achieve a small fraction of it – in all dwellings but the most airtight ones.
- The contribution of each pathway to the total leakage is variable. However, noteworthy is the predominance of:
  - Joint leakages, particularly window-wall joints
  - Leakage pathways into the roof
  - Background air leakage, referring to the many openings and cracks in the building fabric. These are both difficult to quantitively assess and impractical to seal after the building's completion.

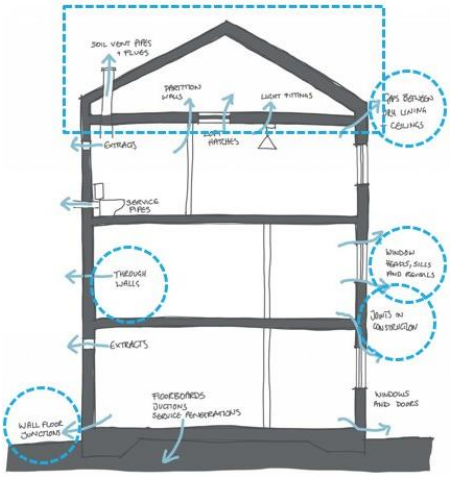

Figure 4: Air Leakage Main Pathways

The aforementioned further highlights the significance of exploiting a building's existing air leakage in its retrofit, particularly the background air leakage, rather than spending resources on challenging sealing attempts.

2.2.2. Air Leakage Classification

A good classification of the air leakage phenomenon addresses the nature of the air leakage pathways (Prignon & Van Moeseke, 2017; Younes et al., 2012), as detailed in Figure 5.

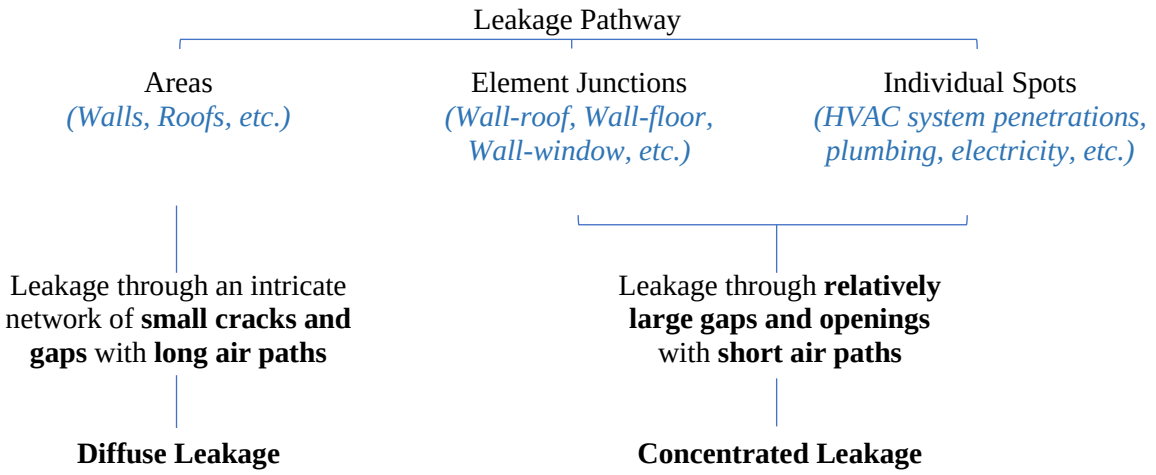

Figure 5: Air Leakage Classification

If both diffuse and concentrated leakage types are found in practice, some cases are considered hybrid (Refer to Figures 6 and 7). These are, however, classified as either of the two main leakage types based on their dominant behavior (Prignon & Van Moeseke, 2017). Applying an air permeable insulation layer inside the existing envelope could then possibly allow to treat any envelope leakage, whether concentrated or diffuse, as a diffuse air leakage through the insulation (Refer to Figure 7).

The distinction between diffuse and concentrated leakage is important due to the differences in their leakage flow regimes (Refer to Chapter 2.2.3) and leakage heat loads (Refer to Chapter 2.2.4).

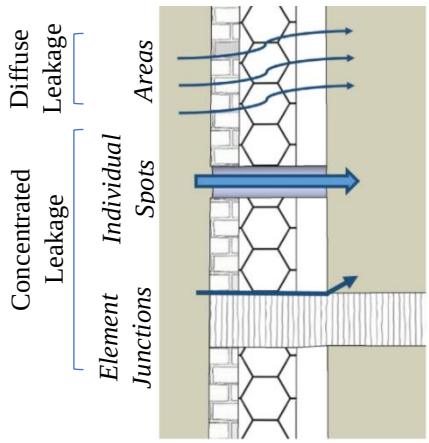

Figure 6: Air Leakage Pathway Types (Prignon & Van Moeseke, 2017).

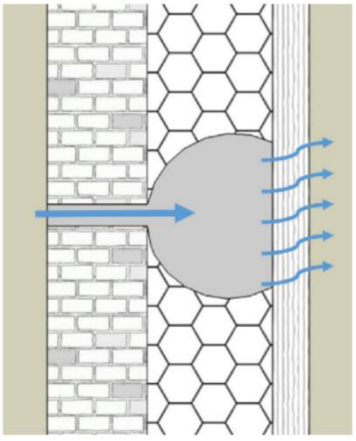

Figure 7: Air Leakage Hybrid Pathway (Prignon & Van Moeseke, 2017).

2.2.3. Airflow Types

The underlying physical concept to any air leakage model consists of a mass flow balance, which entails the understanding of the flow mechanisms (Younes et al., 2012). The flow regime allows to define the leakage flow equation, which characterizes the building's dynamic air leakage behavior at different pressure gradients.

A distinction is, however, made between the airflow through large openings (concentrated leakage) and small cracks (diffuse leakage) (Younes et al., 2012).

Concentrated Leakage

In case of **short leaks**, friction forces are assumed negligeable and the flow **turbulent** and governed by the **orifice equation**.

$$Q = C_d A[\frac{2}{\rho}\Delta P]^{\frac{1}{2}}$$

Q – airflow rate [m^3/s]
C_d – discharge coefficient [-]
A – opening area [m^2]
ρ – air density [kg/m^3]
ΔP – pressure gradient across the opening [Pa]

Diffuse Leakage

In case of **low flow rates** and **long airflow paths**, the **viscosity effect** is dominant and the flow is **laminar**.

$$Q = \frac{\Delta P}{8\mu L}[\pi r^4]$$

Q – airflow rate [m^3/s]
μ – dynamic viscosity in air [Pa.s]
L – flow path length [m]
r – opening's radius [m]
ΔP – pressure gradient across the opening [Pa]

Power Law

In practice, a building's air leakage is attributable to wide-ranging pathways (Refer to Chapter 2.2.1), and the dominating airflows are rarely fully-turbulent or fully-laminar (Refer to Chapter 2.2.2).

The flow mechanism thus combines both airflow schemes and may be represented by one overarching equation referred to as the **Power Law** (De Hoon, 2016; Prignon & Van Moeseke, 2017; Younes et al., 2012), detailed below:

$$Q = C\,(\Delta P)^n$$

C – flow coefficient [$m^3/s.Pa^n$]
n – flow exponent [-]

Any leakage flow may thus be represented by the Power Law equation, by defining its characteristic **C** and **n** parameters:

$$\boldsymbol{C} \propto \frac{\rho^{n-1}}{\mu^{2n-1}}$$

As per the dimensional analysis (Walker et al., 1998), the **flow coefficient (C)** is independent of the viscosity for a turbulent orifice flow (where n = 0.5) and of the density for a laminar flow (where n = 1).
Giving the correct behavior of the flow at the limiting flow regimes, it is in agreement with the specific flow equations for the fully-developed turbulent and laminar flows above.

$$\boldsymbol{n} = [0.5; 1]$$

The **flow exponent (n)** varies between 0.5, for a fully-developed turbulent flow, and 1, for a fully-developed laminar flow (De Hoon, 2016; Younes et al., 2012).

A good indicator of the flow regime, **n** helps estimate the size of dominant leakage pathways. A change in the exponent post-retrofit also characterizes the effect of the applied measures (De Hoon, 2016).

For building envelope leakage, **n** is typically in the vicinity of 0.65 or 2/3.

2.2.4. Leakage Heat Loads and Infiltration Heat Recovery

Identified as the main contributor to the ventilation demand in a majority of residential buildings (Stephen, 1998), air leakage is also accountable for a measurable share of its heating demand (Emmerich et al., 2019; Gillott et al., 2016; Younes et al., 2012; Zmeureanu, 2000).
Another important distinction could, however, be raised as to the heat load of concentrated and diffuse leakages.

Air leakage heat load is conventionally computed as the product of the leakage mass flow rate to the indoor-outdoor sensible enthalpy difference (Buchanan & Sherman, 2000), neglecting the interaction between conduction and air flows in the construction (Solupe & Krarti, 2014; Younes et al., 2012).

$$Q_{inf} = \dot{m} C_p (T_i - T_o)$$

Q_{inf} – air leakage energy flow [W]
$\dot{m}$ – leakage mass flow rate [kg/s]
C_p – air specific heat capacity [J/K°C]
T_i & T_o – indoor and outdoor temperatures [°C]

Decoupling conduction and air leakage, their combined thermal load through the envelope is then conventionally estimated as the simple summation of their distinct heat loads (Solupe & Krarti, 2014; Younes et al., 2012).

$$Q_{convention} = Q_{conduction} + Q_{leakage}$$

$$Q_{convention} = UA\,(T_i - T_o) + \dot{m} C_p (T_i - T_o)$$

$Q_{convention}$ – air leakage energy flow [W]
U – construction thermal transmittance [W/m^2.K]
A – construction surface area [m^2]

Albeit acceptable for concentrated leakage, this decoupling entails significant overestimation when it comes to the energy impact of diffuse leakage (Younes et al., 2012).

In contrast with concentrated leakage, diffuse leakage occurs through a network of minute cracks and openings with long air paths in the envelope. The larger contact surface and transit time of the leakage air within the building fabric entails much greater heat exchange between the solid and air phases. These exchanges, often referred to as **Infiltration Heat Recovery** (**IHR**), shift the temperature distribution in the construction from the conduction's linear distribution to a curved distribution (Solupe & Krarti, 2014; Younes et al., 2012).

The temperature gradient within a building's envelope is thus controlled by the indoor-outdoor temperature gradient, as well as the direction and velocity of the leakage airflow, as illustrated in Figure 8 (Solupe & Krarti, 2014).

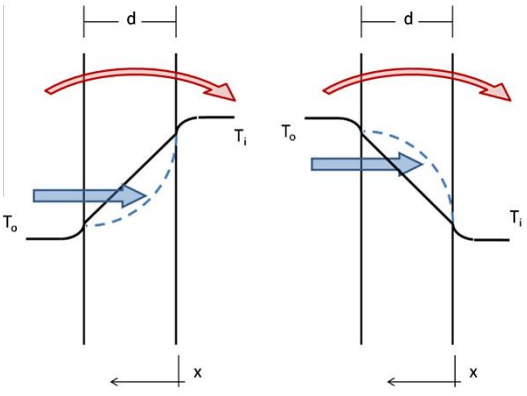

Figure 8: Airflow's Impact on Constructions' Temperature Distribution (Solupe & Krarti, 2014)

In terms of energy demand, the conventional decoupled method is found to overestimate the leakage's energy load by 10-95% (Buchanan & Sherman, 1998, 2000).
The variability of the IHR effectiveness is attributed to various parameters, influencing the air leakage's transit time: the shorter the transit time of the air in the construction, the less energy exchange between the leaking air and the building fabric and, consequently, the less heat recovered (Buchanan & Sherman, 1998; Sherman & Walker, 2001).

Accordingly, the IHR efficiency:

- Decreases at higher **airflow rates**
- Increases with the **leakage path length**
- Increases with the envelope participation fraction, determined by the **envelope's construction**.

Constructions subject to low flow rates and long leakage pathways thus achieve the highest heat recovery rates. A trade-off is, however, arising (Sherman & Walker, 2001).

- At low leakage rates, the high IHR rate is implemented to small leakage heat loads.
- At high leakage rates, the low IHR rate is implemented to large leakage heat loads.

In terms of total building energy, an optimum air leakage rate could be defined to balance the IHR and leakage rates, and maximize the building's energy savings while exploiting the leaking air for ventilation.

The heat recovery effect resulting from the interaction between the building fabric and the leaking air thus appears as a key factor in the overall building physics and building energy loads (Younes et al., 2012). This is further emphasized in buildings with breathable, such as traditional masonry buildings, where practically the whole envelope interacts with the airflow (Jokisalo et al., 2009).

Intentionally integrating and enhancing this heat recovery phenomenon in constructions, for energy-efficiency purposes, has been studied and incorporated into purpose-designed building fabric systems commonly referred to as **Dynamic Insulation**.

2.3. Dynamic Insulation

2.3.1. Definition

Dynamic Insulation (DI) is a building envelope system whose base principle consists of introducing a running fluid into the building's static construction layer to recover some of the heat loss through the envelope (Fawaier & Bokor, 2022): The greater the fluid flow, the smaller the heat loss (Refer to Figure 9).

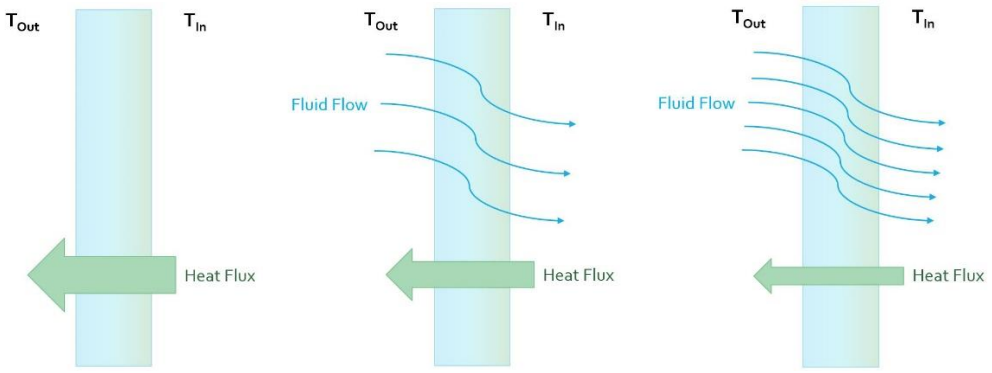

Figure 9: Fluid Flow's Impact on the Envelope Construction's Heat Flux

Dynamic Insulation systems have two primary functions:

1. Allow to adapt the building envelope's thermal resistance to the outdoor conditions, by controlling the heat transfer rate into and out of the building (Fawaier & Bokor, 2022).
2. Allow to utilize the recovered conductive heat to pre-condition incoming ventilation air, by acting as a heat exchanger, reducing the building's energy use while contributing to satisfactory air change levels (Zhang & Wang, 2021).

2.3.2. Dynamic Insulation Types

Currently available DI structures are mostly research prototypes or small-scale demonstration projects. As per their base principle, DI technologies may be classified based on their fluid and construction types, as described in the following scheme (Fawaier & Bokor, 2022).

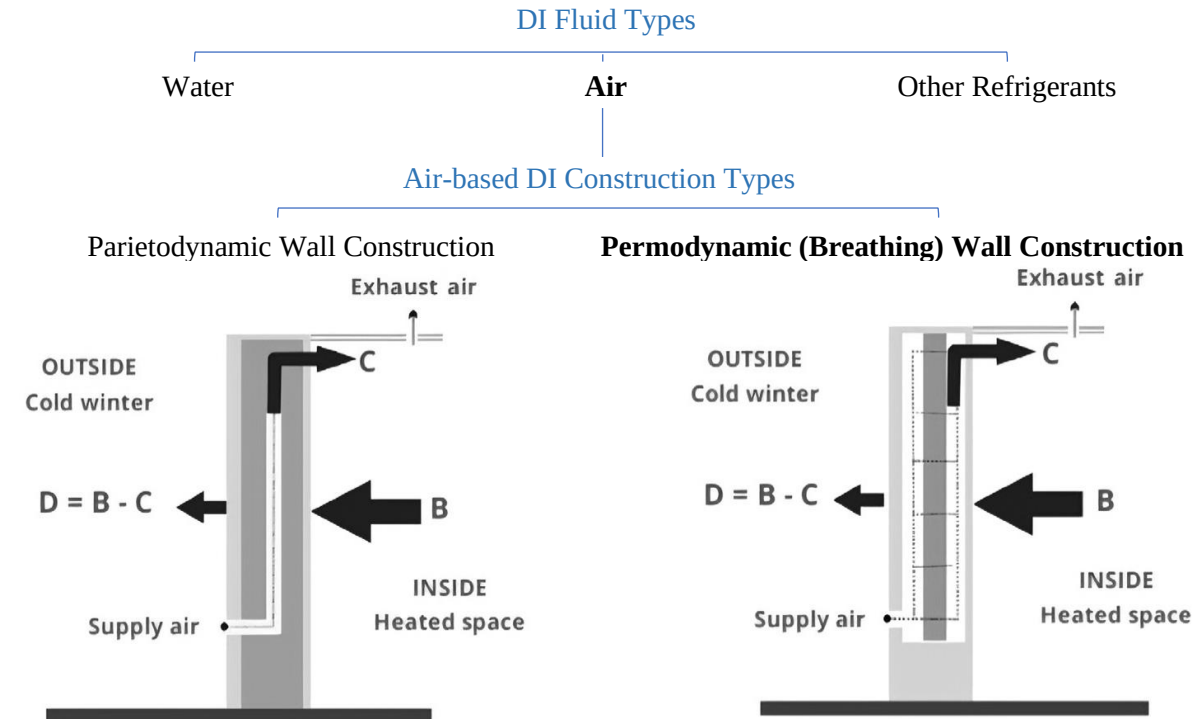

Figure 10: Air-based DI Construction Types (Fawaier & Bokor, 2022)

- Airflow direction is perpendicular to the heat transfer direction.
- Airflow is constrained in ideally-airtight channels.

Solution is not compatible with the studied problem:
Relying on the airtightness of the building fabric, this approach contradicts the research goal of investigating a potential retrofit strategy preserving the building's air leakage.

- Airflow direction is parallel to the heat transfer direction.
- Airflow travels through the air-permeable construction.

Solution is compatible with the studied problem:
The approach is a distributed ventilation air supply system, where the construction acts as a **supply source**, **heat exchanger**, and **airborne contaminant filter** – and thus provides for the optimization of the energy use and the supply of filtered outdoor air, using air leakage (Alongi et al., 2017; B. Taylor & Imbabi, 1998).

Air-based DI systems are deemed the most common application in buildings (Fawaier & Bokor, 2022). Such systems, particularly under a **Permodynamic (Breathing) Wall construction**, are also conveniently the most suited within the context of this study, due to the possibility of preserving the construction's breathability and exploiting its air leakage flow in the dynamic insulation's operations.

Providing for the movement of air and moisture through the envelope, Breathing Wall Dynamic Insulation is thus identified as a potential solution for the simultaneous reduction in ventilation and envelope heat losses, and improvement of the Indoor Air Quality (IAQ) (B. Taylor & Imbabi, 1998).

2.3.3. Breathing Wall Dynamic Insulation: Potential Solution for Traditional Heritage Buildings

The trade-off between the building's energy-efficiency and its indoor environment quality (IEQ) highlights the existence of an optimal airtightness limit beyond which further sealing of the envelope would no longer be suited for satisfactory levels of indoor health and comfort (Ridley et al., 2003; Salehi et al., 2017).

The exploitation of the Infiltration Heat Recovery (IHR) effect is one potential solution to the optimization of the retrofit's energy-saving benefits with satisfactory indoor environment quality (IEQ) levels. Although a naturally-occurring phenomenon in any air-permeable construction, the IHR effect is further emphasized through Dynamic Insulation (DI) systems.

Dynamic insulation's Breathing Wall (BW) systems particularly address many of the limitations faced in the retrofit of heritage buildings with breathable constructions (Fawaier & Bokor, 2022; B. Taylor & Imbabi, 1998; B. J. Taylor & Imbabi, 1997).

In terms of Building Construction, BW systems ensure:

Air-Permeable Constructions

BW dynamic insulation systems depend on air-permeable constructions – which allows the exploitation of the air leakage in traditional historic buildings, rather than sealing them.

Reduced Insulation Thickness

BW systems act as heat exchangers, reducing the combined conductive and ventilation heat losses – which calls for reduced insulation thicknesses, and limits the decrease in usable floor area resulting from the added internal insulation in heritage buildings.

In terms Building Performance, BW systems provide for the potential optimization of the energy-efficiency and IEQ through:

Adaptable Thermal Comfort

BW systems allow to achieve the desired indoor climate by either restricting or enhancing the heat fluxes across the building envelope – which provides adaptable building envelope properties for the different needs of the heating and cooling seasons.

Filtered Outdoor Air Supply

BW systems allow the movement of air and moisture through the building envelope and thus operate as a component of the ventilation system – which provides fresh and filtered outdoor air and enhances the Indoor Environment Quality (IEQ).

2.3.4. Breathing Wall Construction and Operation

Typical Breathing Wall systems consist of three layers (Fawaier & Bokor, 2022):

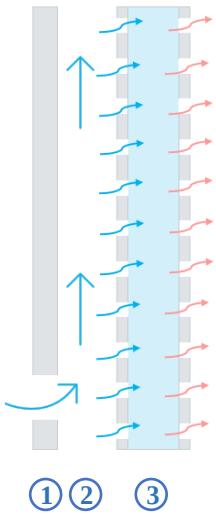

Figure 11: Breathing Wall Systems Layers

1 External Layer – exposed to ambient air.

- In existing buildings, the external layer corresponds to the existing construction.
- The air pathways in the external layer could be concentrated or diffuse; either way the leaking air will be converted into a diffuse airflow within the internal breathing layer.

2 Air Gap – between the external layer and the internal breathing layer

- The vertical airgap allows the circulation of air and its distribution between the external construction layer and the breathing layer.

3 Breathing Internal Layer – made of porous insulation material

- The breathing internal layer allows the circulation of the ventilation airflow through the building fabric driven by the outdoor-indoor pressure gradient.
- The porosity of the material emphasizes a diffuse airflow with long airpath and, consequently, the heat exchange between the air and solid matrices.

Acting as a distributed ventilation system, BW constructions are integrated with the building's HVAC system. Their thermal and ventilation performance is attributed to the leakage process through their air-permeable construction (Zhang & Wang, 2021), driven by the pressure gradient across it (as detailed in Chapter 2.1.3).

They thus present two operation modes (Refer to Table 2) (Alongi et al., 2017; Fawaier & Bokor, 2022; B. Taylor & Imbabi, 1998; B. J. Taylor et al., 1998) and may be driven by two main ventilation regimes (Refer to Table 3) (Zhang & Wang, 2021).

Table 2: Breathing Wall Systems' Operation Modes

Modes of Operation	
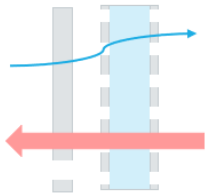	***Contra-Flux Operations*** · The airflow and the heat flux move in opposite directions. · The system operates as a: 〉 Heat-exchanger – reducing heat loss in the heating season. 〉 Air Filter – filtering the incoming air against outdoor pollutants. 〉 Diffusion Barrier – preventing interstitial condensation.
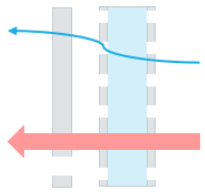	***Pro-Flux Operations*** · The airflow and the heat flux move in the same direction · The system operates as a: 〉 Heat Dissipator – enhancing the heat dissipation in the cooling season, improving the summer thermal comfort, and reducing overheating risks and cooling demands

Table 3: Breathing Wall Systems' Ventilation Regimes

Ventilation Regimes	
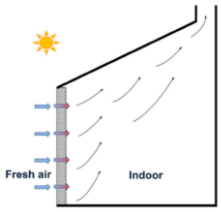	***Natural Ventilation*** · The pressure gradient across the envelope is governed by the natural pressure components (wind and stack) · Operations are highly influenced by the surrounding environment. 〉 The greatest challenge is sustaining the desired flow direction under varying weather conditions. The flow magnitude is not as important. · Theoretically, DI systems may successfully perform without mechanical ventilation. 〉 Some studies (Etheridge & Clare, 2001) suggest wind-powered extract fans to help maintain counter-flow at high wind speeds and achieve the needed operations.
	***Mechanical Ventilation*** · The pressure gradient across the envelope is governed by the mechanical fans' induced pressure. · Operations are more controllable and predictable. 〉 System is less challenging in terms of design. But it entails more intrusive systems, with additional materials and system-energy consumption.

2.4.State-of-the-art Retrofit, and Air Leakage Building Performance

2.4.1. Conventional Approach

The implications of low airtightness levels and their associated air leakage in buildings are well- and widely-documented.

Conventional Approach and Applications

Air leakage exhibits risks of uncontrolled:

〉 Introduction of unconditioned air into the building.
〉 Release of conditioned air out of the building, bypassing the ventilation system's heat recovery process.

It is thus often depicted as a source of unnecessary energy waste and overconsumption, altering the envelope's thermal performance and the heat flow through it (Younes et al., 2012).

As discussed under Chapter 2.2.4, the air leakage's heat load is conventionally calculated as:

$$Q_{inf} = \dot{m} C_p (T_i - T_o)$$

Q_{inf} – air leakage energy flow [W]
$\dot{m}$ – leakage mass flow rate [kg/s]
C_p – air specific heat capacity [J/K°C]
T_i & T_o – indoor and outdoor temperatures [°C]

Under this conventional estimation, air leakage is identified as a major contributor to the building's heat loss and energy use (Younes et al., 2012). Various studies have indeed attributed between 25-50% of the building's heating load to the air leaking through its envelope (Prignon & Van Moeseke, 2017; Younes et al., 2012), while improved airtightness is credited with significant energy-saving potential (Emmerich et al., 2019; Gillott et al., 2016; Zmeureanu, 2000).

Strongly influenced by the current building regulations and standards, catering for stricter energy performances, the building field has thus conventionally reduced the buildings' air leakage through airtight constructions (Emmerich et al., 2019; Gillott et al., 2016; Zmeureanu, 2000).

A predominant reliance on the same retrofit strategies is indeed detected, despite the contrasting climates and building characteristics (Blázquez et al., 2019; Cabeza et al., 2018; Doran et al., 2014; Martínez-Molina et al., 2016; Zagorskas et al., 2013). Renovation programs focus on (Ortiz & Bluyssen, 2022):

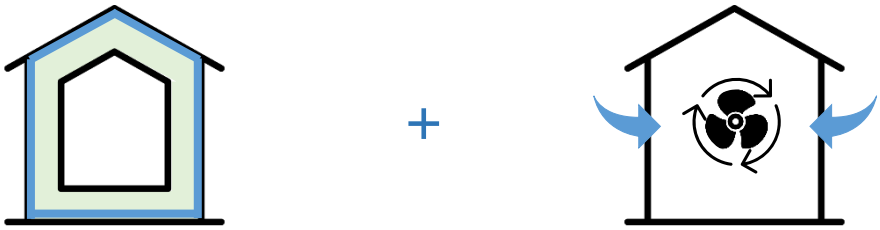

Improvement of the **building envelope's insulation and airtightness** as practically possible, to minimize envelope heat loss and focus on purpose-designed openings and systems to meet the ventilation demand.
Fundamental strategy to increase buildings' energy-efficiency

Implementation of **advanced low-energy HVAC systems**, for thermal conditioning the indoor environment and compensating the building's air change rate to meet the ventilation demand.
Popular support strategy to improve buildings' health and comfort

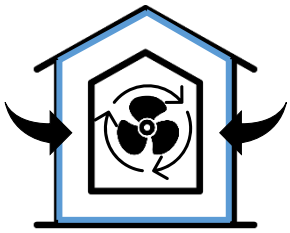

Conventional Retrofit Case
[CRC]

Figure 12: Conventional Retrofit Case (CRC) Components

Conventional Retrofit Approach: Limitations

Limitations in the conventional retrofit strategy are related to the neglection of two aspects of the relationship between the building's air leakage and its overall performance:

Infiltration Heat Recovery (IHR)

The airtightness implications on the building's energy-efficiency are often misrepresented, particularly in breathable constructions.
The conventional approach to the air leakage's heat load overestimates it by 10-95% (Buchanan & Sherman, 1998, 2000), due to neglecting the interaction between the air leakage and conduction fluxes in the envelope (as detailed in Chapter 2.2.4).

This interaction entails a heat exchange between the solid and air phases, referred to as the IHR. Although negligeable for concentrated leakages, the IHR may be significant in constructions with a wide network of minute cracks with long air paths, a characteristic feature of traditional masonry buildings (Solupe & Krarti, 2014; Younes et al., 2012).

The relationship of the air leakage's mass flowrate to its heat load thus diverges from the positive linear relationship assumed in the conventional approach.
Accordingly, an **increase in air leakage flow** does not necessarily entail a **proportional increase in its heat loss**:

- Under pro-flux operations, the heat released might increase faster
- Under contra-flux operations, the heat loss might increase slower, or even decrease

Although addressed in many studies (Buchanan & Sherman, 2000; Fawaier & Bokor, 2022; Qiu & Haghighat, 2007; Solupe & Krarti, 2014), this effect is typically **not accounted for in research and industry**.

The leakage's contribution to building energy demand, and accordingly **the energy-savings achieved by airtightness improvements,** are often overestimated**.**
This affects retrofit projects, as it results in performance gaps between estimated and actual building performances and misinforms retrofit decisions (Jokisalo et al., 2009; Solupe & Krarti, 2014).

Indoor Environment Quality (IEQ)

Building airtightness is not limited to heat loss reduction and energy-savings.
Applications of the conventional retrofit reveal counter-productive trends, of particular importance in traditional and monumental buildings (Blázquez et al., 2023; Doran et al., 2014; Fawaier & Bokor, 2022; Ortiz & Bluyssen, 2022; Stephen, 1998):

- Build-up of stale-air & indoor contaminants and decreased Indoor Air Quality (IAQ)
  - Air leakage is a major contributor to buildings' air change rate and indoor contaminant removal. It was indeed found as the primary ventilation source in most traditional UK dwellings (Stephen, 1998).
  - Airtightness measures thus risk tipping the balance between sufficient and insufficient ventilation (Stephen, 1998).
- Build-up of humidity and increased risk of moisture, condensation, and mold growth.
  - Air leakage is critical to the hygrothermal balance of breathable buildings (Doran et al., 2014; Little et al., 2015).
  - It is also identified as a crucial component of the wetting and drying cycles of masonry walls (Cassar et al., 2007).
- Reduced heat removal in summer and increased risk of summer overheating.
  - Higher thermal resistance and airtightness render buildings more sensitive to solar and internal heat gain, potentially causing higher or previously non-existent cooling demands (Fawaier & Bokor, 2022; Ortiz & Bluyssen, 2022).

The worsening of the IEQ is often neglected as a primary performance indicator to retrofit strategies, despite its implications on the health and comfort of building occupants (d'Ambrosio Alfano et al., 2016; Gillott et al., 2016; Salehi et al., 2017), and degradation of the construction (Younes et al., 2012).

2.4.2. Air Leakage in Breathable Constructions and Breathing Wall Approach

Breathable Constructions' Performance Trade-off

The performance and limitations of the conventional retrofit strategy (Refer to Chapter 2.4.1), particularly in traditional heritage buildings, clear up the actual relationship of a building's overall performance to its air leakage. It embodies a complex trade-off between the building's energy-efficiency and IEQ, that considers three situations detailed in Table 4 below.

For buildings with mechanical heating and no mechanical cooling, characteristic of the majority of the dwellings in Central and Northern Europe, the thermal energy demand is highly-dependent on the heating season. Accordingly, the heat flux's positive direction is assumed to be outward.

Table 4: Air Leakage's Complex Trade-off between Energy-Efficiency and IEQ

Pro-flux operations	Contra-flux operations	
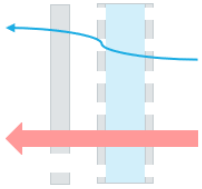	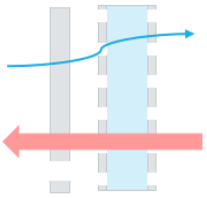	
Air leakage (Q_A) and conduction (Q_c) heat fluxes are in the same direction $Q_A > 0$ & $Q_c > 0$	Air leakage (Q_A) and conduction (Q_c) heat fluxes are in opposite directions $Q_A < 0$ & $Q_c > 0$	
$Q_A + Q_c > 0$	$Q_A + Q_c > 0$	$Q_A + Q_c < 0$
As $\dot{m}$ increases by $\Delta\dot{m}$, building energy **increases** by **more** than $\Delta\dot{m} \times C\Delta T$	As $\dot{m}$ increases by $\Delta\dot{m}$, building energy **increases** by **less** than $\Delta\dot{m} \times C\Delta T$	As $\dot{m}$ increases by $\Delta\dot{m}$, building energy **decreases** by **less or equal** than $\Delta\dot{m} \times C\Delta T$
Severe trade-off between energy-efficiency and IEQ	**Mild trade-off** between energy-efficiency and IEQ	**No trade-off** between energy-efficiency and IEQ
Air Leakage Load Case 1	Air Leakage Load Case 2	Air Leakage Load Case 3

Through breathable constructions, the building performance's relationship to the air leakage is then variable, depending on: the direction of the air leakage, the air leakage flow, and the envelope's thickness and thermal conductivity (Buchanan & Sherman, 1998, 2000; Solupe & Krarti, 2014; B. Taylor & Imbabi, 1998; B. J. Taylor et al., 1996).

Breathing Wall Approach and Applications

The exploitation of the building's air leakage in its post-retrofit performance is favored by treating its breathable construction as a Breathing Wall Dynamic Insulation (Refer to Chapter 2.3.3). As for all DI systems, the air leakage limit up to which it is benefiting the building performance depends on the system's design: ventilation regime and flow, and envelope material and thickness (Refer to Chapter 2.3.4).

Ideally, the best configuration would seek to maximize the operation of the construction under the ***Air Leakage Load Case 3*** defined above, and minimize its operation under the ***Air Leakage Load Case 1***. A well-designed DI system would indeed contribute to the IEQ while simultaneously saving-energy (Fawaier & Bokor, 2022).

A recent review of the literature on DI systems (Fawaier & Bokor, 2022) distinguishes the various existing air-based systems and supports that their application in building envelopes potentially results in yearly savings on space-conditioning and ventilation.

The DI technology's basic timeline is shown in Figure 13 (Fawaier & Bokor, 2022).

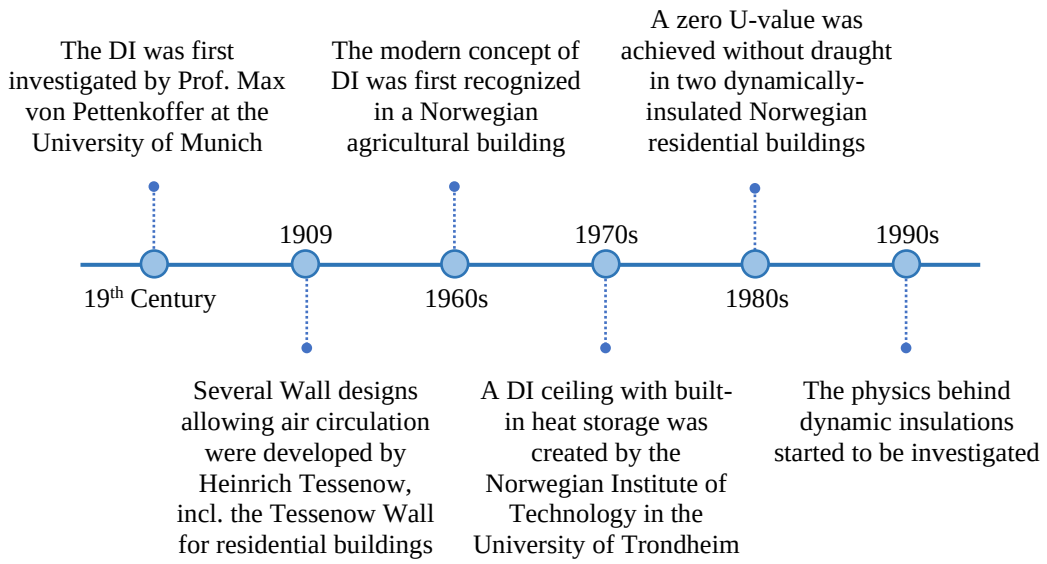

Figure 13: The DI Technology's Historical Timeline

The modern concept of Dynamic Insulation was introduced in the 1960's in Norwegian agricultural buildings as dynamically-insulated ceilings, which combined the natural stack ventilation with heat storage in the barns' hayloft. The idea of air permeable constructions as dynamic insulations may, however, be traced back to the mid-19th century when research at the University of Munich investigated the air and moisture transport through building materials, and described the airflows through porous composite envelopes (Fawaier & Bokor, 2022).

The DI concept was first implemented in a residential configuration in the 1980's; two Norwegian residential buildings with dynamically-insulated ceilings were monitored and found to achieve a U-value of zero with no draught. The construction details were, nonetheless, found to be critical for achieving such performance Co(Fawaier & Bokor, 2022; Halliday, 2001).
Along the same lines, a 1993 study noted a 50% recovery of conduction heat losses in a Japanese family dwelling by dynamic insulations, associated with a well-distributed and pre-conditioned draught-free ventilation ((Halliday, 2001).

More recent examples have considered the implementation of DI systems in residential buildings as a strategy for reducing heating loads under cold climates (Etheridge & Clare, 2001; Park et al., 2016; Samuel et al., 2003), cooling loads under warm humid climates ((Ascione et al., 2015; Elsarrag et al., 2012; M. Imbabi et al., 2006), or both (A. A. Samuel, 2002).Besides the improvements in indoor air quality and thermal comfort, the considered dynamic insulation systems noted measurable energy-savings in both seasons: Park et al. (2016) estimate a 15.5-40.2% reduction in the heating loads of a Tokyo model house, for different DI installation points over its envelope, while Elsarrag et al.B(2012) achieves a drop in the conduction gains of the EcoVilla in Qatar by a measured 41% , against a simulated 38%.

The vast majority of the dynamic insulation literature, however, focuses on the specific performance of dynamic insulations at the component level, rather than the building level. The latter considers development of models and their validation (Alongi et al., 2017, 2020a, 2021; Krarti, 1994; Qiu & Haghighat, 2007; B. J. Taylor et al., 1996), as well as the evaluation and optimization of the performance of DI materials and prototypes (Alongi et al., 2020b; Baker, 2003; W. Chen & Liu, 2004; Craig et al., 2021; Craig & Grinham, 2017; Dimoudi et al., 2004; M. S.-E. Imbabi, 2006; Wong et al., 2007; Zhang & Wang, 2021).

Despite the dynamic insulation concept being introduced more than 30 years ago, design guidelines for the their implementation as an applicable solution are thus not well-developed, for either new or existing buildings, resulting in its lack of application in building design.

Although the implementation of purpose-designed dynamic insulation components has been limited, the IHR effect is still a naturally-occurring phenomenon in all breathable constructions with significant diffuse leakage (Jokisalo et al., 2009). Dynamic Insulation is thus already existing in a majority of traditional historic constructions, in the form of their air permeable massive constructions and insulation layers.
Their primary limitation lies in their original design, which have not been tailored to operate as a dynamic insulation. This raises the question of how optimal their existing configurations and operational modes are to fully harness their potential dynamic insulation benefits. Addressing these limitations may yield measurable improvements with minimal interventions.

DI systems indeed adopt various configurations and operational modes, affecting their infiltration heat recovery (IHR) efficiency. For instance, Murrata *et al.* (2015) investigated a system of inorganic concrete breathable walls, alternatively acting in supply and exhaust. They established that Breathing Wall DI systems may achieve similar energy-saving performance as the combination of increased thermal insulation with a ventilation system with a heat recovery efficiency of 90%.

Breathing Wall Approach: Limitations and Design Considerations

The promising benefits of BW constructions depend upon a number of conditions and considerations (B. Taylor & Imbabi, 1998), addressing their basic Design Principles and three buildings aspects:

Supporting Systems Design	Building Design	DI System Design

Design Principles

In **conventional airtight buildings**, all HVAC loads are fully-addressed through purpose-designed systems. The extent of the external environment's influence on the internal loads is thus, more or less, in the control of the designer. This allows the implementation of the same system **under various contexts** (B. J. Taylor & Imbabi, 2000).

In retrospect, in case of **breathing wall systems**, the external and internal environments are intricately-coupled; temperature or wind variations may influence the behavior of DI constructions . J. Taylor & Imbabi, 2000).
The extent of the system's sensitivity to weather and design variables is also different under varying DI configurations, structures, and climatic contexts (Fawaier & Bokor, 2022).
The efficiency of a DI system is thus strongly **context-dependent**.

While an environmental design is, to an extent, optional in airtight buildings, it is imperative in the design of breathable constructions. The design of durable, energy-efficient, and comfortable dynamically-insulated buildings must be based on strong environmental design principles, accounting for the highly-variable external environment B. J. Taylor & Imbabi, 2000).

1 Supporting Systems Design

- In the heating season, when the system operates in contra-flux, the reduced heat loss across the envelope entails a higher heat input into the construction's interior surface to ensure sufficient warming of the incoming air (B. Taylor & Imbabi, 1998).
  - If the incoming air leakage is introduced without going through the IHR process, little savings are achieved.
  - This heat demand may be covered by the space-heating system or through a complementary heat-recovery system on the indoor air.
- In the heating season, reasonably uniform inward leakage airflows (i.e. air infiltration) must be ensured under all environmental conditions. Fans may then be required for the reliable and sufficient depressurization of the system in mild and variable climates (B. Taylor & Imbabi, 1998).
  - Colder climates (e.g. Northern Europe) with indoor-outdoor temperature gradients of 40°C provide for a reliable stack effect. This is not guaranteed in temperate climates.
  - The depressurization must not exceed the limit beyond which users would experience discomfort and difficulty opening doors/windows.
- As the breathing wall acts as an air filter, there is a potential risk that dust trapped in its pores sustains bacterial growth and produces toxins and microbes that could spread to the indoor living space. As some bacteria provide the needed environment for mold and fungi growth, this could constitute a potential health hazard (B. Taylor & Imbabi, 1998).
  - An investigation of the conditions under which the DI may become an amplifier and disseminator of viruses, spores, and bacteria must be in order.
  - The dust accumulation has been proven insignificant in barns. Dwellings presenting smaller ventilation rates, their dust accumulation rate is expected to be correspondingly smaller and even less problematic.

2 Building Design

- At low air change rates, conventional airtight buildings with balanced MVHR are expected to perform better than dynamically-insulated buildings (B. Taylor & Imbabi, 1998).
  - The more effective the heat exchanger, the higher the ACH at which DI systems become worthwhile.
- The most effective DI performance considers as much of the building envelope as practical to be air permeable (B. Taylor & Imbabi, 1998).
  - This typically affects the building's glazed-opaque surface distribution, which is not of concern in monumental retrofit as such distribution is pre-set.
- The smaller the building's volume to envelope-area ratio, the greater the energy-savings (B. Taylor & Imbabi, 1998).
  - As the volume-to-area ratio increases, so does the ventilation-to-envelope heat losses.
  - Detached dwellings are better suited candidates for DI systems relative to apartments, particularly when energy-conservation is the main objective.
- Besides the dynamically-insulated surfaces, the building must be airtight (Gan, 2000).
  - DI systems in particular, and heat recovery systems in general, are not effective in buildings where the heat-exchanger system may be by-passed through the construction.
  - It is necessary to ensure that virtually all leakage goes through the DI surfaces in the form of diffuse leakage, which implies the sealing of concentrated leakage pathways.

- Achieving low effective U-values in the Breathing Wall typically requires higher ventilation rates (Fawaier & Bokor, 2022).
  - Heat is recovered with increasing flow rates, that decrease the conduction heat losses and provide pre-conditioned ventilation air.
  - For instance, low heat loss ($0.1 < U < 0.3$ W/m^{2}K) may only be achieved in timber panels for high heat exchange efficiencies at ventilation rates of 18-72 m/h (Craig et al., 2021).
- Achieving low effective U-values at lower airflows requires higher static thermal resistance of the construction (B. Taylor & Imbabi, 1998; B. J. Taylor et al., 1997).
  - Although naturally-occurring in all air permeable materials, the IHR effect is most efficient in inherently well-insulating materials (low λ) with large thicknesses. Otherwise, higher airflows would be required to achieve equivalent DI performance.
  - For instance, a masonry wall needs nearly 10 times the airflow through cellulose to achieve comparable relative improvements in U-value ($U_{dynamic}/U_{static}$), and 100 times that airflow to attain the same dynamic U-value ($U_{dynamic}$).
  - A composite permeable construction with both high thermal storage and low U-value may, however, be achieved by combining the properties of masonry and cellulose.
- Under mechanical ventilation, Breathing Walls have a critical thickness for minimizing the total energy loss (Fawaier & Bokor, 2022; B. Taylor & Imbabi, 1998).
  - Heat loss through the BW system may be reduced to practically zero with an increasing thickness of the porous medium. However, the greater thickness results in higher leakage pressure drop, and consequent energy loss through the mechanical ventilation system.
  - A critical thickness of the porous medium exists, achieving minimal overall energy loss, considering both convective and mechanical ventilation losses. Any increase of the thickness beyond the critical value is ineffective, and rather increases the net energy loss (Zhang & Wang, 2021).

3. Research Methodology

This Chapter defines the overall methodology adopted in answering the research questions presented under Chapter 1.4.

In an attempt to develop retrofit strategies addressing the particular characteristics of historic traditional buildings, the research investigates the potential of exploiting the building's existing air leakage as an integral part of its HVAC system and assesses the prospects of Dynamic Insulation (DI) as a solution to the trade-off between energy-savings and Indoor Environment Quality (IEQ).

The study is carried out as a comparative analysis simulating a single-family dwelling under different retrofit scenarios, and evaluating their respective performances relative to each other and to the baseline (BC) and conventional retrofit (CRC) cases.

Figure 14 summarizes the complete workflow of this research. The elements in blue highlight the solutions to the sub-questions of the corresponding research question group (RQG), leading up to the research's final output and answer to its main research question (highlighted in green).

A thorough **review of the literature** was carried out to define the air leakage's properties, behavior and observed impacts on the building and its occupants, particularly in traditional historic dwellings. This revealed a natural phenomenon, the Infiltration Heat Recovery (IHR), that is conventionally neglected in building energy assessments despite its influence on the air leakage's heat load. The applications of the IHR effect were thus further investigated, introducing the concept of Dynamic Insulation (DI), as a potential solution to the retrofit. The state-of-the-art (SoA) retrofit approaches to addressing air leakage in buildings are presented, with their limitations and design considerations.

The retrofit variants explored into the tailored retrofit strategy for historic traditional dwellings draw inspiration from the SoA retrofit strategies and the existing Dynamic Insulation literature and applications. The performance of such variants is evaluated against comparative reference cases: the base case (BC), built from the case study building's layout and properties, and the conventional retrofit case (CRC), taken as the benchmark of target retrofit improvements.

By highlighting the aspects of the overall building performance that are of interest in evaluating retrofit variants, the review of the air leakage properties and impacts helped define a relevant performance evaluation framework. The latter consisted of the relevant performance parameters and their corresponding criteria.

In order to carry the analysis, a **Building Performance Simulation (BPS) model** was built integrating three components:

the building model	the air leakage model	the dynamic insulation model
		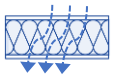

This allowed a more comprehensive and realistic assessment of the building performance, pre-and post-retrofit, by translating the air leakage's dynamic behavior and its associated IHR effect into the building simulation.

- The **building model** is based on an existing case study building, located at Herengracht 15, in Leiden. It conveys the case study building's layout and properties; its technical features are, however, standardized to simplify the model and be representative of the average historic traditional row dwelling in the Netherlands.

The **air leakage model** is defined and calibrated on the basis of the case study building's air leakage characterization. The latter is achieved through in-situ fan-pressurization and IR-thermography measurements, based on a reductive sealing strategy to allocate the total leakage into its component contributions. The model follows a crack template, defining the air leakage through each building component as a function of the pressure gradient. This translates into a more representative and dynamic distribution of the air leakage in the building and its performance.

The **DI model** is based on a well-established analytical DI model from authoritative literature references, referred to as the Taylor Model (B. J. Taylor et al., 1996). The analytical model was used to both build and validate the dynamic DI model, which was integrated into the BPS by coding it into its Energy Management System (EMS). It allows to consider the dynamicity of the construction in the evaluation of the building performance and, therefore, in the optimization of the retrofit approach.

To be able to cover all desired aspects of the retrofit alternatives, while reducing the computational costs, the analysis is carried out in two steps:

1. Sensitivity Analysis
2. Evolutionary Optimization

Both steps, detailed below, are implemented using the JEPlus v2.1 and JEPlus+EA v2.1 software tools in combination with EnergyPlus v23.1.

1. The Conditioned Zone Boundary (CZB) adopted in the retrofit analysis is selected on the basis of a **Sensitivity Analysis (SA)**. Examining the sensitivity of the building energy demand to the envelope surface permeabilities under different CZB, the configuration that shows better potential of preserving the surface permeability into the building's post-retrofit operations was adopted for the rest of the analysis.

2. The remaining variants were then examined in multiple **Evolutionary Optimization (E.Opt)** runs, optimizing the building's design to meet performance objectives set in accordance with the performance evaluation framework.

   For each optimization run, and corresponding retrofit scenario, a set of Pareto Optimal solutions is generated. The evaluation of each resulting set of solutions, against each other and the comparative reference cases (BC and CRC), is carried using the **Technique for Order of Preference by Similarity to Ideal Solution (TOPSIS)**.

The latter helps conclude the research with a final tailored recommendation and application frameworks for the retrofit of historic traditional buildings of varying levels of baseline performance and heritage protection restrictions.

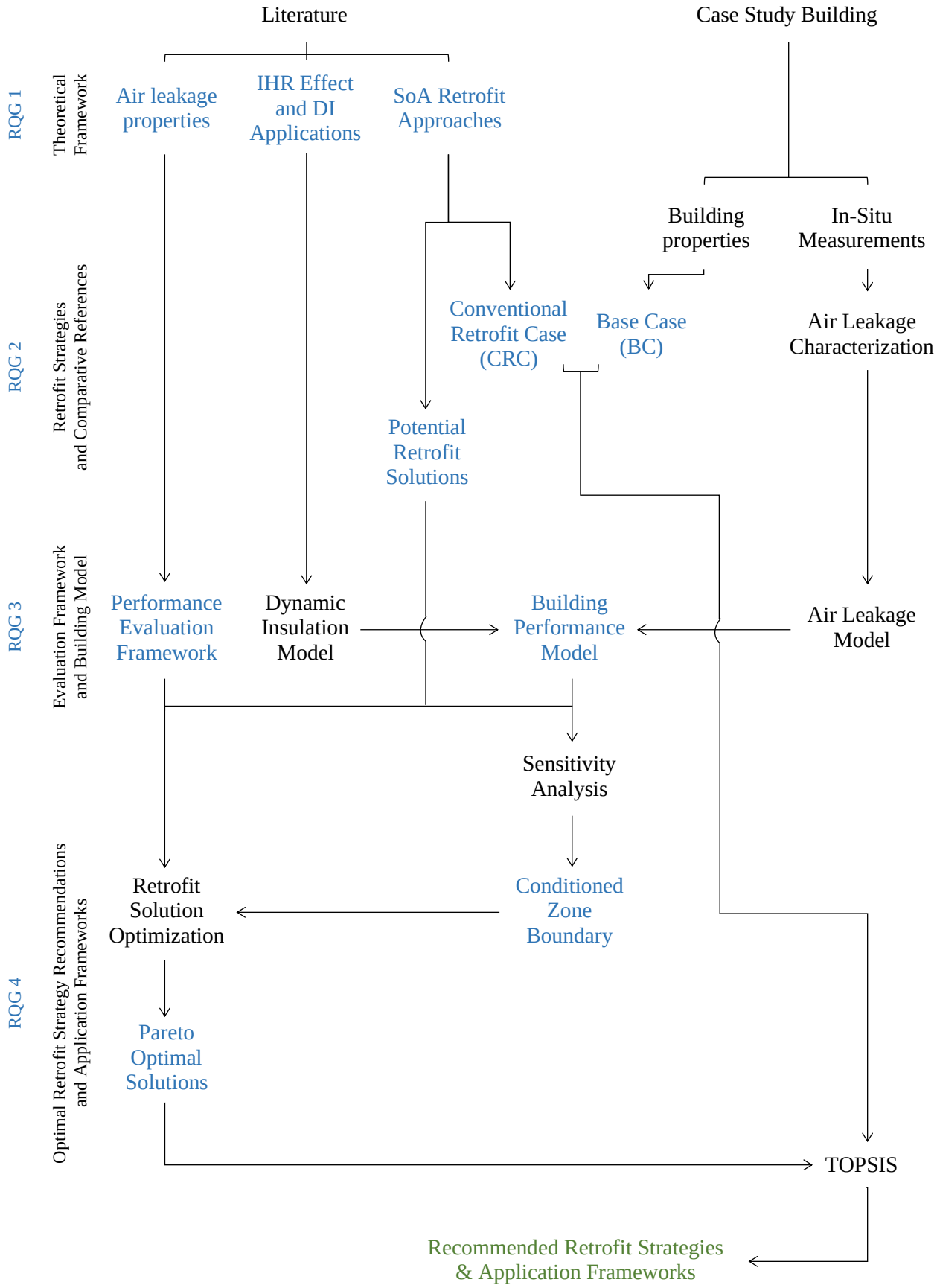

Figure 14: Overall Methodology of Research

4. Retrofit Strategy Alternatives

This Chapter defines the retrofit variants investigated as potential solutions to the retrofit of traditional historic buildings (Chapter 4.1) and their comparative reference cases (Chapter 4.2).

4.1. Solution Retrofit Strategies

The present work seeks the optimal airtightness and ventilation retrofit strategies for historic traditional dwellings, investigating the potential exploitation of their air leakage in their post-retrofit performance.

Addressing the complex trade-off between energy-efficiency, IEQ, and heritage preservation, the retrofit optimization explores all possible combinations (if applicable) of air permeability levels, insulation thickness, and fan air flow rate under the different retrofit scenarios.

Table 5: Performance Trade-offs of airtightness, insulation, and fan flowrates.

· The building airtightness level	for:	〉 The needed breathability of the construction 〉 Lower airtightness 〉 The leakage heat loss reduction 〉 Higher airtightness
· The building insulation thickness	for:	〉 The preservation of the building's original surfaces and usable indoor space 〉 Lower thickness 〉 The conduction heat loss reduction 〉 Higher thickness
· The fan airflow rate	for:	〉 The indoor air quality and ventilation needs 〉 Minimal flowrates 〉 The IHR depressurization of the building 〉 Higher flowrates

The retrofit scenarios are categorized in three groups based on the building feature they address: the conditioned zone, the envelope properties, and the ventilation strategy.

The **conditioned zone boundary** at the loft level is tested to identify the configuration providing for a better potential to exploit the building's air leakage into its post-retrofit performance. In other words, the configuration of interest would encourage the preservation of the envelope surface permeability by minimizing its impact on the building's energy demand.

Conditioned Zone Boundary

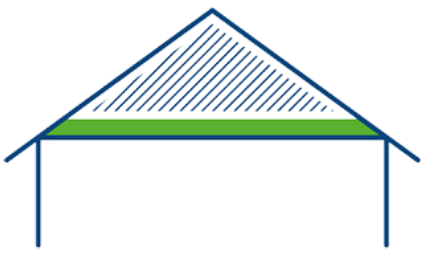

Cold Loft Configuration

〉 Conditioned zone boundary at the Attic Floor
〉 Insulation and air leakage boundary at the Attic Floor

Warm Loft Configuration

〉 Conditioned zone boundary at the Pitched Roof
〉 Insulation and air leakage boundary at the Pitched Roof

The **envelope properties** consider two aspects, the addition of insulation and the dynamicity of the construction. The former evaluates the importance of added insulation on the achieved retrofit improvements, and addresses the implications of varying levels of protection and allowable interventions in heritage buildings. The latter assesses the significance of the construction dynamicity in the BES analysis and the impact it may have on the resulting optimal retrofit strategy.

Insulation of the Construction

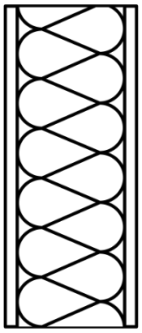

Insulated Construction

- Insulation added on all envelope surfaces
  - Suitable for monuments with only exterior heritage-protected surfaces.

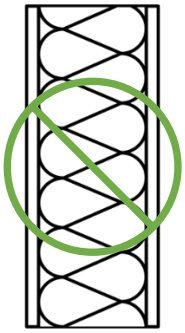

Non-Insulated Construction

- No added insulation of the envelope surfaces, preserving the existing minimal insulation of the roofs
  - Suitable for monuments with heritage-protected exterior and interior surfaces

Envelope Properties

Dynamicity of the Construction

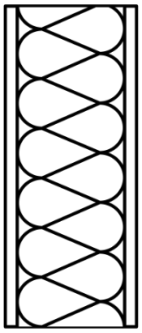

Static Construction

- Conventional decoupling of conduction and air leakage flow heat transfers
  - Without Dynamic Insulation EMS model

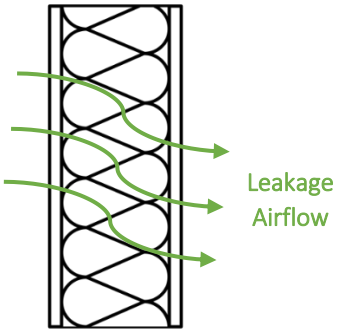

Dynamic Construction

- Coupling of conduction and air leakage flow heat transfers, with infiltration heat recovery (IHR) effect.
  - With Dynamic Insulation EMS model

The **ventilation strategy** also considers two aspects, the ventilation regime and the sizing factor of the mechanical ventilation, if any. The former considers ventilation systems of increasing intrusiveness on the heritage building, and assesses their potential at building performance improvements. The latter considers the significance of over-sizing the mechanical ventilation system, if any, for the dynamic operation of the construction instead of the normal ventilation-based sizing.

Ventilation Regime

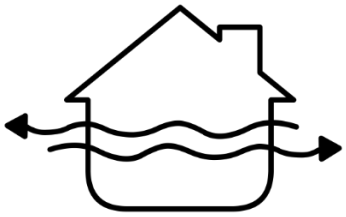

Natural Ventilation

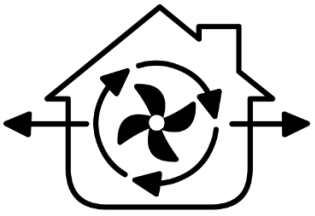

Local Exhaust Fans

- On All Year
- On Heating Season

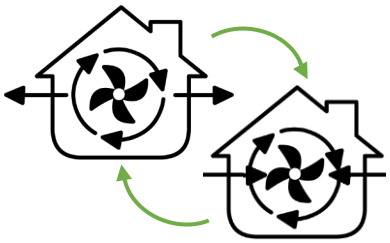

Local Reversible Fans

- Exhaust On Heating Season & Supply On Cooling Season

Ventilation Strategy

Sizing Factor of the Mechanical Fans

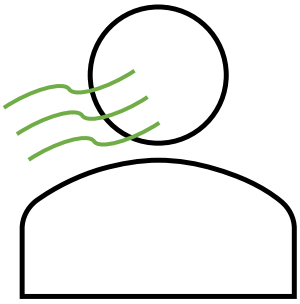

Ventilation-based Flowrate

- Local fans, if any, are sized to meet the minimum ventilation demand
  - Fans have normal operations, without oversizing for a cohesive under-pressurization of the building

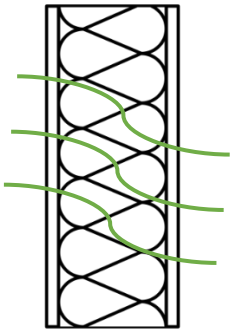

IHR-based Flowrate

- Local fans, if any, are sized to meet the needed flow for optimal IHR effect
  - Fans have special operations, with oversizing for cohesive under-pressurization of the building

4.2. Comparative Reference Cases

In an aim to situate their performance in the specific context of this research, the explored retrofit alternatives are compared against 3 main reference scenarios.
The assessment of each alternative is based on its achieved overall performance improvement from the base case (BC and BRC). This improvement is weighed against the improvement achieved by the conventional retrofit case, which is regarded as the benchmark for retrofitting enhancements.

The 3 reference scenarios, described below, are evaluated under both static and dynamic construction conditions for a fair comparison with the studied static and dynamic retrofit analyses:

Base Case [BC]

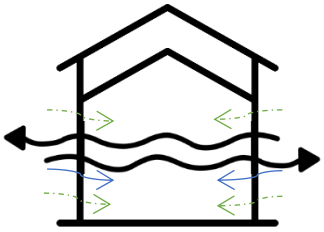

No retrofit measures

- Airtightness:
  - Base Case crack template (Refer to Table 44)
- Insulation:
  - No Wall Insulation
  - Base Case roof rockwool insulation
    40mm pitched roof
    40mm flat roof
- Ventilation Regime:
  - Natural Ventilation

Base Retrofit Case [BRC]

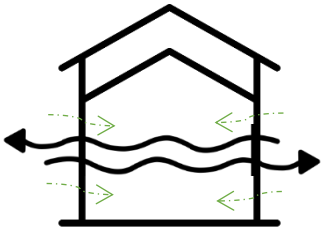

Sealing of concentrated air leakages

- Airtightness:
  - Retrofit crack template (Refer to Table 45)
- Insulation:
  - No Wall Insulation
  - Base Case roof rockwool insulation
    40mm pitched roof
    40mm flat roof
- Ventilation Regime:
  - Natural Ventilation

Conventional Retrofit Case [CRC]

Conventional retrofit measures

- Airtightness:
  - Airtight crack template (Refer to Table 46)
- Insulation:
  - *150 mm rockwool wall insulation*
  - *300 mm rockwool pitched roof insulation*
  - *300 mm rockwool flat roof insulation*
- Ventilation Regime:
  - Balanced Mechanical Ventilation with Heat Recovery (MVHR)

The characteristics of the Base Case are established to accurately represent the Case Study Building, as outlined under Chapter 5. The crack templates of the reference scenarios were accordingly developed and calibrated against the in-situ air leakage measurements in the Case Study Building. These crack templates are the foundation of the building's air leakage model. Their detailed description is provided under Chapter 7.2.

For the sake of a fair comparison of the retrofit improvements achievable in heritage buildings of varying levels of protection, the Non-Insulated Construction scenarios are compared against an additional reference case, described on the right.

In case of heritage-protected interior surfaces, the CRC would not be an attainable reference. An alternative potentially attainable retrofit would then focus on achieving airtight surfaces without obscuring them with added insulation.

Non-Insulated Conventional Retrofit Case [NCRC]

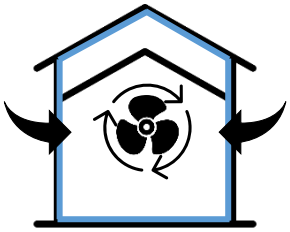

Conventional retrofit measures

- Airtightness:
  - Airtight crack template (Refer to Table 46)
- Insulation:
  - No Wall Insulation
  - Base Case roof rockwool insulation
    40mm pitched roof
    40mm flat roof
- Ventilation Regime:
  - Balanced Mechanical Ventilation with Heat Recovery (MVHR)

Additionally, both the MVHR and the Exhaust Fan ventilation systems consider a heat recovery on the exhaust air with an efficiency of 85%, typical of standard counter-flow plate heat exchangers. While the MVHR system returns the recovered energy directly to the conditioned space in the form of heat, the exhaust heat recovery system transfers the energy to other building systems, such as the DHW system. In both cases, the recovered energy entails savings on the building's total energy demand.

5. Case Study Building and Air Leakage Characterization

5.1. Case Study Building

The case study building, at Herengracht 15 in Leiden, was selected for its befitting characteristics to the scope of the study, as well as its suitability and availability for in-situ measurements.

Figure 15: Case Study Building

Accordingly, the building is a historic traditional single-family dwelling, with a solid wall brick masonry construction and a pitched clay-tiled roof. Built in 1750, it is registered as a National Monument and is thus subject to the associated monumental restrictions on its renovation works.

Although the building was already renovated twice, in the 1980's and the 2020's, the modifications made were found to not significantly alter the building's air leakage behavior.

- The insulation applied on some of the façades is all breathable rockwool insulation.
- The draught-proofing of glazed doors and windows employed a removable system: Instead of replacing the historic windows or directly draught-stripping them, a second draught-sealed internal window was installed, creating a sort of double-glazing system. Opening the second window would thus eliminate its sealing effect and, consequently, allow to measure the performance of the original openings.

In terms of layout, the building is comprised of three stories with an attic. It has 3 bedrooms, 2 workspaces, a kitchen, a dining room, and the ground floor presents an extension holding the living room. The detailed plans of the building may be referred to under Appendix A.

5.2. Fan-Pressurization and IR-Thermography Tests

The in-situ air leakage measurements consist of fan-pressurization and Infra-red thermography tests, conducted in multiple rounds based on a reductive sealing strategy.
The measurements were carried on June 2, 2023, between 9am and 4pm. The measurement conditions consider a rather dry day with little wind, and outside and inside temperatures of around 18°C and 21°C, respectively.

The aim of the measurements was, first, to characterize the building's air permeability. The results were then used for the validation of the power law coefficients (C) and exponents (n) characterizing its dynamic air leakage behavior at the component level (as shown in Chapter 2.2.3).
The adopted measurement approach indeed allows to identify the main air leakage pathways and quantify their individual contribution to the building's total air leakage.

Fan-Pressurization Test

The fan-pressurization test, also known as "blower door test", provides baseline air permeability characterization for existing buildings. Its basic principle consists in the mechanical pressurization and depressurization of the enclosed space using calibrated fans, while monitoring the fan's airflow and the pressure difference across the envelope (Refer to Figure 16).

Advantages of the method include its non-sensitivity to the environmental and climate conditions, and its compatibility with low-rise residential buildings (Salehi et al., 2017). It is a widely standardized method with prescribed best-practice guidelines (Berge, 2011; Doran et al., 2014; Gillott et al., 2016; Kölsch et al., 2019).

Its combination with thermographic measurements allows to identify air leakage pathway locations (Berge, 2011).
Other measurement methods, such as the tracer gas method, face greater limitations and sensitivities, and only measure air leakage rather than air permeability (Gillott et al., 2016).

The fan-pressurization measurements were conducted using a *Retrotec5000* Blower Door Set, in accordance with the NEN 2686 and NEN-EN 13829 standards.

The blower door was set up in the dwelling's front door opening. Throughout the measurements, all ventilation facilities (i.e. vents and extraction hoods) were sealed, all external openings were closed, and all internal doors were open. Adjacent building leakage is, however, integral to the results.
The building's characteristic air leakage data was taken as the average of the pressurization and depressurization results for each round of measurements.

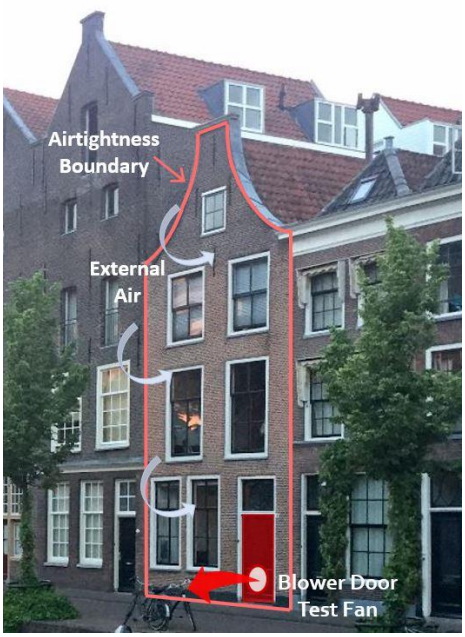

Figure 16: Fan-pressurization Test Setup

Infra-Red (IR) Thermography Imaging

The infra-red thermography, or IR thermography, provides visual evidence of leakage pathways in the building's envelope. It is based upon a thermal imager that detects the surface's thermal radiation, converts it into its temperature, and displays the resulting temperature distribution as a color gradient on a thermal image.

Figure 17 presents an example of thermal image taken in the building. The red and yellow colors show higher temperatures, while the green and blue colors are lower temperatures. The temperature range, however, varies for each situation.

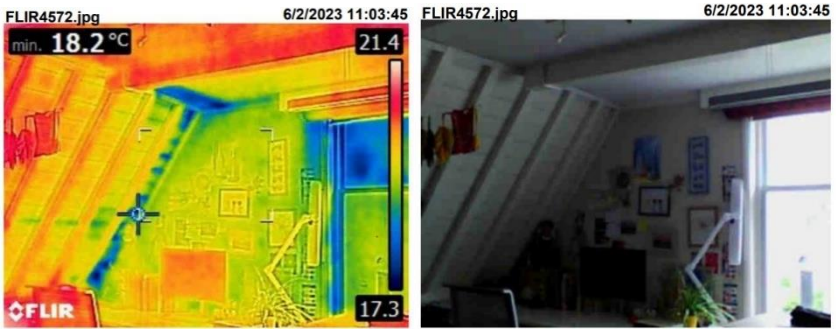

Figure 17: IR Thermography Images from In-situ Measurements

Observed temperature anomalies identify potential leakage locations. This is, however, dependent on the existence of a measurable indoor-outdoor temperature difference, and is restricted by the inability to distinguish anomalies resulting from air leakage and thermal bridges (Berge, 2011).

The measurements were conducted in parallel with the fan-pressurization test using a *FLIR E8* thermographic camera, in accordance with the NEN-EN 13187 standard. The images were taken from inside the building while it was depressurized, making leakage pathways detectable.

Reductive Sealing Measurement Strategy

The reductive sealing strategy consists in conducting the air leakage measurements in multiple rounds. Starting with the base case, additional components in the envelope are progressively sealed with each new round. The difference in the air leakage measured between two consecutive rounds is then attributed to the sealed component. The more reductive sealing rounds are taken, the more detailed the picture of the air leakage's distribution over the building envelope (Stephen, 1998).

The reductive sealing strategy provides the ability to identify the air leakage pathways and quantify their contribution to the building's total leakage. Although very informative, these measurements push the resolution of the fan-pressurization apparatus to its limits and may not be perfectly accurate.

The measurements at the Herengracht 15 dwelling were carried in **4 reductive sealing rounds**, specified on the right.

The components sealed at each round are identified by examining the envelope for potential leakage pathways in the previous rounds. These were identifiable as detectable draughts and/or clear temperature anomalies on the thermographic images.

Due to missing data and inconclusive results, the **Round 4** was disregarded in the analysis.

Round 1: Base Case
with the inner draught-proofed windows, the living room's plenum hatch, and loft hatch open

Round 2: Sealing of windows and glazed doors
with the living room's plenum hatch and loft hatch open

Round 3: Closing and sealing of the living room's plenum hatch.
with the loft hatch open

Round 4: Closing and sealing of the loft hatch.

The fan pressurization measurements' outcomes are summarized in the Chapter 5.3. below, and the estimated components' air leakage contributions are displayed in the Chapter 5.4.
Detailed air leakage characterization information for both the building and its components may be referred to in Appendix B and C, respectively.

5.3. Building Air Leakage Characterization Results

The fan pressurization results consist of a set of paired leakage flow and pressure gradient measurements, under both pressurization and depressurization conditions. The resulting data are processed to characterize the building's air leakage properties, as detailed under Appendix B.

The final power law equations characterizing the building's air leakage under each reductive sealing rounds are summarized in Figure 18. They describe how the air leakage flowrate varies with the pressure gradients across the envelope in the base case (Round 1), with the openings sealed (Round 2), and with both the openings and the living room's plenum hatch sealed (Round 3).

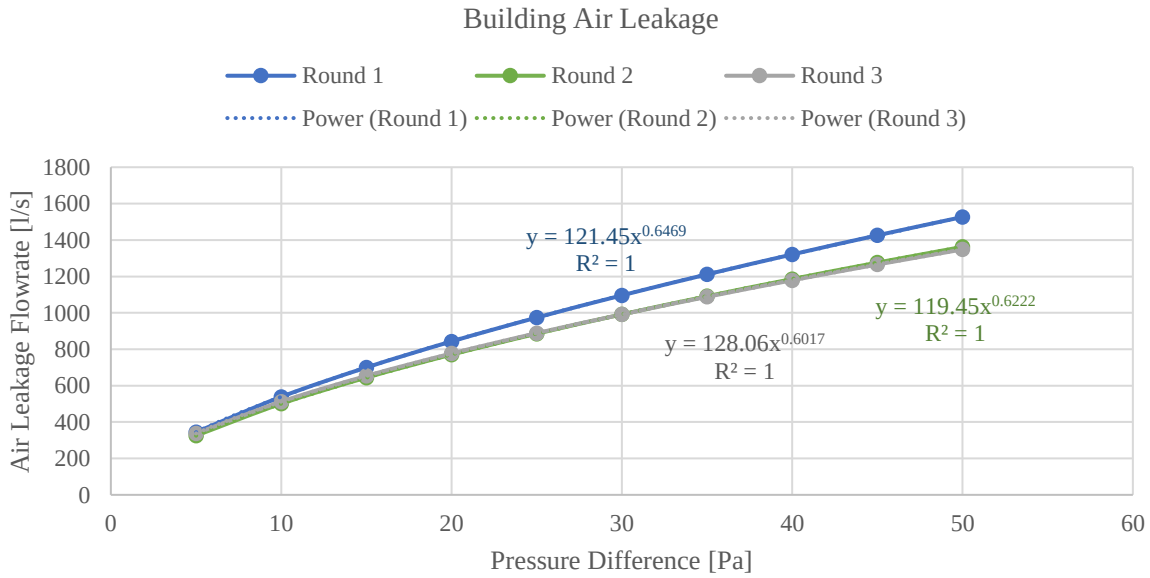

Figure 18: Building Air Leakage Characteristic Power Law Equations

Given the close alignment of the Round 2 and 3 results, it is reasonable to infer that the living room hatch's leakage fails to meet the measurement apparatus' detection threshold. This could justify it as negligible. This is, however, further explored in the components' air leakage characterization below.

5.4. Components' Air Leakage Characterization Results

The reductive sealing measurement approach helps quantify the individual air leakage pathways' contribution to the building's total air leakage. The contribution of the sealed components is estimated as the difference in the measured flows between consecutive rounds, as detailed under Appendix C.

The components' air leakage characterization generates their individual power law equations. Given the negligeable contribution of the living room's plenum hatch (as detailed under Appendix C), the building's total measured air leakage is divided between the openings' concentrated leakage (windows & doors) and envelope surfaces' diffuse leakage (walls & roofs). Each component's contribution is then normalized by their respective perimeter length or surface area.
Final, non-normalized and normalized, results are displayed in the following graphs (Refer to Figures 19 and 20, respectively).

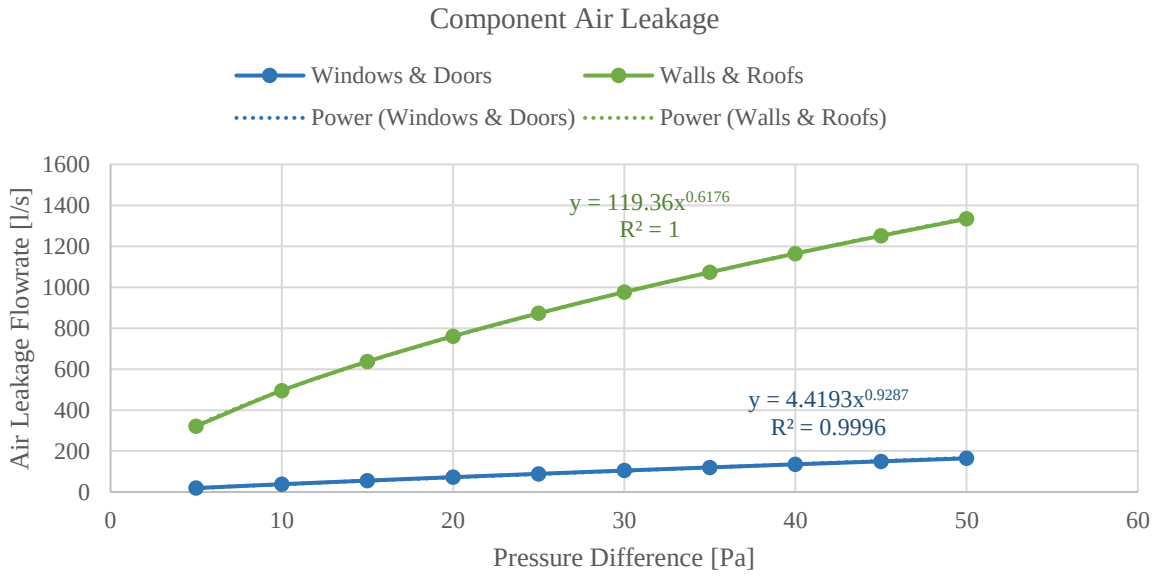

Figure 19: Component Air Leakage Characteristic Non-normalized Power Law Equations

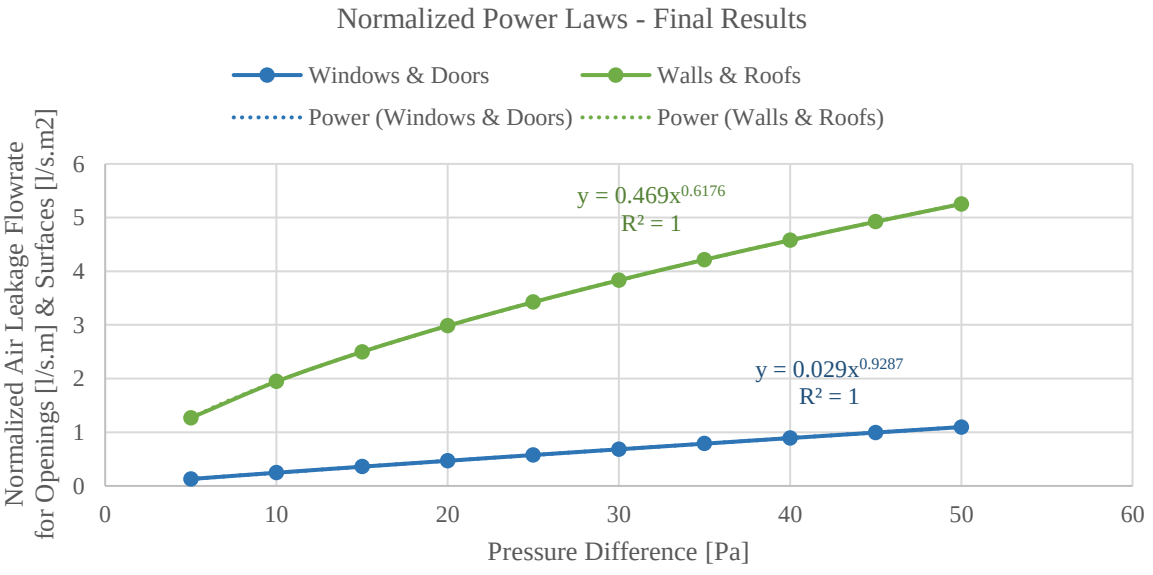

Figure 20: Component Air Leakage Characteristic Normalized Power Law Equations

6. Building Performance Evaluation Framework

6.1. Building Performance Parameters and Criteria

The building's post-retrofit performance addresses the trade-off between its **energy-efficiency** and its **indoor health and comfort**.

Energy-efficiency considers a single evaluation parameter, while the building's indoor health and comfort is typically associated with respect to 5 parameters, shown below.
Although lighting and acoustics present important criteria for a building's overall performance, only the first three parameters for indoor health and comfort are of interest within the scope of this research, due to their direct association with the building's airtightness and ventilation performance.

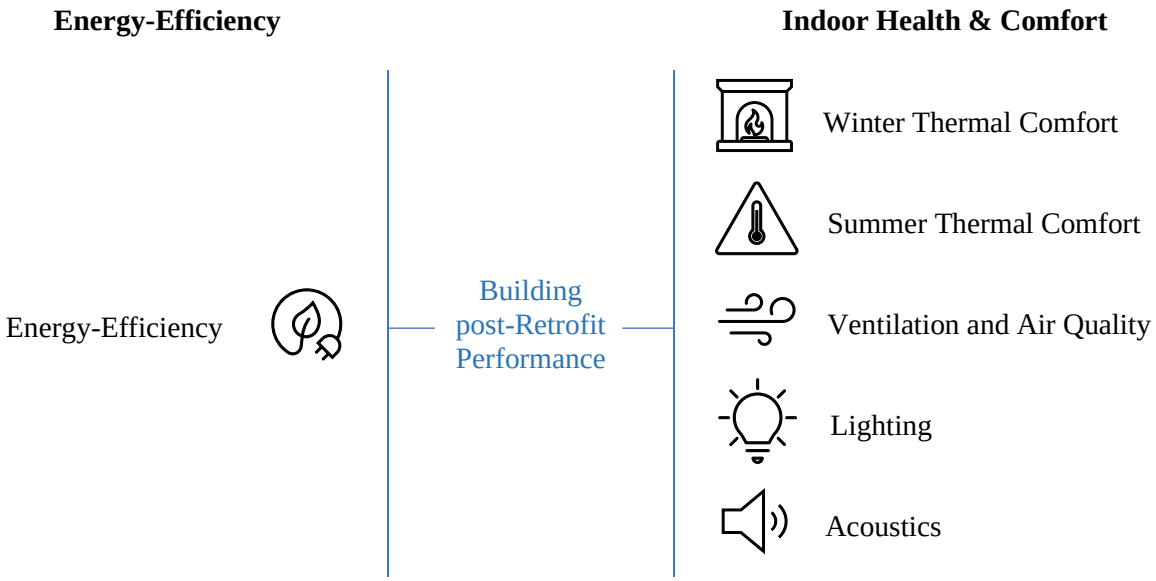

Figure 21: Building Performance Parameters

The assessment of the building's post-retrofit performance with respect to the relevant evaluation parameters must be based on clearly defined criteria.

6.2. Energy-Efficiency

A building's energy performance may be assessed based on different energy quantities. These quantities are distinguished by their position on the building' energy chain and their end-purposes, as detailed in the following scheme (Refer to Figure 22).

The study's scope is concerned with the post-retrofit performance of buildings under different airtightness and ventilation strategies. The building's energy-efficiency then relates to its performance at the final energy use level. The energy-efficiency evaluation criteria are then based on the building-related energy demand.

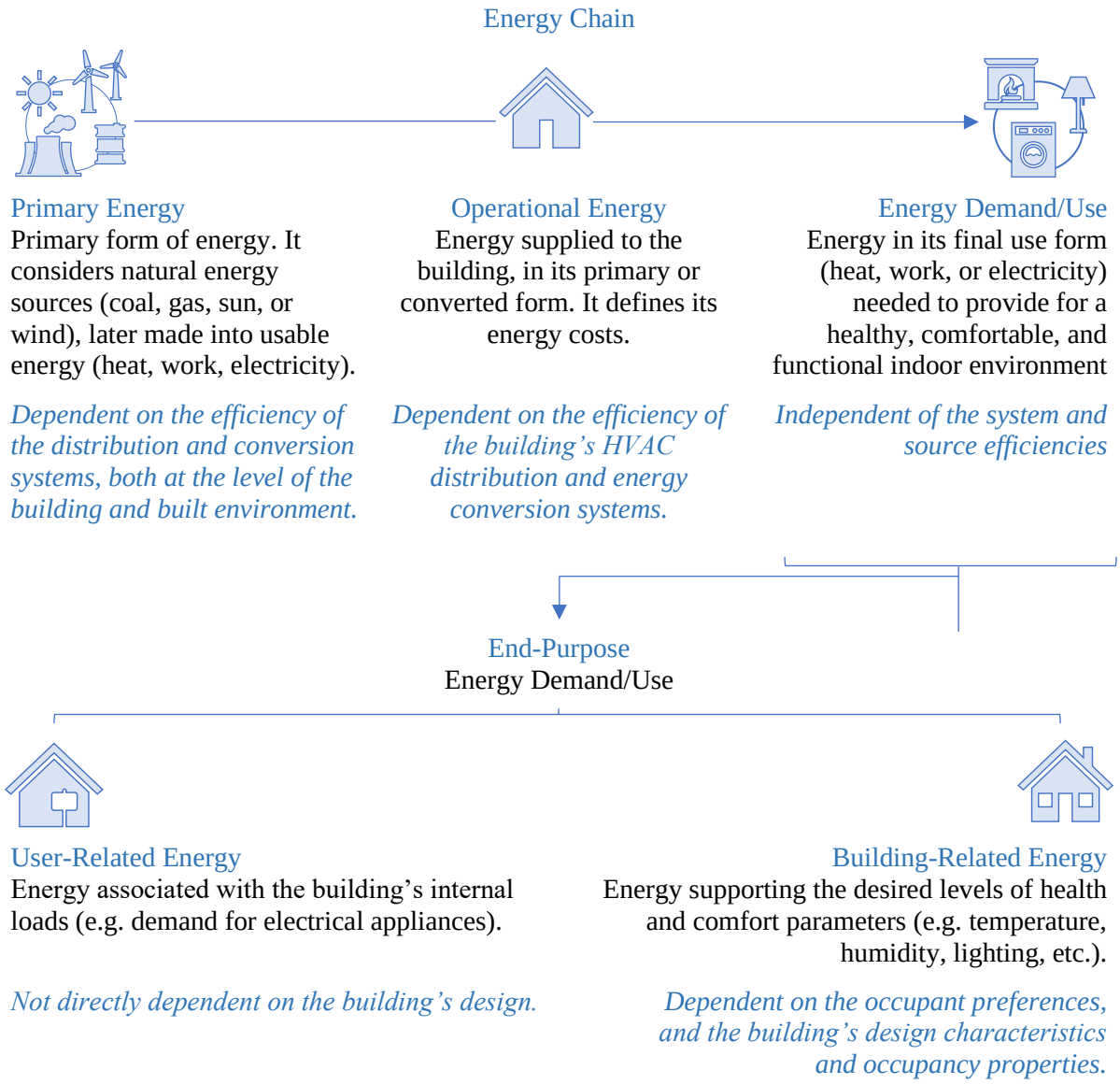

Figure 22: Categorization of Buildings' Energy Quantities

Considering heat recovery on the exhaust air, the net energy demand is defined as:

$$E_{net} = E_{total} - \eta_{HR} \times E_{exhaust}$$

E_{net} – net annual energy demand [kWh]
E_{total} – total annual energy demand [kWh]
η_{HR} – exhaust air heat recovery efficiency [-]
$E_{exhaust}$- exhaust air annual heat loss [kWh]

with:

$$E_{total} = E_{ideal} + E_{vent} + E_{internal}$$

E_{ideal} – annual ideal heating demand [kWh]
E_{vent} – annual ventilation energy demand [kWh]
$E_{internal}$ – annual internal energy demand (incl. electricity, lighting, appliances, DHW) [kWh]

The building's estimated energy consumption is then to be minimized as practically possible.

Table 6: Energy-Efficiency Evaluation Criteria

Building-Related Energy Demand Criteria	Annual Heating Demand 〉Minimize Annual Ventilation Demand 〉Minimize

6.3.Indoor Health and Comfort

The indoor health & comfort criteria consider a classification of the building performance into IEQ categories. This classification (Refer to Table 7) is inspired by the EN 16798 standard (European Committee for Standardization, 2019b), for building energy and comfort evaluation.

Table 7: Building IEQ Performance Categories (EN 16798)

IEQ Categories	Expectation Level	
IEQ I	High	〉For occupants with special needs (elderly, children, etc.)
IEQ II	Medium	〉For normal design and operations
IEQ III	Moderate	〉For an acceptable environment, with risk of reduced occupants' performance
IEQ IV	Low	〉For short times of occupancy only

As per the standard, the target IEQ category for normal design and operation is at least an IEQ II. The current analysis is, however, a comparative analysis. The focus is to evaluate the prospects of a dynamic insulation-based retrofit strategy in achieving higher IEQ levels than the base case and conventional retrofit strategy.

An equivalent weighted performance score is then defined to quantify the distribution of the building's annual performance over the above IEQ categories, based on the hourly score weights presented in Table 8.

Table 8: IEQ Categories' hourly score weights

IEQ Categories	Hourly Weight
IEQ I	+2
IEQ II	+1
IEQ III	0
IEQ IV	-2

For each of the IEQ evaluation parameter, the weighted score is therefore computed as:

$$S_{IEQ_p} = \sum_i n_i \times W_{IEQ_i}$$

S_{IEQ_p} - weighted IEQ score for parameter p [hr]
n_i – number of hours in IEQ category i [hr]
W_{IEQ_i} – hourly weight of IEQ category i [-]

The classification of the building's hourly performance to its corresponding IEQ category is based upon a set of criteria for each of the evaluated IEQ parameters, as referenced in the EN 16798 standard and detailed in the sub-chapters below.

Considering all relevant IEQ parameters and their corresponding scores, the building's overall health and comfort performance is to be improved as practically as possible.

Table 9: IEQ Evaluation Criteria

Building IEQ Criteria	Winter Thermal Comfort Score 〉Maximize Summer Thermal Comfort Score 〉Maximize Ventilation & IAQ Score 〉Maximize Indoor Humidity Score 〉Maximize

Thermal Comfort

Thermal comfort is the "state of mind that expresses satisfaction with the thermal environment" – as per the ISO 7730 (International Organization for Standardization, 2005). As the occupant expectations of the thermal environment differ under different contexts, thermal comfort is a subjective performance aspect (Ortiz & Bluyssen, 2022).
It may, however, be expressed through a set of observable parameters, specified below. While the last two depend on the occupant, the remaining parameters are characteristic of the thermal environment.

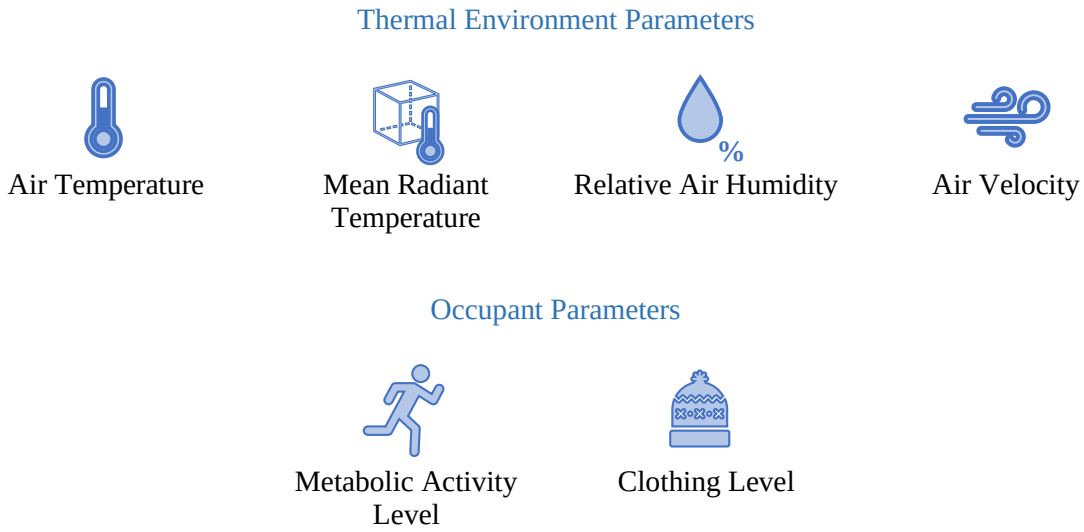

Figure 23: Thermal Comfort's Component Parameters

Accordingly, the thermal comfort performance may be evaluated with respect to both objective and subjective criteria, depending on the building's operation.

Mechanical heating and/or cooling

In mechanically heated and/or cooled buildings, the thermal environment's objective and subjective criteria consider its operative temperatures and PMV-PPD indices, respectively.

Comfortable operative temperature ranges are defined to achieve the same comfort levels set by the PMV-PPD limits.
Operative temperature limits, however, assume a set combination of clothing and activity levels, relative humidity, and air velocity. They must then be adjusted when such conditions differ.

No mechanical heating and/or cooling

In buildings with no mechanical cooling systems (as in most of Central and Northern Europe), the indoor thermal conditions are primarily regulated by the occupants.

In residential buildings, occupant adaptation opportunities are relatively wide. They address the occupant's metabolism, clothing, as well as the indoor temperatures.

The thermal environment's performance may then only be assessed subjectively.
Adaptive comfort criteria are characterize the summer and shoulder seasons. The comfortable indoor operative temperature ranges are a function of the outdoor running mean temperature and are, therefore, dynamic.

Winter Thermal Comfort

Considering mechanical heating during the heating season, assumed to extend between October and April, winter thermal comfort considers either the objective or subjective criteria in defining the IEQ categories.
Such criteria are detailed in Table 10.

Table 10: Winter Thermal Comfort's Evaluation Criteria (EN 16798)

IEQ Categories	Operative Temperature Criteria *Objective*	PMV-PPD Criteria *Subjective*	
	Temperature Range [°C]	PPD [%]	PMV [-]
IEQ I	21 – 25	< 6	[-0.2; 0.2]
IEQ II	20 – 25	< 10	[-0.5; 0.5]
IEQ III	18 – 25	< 15	[-0.7; 0.7]
IEQ IV	16 – 25	< 25	[-1; 1]

The objective and subjective criteria being equivalent for an assumed sedentary activity level (1.2MET) and winter clothing level (1.0 clo), the objective operative temperature limits are adopted in the building performance assessment for their relatively lower computation complexity and costs.

Summer Thermal Comfort

As the building is not mechanically-cooled, an adaptive comfort model is applicable over the summer and shoulder seasons. The subjective thermal comfort criteria then consider a dynamic comfortable operative temperature, defined as a function of the outdoor running mean temperature.
The dynamic adaptive criteria are plotted in Figure 24.

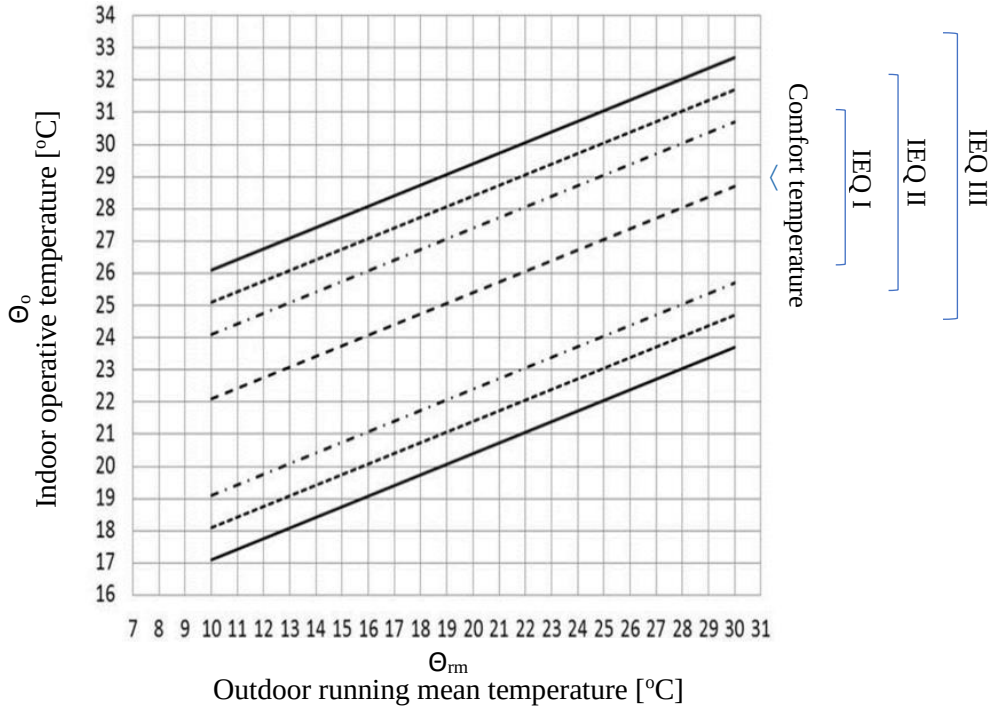

Figure 24: Adaptive Summer Thermal Comfort Evaluation Criteria (EN 16798)

Ventilation & Indoor Air Quality

The discomfort and health implications of indoor air pollution, substantiated by wide scientific evidence, bring about criteria characterizing the building's indoor air quality (IAQ). The main priority is ensuring a healthy and comfortable indoor environment, followed by preventing building damage from excess moisture.

Indoor Air Pollution & Ventilation

Indoor air pollution sources often being predominant in residential buildings, source control and ventilation constitute primary IAQ control and improvement strategies – as per the CEN/TR 16798 – 2: 2019 (European Committee for Standardization, 2019a). In the absence of a common standard IAQ index, the health & comfort (or perceived) criteria typically address ventilation levels and CO_2 concentration limits.
Such criteria are detailed in Table 11.

Table 11: Indoor Air Pollution & Ventilation Evaluation Criteria (EN 16798)

IEQ Categories	Ventilation Rate Criteria *Objective*		CO_2 Concentration Criteria *Subjective*
	q_v [l/s.m^2]	ACH [hr^{-1}]	ΔCO_2 [ppm]
IEQ I	0.49	0.7	550
IEQ II	0.42	0.6	800
IEQ III	0.35	0.5	1350
IEQ IV	0.23	0.4	1350

Often misinterpreted, the CO_2 concentration limits do not consider the effects of the pollutant itself, but rather interpret it as an indicator of bio-effluents and body odor (American Society of Heating, 2022; Ng et al., 2013). Although such indicator fails to account for occupant-independent contaminant sources, it still provides a tool for IAQ assessment on the basis of the tracer gas concepts. Its accuracy as an outdoor air ventilation criterion is, however, dependent on the accuracy of the input values and the validity of various assumptions regarding the building's function, occupant density, and indoor emissions (American Society of Heating, 2022).

Evaluating the building's total ventilation inclusive of the infiltration, the ACH criterion is then adopted for the IAQ performance assessment to ensure the reliability and computational efficiency of the results.

Humidity

The indoor environment's humidity criteria are set to satisfy the thermal comfort and IAQ requirements, on the one hand, and the construction durability requirements (relating to risks of condensation, mold growth, etc.), on the other hand.

Such relative humidity criteria are detailed in the Table 12 (European Committee for Standardization, 2019b).

Table 12: Relative Humidity Evaluation Criteria (EN 16798)

IEQ Categories	Relative Humidity Criteria *Objective*	
	RH_{min} [%]	RH_{max} [%]
IEQ I	30	50
IEQ II	25	60
IEQ III	20	70

7. Building Performance Simulation (BPS) Model

The dynamic simulation's objective is to evaluate the building's energy-efficiency and IEQ performance under varying airtightness and ventilation scenarios, in an attempt to identify an optimal and minimally-intrusive retrofit strategy for monumental historic buildings.
The simulation model was based on a real case study building, the Herengracht 15 dwelling in Leiden (described under Chapter 5).

The simulation was run in EnergyPlus v23.1, a state-of-the-art open-source and cross-platform building energy simulation (BES) tool. It provides for the multi-zone airflow and energy modelling of buildings, and accounts for the dynamic aspects of the outdoor environment, internal loads, and occupant behavior and comfort (*EnergyPlus*, n.d.). Due to its lack of an integrated graphical user interface (GUI), the EnergyPlus simulation engine is combined with the DesignBuilder v7.2.0.032 tool. It comprises of an integrated 3D modeler for the in-depth analysis of building performances.

The implementation of DesignBuilder and EnergyPlus has been validated through various case studies (Baharavand et al., 2013; *EnergyPlus Validation Reports*, n.d.; Fathalian & Kargarsharifabad, 2018; Goia et al., 2018; Mateus et al., 2014; Ozdenefe et al., 2016; U.S. Department of Energy, 2023).

Although DesignBuilder is currently the most capable GUI to EnergyPlus, it integrates an older version (EnergyPlus v9.4), which does not hold the tools needed for the implementation of Dynamic Insulation into the building's energy performance analysis. Accordingly:

1. The model is built within the DesignBuilder modeling interface, with static insulation.
2. The EnergyPlus Input Data File (IDF) is extracted from DesignBuilder.
3. The IDF is converted from a v9.4 to a v23.1 file, using EnergyPlus IDF Version Updater.
4. The Dynamic Insulation model is coded manually into the EnergyPlus IDF text file.
5. The complete model, with Dynamic Insulation, is run directly in EnergyPlus.

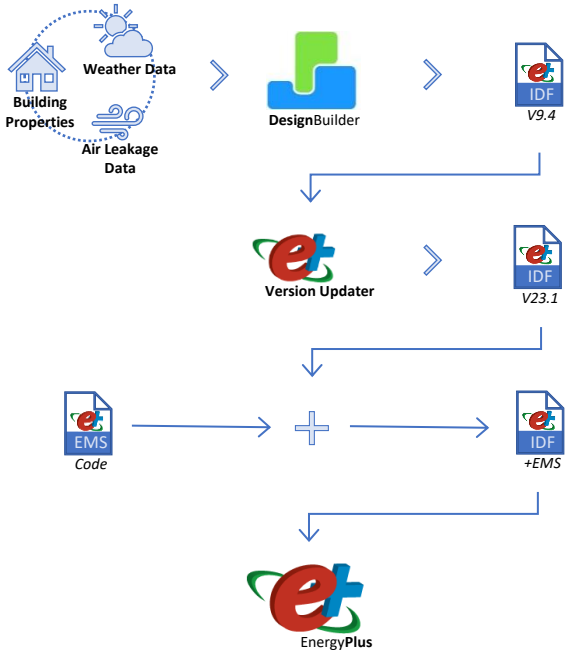

Figure 25: BPS Model Software Workflow

The simulation model was validated at two levels:

Air Leakage Model

The power law equations building's components air leakage (walls, roofs, windows, and doors) were validated against the air leakage rates resulting from the Fan-pressurization test (Refer to Chapter 7.2 and Appendix D).

Dynamic Insulation Model

The simulation's Dynamic Insulation (DI) model is based on a well-established analytical model. Its integration into the simulation tool was then validated, through a comparative analysis, against the existing analytical model (Refer to Chapter 7.3 and Appendix F).

7.1. Simulation Model Description

As per the case study building, the modeling object is a three-story historical row dwelling with a total floor area of 280 m^2, 245 m^2 of which are occupied living space (detailed plans are in Appendix A).

The building has a traditional construction of brick masonry solid walls and wooden roofs, with rockwool insulation and a vapor barrier. The ground floor is an on-ground concrete slab, insulated with expended clay ("argex") granules. Windows and skylights are double-glazed; the former have air cavities (U=2.7 W/m^2K) while the latter have argon-filled cavities (U=1.35 W/m^2K).
The main building has three floors, connected by a staircase shaft, and an attic with a pitched clay-tiled roof. The ground floor extension has a single floor, connected to the main building through a 1m-wide corridor, and a flat roof.

All envelope and system features are assumed uniform throughout the building. These include the envelope construction and treatments, the window types and glazing, the skylight types and glazing, and the HVAC systems.
The modeled house's living space is naturally-ventilated and mechanically heated via hydronic radiators; the attic is non-conditioned. No mechanical cooling is provided.
The building's heating setpoint is at 21°C, its natural ventilation setpoint is set at 24°C, and its internal loads and schedules are based on the EN 16798-1:2019 standard values (European Committee for Standardization, 2019b), and summarized in the Tables 13 and 14, respectively.

Table 13: BPS Model Inputs – Occupants & Internal Loads

Occupant Comfort

Density	Metabolic Rate		Metabolic Factor	Latent Fraction	Winter Clothing	Summer Clothing
[people/m2]	[MET]	[W/person]	[-]	[-]	[clo]	[clo]
0.0235	1.2	126	0.9	0.5	1	0.5

Internal Loads

Equipment		Lighting			Domestic Hot Water	
Power Density	Radiant Fraction	Power Density	Radiant Fraction	Illuminance	Consumption Rate	
[W/m2]	[-]	[W/m2]	[-]	[lux]	[l/p.day]	[l/m2.day]
2.4	0.2	7.5	0.42	150	73	1.718

Table 14: BPS Model Inputs - Occupancy Schedules

Occupancy Schedule

Weekday

Hour	1	2	3	4	5	6	7	8	9	10	11	12	13	14	15	16	17	18	19	20	21	22	23	24
Fraction	1						0.5			0.1				0.2			0.5			0.8			1	

Weekend

Hour	1	2	3	4	5	6	7	8	9	10	11	12	13	14	15	16	17	18	19	20	21	22	23	24
Fraction	1						0.8																1	

Equipment Schedule

All Week

Hour	1	2	3	4	5	6	7	8	9	10	11	12	13	14	15	16	17	18	19	20	21	22	23	24
Fraction	0.5							0.7		0.5		0.6				0.5		0.7			0.8		0.6	

Lighting Schedule

All Week

Hour	1	2	3	4	5	6	7	8	9	10	11	12	13	14	15	16	17	18	19	20	21	22	23	24
Fraction	0						0.15				0.05						0.2						0.15	

The simulation model combined the rooms on each floor into one zone. A separate zone was attributed to the ground floor extension, to account for its distinct features, and the attic, which is unoccupied and unconditioned. The model thus has a total of 5 zones, 4 occupied and 1 unoccupied.

As per the importance of environmental design for breathable constructions, the model considered the annual simulation of the building's performance in response to the local dynamic weather data. Set in the context of the Netherlands, the weather data for the building performance simulation are taken from Amsterdam's EPW file, acquired from the EnergyPlus Weather (EPW) map (*EPW Map*, n.d.).

7.2.Air Leakage Model

The building's air leakage is highly dependent on the interaction between the envelope's distribution of the pressure gradients and the air leakage pathways. If the leakage pathways distribution may be assumed static over a short-term period, the pressure gradient's distribution is dynamic and varies with the wind, stack, fan effects (Refer to Chapter 2.1.3).

In order to account for the combined effect of these factors on the air leakage, the BES models' leakage component is estimated using the integrated Airflow Network (AFN) of EnergyPlus.
The AFN estimates multi-zone pressures and airflows, including leakage and forced air flows, and their associated sensible and latent heat loads. These estimates consider:

- The dynamic wind and stack effect – based on the weather file data and building construction.
- The fan effect – based on the detailed HVAC definition, and specific fan flowrates and availability schedules.
- The air leakage path distribution – as Crack Templates, defining the power law coefficients (C) and exponents (n) of different building components (windows, doors, walls, and roofs).

The weather data are based on the Amsterdam EPW file. And the building's construction and HVAC were specified with respect to the case study's standardized properties for the base case and varied with the studied retrofit scenarios (Refer to Chapter 4).
Following the same logic, the base Crack Template was defined to be representative of the case study building's air leakage distribution, as characterized by the Blower Door Test (BDT) results (Refer to Chapters 5.3 and 5.4), and was only varied with the retrofit scenarios.

The BDT measurements give insight into the distribution of the air leakage between concentrated leaks from openings and diffuse leaks from envelope surfaces. However, the measured data lacks the information for a greater detailing of this distribution over the distinct building components.
To define a detailed Crack Template, the coefficients (C) and exponents (n) of the AIVC Guide 5 for Ventilation Modeling Data (Orme & Leksmono, 2002) were used, then calibrated and validated against the in-situ air leakage measurements (Under Chapters 5.3 and 5.4).

Detailed information about the Air Leakage Model's development and calibration may be referred to under Appendix D; while the detailed AIVC power law coefficients (C) and exponents (n) that underpinned the reference leakage estimates are outlined under the Appendix E.

The calibration process supports the compatibility of the AIVC estimates with the measured leakage flows through windows, doors, and wall surfaces, provided by a sufficient detailing of their specific types and treatments. But it also reveals a notable overestimation of the building's total leakage, attributed to the limited AIVC estimates for roof leakage and their failure to encompass the specific roof properties of the Case Study building.

The calibration results provide the definition the air leakage model, in the form of detailed Crack Templates for each of the building scenarios described below.

Blower Door Test	[BDT]	Reflects the Case Study building's conditions at the time of the blower door test measurements
Base Case	[BC]	Assumes the Case Study building's conditions prior to the 1980's and 2020's partial retrofits, considering all walls bare and the flat roof not sealed.
Base Retrofit Case	[BRC]	Defines the Case Study building's base leakage conditions for the developed retrofit strategies, by sealing concentrated leaks to prevent risks of draughts and by-passing of the DI system.
Conventional Retrofit Case	[CRC]	Defines the Case Study building's leakage conditions under the conventional "build tight-ventilate right" approach, assuming high airtightness of all envelope components.

The normalized power law equations characterizing each defined Crack Template are outlined in Figure 26. The corresponding airflows are expressed in **kg/s.m²** of surface area for surface leakages (walls, roofs, and floors), and in **kg/s.m** of perimeter for opening leakages (windows and doors).

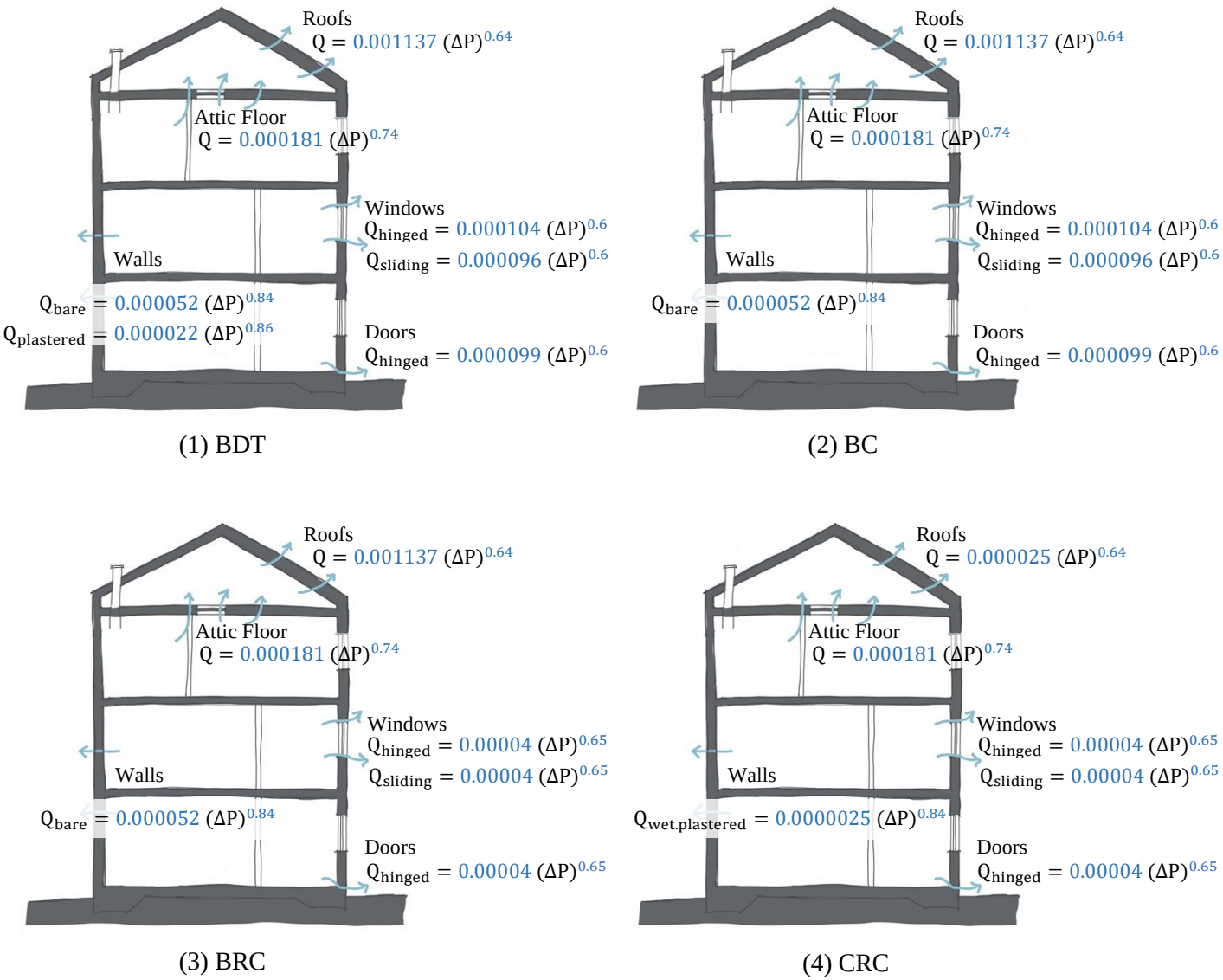

Figure 26: Air Leakage Model's Crack Templates

7.3. Dynamic Insulation Model

As per the basic principle of Breathing Wall (BW) dynamic insulations, the diffuse infiltration air recovers part or all of the conduction heat loss across the permeable construction due to the thermal interaction between the fluid and solid matrix.

A main limitation of the available building energy simulation (BES) tools is their reliance on the conventional decoupling of conduction and airflow heat transfers through the building envelope, as shown below (and detailed in Chapter 2.2.4), and their consequent failure in modeling the infiltration heat recovery (IHR) phenomenon characteristic of dynamic insulations' operations.

$$Q_{convention} = Q_{conduction} + Q_{leakage}$$

$$Q_{convention} = UA\,(T_i - T_o) + \dot{m}C_p(T_i - T_o)$$

Q – envelope energy flow [W]
U – construction thermal transmittance [W/m^2.K]
A – construction surface area [m^2]

Introducing this behavior into the building's energy and thermal balance thus requires the integration of a distinct analytical DI model into the BES tool.

Stand-alone DI Model

The plethora of models representing the behavior of Dynamic Insulations may be distinguished into two approaches, hereon referred to as the IHR and DI approach described below.

IHR Approach

- Defines an **IHR factor (f)** correcting the leakage heat load for the heat exchanged between the air and solid matrix.

$$Q_{IHR} = Q_{conduction} + Q_{leakage}$$

$$Q_{leakage} = (1 - f)\,\dot{m}C_p(T_i - T_o)$$

- All models are steady-state analytical models that correct the building's total annual energy demand, and often fail to consider the impact on the dynamic indoor environment (Solupe & Krarti, 2014).

〉 Steady-state analytical IHR models include:
  〉 *Anderlind Model (1985)*
  〉 *Claridge Model (1991)*
  〉 *Liu Model (1992)*
  〉 *LBNL Model (2000)*

DI Approach

- Defines a **Dynamic U-value (U_{dyn})** correcting the conduction heat flux for the heat recovered by the air leakage.

$$Q_{DI} = Q_{conduction} + Q_{leakage}$$

$$Q_{conduction} = U_{dyn}A_{inf}\,(T_i - T_o)$$

- Models are either steady-state analytical or transient numerical models.

〉 Steady-state analytical DI models include:
  〉 *Krarti Model* - (Krarti, 1994)
  〉 *Taylor Model* - (B. J. Taylor et al., 1996; B. J. Taylor & Imbabi, 1997).

〉 Transient numerical DI models include:
  〉 *Qiu Model* - (Qiu & Haghighat, 2007)
  〉 *Ascione Model* - (Ascione et al., 2015)
  〉 *Alongi Model* - Alongi et al., 2017)

- Annual simulations of the construction's transient state have been mainly addressed through numerical models. But analytical models coupled with dynamic BES tools, to account for the time-dependent regime, are found sufficiently accurate and allow a reduced computational effort.

The Taylor Model (B. J. Taylor et al., 1996) constitutes the most authoritative DI reference. It introduced the concept of dynamic U-value and defined it as a function of the air flow, density, and specific heat capacity, and the material's static thermal resistance (as shown in the equations below). Although it is a one-dimensional model developed upon the steady-state behavior of 3-layered building components, it is readily expandable to any number of layers. Its main simplification considers the neglection of the indoor and outdoor air film resistances, which would account for the variation of the surface temperature with the airflow through the wall. Nonetheless, the model was found valid for buildings with relatively low air change rates, such as dwellings, unlike sport centers and swimming pools (Alongi et al., 2017; B. J. Taylor et al., 1996; B. J. Taylor & Imbabi, 1997).

$$U_{dyn} = \frac{Pe}{R\,(e^{Pe} - 1)}$$

$+$

$$Pe = \frac{v \rho_a C_a L}{\lambda}$$

$\rangle$ $$U_{dyn} = \frac{v \rho_a C_a}{e^{v \rho_a C_a R} - 1}$$

U_{dyn} – dynamic U-value [W/m^{2}K]

v – air infiltration flow velocity [m/s]
ρ_a – air density – 1.204 kg/m^3
C_a – air specific heat capacity – 1006 J/kgK
L – material thickness [m]
λ – material static thermal conductivity [W/mK]

R – material static thermal resistance – L/λ [m^{2}K/W]

Based on Taylor's (1996) dynamic U-value, an equivalent dynamic thermal conductivity could be defined to act as a the time-variant building material property in the BES model (M. Imbabi & Elsarrag, n.d.; M. S.-E. Imbabi, 2012). The main limitation of this model representation is that it assumes a rather homogeneous spread of the diffuse air leakage and IHR effect on each envelope surface, which may not be guaranteed in existing buildings.

Considering that $U = \frac{1}{R}$

$\rangle$ $$R_{dyn} = \frac{e^{v \rho_a C_a R} - 1}{v \rho_a C_a}$$

And $R = \frac{L}{\lambda}$

$\rangle$ $$\lambda_{dyn} = \frac{v \rho_a C_a L}{e^{v \rho_a C_a L/\lambda} - 1}$$

R_{dyn} – dynamic thermal resistance [m^{2}K/W]
λ_{dyn} – dynamic thermal conductivity [W/mK]

v – air infiltration flow velocity [m/s]
ρ_a – air density – 1.204 kg/m^3
C_a – air specific heat capacity – 1006 J/kgK
L – material thickness [m]
λ – material static thermal conductivity [W/mK]
R – material static thermal resistance – L/λ [m^{2}K/W]

Integration of the DI and BES Model

The available literature on Dynamic Insulation (DI) seldom assists users on modeling dynamically-insulated elements in BES tools.
Despite the abundance of software tools simulating the building's energy and comfort performance, the majority were developed when the dynamicity of building systems and materials was not of major importance. They thus show limitations in the simulation of time-variant building parameters: the thermophysical properties of the materials are often not changeable during the simulation runs.

EnergyPlus provides more flexibility in that respect, based on its advanced control methods emulating a building's Energy Management System (EMS). The EMS allows coding custom supervisory algorithms into the simulation tool, to override selected aspects of the model's regular operations. This is possible through a set of sensors, control logics, and actuators, using a simplified programming language – the EnergyPlus Runtime Language (Erl).

EnergyPlus then parses and executes the defined Erl program during the simulation run. It then provides the possibility to model the dynamicity of building properties (Homem, 2017; U.S. Department of Energy, 2022).

Accordingly, at each timestep:

1. The BES generates the EnergyPlus output variables
2. Sensors extract the needed parameter values from the BES environment
3. The information provided by the sensors is processed by the user-defined control algorithm
4. The algorithm's output controls the actuator, setting its behavior by means of "IF" commands.
5. The resulting proposed action is then implemented by the actuator into the building model.

The EMS process is summarized in the Figure 27.

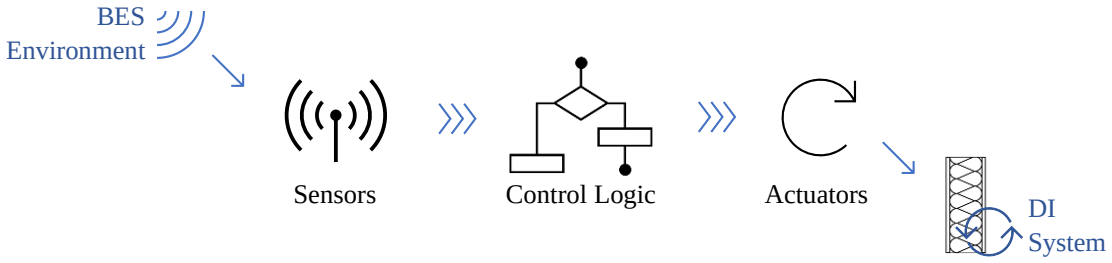

Figure 27: EnergyPlus' EMS Process for DI System Modelling

EnergyPlus' EMS provides two actuator functions for the modeling of different types of dynamic insulation. Both functions offer the possibility to modify a material layer's properties, but using different approaches. The two functions and their corresponding approaches are summarized in the following scheme (U.S. Department of Energy, 2022).

Surface Construction State Actuator

Actuates the properties of a building surface by replacing its whole construction with another pre-defined construction in the database.

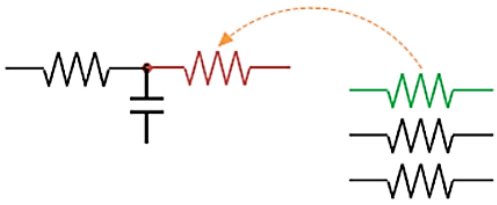

The red and green resistances are the constructions being removed and added, respectively (Homem, 2017).

Conduction Finite Difference (CondFD) Surface Material Layer Actuator

Actuates the properties of a building surface by controlling a specified material property of a layer in its construction.

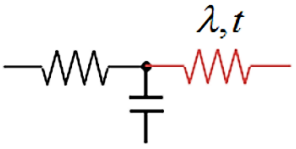

The red resistances are the elements having modfied thermo-physical properties (Homem, 2017).

For the purpose of modeling the breathing walls as having a conductivity varying with the leakage airflow through it, the CondFD Surface Material Layer actuator appears more fitting. Implementing the Surface Construction State actuator would require the creation of a constructions database covering all of the material's possible thermal conductivity values, which are indefinite in this case. This actuator is only efficient in case of a limited number of construction variants.

The CondFD Surface Material Layer actuator allows to compute the material's dynamic thermal conductivity during the simulation as a function of the airflow estimated by the model's integrated Airflow Network (AFN). It avoids the need to predict each surface's expected airflow range or limit the dynamicity of the material properties to a pre-defined set.

To the best of knowledge, there is no prior implementation of the Taylor's DI model in whole-building BES tools. The EnergyPlus EMS algorithm logic is described in the following flow-chart.

At each timestep, for all DI surfaces:

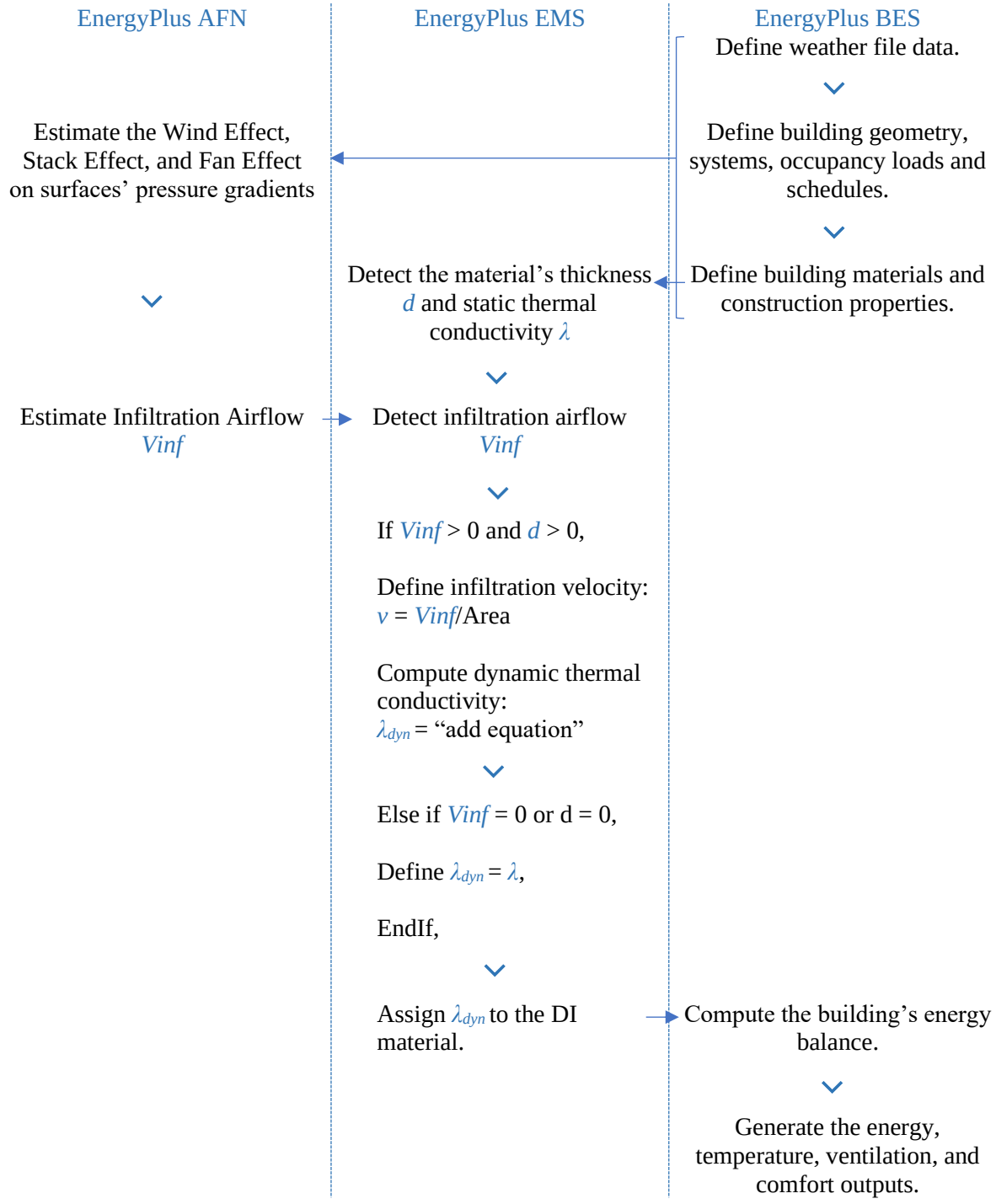

Figure 28: Flowchart of the EnergyPlus' EMS algorithm logic for DI System Modelling

Validation of EMS Model

The analytical Taylor model is a well-established model (Alongi et al., 2017). Its implementation into EnergyPlus' EMS, however, lacks validation.

To ensure the reliability of the EMS-integrated BES tool, the developed script was validated against the existing steady-state analytical model. Detailed information on the validation process and results can be found under Appendix F and G.

The results prove the validity of the DI model under different construction configurations:

Single-layered Constructions	Multi-layered Constructions without Air Gap	Multi-layered Constructions with Air Gap
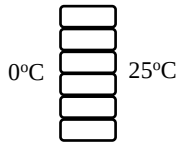	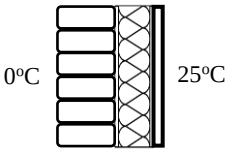	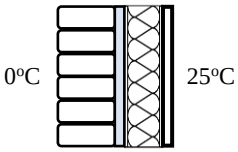

However, two key validity limitations and corresponding conditions are highlighted for the EMS Script's application on multi-layered constructions:

1. A validity limit on the air leakage flowrate – the flowrate must not exceed 0.008 $m^3/s.m^2$.
2. An incompatibility with constructions having "NoMass" materials, which are materials defined only by their thermal resistance – conventional material definition must be adopted for all dynamic constructions.

8. Conditioned Zone Boundary

8.1. Methodology

A sensitivity analysis (SA) is carried out to select the conditioned zone boundary configuration with higher potential for the preservation of the building's air permeability without hindering its energy-efficiency.

Sensitivity Analysis

Sensitivity Analysis (SA) refers to a set of statistical methods aiming to characterize, qualitatively or quantitatively, the influence of independent input variables on dependent output variables. It is a fundamental practice for the analysis of a model behavior under varying conditions (Saltelli et al., 2008), and may be carried for various purposes: to support, reduce, or calibrate model analyses, or to support decision making (Paleari et al., 2021).

SA methods are sorted into (Balesdent et al., 2016; R. Chen & Tsay, 2021; Menberg et al., 2016):

- Local Sensitivity Analysis (LSA)
  - 〉 Explore a reduced space of the independent variable inputs around a baseline
- Global Sensitivity Analysis (GSA)
  - 〉 Explore the whole domain of the independent variable inputs

Although both are widely implemented in Building Energy Performance (BEP) analysis, the GSA is considered more reliable and effective. Its higher computational cost is its only shortcoming against LSA (R. Chen & Tsay, 2021).
Characterizing the input variables' global influence, the GSA identifies the most influencial inputs and, consequently, the variables to be considered in the analysis (Balesdent et al., 2016).

GSA methods may be screening-based, regression-based, or variance-based (R. Chen & Tsay, 2021). A comprehensive overview of the methods used in BEP analysis, their theoretical frameworks and practical applications, is provided by Tian (2013) and Iooss & LeMaitre (2015), while Chen & Tsay (2021) and Menberg *et al.* (2016) present comparative analyses of the reliability of their sampling and assessment methods.

For building simulations, the correlation-based Pearson method and the standardized regression coefficient method provide the most reliable results (R. Chen & Tsay, 2021). The regression method is generally favored due to its moderate computational complexity and costs (Tian, 2013).

However, in case of computationally-intensive building simulations with larger parameter sets, the parameter-screening Morris Method (MM) is recommended for providing good compromise between accuracy and efficiency (R. Chen & Tsay, 2021; Menberg et al., 2016; Tian, 2013). Although significantly reducing the simulation time, the Morris Method is comparable to the computationally expensive methods, in terms of qualitative analysis and parameter ranking results (R. Chen & Tsay, 2021; Menberg et al., 2016; Tian, 2013).

Morris Method

The Morris Method (MM) is derived from the LSA method. It is based on an OAT (One-at-a-time) sampling approach with several paths of stepwise parameter changes, varying a single factor between consecutive runs.

It overcomes the LSA's limitations by varying the input variables over their entire definition domain, solving their partial derivatives and averaging the local measures to generate GSA information (Balesdent et al., 2016; Menberg et al., 2016; Wang & Ierapetritou, 2018).

The method ranks input variables based on their influence on the output, and identifies non-linearity and interactions with other input variables. However, it is unable to distinguish non-linearity from variables-interactions, which may be important in some analysis (Wang & Ierapetritou, 2018).

The Morris Method is based on the calculation of the Elementary Effect (EE) (Wang & Ierapetritou, 2018). The EE of the i[th] variable is given by:

$$EE_i = \frac{Y(x_1, \dots, x_{i-1}, x_i + \Delta_i, x_{i+1}, \dots, x_k) - Y(x_1, \dots, x_k)}{\Delta_i}$$

k – number of inputs
Δ_i – i[th] factor's step change
$(x_1, \dots, x_k)$ – base point
Y – model output

Based on the EE results, three sensitivity metrics are generated (Wang & Ierapetritou, 2018).

$\mu_i = \frac{1}{r}\sum_{j=1}^{r} EE_i^j$	μ_i – average of EE_i	〉 Reflects the input's individual sensitivity information 〉 Vulnerable when EE_i has different signs
$\sigma^2{}_i = \frac{1}{r}\sum_{j=1}^{r}(EE_i^j - \mu_i)^2$	$\sigma^2{}_i$ – variance of EE_i	〉 Reflects non-linearity and interaction in the input's effect
$\mu_i^* = \frac{1}{r}\sum_{j=1}^{r}\lvert EE_i^j \rvert$	μ_i^*- average of EE_i's absolute value	〉 Reflects the input's individual sensitivity information 〉 Not vulnerable when EE_i has different signs

The Morris Method's sampling cost is (Iooss & Lemaitre, 2015; Wang & Ierapetritou, 2018):

$$cost = R\ (k + 1)$$

R – number of trajectories, or radial base points. A value between 2 and 10 is recommended.
$(k + 1)$ – number of simulation locations per trajectory, or radial base point
k – number of input variables

The Morris Method is a qualitative method. It ranks the inputs in order of significance to the outputs, but fails to quantify the extent by which an input is more influential than another.
Inputs with large μ_i, $\sigma^2{}_i$, and/or μ_i^* values are classified as significant. While inputs with sensitivity metrics under 10% of the largest metrics are considered insignificant (Wang & Ierapetritou, 2018).

Sensitivity Analysis Runs

The intention behind the Sensitivity Analysis (SA) was determining the configuration with the greatest potential of preserving air leakage into the building's post-retrofit operations, without sacrificing its energy-efficiency.

For this purpose, the influence of the surface permeabilities on the building's energy demand was assessed for both loft configurations (i.e. warm loft and cold loft), under varying conditions. These considered two ventilation operation modes (with ventilation-based and IHR-based fan flowrates), under both static and dynamic construction behavior.

The building model was configured to emphasize the IHR effect, as to make any potential contribution detectable:

- The boundary surfaces are insulated with 200 mm rockwool layers (λ_s = 0.04 W/mK).
  - Although the IHR is a naturally-occurring phenomenon in any air permeable construction with diffuse leakage, Taylor *et al.* (1997) highlights that DI is most effective with inherently good insulating materials (low λ) and large thicknesses. Otherwise, higher air flows would be needed for the same DI performance.
- The building's ventilation is controlled with a continuously running exhaust fan
  - A reliable building depressurization in mild and variable climates is only possible using exhaust fans. In temperate climates, unlike in colder climates, the natural stack effect may not reliably meet the pressure requirements (B. Taylor & Imbabi, 1998).
  - Two scenarios are considered, distinguished by the exhaust fan's flow rate:

Normal Operations

- Sizing to the ventilation demand
  - Fan flowrate: 0.9 l/s.m^2 – minimum allowable ventilation for IAQ (*Bouwbesluit Online 2012*, n.d.).
  - Building under-pressure: 1-2 Pa

Under-pressure Operations

- Sizing to depressurize the building for full-infiltration leakage
  - Fan flowrate: 5.93 l/s.m^2.
  - Building under-pressure: 30 Pa – maximum allowable under-pressure for doors' operability and indoor comfort

The SA analysis for both exhaust scenarios is defined as follows:

Table 15: SA Analysis Settings

Algorithm Settings	
Method	Morris Method
Number of Independent Input Variables – k	3
Number of Dependent Output Variables – n	1
Initial Sample Size – R	10
Sample Size – R (k+1)	400
Scenarios	
Runs (under each mode of operation)	Run 1 – Cold Loft, Static Insulation Run 2 – Cold Loft, Dynamic Insulation Run 3 – Warm Loft, Static Insulation Run 4 – Warm Loft, Static Insulation
Variables	
Input Parameters (Independent Variables)	W – Walls' leakage coefficient (Runs 1-4) AF – Attic Floor's leakage coefficient (Runs 1-2) PR – Pitched Roof's leakage coefficient (Runs 3-4) FR – Flat Roof's leakage coefficient (Runs 1-4)
Output (Dependent Variable)	Building's Annual Energy Demand

The parameter range of the input variables encompass virtually all achievable values for the considered type of construction under different types and levels of finishing, retrofitting, or replacement. These values are identified based on the results of the Meta-analysis on building components' airtightness (Prignon et al., 2021), and summarized in Table 16.

Table 16: Sensitivity Analysis Input Definition - Surface Permeability

Input	Range [kg/s.m^2]	Steps	Values [kg/s.m^2]
W	[0.000001, 0.0004]	21	0.000001, 0.0000025, 0.000005, 0.0000075, 0.00001, 0.000025, 0.00005, 0.000075, 0.0001, 0.000125, 0.00015, 0.000175, 0.0002, 0.000225, 0.00025, 0.000275, 0.0003, 0.000325, 0.00035, 0.000375, 0.0004
AF, PR, FR	[0.00001, 0.004]	21	0.00001, 0.000025, 0.00005, 0.000075, 0.0001, 0.00025, 0.0005, 0.00075, 0.001, 0.00125, 0.0015, 0.00175, 0.002, 0.00225, 0.0025, 0.00275, 0.003, 0.00325, 0.0035, 0.00375, 0.004

8.2. Results

The complete SA analysis took a total of 32 calculation hours to run. Each of the 8 scenarios takes 4 calculation hours, with a single iteration's average duration of 1 hour for 10 simultaneous simulations.

The Sensitivity Analyses' results consisted of Morris Method's 3 sensitivity metrics (μ, σ^2, and/or μ^*), as defined under Chapter 8.1 above. The complete analysis' results are summarized in the Tables 17 and 18 for normal and under-pressure operations, respectively.

The graphical representation proposed by Morris to show each input's importance considered a two-dimensional plot of EE's mean (μ^*) and standard deviation (σ). Inputs with both low values (lower left corner) are the least-influential inputs, while inputs with both high values (upper right corner) are the most influential (Tian, 2013).
The resulting Morris metrics and corresponding graphical representation are thus shown below for both normal and under-pressure operations (Refer to Figures 29 and 34, respectively).

As per the definition of the μ and μ^* metrics, their relative values highlight the nature of the relationship between each input variable and the dependent energy demand in each run. This reveals potential changes in such relationships as a result of the construction dynamicity.
The relative μ and μ^* values for each input variable under static and dynamic construction conditions are then compared for normal (Figures 30 and 32) and under-pressure operations (Figures 35 and 37).

Also, the inputs with metrics smaller than 10% of the largest metric may, in practice, be considered insignificant (Wang & Ierapetritou, 2018).
The comparison of the input metrics and their relative significance may then be inferred from the below charts for normal (Figures 31 and 33) and under-pressure operations (Figures 36 and 38).

Normal Operations (1-2Pa)

Table 17: Sensitivity Analysis' Comprehensive Results – Normal Operations

Cold Loft

Input Parameter	Static Insulation				Dynamic Insulation			
	Run 1				Run 2			
	μ	μ^*	c	%	μ	μ^*	σ	%
W	5055	5055	448.9	**25.61**	3943	3943	1141	**20.02**
AF	19740	19740	2537	**100.00**	19700	19700	3340	**100.00**
FR	5990	5990	1776	**30.34**	6048	6048	1178	**30.70**

Warm Loft

Input Parameter	Static Insulation				Dynamic Insulation			
	Run 3				Run 4			
	μ	μ^*	σ	%	μ	μ^*	σ	%
W	5761	5761	1893	**9.22**	4294	4294	973.3	**6.79**
PR	62520	62520	29090	**100.00**	63200	63200	27800	**100.00**
FR	14270	14270	7557	**22.83**	12210	12210	5608	**19.32**

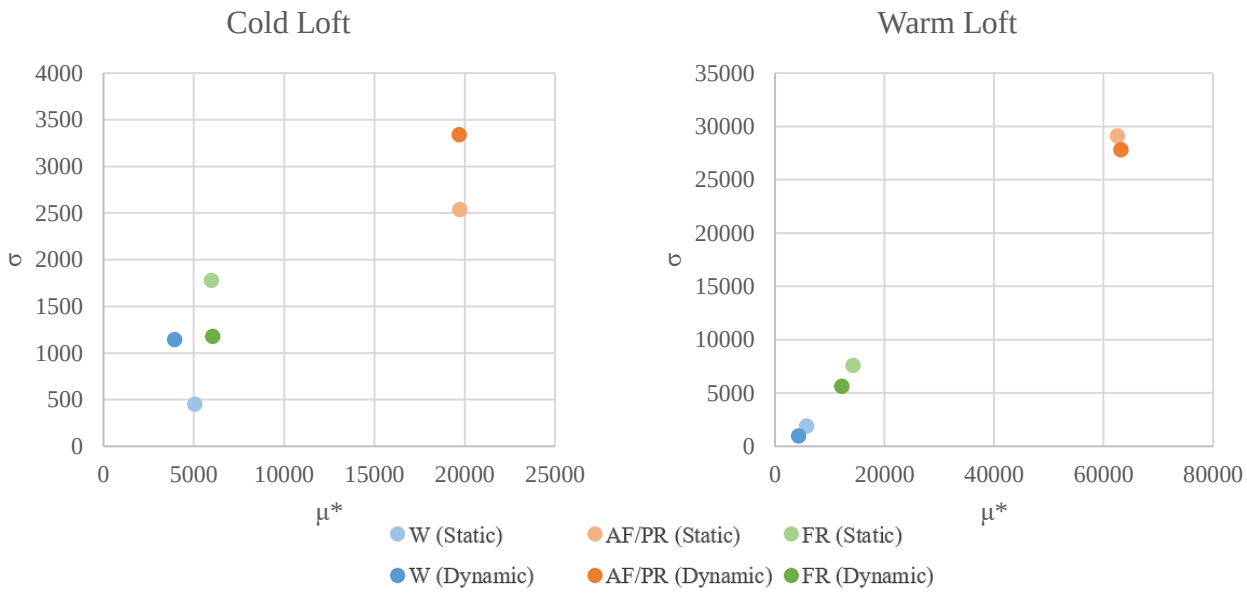

Figure 29: Morris SA Metrics' Plot – Normal Operations

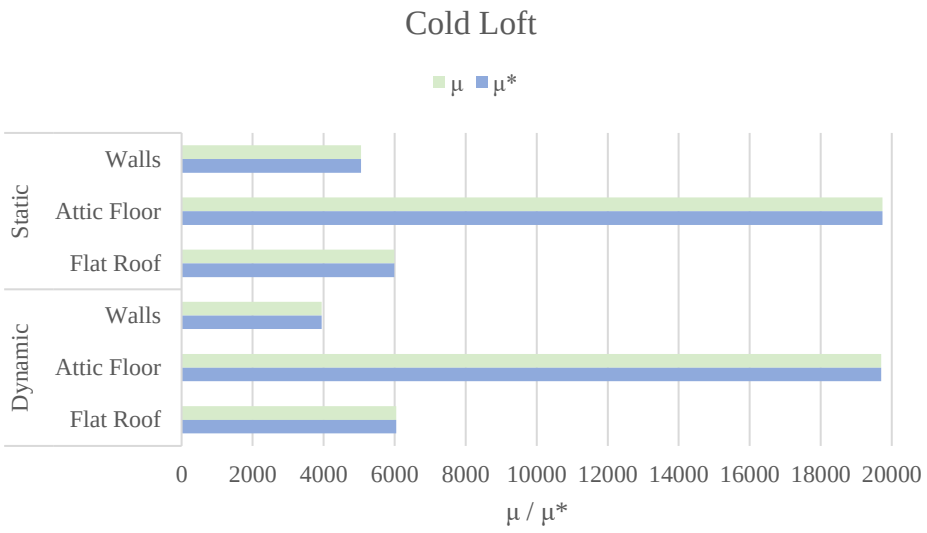

Figure 30: Morris SA Metrics (μ/μ*) under Cold Loft Case – Normal Operations

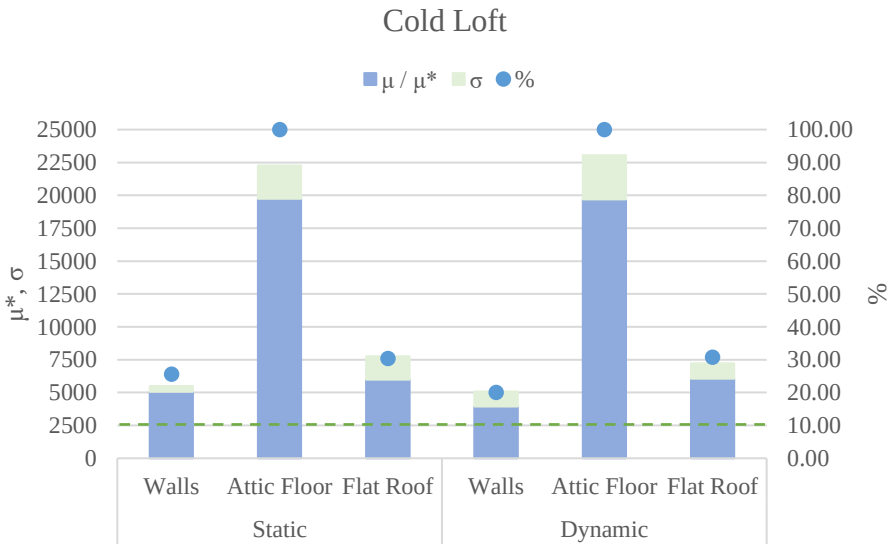

Figure 31: Morris SA Metrics' Significance under Cold Loft Case – Normal Operations

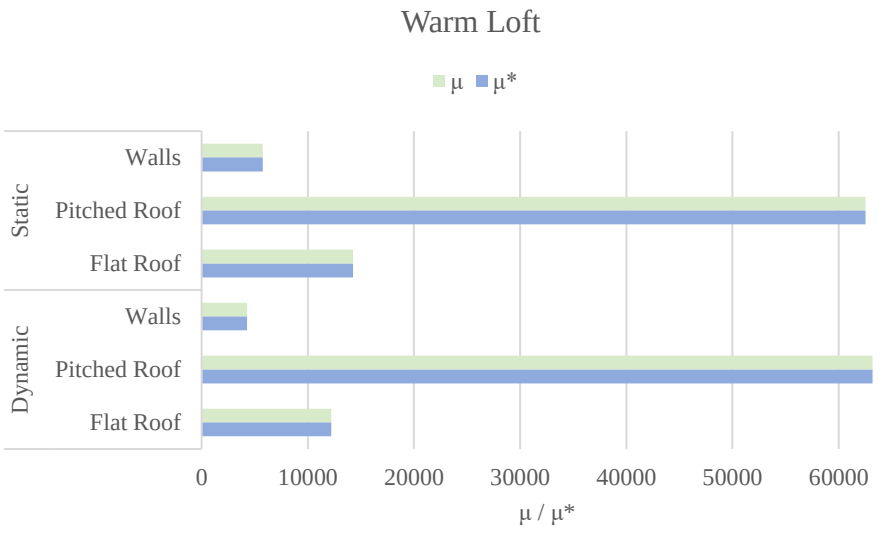

Figure 32: Morris SA Metrics (μ/μ*) under Warm Loft Case – Normal Operations

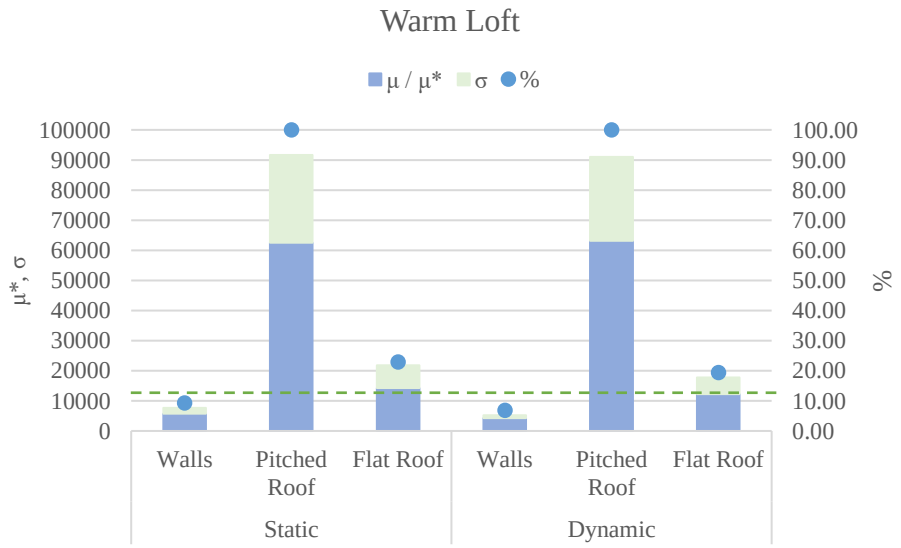

Figure 33: Morris SA Metrics' Significance under Warm Loft Case – Normal Operations

Under-pressure Operations (30Pa)

Table 18: Sensitivity Analysis' Comprehensive Results – Under-pressure Operations

Cold Loft

Input Parameter	Static Insulation				Dynamic Insulation			
	Run 1				Run 2			
	μ	μ^*	σ	%	μ	μ^*	σ	%
W	2341	2341	759.7	**59.69**	-267.9	2565	1993	**48.17**
AF	3199	3199	1135	**81.57**	1856	3690	2316	**69.296**
FR	3922	3922	1501	**100.00**	3362	5325	2613	**100.00**

Warm Loft

Input Parameter	Static Insulation				Dynamic Insulation			
	Run 3				Run 4			
	μ	μ^*	σ	%	μ	μ^*	σ	%
W	3319	3321	2410	**47.76**	1319	2526	2223	**31.41**
PR	6954	6954	3722	**100.00**	3663	8041	5844	**100.00**
FR	6281	6281	3783	**90.32**	4358	4933	4211	**61.35**

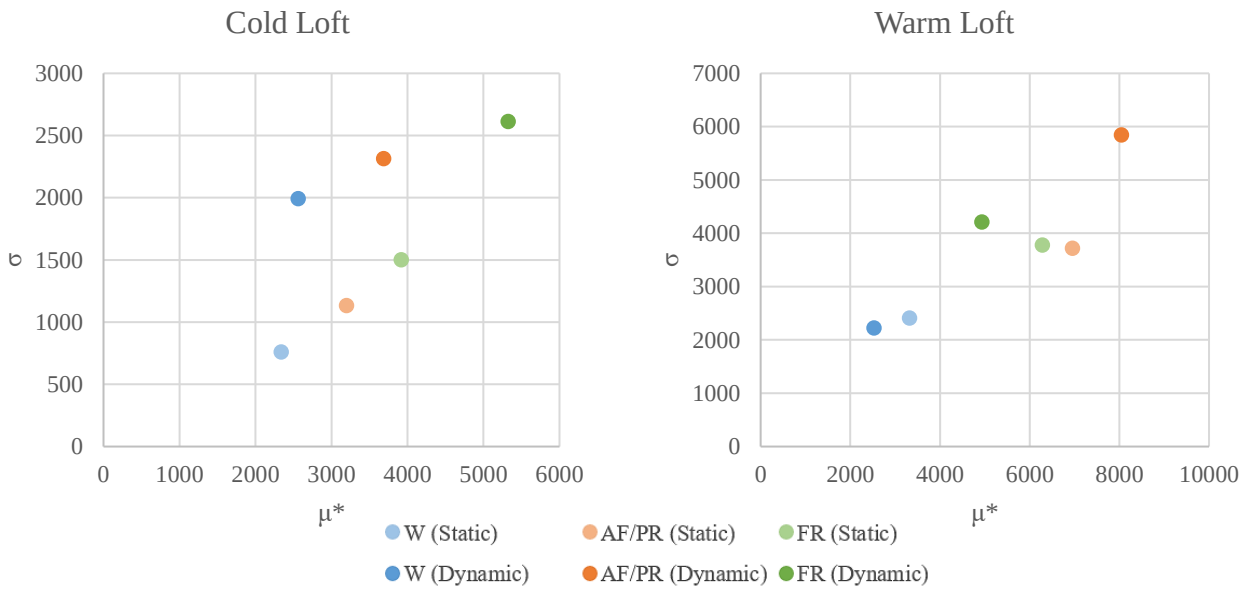

Figure 34: Morris SA Metrics' Plot – Under-pressure Operations

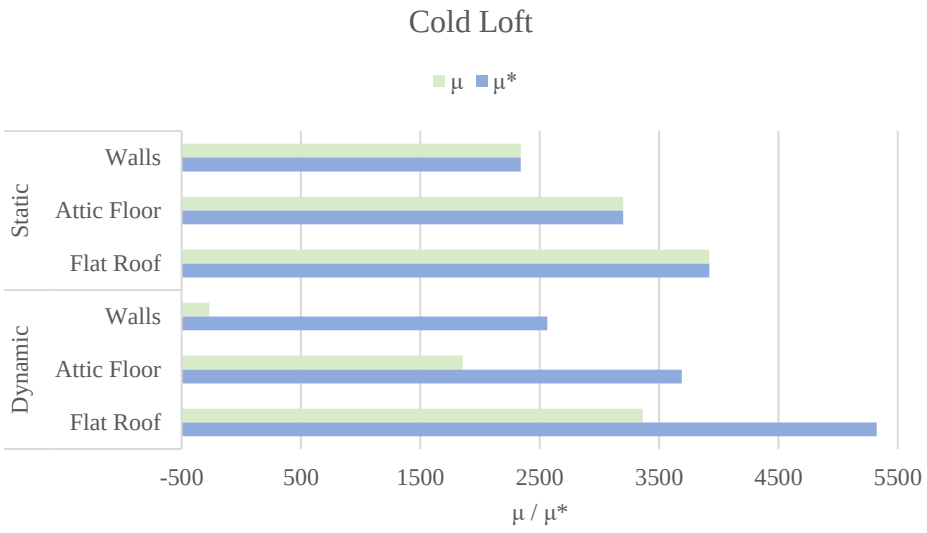

Figure 35: Morris SA Metrics (μ/μ*) under Cold Loft Case – Under-pressure Operations

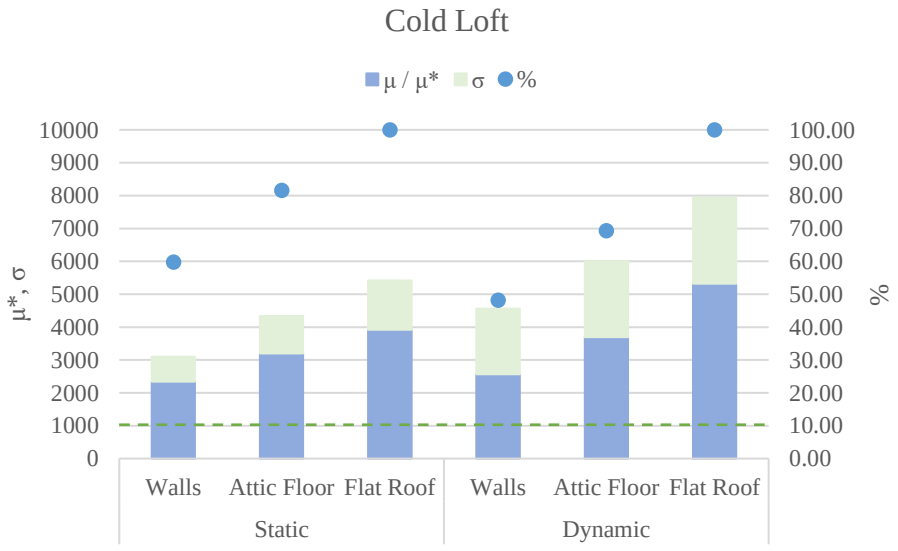

Figure 36: Morris SA Metrics' Significance under Cold Loft Case – Under-pressure Operations

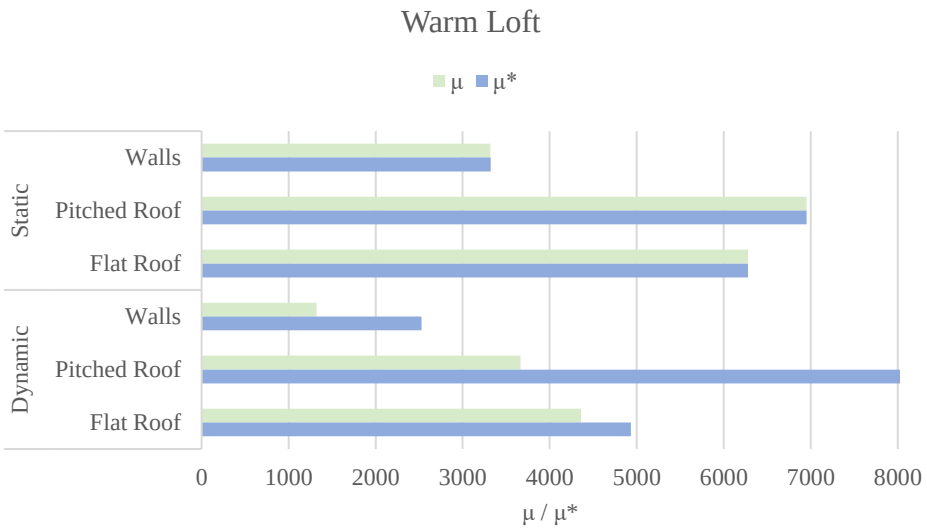

Figure 37: Morris SA Metrics (μ/μ*) under Warm Loft Case – Under-pressure Operations

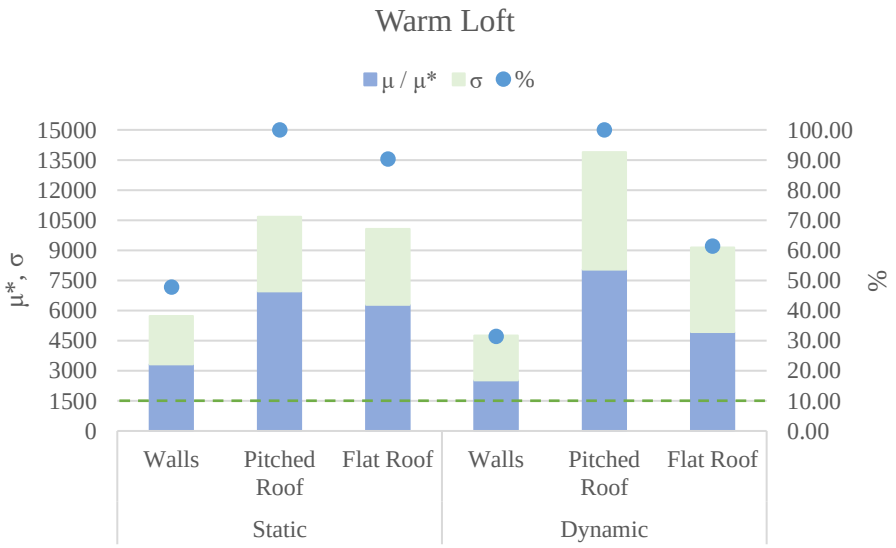

Figure 38: Morris SA Metrics' Significance under Warm Loft Case – Under-pressure Operations

8.3.Analysis & Discussion

As per the Morris Method's definition (Refer to Chapter 8.1), the sensitivity metrics establish a qualitative ranking of the input parameters on the dependent variable (the building's energy demand, in this case) and establishes the relative significance of their influence.

Extent of Infiltration Heat Recovery

The air leakage's effect on the building energy demand is conventionally depicted as a positive relationship, meaning that an increase in the air leakage would entail greater heat loss, and consequently higher energy demand.

Normal Operations

This positive relationship is clear under all normal operation scenarios (cold/warm loft and static/dynamic constructions) through equal values of μ and μ^* (Refer to Figures 30 and 32). The former being the average of the EE values and the latter the average of their absolute values, their equality indicate that all EE values are positive. This supports the consistently positive relationship of the envelope's air permeability and the building's energy demand. The negligeable changes between the equivalent static and dynamic cases also emphasize the little potential for IHR exploitation under such operative conditions.

Under-pressure Operations

However, for under-pressure operations, deviations become apparent: While analogous findings are observed in cases where the construction is presumed to exhibit static behavior, notable discrepancies emerge between the values of μ and μ^* when the construction's dynamicity is considered, under both loft configurations (Refer to Figures 35 and 37). This difference between μ and μ^* indicates that the EE values include both positive and negative components. In practical terms, an increase in the envelope's permeability causes the building's energy demand to increase in some cases and decrease in others.
This inconsistent relationship between air permeability and building energy demand may be attributed to the IHR effect: An increase in the air infiltration is associated to increased convection heat losses but reduced conduction heat losses, due to greater infiltration heat recovery. Depending on which of the two outcomes is dominant, the total heat loss and, consequently, the building energy demand will either increase or decrease.

Accordingly, the results of the analysis align with the literature findings. The IHR may entail savings under normal fan operations (depressurization of 1-2Pa) by mitigating the increase in energy demand. However, there is a clear need for exhaust fans and the oversizing of their design flowrates to ensure a reliable and sufficient building depressurization under the temperate Dutch climate, and to fully realize measurable IHR-related savings.

Input Parameter Ranking

The comparison of the μ and μ^* gives an indication as to the nature of the relationship between the surface permeabilities and the building energy demand. The relative importance of the inputs effect is then expressed in the form of a qualitative ranking, evident through the corresponding σ vs μ^*graphs (Figures 29 and 34, above).

Normal Operations (1-2Pa)

〉 Under a Cold and Warm Loft configurations

The energy demand is governed by the permeability of the Attic Floor or Pitched Roof. The Flat Roof and Walls follow, with a significantly lower effect.

Under-pressure Operations (30Pa)

〉 Under Cold Loft configurations

The energy demand is mostly influenced by the permeability of the Flat Roof, followed by the Attic Floor, and finally the Walls.

〉 Under Warm Loft configuration

The energy demand is governed by the Pitched Roof, followed by the Flat Roof, and finally the Walls.

The difference in the rankings between the static and dynamic cases is most significant under the Under-pressure operations of the Warm Loft configuration. This potentially suggests a greater IHR impact.

Input Parameters' Significance

The analysis focuses on the μ^* metric as percentage ratio (%) of the largest metric value in each run. The resulting percentage value are summarized in the Tables 17 and 18, for normal and under-pressure operations, and depicted in the corresponding charts (Figures 31 and 33, and 36 and 38).

Normal Operations (1-2Pa)

〉 Under a Cold Loft configuration

The permeability of all considered envelope surfaces (walls, attic floor, and flat roof) are attributed percentage ratios greater than 10% and are thus identified as significant. This implies that an increase in any of them would cause measurable increases in the building's energy demand.

〉 Under a Warm Loft configuration

The permeability of the permeability of the wall surfaces is attributed a μ^* is smaller than 10% of the largest value, and is thus not significant to the building's energy demand. It is thus possible to preserve a high permeability of the walls without compromising the building's energy-effectiveness.

Under-pressure Operations (30Pa)

〉 Under Cold and Warm Loft configurations

The permeability of all considered envelope surfaces have μ^* values with relatively high percent ratios. All surface air permeabilities are thus attributed a significant impact on the building's energy demand.

〉 It is, nonetheless, important to note that the impact the surface air permeability is not necessarily an increase of the demand in this case, as shown under Chapter 2.4.2, and may actually be beneficial to the building's energy-efficiency.

8.4. Conclusions

Building upon the sensitivity analysis results, several observations are made:

- Although exhaust fans consistently allow the mitigation of the air leakage's thermal load through some Infiltration Heat Recovery (IHR), achieving a strict and significant decrease in energy demand from higher surface permeabilities requires fan flowrates exceeding those dictated by minimum ventilation requirements.
- The ranked influence of different envelope surface permeabilities on the building's energy demand remains consistent at varying airflow rates under the Warm Loft configuration, but varies under a Cold Loft configuration. Wall permeabilities yet consistently exhibit the least influence across all scenarios.
- All surface permeabilities show measurable effect on the energy demand for most scenarios.
  - At high exhaust flow rates, this effect may be beneficial under both configurations. With high IHR, they provide the possibility to preserve the envelope's permeability while improving the building's performance.
  - At low exhaust flow rates, the air leakage's effect on the energy demand is mostly unfavorable, due to limited IHR effect. Nonetheless, the walls' air permeability may be deemed negligible under a Warm Loft configuration, thereby offering the possibility of preservation without compromising the overall energy-efficiency.
- The dynamicity of the construction introduces the most substantial variations in results under the Warm loft configuration, suggesting a more pronounced influence of the IHR on the Walls and Flat Roof under this configuration.

Comparing the two conditioned zone boundary configurations, the Warm Loft configuration presents several advantages in terms of the potential of preserving the building's permeability in favor of its post-retrofit performance:

1. Negligible impact of Wall permeability under low exhaust flowrates (Normal Operations), allowing its potential preservation without adverse effects on the building's energy-efficiency even in the absence of IHR.
2. Consistent ranking of surface permeabilities' influence on the building's energy demand under varying exhaust rates (Normal and Under-pressure Operations), allowing for consistent retrofit focus and reliable benefits at all air flowrates.
3. Greater potential impact of the IHR effect on the relationship between surface permeabilities and the building's energy demand, and greater potential of exploiting the building's air leakage into its post-retrofit performance under both modes of operation.

The Warm Loft configuration, setting the conditioned zone boundary at the Pitched Roof level, is then favored and, consequently, selected for further analysis.
The analysis encompasses the whole range between Normal and Under-pressure modes of operation, each offering distinct advantages in need of further investigation:

> While the Under-pressure operations introduce a significantly greater Infiltration Heat Recovery (IHR) effect, resulting in substantial energy demand reductions, the Normal operations consistently provide energy savings and system efficiency.
> It removes the need for over-sizing the fan systems beyond ventilation requirements and even suggests a potential for natural ventilation that could be explored.

9. Envelope and Ventilation Strategies and Application Frameworks

9.1. Optimization Analysis Methodology

An evolutionary optimization (EOpt) of the envelope's air permeability and insulation thickness, and the fans' flowrate under the retrofit variants aims to identify the optimal retrofit approach for historic traditional buildings, balancing the their energy-efficiency, IEQ, and heritage preservation.

Optimization Analysis

Optimization problems are typical of the design process, comparing various solutions as per their ability to fulfill one or more contrasting objectives (Lara et al., 2017). Such optimization problems are built upon three components:

- $f(x)$ Objective function – *to be maximized or minimized*
- (x) Set of unknown variables – *affecting the objective function*
- $[f(x)]$ Set of constraints – *limiting the permissible values the variables may take*

If parametric analysis tools allow exploring potential alternatives, they are not solution techniques: often referred to as "exhaustive search", they evaluate all possible variable combinations. Although guaranteeing the best solution, they entail high computational time and cost (Lara et al., 2017).
To overcome this drawback, a variety of optimization methods have been developed. Unlike the exhaustive search approach, some of these solutions may not be guaranteed, but provide for a measurably more efficient search process (Lara et al., 2017).

The classification of optimization strategies is described in the scheme below.

Optimization Algorithms	
Linear Algorithms	Optimization problems defined by a set of perfectly linear equations
Non-linear Algorithms	Optimization problems defined by a set of non-linear equations
Deterministic	Classic deterministic approach, reliant on the knowledge of gradients and/or higher order derivatives of equations, that are not always available for practical problems.
Enumerative	Exhaustive approach, examining all possible solutions in the objective function's domain space for the true optimum solution, and potentially computationally expensive.
Stochastic	Non-deterministic approach introducing randomness through a "Guided Random Search" across the search space.
Simulated Annealing (SA)	Algorithm emulating the physical annealing process to minimize energy states.
Evolutionary Algorithm (EA)	Algorithm emulating natural evolutionary behavior, improving potential solutions over generations using biologically-inspired processes.

Figure 39: Optimization Strategies Classification

Identifying the retrofit variants optimizing multiple contrasting objectives poses a multi-objective optimization (MOO) problem.
MOO typically yields a set of dominating optimal solutions, known as Pareto-optimal solutions, instead of a single optimum (Deb et al., 2002; Penna et al., 2015). This approach considers the dominance concept; a solution X dominates a solution Y when both of these conditions are satisfied:

- Solution X is not worse than solution Y in all objectives
- Solution X is strictly superior to solution Y in no less than one objective

Accordingly, moving from Y to X entails an improvement in all objectives, or in some without a detriment to others (Penna et al., 2015), as shown in Figure 40.
Pareto-optima, representing non-dominated solutions, collectively form the "Pareto Front", in case of two objectives, or "Pareto Surface", in case of multiple objectives (Penna et al., 2015).

Given that none of the Pareto-optimal solutions may be regarded as superior in absence of additional information, it becomes imperative to identify as many of these solutions as possible (Deb et al., 2002).

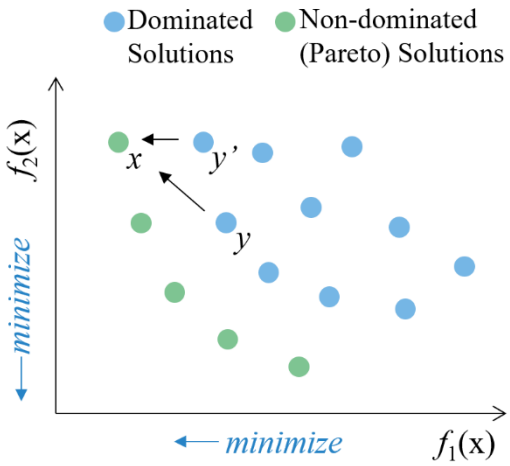

Figure 40: MOO's Pareto Front

The classical approach suggests converting the MOO problems into single-objective optimization (SOO) problems by addressing the Pareto-optima sequentially. This approach necessitates multiple runs to identify multiple solutions, resulting in increased computational costs (Deb et al., 2002).

Multi-objective Evolutionary Algorithms (MOEA) then offer a solution (Deb et al., 2002). Evolutionary algorithms (EA), particularly Genetic Algorithms (GA), are well-regarded for their advantages in building design and retrofit optimizations (Lara et al., 2017; Penna et al., 2015) and have gained popularity in Building Energy Performance (BEP) research due to their ability to efficiently identify multiple solutions in a single run (Deb et al., 2002; Wurtz et al., 2021).

The Non-dominated Sorting Genetic Algorithm (NSGA) is one of the first algorithms in this category. However, non-dominated MOEA have often faced criticism for (Deb et al., 2002):

- The non-dominated sorting's high computational complexity.
- The lack of elitism, that enhances performance and prevents the loss of prior good solutions.
- The reliance on a specified sharing parameter for diversity preservation.

The NSGA-II was thus developed by Deb *et al.* (2002) to alleviate such limitations:

- Relative to other elitist MOEA, the NSGA-II improves the solutions' spread and convergence around the true Pareto-optimal region (Deb et al., 2002).
- Relative to other constrained multi-objective optimization (CMOO) algorithms, the NSGA-II efficiently addresses CMOO problems by redefining dominance (Deb et al., 2002).

The NSGA-II thus gained substantial relevance in practical applications due to its fast non-dominated sorting approach, elitist strategy, parameter-less diversity-preservation method, and efficient constraint-handling approach (Deb et al., 2002).

NSGA-II

The Non-dominated Sorting Genetic Algorithm (commonly referred to as "NSGA-II"), developed by Deb *et al* (2002), was first implemented in 1975 (Holland, 1992) and since gained increasing relevance, owing to its ability to efficiently address multiple optimization objectives, while preserving the diversity of the solutions and identifying the Pareto-optima (Deb et al., 2002; Long, 2023).

Inspired by Darwin's evolution theory, the NSGA-II's algorithm represents all potential solutions as **individuals of a population**, with their characteristics defined as the individual's **genetic information**, and the input variables set as a **gene sequence** on a **chromosome** (Deb et al., 2002).

The NSGA-II's algorithm indeed employs (Deb et al., 2002; Long, 2023):

- Genetic Algorithm (GA) general principles
  - A population of individuals is represented as state vectors.
  - The population is evolved through generations to identify the optimal solutions.

- Revised mating selection and survival selection strategies

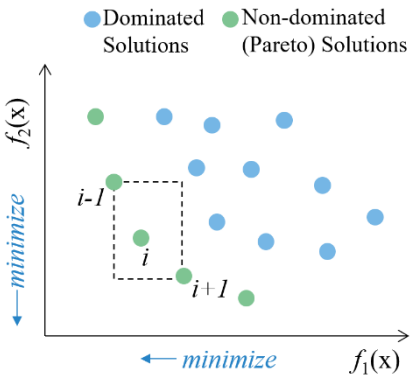

Figure 41: NSGA II's Crowding Distance

  - **Survival selection strategy**
    Surviving solutions are selected in the splitting front based on crowding distance and preserving extreme points.
    In Figure 41 (Deb et al., 2002), the front is represented by the circles, and the i^{th} solution's crowding distance is the average length of the square's sides.
  - **Mating selection strategy**
    Following a binary tournament mating selection approach, each individual is compared on the basis of its rank or domination criterium first, then its crowding distance.

- Non-dominated sorting approach for assessing the fitness of individuals (Refer to Figure 42)
  - Individuals are compared and sorted based on the objective criteria.
  - The non-dominated and best individuals are preserved in the population, and participate in the subsequent generations' evolution process.

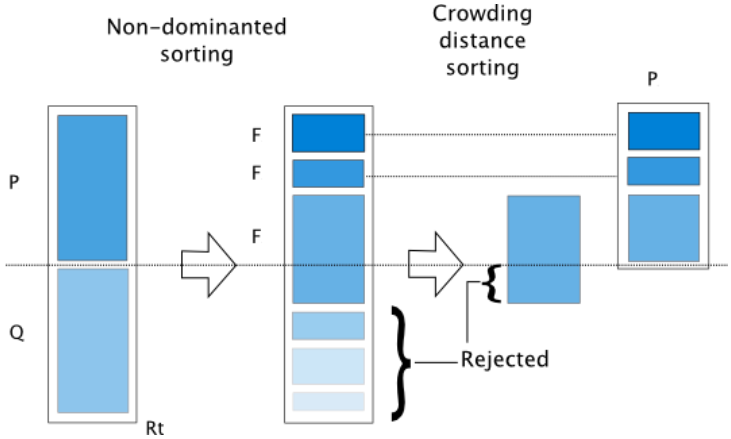

Figure 42: NSGA II's Non-dominated Sorting Approach (Deb et al., 2002).

Accordingly, once a population of randomly selected individual (the **first generation**) is initialized, the algorithm follows a **generational** loop (Deb et al., 2002; Lara et al., 2017; Long, 2023; Wurtz et al., 2021):

1. Evaluating the individuals' fitness relative to the multiple objectives
2. Sorting to identify the non-dominated individuals
3. Selecting the best and non-dominated individual for reproduction
4. Creating a new generation of offspring individuals, by implementing:
    - Cross-over – replacing the "genes" from the distinct solutions
    - Mutation – instilling random changes

Generational iterations are ended when a termination criterion is met, meaning either of:

- enough fit solutions are obtained
- the pre-defined maximum number of generations is met

The Pareto-optimal solutions identified in the final population are the output solutions.

The NSGA-II's Evolutionary Algorithm process is summarized in Figure 43 (Lara et al., 2017).

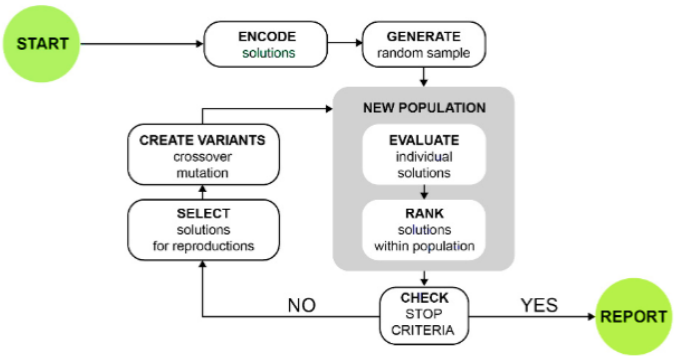

Figure 43: Evolutionary Optimization Algorithm Process (Lara et al., 2017)

Evolutionary Optimization Runs

After establishing the recommended conditioned zone boundary for the surface permeability in the building post-retrofit, the subsequent analysis aimed to assess the importance of the ventilation regime and construction dynamicity in formulating the ideal retrofit strategy for historic traditional buildings of varying levels of protection. To determine the optimal combinations of airtightness level, insulation thickness, and fan flowrates conductive to the successful implementation of the recommended retrofit strategies, a set of evolutionary optimization runs were conducted, as outlined below.

The conditioned zone boundary considers the loft configuration selected as a result of the Sensitivity Analysis. For the sake of time-efficiency, the other configuration will not be examined.

The intention of each EOpt run is to identify the combination of airtightness level, insulation thickness, and fan flowrates (if applicable) that achieves the optimal balance of energy-efficiency and IEQ, under each ventilation and envelope retrofit variant.
For this purpose, five objective functions are defined, and may be distinguished into two categories.

Energy-Efficiency

The building's **annual net energy demand** is attributed an objective function, as defined in Chapter 6.3.

The **internal energy** is independent of the building's construction and ventilation performance, and is a **constant** throughout the retrofit variants.

The building's **net annual energy demand** thus varies with the variation of the **heating and ventilation energy**, and **exhaust energy recovery**.

〉 The resulting building's net annual energy demand is set to be **minimized**.

Indoor Health and Comfort

The building's **indoor comfort** considers 4 different scores, corresponding to each IEQ parameter defined in Chapter 6.3: **Winter thermal comfort**, **Summer thermal comfort**, **Ventilation ACH** (Air Change Rate), and **Ventilation RH** (Relative Humidity).
Each score is attributed an objective function.

As per the EN 16798 standard (European Committee for Standardization, 2019b):

A building meets the requirements for a given IEQ category if at least 95% of its area meets the requirements for this category.

Accordingly, the building's hourly performance is the IEQ category of the zone with the lowest performance (i.e. lowest IEQ category).
The building's **annual comfort scores** are then estimated using the equation and hourly weights defined in Chapter 6.3.

〉 The resulting 4 building annual comfort scores are set to be **maximized**.

The yielding of reliable and relevant results is dependent on the proper configuration of the NSGA-II optimization algorithm. Accordingly (Lara et al., 2017):

Table 19: NSGA-II Algorithm Configuration

A population size of 10 individuals is adopted	〉 Provides enough variability in the creation of new solutions
A maximum number of generations (i.e. iterations) of 200 is set	The maximum number of simulations is set at: $N_{simulation} = 10 \times 200 = 2000$ 〉 Provides sufficient generations for BEP applications, while allowing the use of the lower computational capacity of a local computer (Lara et al., 2017).
The cross-over rate (i.e. rate of generation of new solution from existing solutions) is maximized at 1	〉 Enhances the exploration of the solution space, and its convergence around the true Pareto-optima.
The mutation rate (i.e. rate of inducing random changes into new solutions) is set at 0.2	〉 Prevents random "trial & error" processes in the optimization algorithm

The EOpt analysis' configuration is summarized as follows:

Table 20: EOpt Analysis Settings

Algorithm Settings	
Method	NSGA-II
Number of Variables – k	10
Number of Objective Functions – n	5
Initial Population Size	10
Maximum Number of Generations	200
Cross-over [%]	100
Mutation [%]	20
Tournament Selection Size	2
Scenarios	
Runs	Run 1 – Non-insulated & dynamic construction, Ventilation-based fan flowrate Run 2 – Insulated & dynamic construction, Ventilation-based fan flowrate Run 3 – Non-insulated & dynamic construction, IHR-based fan flowrate Run 4 – Insulated & dynamic construction, IHR-based fan flowrate Run 5 – Non-insulated & static construction, Ventilation-based fan flowrate Run 6 – Insulated & static construction, Ventilation-based fan flowrate
Variables	
Input Parameters (Variables)	W – Walls' leakage coefficient PR – Pitched Roof's leakage coefficient FR – Flat Roof's leakage coefficient Wins – Walls' insulation thickness PRIns – Pitched Roof's insulation thickness FRIns – Flat Roof's Insulation thickness FanSched – Fans' operation schedules FanFlow – Fans' operation flowrate
Output (Objective Functions)	Building's Annual Energy Demand [t1] – *Minimize* Winter Thermal Comfort Score [t2] – *Maximize* Summer Thermal Comfort Score [t3] – *Maximize* Ventilation ACH Score [t4] – *Maximize* Ventilation RH Score [t5] – *Maximize*

The parameter range of air permeability and insulation input variables encompass possibly achievable values, and are summarized in Tables 21 and 22, respectively. For the air permeability, the same values explored in the Sensitivity Analysis are adopted (Refer to Table 16), identified based on the results of the Meta-analysis on building components' airtightness (Prignon et al., 2021).

Table 21: Optimization Input Definition - Surface Permeability

Input	Range	Steps	Values
W	[0.000001, 0.0004]	21	0.000001, 0.0000025, 0.000005, 0.0000075, 0.00001, 0.000025, 0.00005, 0.000075, 0.0001, 0.000125, 0.00015, 0.000175, 0.0002, 0.000225, 0.00025, 0.000275, 0.0003, 0.000325, 0.00035, 0.000375, 0.0004
AF, PR, FR	[0.00001, 0.004]	21	0.00001, 0.000025, 0.00005, 0.000075, 0.0001, 0.00025, 0.0005, 0.00075, 0.001, 0.00125, 0.0015, 0.00175, 0.002, 0.00225, 0.0025, 0.00275, 0.003, 0.00325, 0.0035, 0.00375, 0.004

Table 22: Optimization Input Definition - Insulation Thickness

Input	Range	Steps	Values
WIns	[0, 0.15]	16	0, 10, 20, 30, 40, 50, 60, 70, 80, 90, 100, 110, 120, 130, 140, 150
PRIns, FRIns	[0, 0.30]	16	0, 20, 40, 60, 80, 100, 120, 140, 160, 180, 200, 220, 240, 260, 280, 300

The Fans' operation schedules' options are set to define the 4 ventilation regime variants of the studied retrofit scenarios (Refer to Chapter 4).
Comparing the distribution of the Pareto-optima's performance among the distinct ventilation regimes gives insight into the importance of the ventilation type in the building's post-retrofit performance, and supports the selection of the most desirable variant under specific building contexts.

The Fans' operation schedules are defined in pairs, as "Combinatorial Parameters" (*The Parameters*, 2020), for the exhaust and supply fans (Refer to Table 23)

Table 23: Optimization Input Definition - Fan Operation Schedule

Input	Values
FanSched	Exhaust Off (All Year) & Supply Off (All Year) Exhaust On (All Year) Exhaust On (Heating Season) & Supply Off (All Year) Exhaust On (Heating Season) & Supply On (Cooling Season)

When Exhaust and/or Supply fans are operating under Ventilation-based fan flowrate, the flow rate is set to meet the minimum standard-required flowrate of 0.9 l/s.m^2 (*Bouwbesluit Online 2012*, n.d.). Under IHR-based fan operations, the flowrate is increased to ensure reliable depressurization of the building and efficient IHR. The fan flowrate values are then set to meet under-pressures of up to 30Pa – the maximum allowable under-pressure for doors' operability and indoor comfort. The considered fan flowrates are listed in Table 24.

Table 24: Optimization Input Definition - Fan Flowrate

Input	Range	Steps	Values
FanFlow	[0.9, 5.93]	13	0.9, 1.25, 1.5, 1.75, 2.0, 2.5, 3.0, 3.5, 4.0, 4.5, 5.0, 5.5, 5.93

9.2. Multi-Criteria Decision Analysis

A Multi-Criteria Decision Analysis (MCDA) and Decision-Making (MCDM) process is carried out on the non-dominated solution sets of the evolutionary optimization (EOpt) to efficiently and objectively identify the solutions that best address the specific problems examined in this research, their properties and limitations.
It is to select the optimal solutions that improve the overall building performance from the base case (BC) to an extent that is comparable to (or better than) the conventional retrofit case (CRC), while exploiting as practically possible the building's existing air leakage. Accordingly, the target ranges of air permeability, insulation thickness, and fan flowrate are defined for each studied scenario.

Multi-Criteria Decision Analysis (MCDA) and Decision-Making (MCDM)

Multi-objective optimizations (MOO) with conflicting targets result in a set of non-dominated solutions, the Pareto-optimal solutions. From the perspective of all target objectives, the resulting solutions are considered to be equally good and provide insight into the trade-off between the studied objectives (Wang & Rangaiah, 2017).

Considering the many retrofit variants, the resulting Pareto-optima involve an amalgam of solutions that accommodate a wide range of post-retrofit performances, each prioritizing different aspects of the building properties and performance.

The selection of the solutions of interest for a specific problem must thus follow a methodical strategy. Various selection techniques exist; they may be fundamentally different and result in the selection of different optimal solutions (Wang & Rangaiah, 2017). The choice of the adopted selection method is thus of importance in ensuring the study's desired outcomes.

The method adopted is selected to satisfy three characteristics (Wang & Rangaiah, 2017):

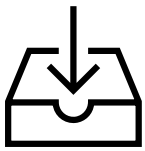

Less User Input Required

For convenience and minimal subjective influence on the selection result

Ability to Manage Objectives of Different Magnitudes

Through normalization steps, for consistency and wider range of applicability

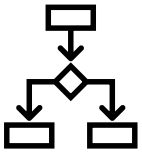

Simplicity of Principles and Algorithms

For simpler and correct interpretations of the selection results

Considering their basic principles, associated algorithms, and resulting recommended solutions, the considered selection methods may be categorized into 4 groups (Wang & Rangaiah, 2017). Their characteristics, similarities and disparities, advantages and disadvantages are displayed and compared in the following scheme (Refer to Table 25).

Table 25: MCDA Methods and their Characteristics

Group 1	TOPSIS Technique for Order of Preference by Similarity to Ideal Solution LINMAP Linear Programming Technique for Multi-dimensional Analysis of Preference VIKOR Viekriterijumsko Kompromisno Rangiranje	〉 Similar Outcomes 〉 Choice based on solutions' distances from ideal solutions 〉 User input for weightage	TOPSIS & LINMAP same optimal solution VIKOR possible different optimal solution LINMAP & VIKOR only consider the positive-ideal point › maximize benefits TOPSIS considers both positive- and negative-ideals › maximize benefits and avoid risks TOPSIS & LINMAP only require objective weights – relative importance of objectives VIKOR also requires strategy weights – decision-making based on maximum group utility, consensus, or with veto.
	› Favored method: TOPSIS For considering both positive and negative effects, and reducing user input		
Group 2	SAW Simple Additive Weighting MEW Multiplicative Exponent Weighing	〉 Similar Outcomes 〉 Restriction on applicability	SAW & MEW result is quite similar solutions SAW & MEW's objectives cannot be 0, being at the denominator of the normalization equation MEW is not suitable for problems with negative values in the objective matrix.
	› Favored method: SAW For being applicable on a wider set of problems		
Group 3	NFM Net Flow Method ELECTRE II Elimination and Choice Translating priority II ELECTRE III Elimination and Choice Translating priority III	〉 Same computationally-expensive base principle 〉 Some similar Outcomes 〉 User input for threshold values	NFM, ELECTRE II & III are based on the pairwise comparison of each objective per solutions' pairs NFM & ELECTRE III often result in the same recommended solutions ELECTRE II often results in different results NFM, ELECTRE II & III require multiple thresholds, difficult to define, as user input
	› Favored method: NFM For requiring fewer and more physically-significant inputs		
Group 4	FUCA Fair Un Choix Adéquat GRA Gray Relational Analysis	〉 Different from other methods	FUCA has the simplest basic principle GRA is the only method with no required user input
	› Favored method: GRA For being objective and providing similar outcomes as other methods, with equal weightage on all objectives		

In terms of user input, principle simplicity, and range of applicability, the TOPSIS, GRA and SAW methods are preferred for selecting an optimal solution from extensive sets of non-dominated solutions. Among these, TOPSIS is the most commonly utilized method (Wang & Rangaiah, 2017).

For the purpose of this study, the **TOPSIS** method is adopted:

> Built upon simple principles and algorithms, it has the ability to address a wider set of problems and account for both positive and negative impacts, while requiring minimal user input.
> The objectivity of the solution may even further be increased to the GRA level by implementing equal weightage on all objectives (Wang & Rangaiah, 2017).

Since the selection method choice is by itself subjective, domain knowledge and desired values of decision variables must be combined with the adopted selection method in recommending an optimal solution.

TOPSIS Method

The Technique for Order of Preference by Similarity to Ideal Solution (commonly known as TOPSIS) is one of the most commonly used methods for Multi-Criteria Decision Analysis (MCDA) and Decision-Making (MCDM).

The TOPSIS selected optimal solution out of a set of non-dominated solutions exhibits (Refer to Figure 44):

- The smallest Euclidian distance S_{i+} from the ideal (or positive-ideal) solution, which combines each objective's best value in the given set of Pareto-optimal solutions.
- The largest Euclidian distance S_{i-} from the negative-ideal solution, which combines each objective's worst value in the given set of Pareto-optimal solutions.

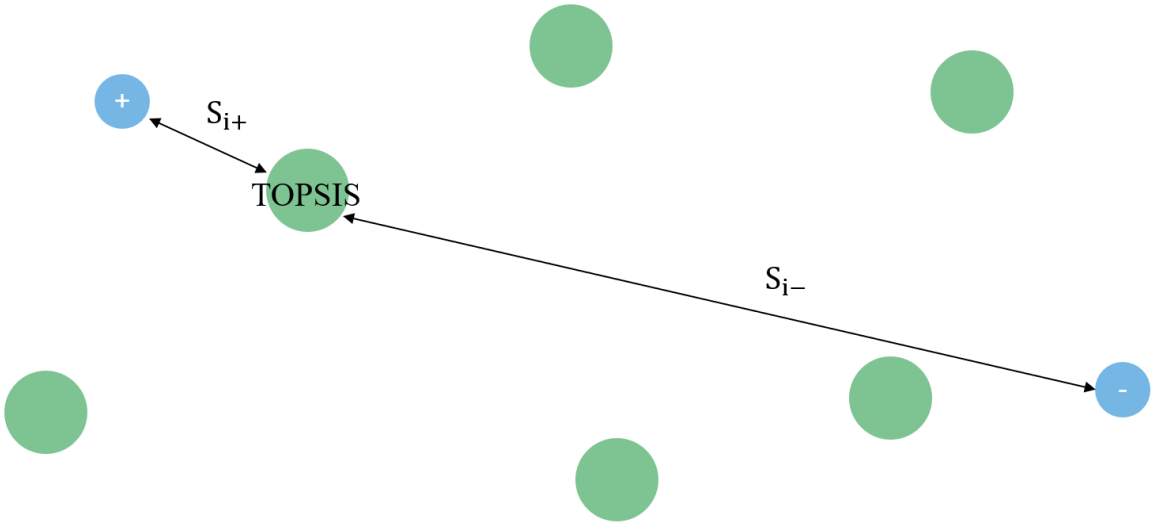

Figure 44: TOPSIS Method Selection Criteria and Solution

The TOPSIS method is implemented following the steps detailed in the below scheme (Wang & Rangaiah, 2017)

Step 1

Construction of the objective matrix

The objective matrix is a matrix of:

- m rows – for each of the m Pareto-optimal solutions generated by the optimization process
- n columns – for each of the n objectives.

It considers each solution's objective function values, and not the optimization problem's decision variables. In practice, however, the decision variables may be important to the selection of solutions based on their relative feasibility, and may then be considered separately in the analysis of the selection's top results.

Step 2

Construction of the normalized objective matrix

$$F_{ij} = \frac{f_{ij}}{\sqrt{\sum_{i=1}^{m} {f_{ij}}^2}}$$

Step 3

Construction of the weighted normalized objective matrix

The normalized matrix multiplies each objective's column by its corresponding weight. For the purpose of objectivity in this study, the five objective functions are assigned the equal weights of 0.2.

$$v_{ij} = F_{ij} \times w_j$$

Where:

$$\sum_{j=0}^{n} w_j = 1$$

Step 4

Definition of the ideal and negative-ideal solutions

The ideal solution considers each objective's best value; the best value in each column is the largest one for maximization objectives and the smallest one for minimization objectives. Mathematically, the ideal solutions are defined by:

$$A^+ = \{(Max_i(v_{ij})|j \in J), (Min_i(v_{ij})|j \in J') \mid i \in 1, 2, \dots, m\} = \{{v_1}^-, {v_2}^-, \dots, {v_j}^-, \dots, {v_n}^-\}$$

The negative-ideal solution considers each objective's worst value; the worst value in each column is the smallest for maximization objectives and the largest one for minimization objectives. Mathematically, the latter translates into:

$$A^- = \{(Min_i(v_{ij})|j \in J), (Max_i(v_{ij})|j \in J') \mid i \in 1, 2, \dots, m\} = \{{v_1}^-, {v_2}^-, \dots, {v_j}^-, \dots, {v_n}^-\}$$

Step 5

Calculation of the Euclidian of each solution to the ideal and the negative-ideal solutions

$$S_{i+} = \sqrt{\sum_{j=1}^{n} (v_{ij} - {v_j}^+)^2}$$

$$S_{i-} = \sqrt{\sum_{j=1}^{n} (v_{ij} - {v_j}^-)^2}$$

Step 6

Calculation of the closeness factor of each solution

$$C_i = \frac{S_{i-}}{S_{i-} + S_{i+}}$$

The closeness factor is the TOPSIS ranking factor, representing each solution as a function of its location with respect to the ideal and negative-ideal solutions.

When $S_{i-} = 0$, $C_i = 0$, meaning that the solution i is closest to the negative-ideal solution.
When $S_{i+} = 0$, $C_i = 1$, meaning that the solution i is closest to the positive-ideal solution.

The non-dominated solution with the largest C_i value is thus the recommended optimal solution.

Knowing that:

f_{ij} – the i[th] value of the objective matrix's j[th] objective
F_{ij} – the normalized f_{ij} value
v_{ij} – the rank or weighted value of f_{ij} or F_{ij}
w_j – the j[th] objective's weight

A^+ – ideal solution
A^- – negative-ideal solution
J – set of maximization objectives
J' – set of minimization objectives

S_{i+} – distance of the i[th] solution to the positive-ideal solution
S_{i-} – distance of the i[th] solution to the negative-ideal solution

i = 1, 2, 3, …, m
j = 1, 2, 3, …, n

TOPSIS Analysis

The TOPSIS method is applied on each set of Pareto-optimal solutions, generated by each optimization run, as defined under Chapter 9.2.

In an attempt to situate the performance of the Pareto-optimal solutions in the specific context of this research, being the retrofit of historic traditional dwellings, three reference solutions were introduced into the TOPSIS analysis of each Pareto-optimal set:

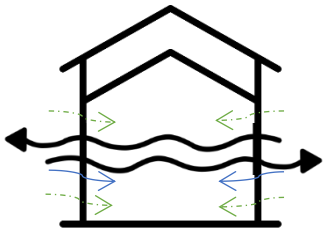

Base Case
[BC]

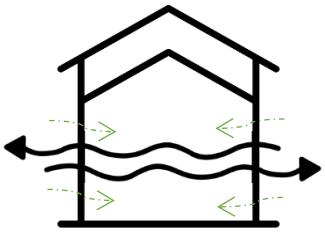

Base Retrofit Case
[BRC]

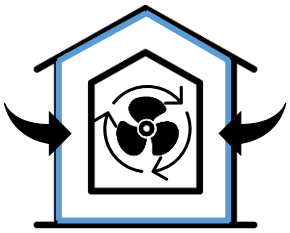

Conventional Retrofit Case
[CRC]

For Non-Insulated Construction scenario runs (Runs 1, 3, and 5), the TOPSIS analysis incorporates an additional reference case to ensure a robust and fair assessment of solutions within their respective context.

All comparative references are described under Chapter 4.2, and help provide a better understanding of the relevance and performance of each retrofit solution in a valid context.

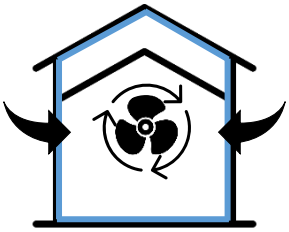

Non-Insulated Conventional Retrofit Case [NCRC]

The TOPSIS closeness factor (C_i) ranks each solution on a linear scale representing its position with respect to the ideal and negative-ideal solutions. The latter bounds are, however, subjective to each optimization run and result in solution rankings that are not objectively comparable between the different runs (Refer to Figure 45).
To efficiently and objectively identify the optimal solutions that improve the overall building performance from the base case (BC and BRC) to an extent that is better than or comparable to the conventional retrofit case (CRC), the solutions are categorized based on their percent distance from the CRC. In other words, for each set of Pareto-optimal solutions:

The normalized distance between BC/BRC and CRC is computed as the difference in their respective closeness factors: $Max(C_{BC}, C_{BRC})$ and C_{CRC}

$$D_{CRC} = C_{CRC} - Max(C_{BC}, C_{BRC})$$

D_{CRC} – CRC's normalized distance [-]
C_{CRC} – CRC's Closeness Factor [-]
$Max(C_{BC}, C_{BRC})$ – Highest base case Closeness Factor [-]

Following the same logic, each Pareto-optimal solution's normalized distance from BC/BRC is also determined.

$$D_i = C_i - Max(C_{BC}, C_{BRC})$$

D_i – Solution i's normalized distance [-]
C_i – Solution i's Closeness Factor [-]
$Max(C_{BC}, C_{BRC})$ – Highest base case Closeness Factor [-]

The solutions are then situated relative to the base and conventional retrofit cases in terms of their relative closeness ratio.

$$R_i = \frac{D_i}{D_{CRC}}$$

R_i – Solution i's Relative Closeness Ratio [-]
D_i – Solution i's normalized distance [-]
D_{CRC} – CRC's normalized distance [-]

Unlike the closeness factor (C_i), the relative closeness ratio (R_i) evaluates the solutions on a linear scale normalized to the study's comparative references, consistent for all runs. This scoring system enables an objective comparison of all Pareto optima within the study's contextual framework.
For the purpose of this study, all solutions that are better than or within a 10% distance worse than the CRC are selected. Meaning, all solutions with a relative closeness ratio greater than 0.9 are considered as comparable to (or better than) the CRC (Refer to Figure 46).

The present research does not aim to identify the optimal retrofit solutions only based on their post-retrofit performance. These solution must also exploit the building's existing air leakage as practically possible and account for traditional historic buildings' properties and restrictions.
Accordingly, the target ranges of airtightness level, insulation thickness, and fan flowrate associated to these optimal solutions (as input variables) are also examined.

For heritage buildings with protected interior surfaces, the non-insulated scenarios' performances are also situated against the NCRC reference. Their corresponding Relative Closeness Ratio (R'_i) is then estimated by simply replacing the CRC results by the NCRC results in the process presented above.

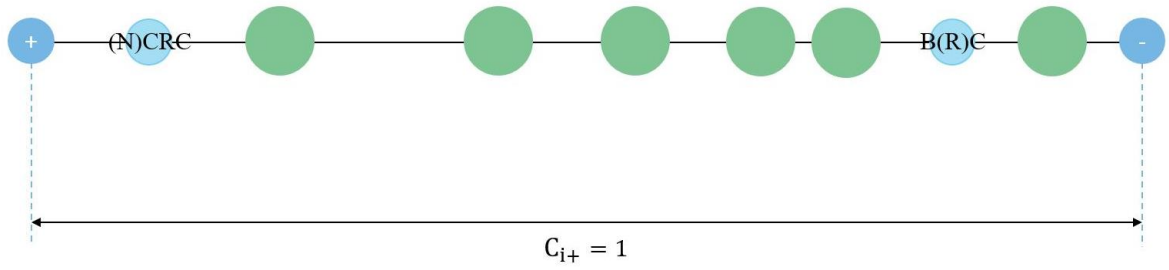

Figure 45: Closeness Factor (C_i) Scale

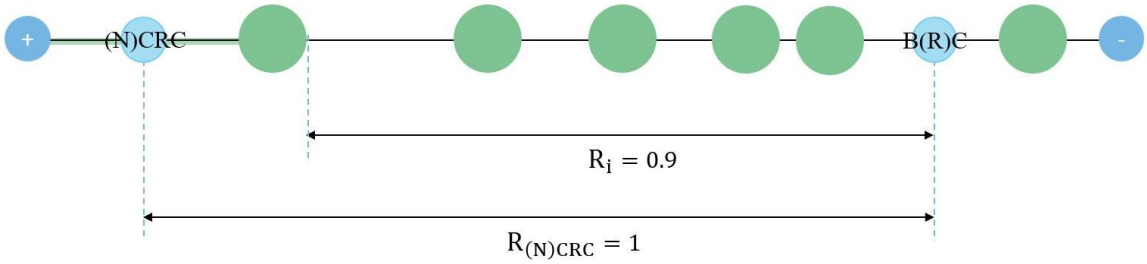

Figure 46: Relative Closeness Ratio (R_i) Scale and Target Scores

9.3. Results

NSGA II Optimization

The complete EOpt analysis took a total of 50 days to run, with an average of 8 days per scenario. Each scenario run considered 200 generations of at most 10 individuals (or building simulations), with each generation requiring around 1 calculation hour to run.

The Evolutionary Optimizations' results consisted of the NSGA II's resulting set of Pareto-optimal solutions, characterized by their respective:
(As defined under Chapter 9.1)

- Input variables
- Output-decision variables
- Output-objective function variables

An overview of the complete analysis' results is summarized in the charts below (Refer to Figure 47).

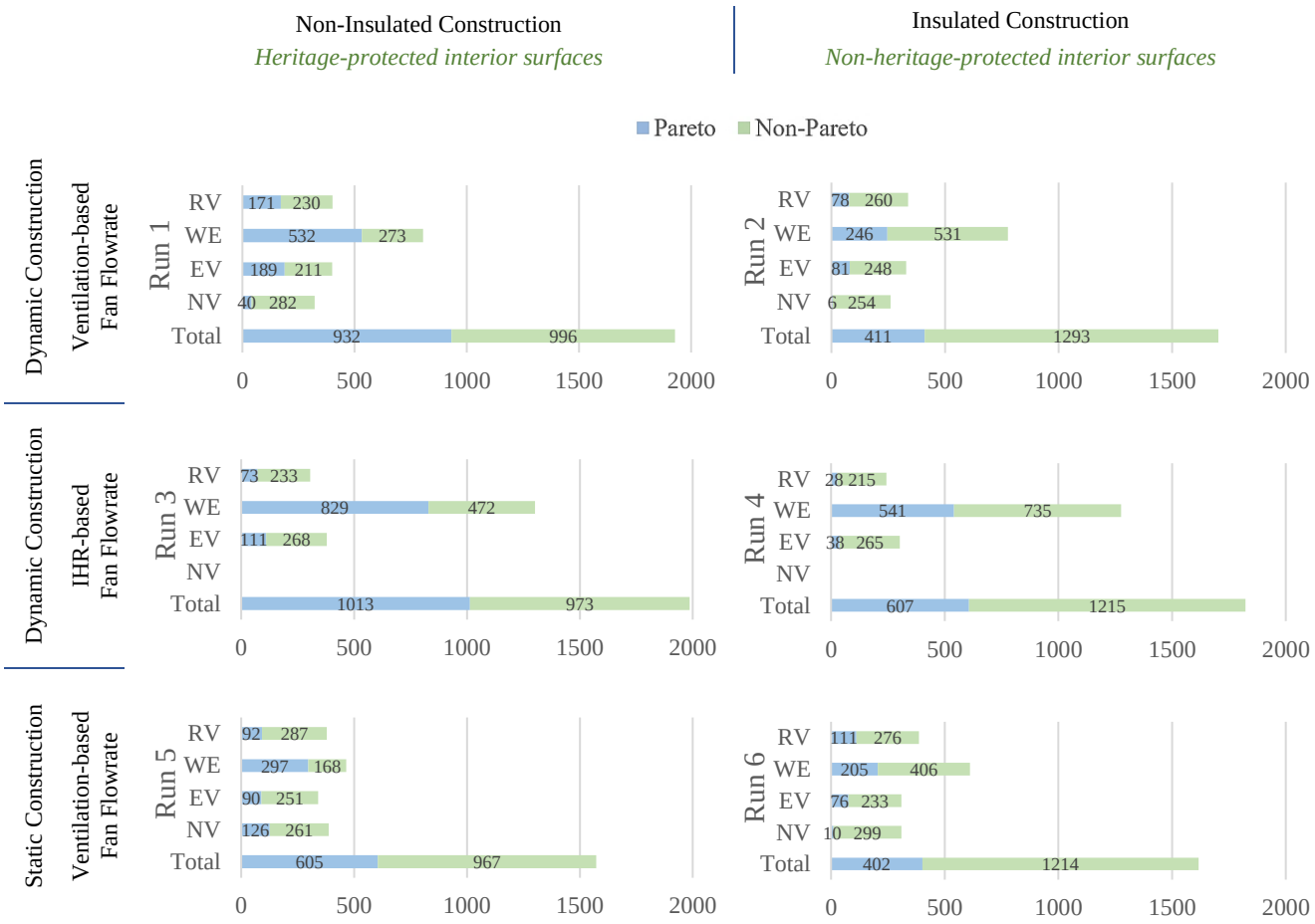

Figure 47: Optimization Results - Overview

The set of Pareto-optimal solutions derived from each run constitute the foundation for defining retrofit strategies recommendation for historic traditional dwellings, both with heritage protected (Runs 1, 3 and 5) and non-protected (Runs 2, 4 and 6) interior surfaces. Analyzing these results serves three primary objectives.

Within each of these heritage-protection contexts, the comparison between the dynamic construction scenarios utilizing Ventilation-based and IHR-based fan flowrates provides for the following:

1. Assessment of the significance of fan flowrates and the potential benefits of exceeding ventilation requirements in enhancing the efficient utilization of air leakage and its associated IHR effect into achieving a balanced overall building performance.
2. Formulation of the recommendations for the most effective ventilation strategy (reducing the trade-off between energy-efficiency, IEQ, and heritage preservation), as well as identifying the requisite air permeability levels, insulation thicknesses, and fan flowrates to meet such optimal performance.

Moreover, the comparison between the dynamic and static construction scenarios gives insight into:

3. Characterization of the importance of accounting for construction dynamicity when evaluating and designing retrofit strategies for historic traditional dwellings.
   This highlights the potential need for the development of Building Energy Simulation (BES) tools capable of more effectively incorporating the dynamic behavior of building materials and their interaction with the dynamic airflows.

As previously defined, the post-retrofit performances achieved by the Pareto-optimal solutions are situated in terms of their achieved improvement from the Base Case (BC and BRC) performance, relative to the improvement attained by the Conventional Retrofit Case (CRC) or Non-insulated Conventional Retrofit Case (NCRC).

For this purpose, the comparative references' results are presented in Table 26, and integrated in the analysis of all identified sets of Pareto-optimal solutions.
The reference cases evaluated under static and dynamic construction conditions reveal subtle disparities in their results and, consequently, their perceived performance. Although not specifically tailored for IHR exploitation, they provide a glimpse of the potential improvements achievable through the consideration of construction dynamicity in the design of retrofit strategies.

Table 26: Comparative References' Results - Objective Functions

Comparative Reference Cases		Objective Functions				
		t1	t2	t3	t4	t5
		[kwh]	[w.hrs]	[w.hrs]	[w.hrs]	[w.hrs]
BC	Static	69780.0	601.1	-4900.9	16812.8	3291.7
	Dynamic	69672.6	609.7	-4893.37	16815.0	3298.9
BRC	Static	69067.6	599.4	-4890.8	16765.4	3318.6
	Dynamic	68946.1	609.5	-4883.8	16767.6	3325.0
CRC	Static	27208.5	3364.8	-1698.1	17369.0	7488.4
	Dynamic	27197.0	3367.2	-1695.4	17368.3	7488.0
NCRC	Static	38783.2	587.6	-3034.7	17429.5	6499.3
	Dynamic	38709.2	590.8	-3031.5	17428.6	6502.9

The trade-off between the **minimization objective** (energy demand) and the **maximization objectives** (IEQ Scores) in each analysis scenario is depicted through scatter plots of all corresponding Pareto-optimal solutions, revealing their Pareto fronts. The results are categorized into non-insulated (Refer to Figures 48, 49 and 50) and insulated cases (Refer to Figures 51, 52, and 53).

Non-Insulated Cases

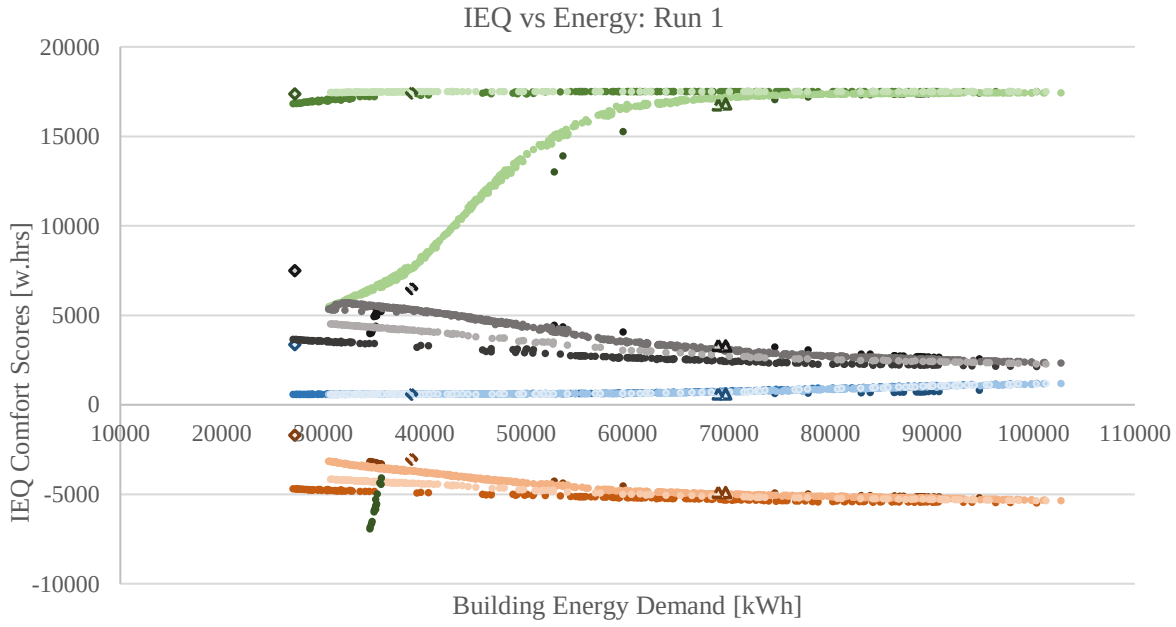

Figure 48: Pareto Optimal Solutions - Run 1

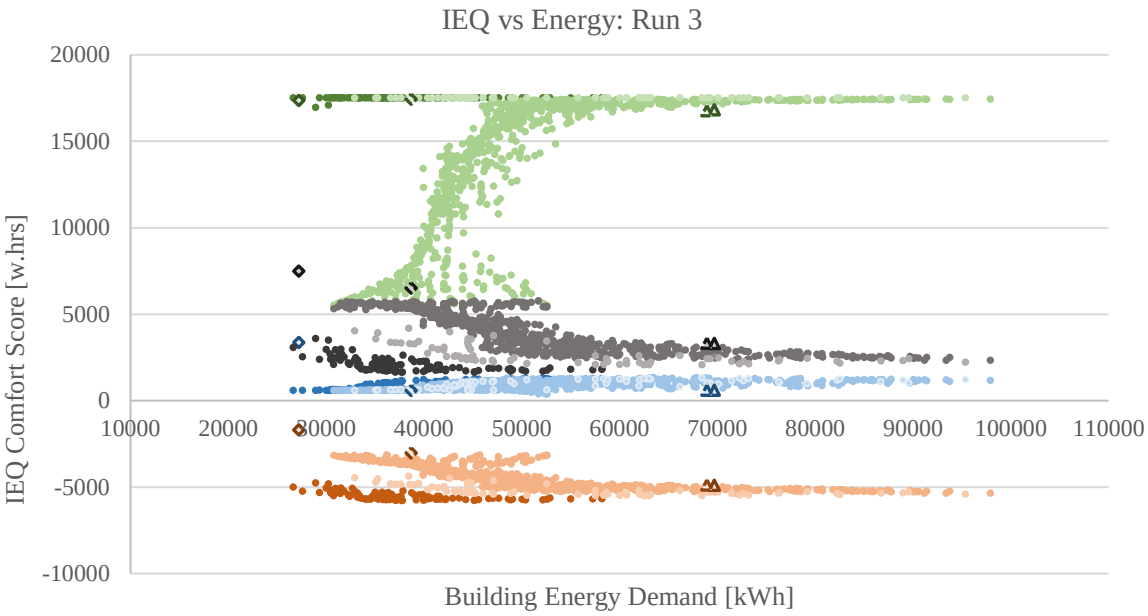

Figure 49: Pareto Optimal Solutions - Run 3

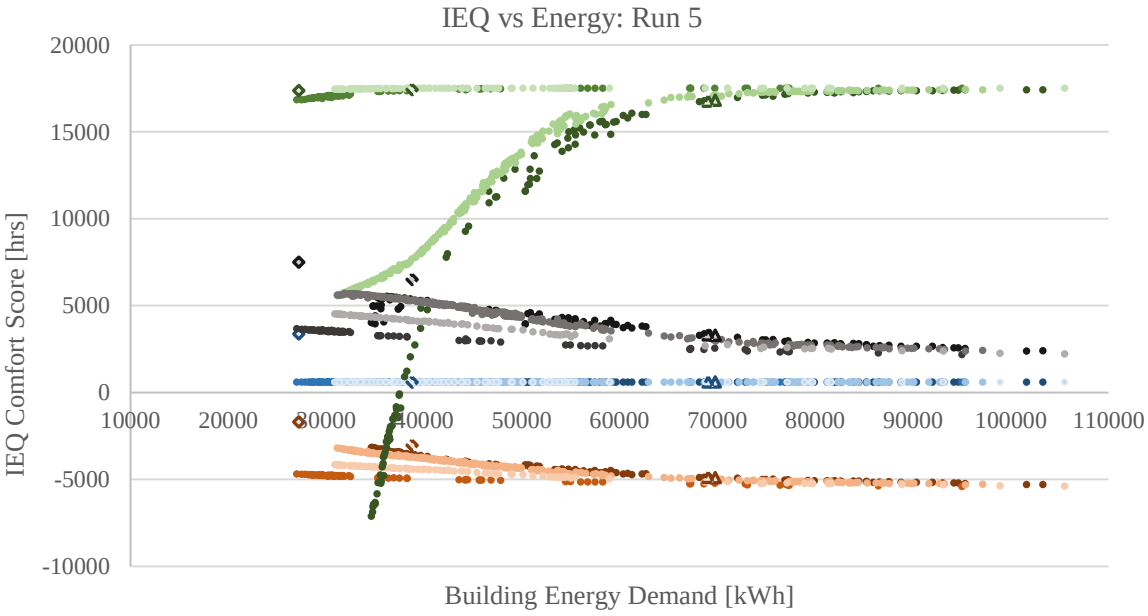

Figure 50: Pareto Optimal Solutions - Run 5

Legend of Figures 48, 49, and 50:

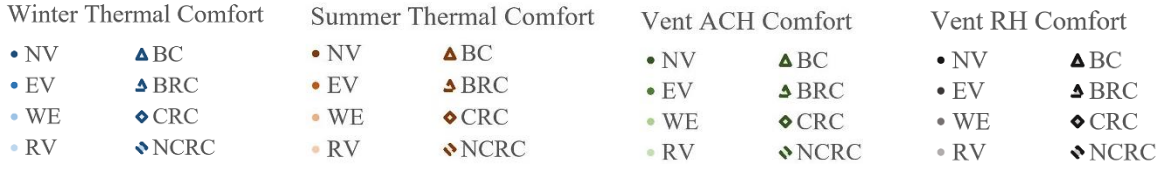

Insulated Cases

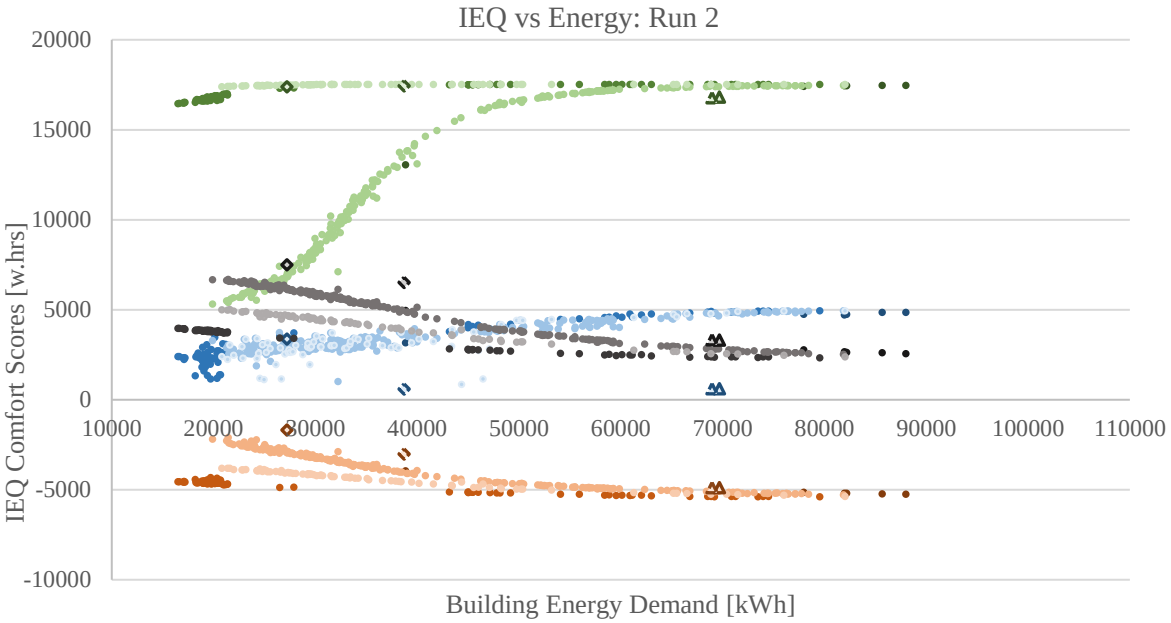

Figure 51: Pareto Optimal Solutions - Run 2

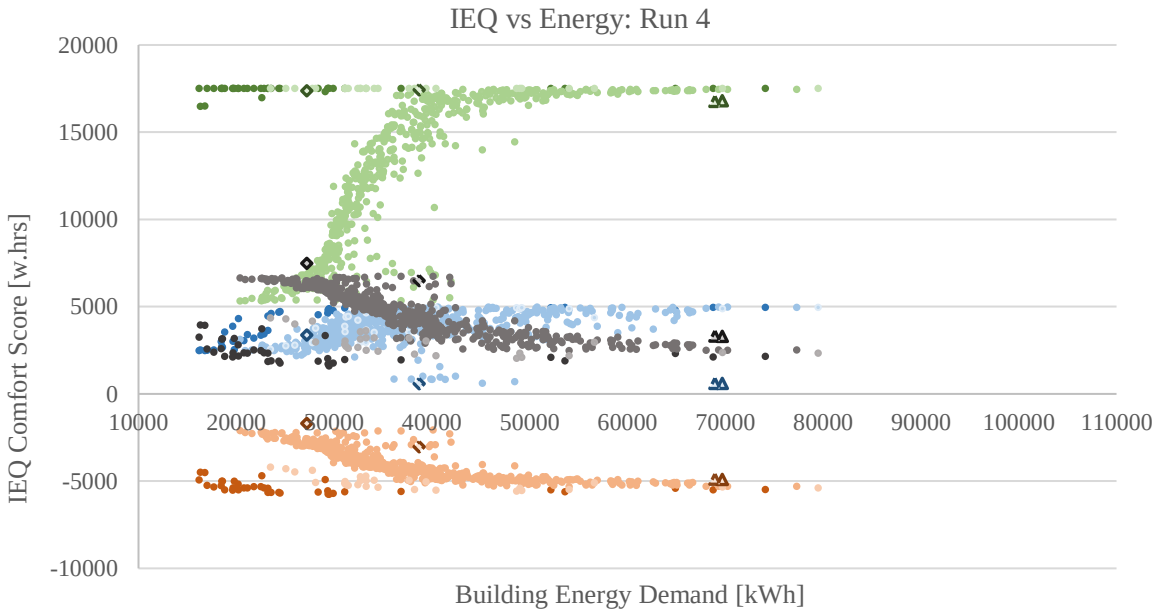

Figure 52: Pareto Optimal Solutions - Run 4

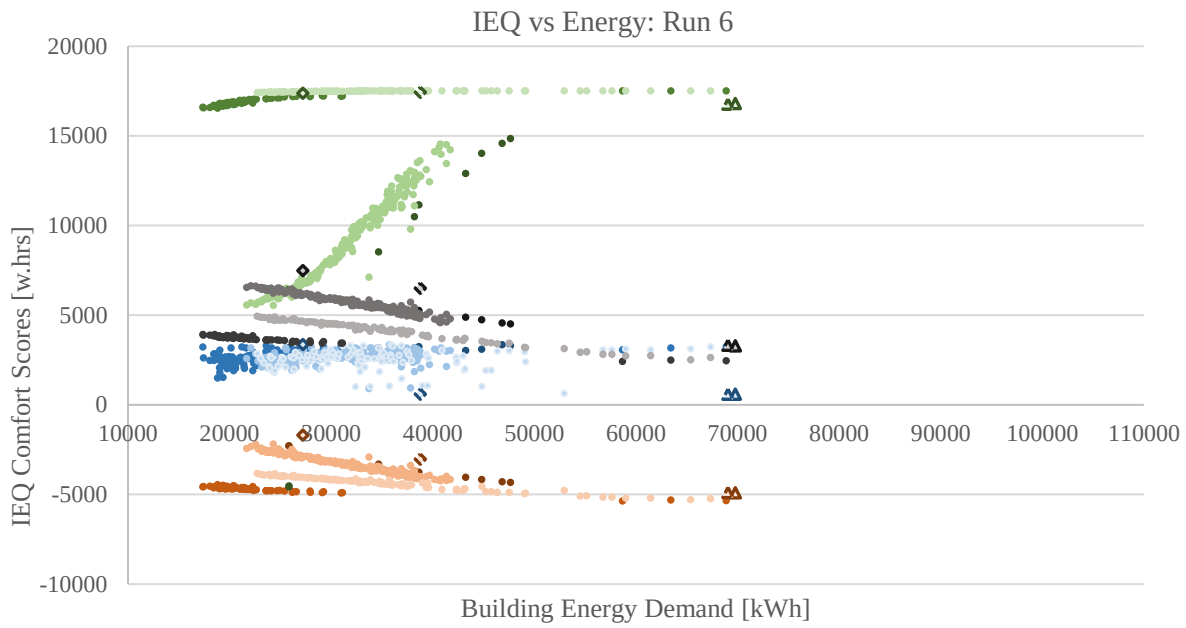

Figure 53: Pareto Optimal Solutions - Run 6

Legend of Figures 51, 52, and 53:

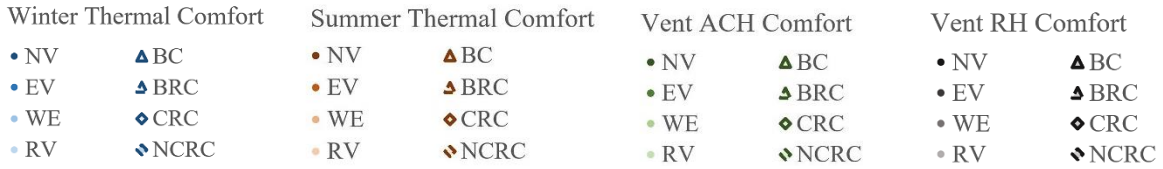

TOPSIS Analysis

The TOPSIS analysis on each set of Pareto-optimal solutions includes the comparative references, for contextualization, and forms the basis for the optimal retrofit recommendation.
The analysis results include each solution's closeness factor (C) and corresponding relative closeness ratio against the CRC (R) or the NCRC (R'), as defined in Chapter 9.2.

The performance distribution of the Pareto-optima relative to the references offers valuable insight into expected improvements across the retrofit variants, and helps identify effective and relevant options.
For non-insulated cases, the relative improvements' distribution is examined concerning CRC and NCRC (Refer to Figure 54 for Runs 1, 3, and 5). Insulated cases are only weighed against the CRC case (Refer to Figure 55 for Runs 2, 4, and 6).

Non-Insulated Cases

Figure 54: Relative Closeness Ratio Distribution - Non-Insulated Cases

Insulated Cases

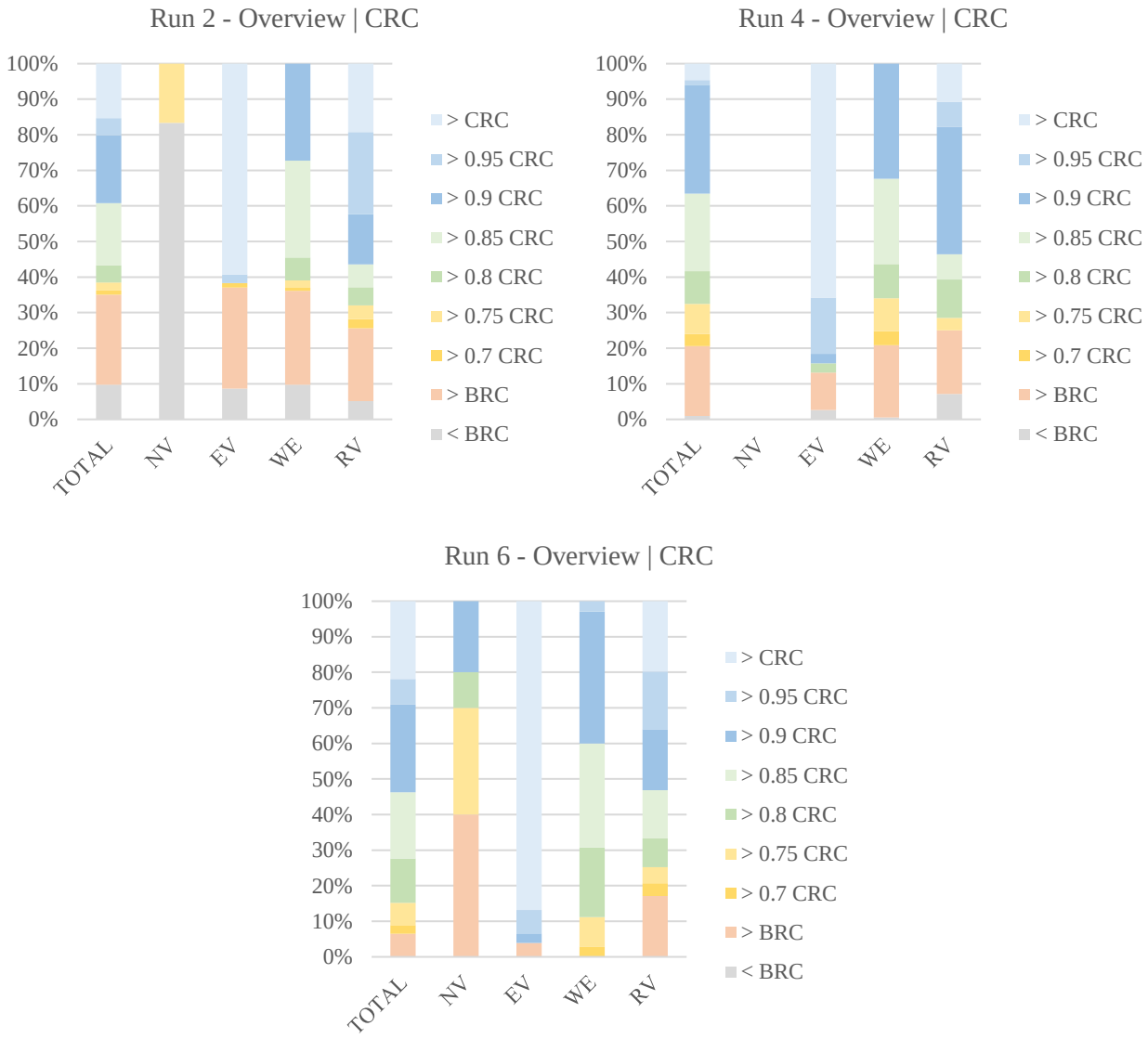

Figure 55: Relative Closeness Ratio Distribution - Insulated Cases

In order to define practicable retrofit recommendations, the focus was set on the solutions that achieve improvements comparable (or better) than the conventional retrofit. For this study, the comparable limit was set at a tolerance of 10% under the conventional retrofit level.

Isolating the top solutions, with a relative closeness ratio greater than 0.9, the results are distinguished between the different retrofit variants and used to develop recommendations.
These results are summarized in the form of boxplots characterizing the solutions' performance parameters, evidence to their achievable overall relative performance (C, R, and R') and detailed energy (t1) and IEQ (t2, t3, t4, t5) performance. The latter are weighed against the requisite airtightness levels, insulation thicknesses, and fan flowrates to achieving such performances.

The results are presented first for the Non-insulated cases, against NCRC (Refer to Figure 56 for Run 1, 57 for Run 3, and 58 for Run 5), and for the Insulated cases against CRC (Refer to Figure 59 for Run 2, 60 for Run 4, and 61 for Run 6).

The exhaustive results for the entire set of Pareto-optimal solutions are found under Appendix H.

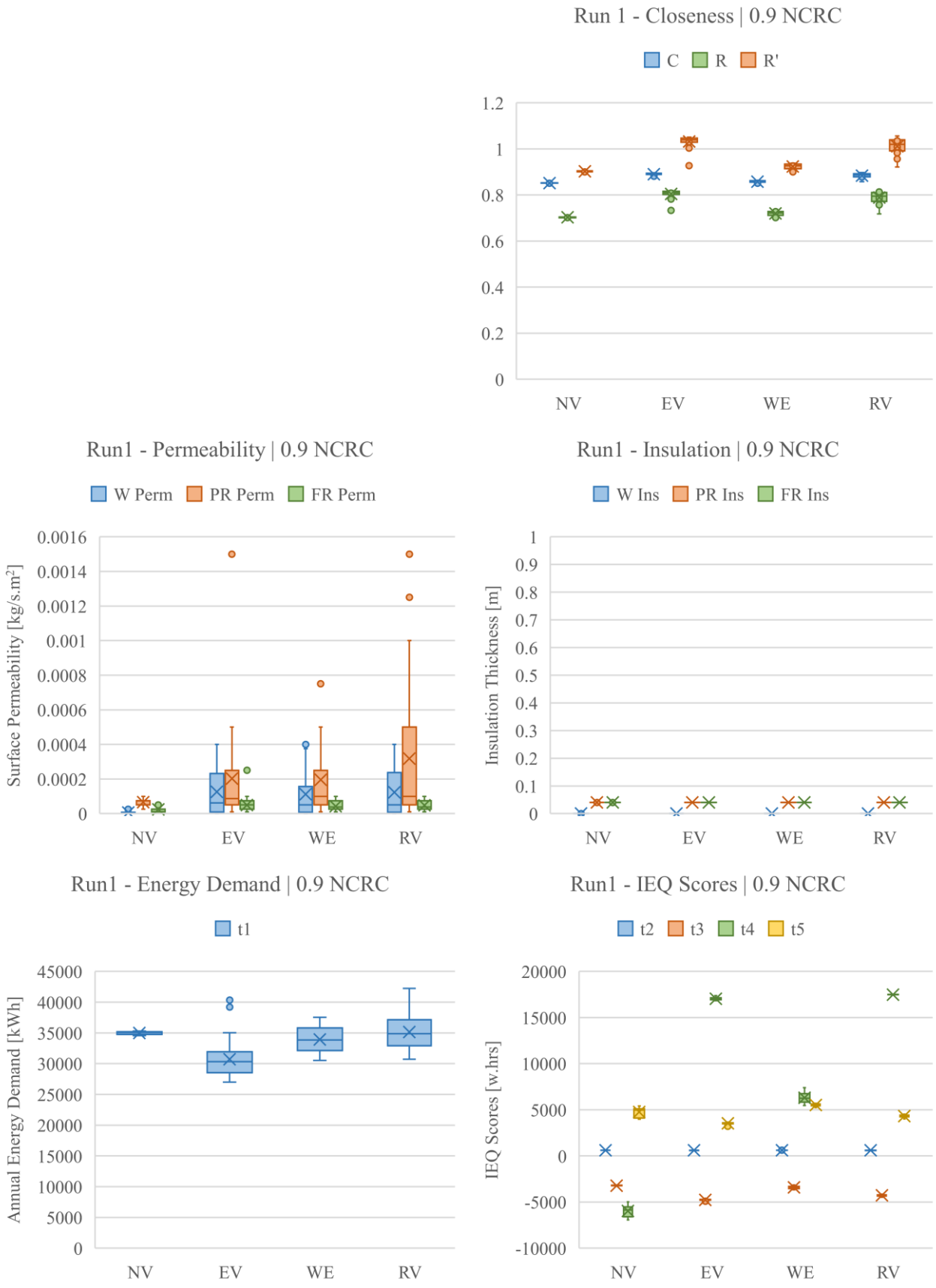

Figure 56: Design and Performance Parameters - Run 1 | 0.9 NCRC

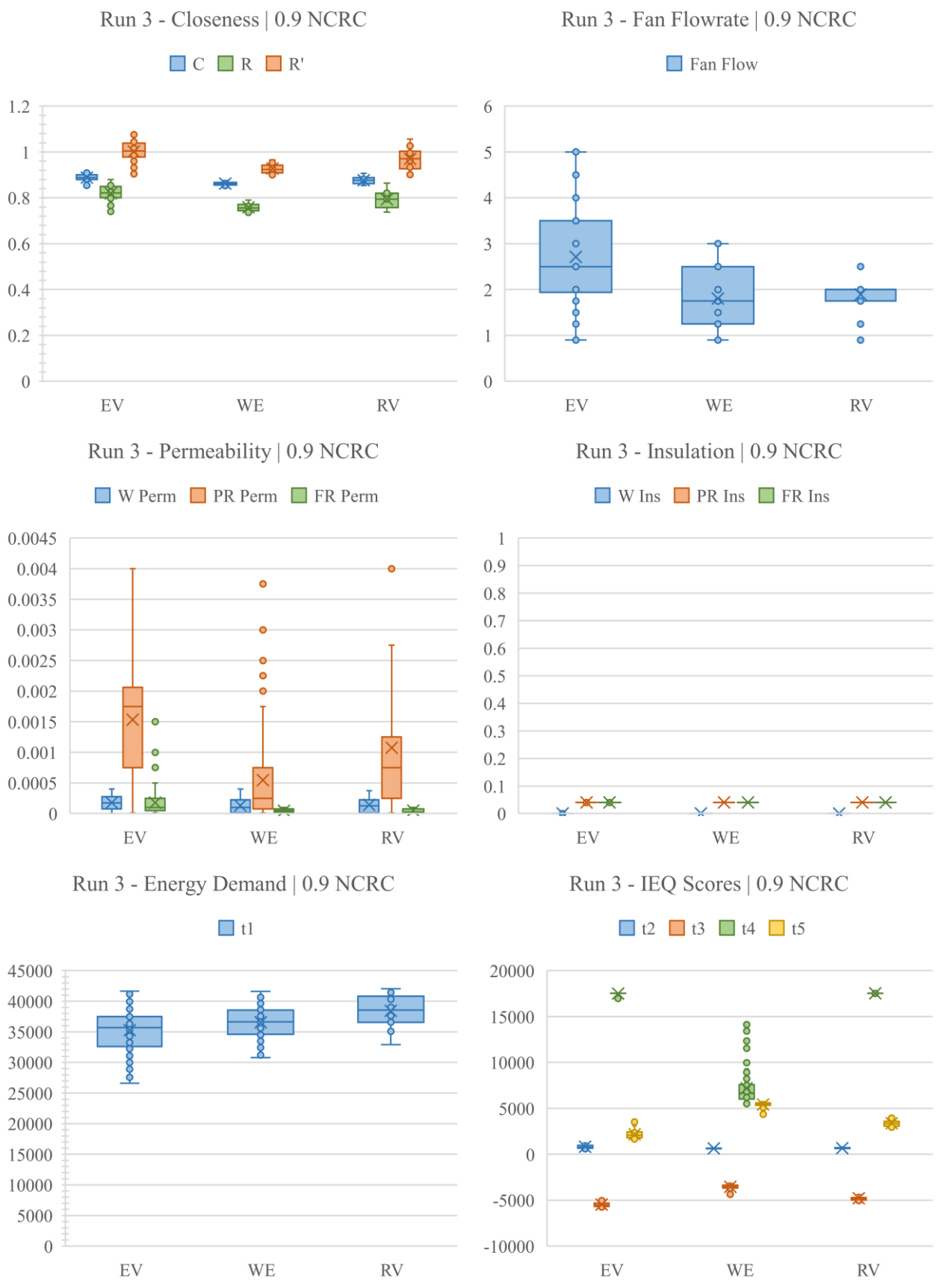

Figure 57: Design and Performance Parameters - Run 3 | 0.9 NCRC

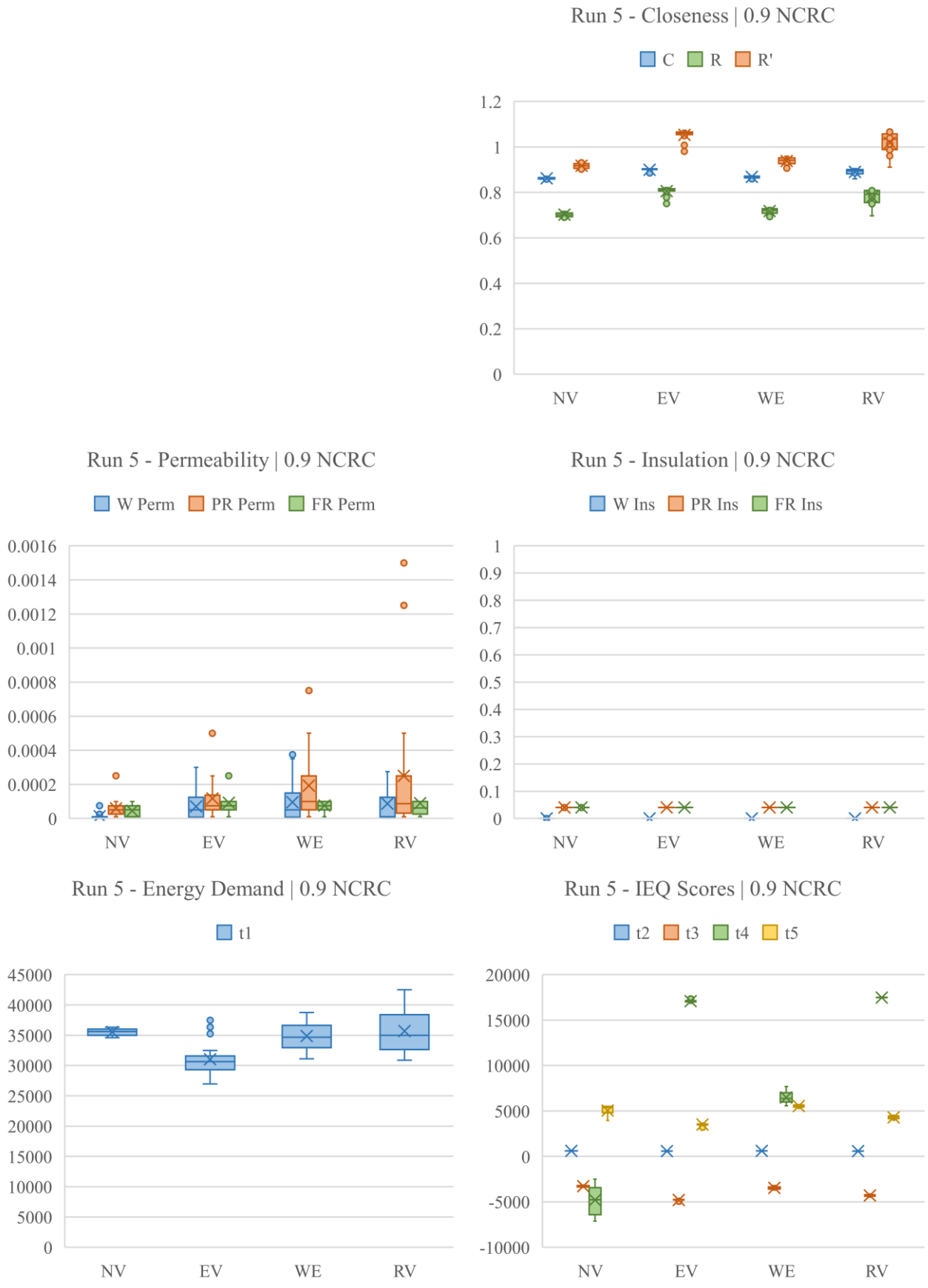

Figure 58: Design and Performance Parameters - Run 5 | 0.9 NCRC

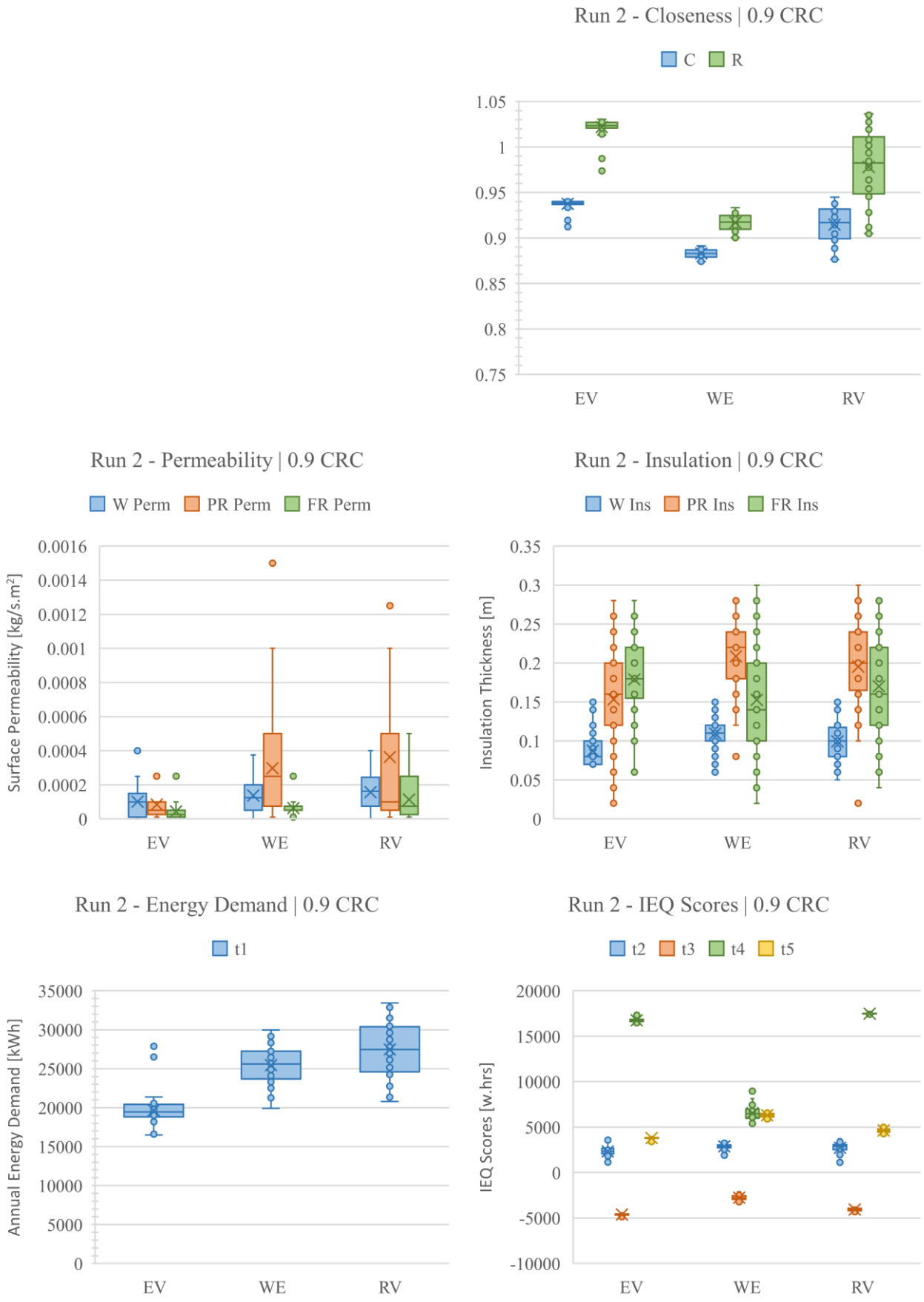

Figure 59: Design and Performance Parameters - Run 2 | 0.9 CRC

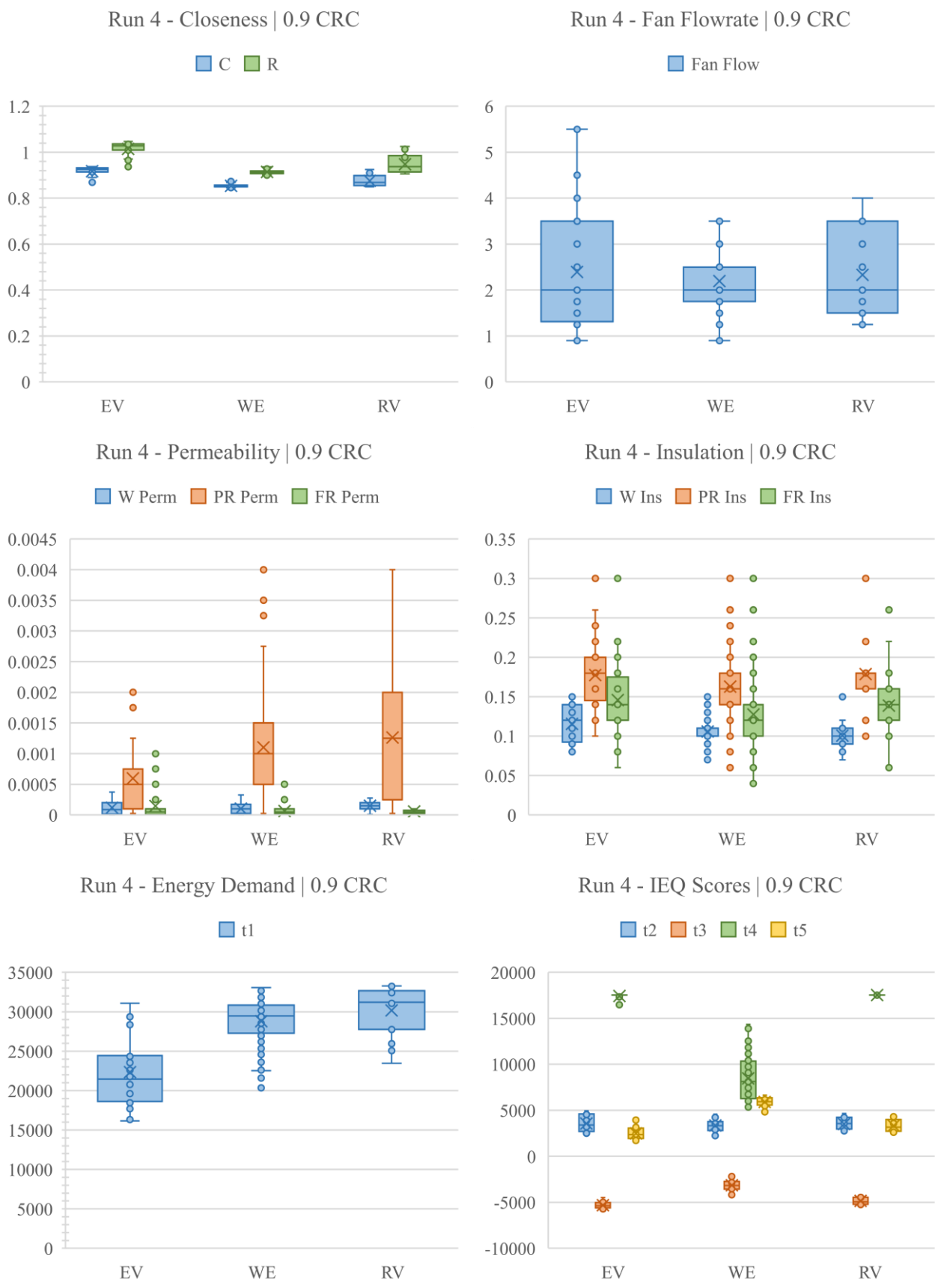

Figure 60: Design and Performance Parameters - Run 4 | 0.9 CRC

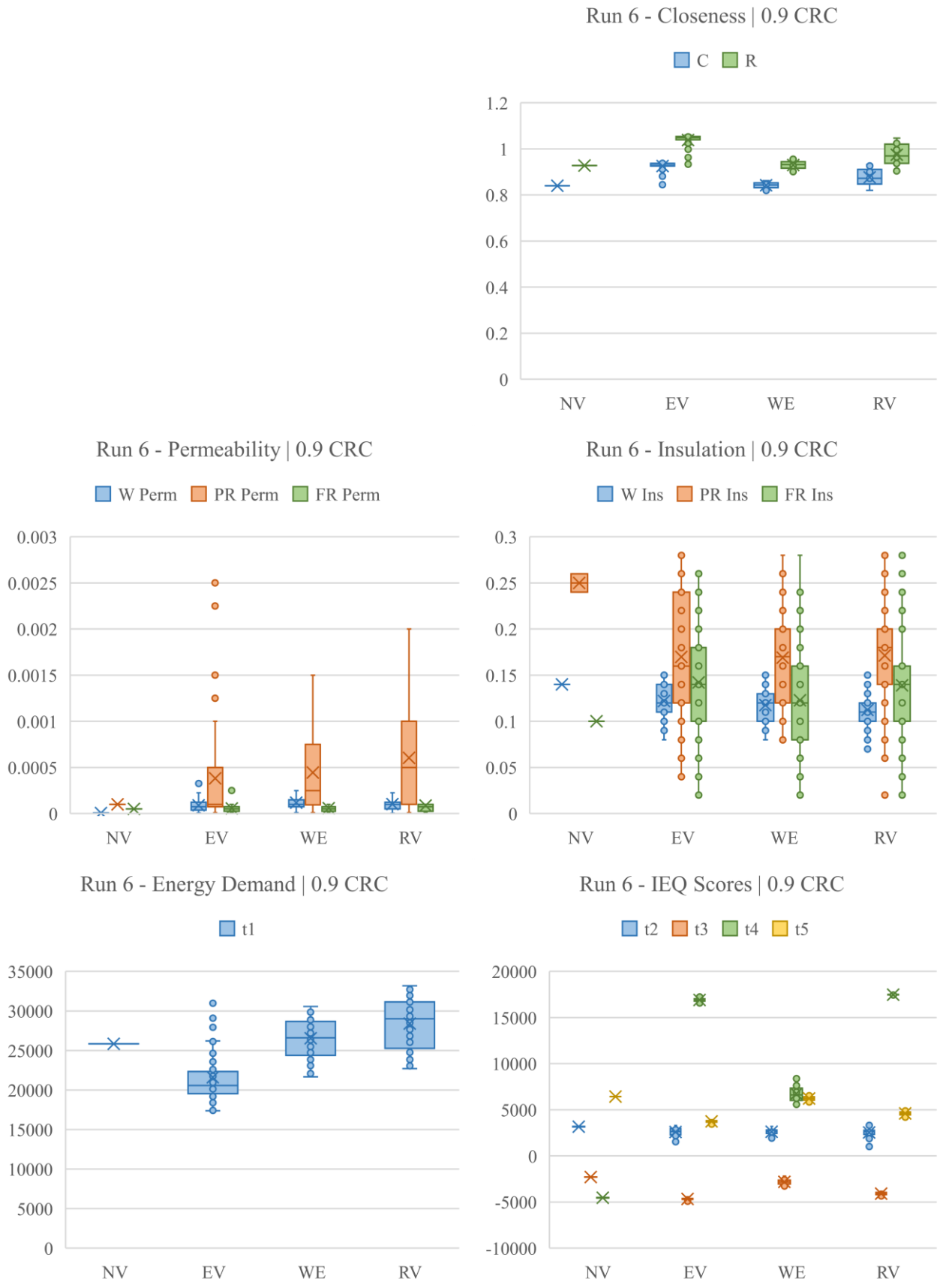

Figure 61: Design and Performance Parameters - Run 6 | 0.9 CRC

9.4. Analysis & Discussion

IEQ Score – Energy Demand Trade-off

Analyzing the Pareto-optimal solutions' distribution in terms of their IEQ Scores and Energy Demand (Refer to Figures 48 to 53) provides valuable insight into the complex variability of the trade-off under various retrofit options, as it was highlighted under Chapter 2.4.2.
This analysis helps pinpointing the variants that best mitigate the severity of the trade-off, allowing for high overall performance without significant compromises on individual performance aspects.

The observed performance improvements are bound to be more pronounced in insulated buildings. Although it can get relatively close to the CRC for most performance aspects, the non-insulated retrofits approach is not comparable to it. The insulated and non-insulated retrofit cases are then respectively set against the CRC and NCRC references.
Similar trends are observed when modifying the fan sizing factor (Ventilation-based vs IHR based) and construction dynamicity (Static vs Dynamic) in both insulated and non-insulated cases. These trends are described below.

Fan Flowrate Sizing

Increasing the fan flowrate beyond ventilation requirements results in a broader performance range, especially under the WE regime.

This reflects a wider range of the trade-off relationship between energy demand and IEQ. Nonetheless, the overall direction of this change leads to improved IEQ for the same energy demand, which could potentially be attributed to a better utilization of the IHR effect.

Different trends are noticeable under EV and RV regimes. While increased fan flowrates enhance winter thermal comfort by effectively utilizing the IHR effect, they marginally compromise summer thermal comfort and relative humidity (RH) performances.

Construction Dynamicity

Neglecting the dynamicity of the construction leads to minimal deviations in results, when the fan flowrate is limited to ventilation demands.

Although resulting in slight energy reductions met by higher IEQ, the difference is relatively small and suggest limited IHR effect at ventilation-based flowrates.

The more significant difference in the energy-IEQ trade-off at higher fan flowrates serves as compelling evidence to the increased IHR effect at these airflow levels.
This observation supports the claim that the variations in the trade-off relationship brought about by increased fan-flowrate (as described on the left) can be attributed to the influence of the IHR effect.

This implies that effective utilization of the air leakage's IHR effect may necessitate both the construction dynamicity and the high fan-assisted depressurization of the building, particularly in the heating season. These findings align with the literature, advocating for a dependable mechanical depressurization of the buildings in temperate climates (Refer to Chapter 2.4.2).
At low fan flowrates, the influence of the fan-induced depressurization on the building's pressure gradient is minimal, and may be dominated by the natural dynamic wind and stack effects driving the air leakage. The result is an unreliable depressurization of the building and consequent inward leakage, which prevents the full exploitation of the IHR effect.

Focusing on the relative performance of the ventilation regime variants in scenarios with dynamic constructions and IHR-based fan flowrates (Runs 3 and 4), two variants emerge as potential solutions that effectively balance energy-efficiency and IEQ. Further analysis of these variants is warranted.

The analysis of their relative performances is presented below.

Eligible Solutions

WE
- highest summer thermal comfort and RH performance
- high winter thermal comfort
- limitations in the ventilation ACH
- high energy savings

EV
- highest winter thermal comfort
- lowest summer thermal comfort and RH performance
- highest ventilation ACH
- highest energy savings

Ineligible Solutions

NV
- overall limited IEQ performance
- minimal energy savings

RV
- moderate summer and winter thermal comfort, and RH performance
- highest ventilation ACH
- good energy savings, but lower than WE and EV

Relative Closeness Ratio Distribution

The retrofit recommendation, however, targets retrofit approaches that improve the overall building performance, rather than specific component performance aspects. Each pareto-optimal solutions' overall performance is situated against its comparative reference case as a function of its relative closeness ratio (R against CRC and R' against NCRC)
Analyzing the distribution of the solutions' relative closeness ratio across the retrofit variants (Refer to Figures 54 and 55) sheds the light on potentially effective and relevant options.

The performance improvement from oversizing the fan flowrates to accommodate a more effective and reliable exploitation of the IHR effect is highlighted through a major decrease in low-performing solutions (represented in red and grey) between Runs 1 and 3 for non-insulated retrofits, and Runs 2 and 4 for insulated retrofits.

Such improvement is best manifested under the EV regime in non-insulated buildings, whereby the fraction of low performing solutions drops from a high 67% to less than 10%, and is met by an opposite increase in high-performing solutions (represented in blue).
In insulated buildings, the EV regime also leads the improvements. However, the decrease in low-performing solutions is less pronounced and more closely followed by the results of the WE regime.

Additionally, high performing solutions (represented in blue) mostly reveal comparable distributions under the dynamic scenarios (Runs 1 to 4), and even higher fractions in the static scenarios (Runs 5 and 6). No conclusions could be inferred from this observation without further knowledge of the airtightness strategy adopted to achieve such high-performing buildings: the modern build tight-ventilate right approach, or the alternative exploitation of the air leakage and IHR effect (described in Chapter 1.1.4).

As comparably high performances are achievable under both low- and high- exploitation of the IHR effect, the determining argument in this case falls on minimizing the level of intrusiveness of their requisite retrofit interventions, including the airtightness level to be realized.

Another key observation is that, under both ventilation-based fan flowrates (Run 1 and 2) and IHR-based fan flowrates (Run 3 and 4), performances comparable to the CRC are not realistically achievable without enhancing the envelope's thermal resistance through insulation. The highest improvement met in non-insulated buildings amounts to around 88% of the CRC improvement, which is still a significant performance considering the complete lack of added insulation.
Nonetheless, non-insulated retrofits can meet and even surpass the realistically attainable performance

of the Non-insulated Conventional Retrofit (NCRC) alternative in buildings with heritage-protected interior surfaces.

These findings further substantiate the existing literature (Refer to Chapter 2.4.2), supporting the following factors for effective performance in buildings with dynamic constructions:

1. An inherently well-insulating construction, designed as a composite masonry-insulation structure for higher IHR efficiency (lower U-values at lower airflow rates).
2. A mechanically-assisted depressurization of the building, sized to accommodate a sufficient and reliable IHR exploitation.

Moreover, a notable finding in both insulated and non-insulated buildings with dynamic constructions is the inherent limitation of achieving high performances, comparable to the CRC, under a natural ventilation (NV) regime. Their maximum attainable performance considers:

Non-insulated Buildings

- Upper limit of > 0.7 CRC
  - However, equivalent to > 0.9 NCRC and meeting high-performance relative to buildings with heritage-protected interior surfaces

Insulated Buildings

- Upper limit of > 0.75 CRC
  - Not ideal in buildings with no heritage-protected interior surfaces

Natural Ventilation is thus not favorable when targeting the optimization of the overall post-retrofit building performance, although providing for acceptable performances under the context of buildings with protected interior surfaces.
In the unlikely case of stringent heritage restrictions with limitations on mechanical fans' installation, natural ventilation could be considered. The requisite design parameters and associated performance objective functions are then presented in the Table 27 below.

Table 27: Design and Performance Parameters - Natural Ventilation

Non-insulated Buildings	**Design Parameters**		
	Air Permeability [kg/s.m2]	W	0.000025
		PR	0.00005
		FR	0.000025
	Insulation Thickness [m]	W	0
		PR	0.04
		FR	0.04
	Performance Objective Functions		
	Energy [kWh]	t1	35142.8
	IEQ Score [w.hrs]	t2	602.3
		t3	-3232.0
		t4	-5649.2
		t5	5123.5
Insulated Buildings	**Design Parameters**		
	Air Permeability [kg/s.m2]	W	0.000175
		PR	0.00005
		FR	0.0005
	Insulation Thickness [m]	W	0.11
		PR	0.26
		FR	0.20
	Performance Objective Functions		
	Energy [kWh]	t1	38828.5
	IEQ Score [w.hrs]	t2	3161.1
		t3	-3951.6
		t4	13062.1
		t5	4955.5

Hence, the achievable performance under a NV regime is suboptimal, both in terms of energy-savings and IEQ performance, and the associated airtightness and insulation requirements are stringent. In other words, the air leakage is still regarded as overhead and not exploited in the post-retrofit design. The NV regime thus fails to serve the main aspect of the target retrofit strategy, namely, the effective exploitation of the air leakage into the optimal post-retrofit building performance

Performance and Design Parameters Distribution

The detailed performance and design parameters results (Refer to Figures 56 to 61) further reflect the above-identified trends. Namely, the role of insulation and the building's mechanical depressurization in efficiently harnessing the IHR effect, as well as the relative performance of the ventilation regime variants in achieving efficient IHR utilization:

- The EV and WE deliver superior energy-savings while accommodating higher surface permeability, and thus efficiently exploiting the IHR effect.
- The RV exhibits performances and requirements almost up to EV and WE standards but with greater implementation intrusiveness.
- The NV, acceptable only in buildings with heritage-protected interiors, offers sub-optimal overall performance and relies on the conventional surface sealing.

The retrofit recommendation, however, focuses on high-performing solutions exploiting the building's air leakage as practically possible.
High-performing solutions are defined as "solutions with overall performances comparable or better than the equivalent conventional retrofit case (CRC or NCRC), assuming a tolerance of 10%". Meaning, these are the solutions with a relative closeness ratio greater than 0.9.

The retrofit recommendations are, accordingly, selected among the studied retrofit variants based on:

1. Their ability to achieve performances comparable (or better) than the conventional retrofits
2. Their ability to achieve such performances while minimizing the interventions on the building as practically possible. This particularly considers the potential to preserve the building's existing air leakage and permeability into its post-retrofit design.

Considerations of particular importance in this selection consider, under all scenarios:

The variability and adaptability of natural ventilation options

Optimal ventilation performance is achieved through fan operations, providing satisfactory air change rates to ensure indoor air quality.

When natural ventilation is adopted, all year for NV and in summer for WE, greater variability is detected in the building's air change rate due to dynamic natural processes governing the pressure gradients across the building envelope.

To maintain sufficient ventilation in these cases, occupants often compensate through more frequent window opening. This approach is suitable under the WE regime, as window opening in summer does not compromise the building's energy demand and might further improve its summer thermal comfort. It is thus safe not to penalize the WE regime for its seeming summer ventilation shortcomings. However, frequent window opening for the NV regime results in increased heat loss during winter and, consequently, higher energy demand or reduced thermal comfort.

The inherent intrusiveness of mechanical ventilation options

Exhaust fan-based ventilation (EV and WE) may rely on exhaust fans in the wet rooms for both the building depressurizion and expulsion of stale air, making them less intrusive and more straight-forward to implement.

In contrast, reversible ventilation (RV) requires fan installation in living or circulation spaces, which is typically more disruptive to the building. Indeed, unlike the exhaust, the supply of air through the wet rooms in not desirable as they lead to the spread of the wet room air into the living spaces (Refer to Figure 62).

All systems are, however, less intrusive than a full balanced ventilation system with heat recovery.
Considering the RV system's inherent intrusiveness, it can only be preferred when it offers significantly higher performance and more flexible design requirements than EV and WE.

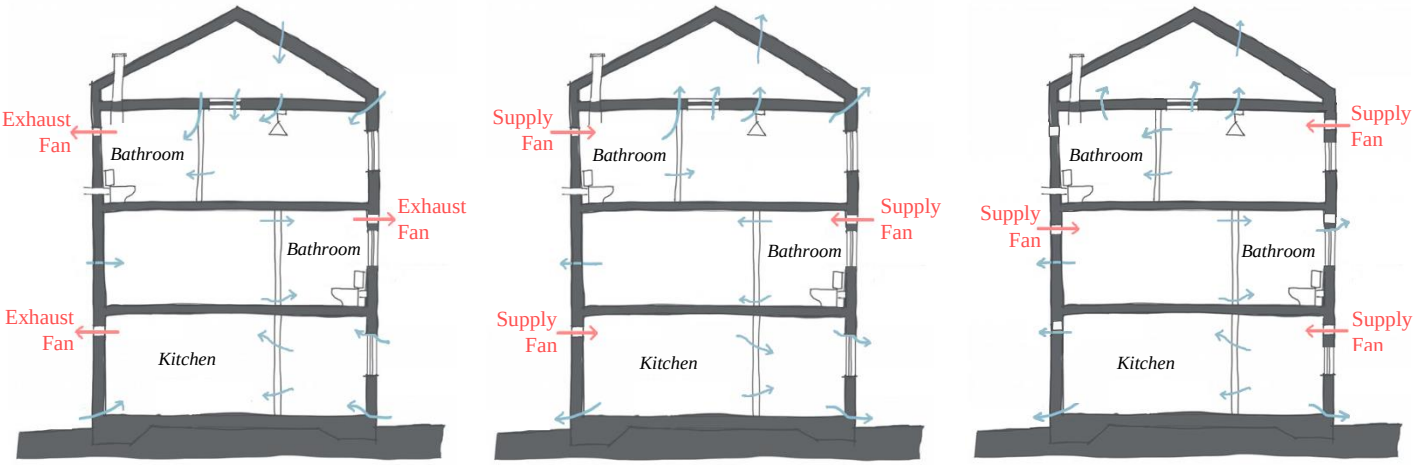

Figure 62: Building Air Movement under Exhaust Ventilation in Wet Rooms (left), and Supply Ventilation in Wet Rooms (middle) and Living Spaces (right)

Accordingly, the ventilation regime identified to hold the highest potential under each of the studied scenarios are presented in the Table 28 below, along with their supporting arguments. The predominance of the EV regime's performance under all scenarios is already clear.

Table 28: Best-performing Ventilation Regimes per Scenario

	Non-Insulated Construction *Heritage-protected interior surfaces*		Insulated Construction *Non-heritage-protected interior surfaces*	
Dynamic Ventilation-based Fan Flowrate	Run 1:	〉 EV	Run 2:	〉 EV
	Energy Savings	Highest	Energy Savings	Highest
	IEQ Scores	All comparable	IEQ Scores	All comparable
	Permeability Levels	Highest on all surfaces	Permeability Levels	Highest (All but PR)
	Insulation Thicknesses	All comparable	Insulation Thicknesses	All comparable
	Intrusiveness Level	Least (after NV)	Intrusiveness Level	Least (after NV)
Dynamic IHR-based Fan Flowrate	Run 3:	〉 EV	Run 4:	〉 EV
	Energy Savings	Highest	Energy Savings	Highest
	IEQ Scores	All comparable	IEQ Scores	All comparable
	Permeability Levels	Highest on all surfaces	Permeability Levels	Highest (all but PR)
	Insulation Thicknesses	All comparable	Insulation Thicknesses	All comparable
	Intrusiveness Level	Least	Intrusiveness Level	Least

Surface Permeability – Energy Performance Relationship

The above results, however, bin all potentially achievable energy and IEQ performances with all potential permeability levels, and fail to transpire the actual relationship between the two. Selecting the best method for the efficient exploitation of air leakage into the building's post-retrofit performance asks for a more detailed examination of the permeability-performance pairs under the different ventilation regimes for each of the 4 dynamic scenarios. Comparing these relationships with the static results highlights whether or not accounting for the construction dynamicity in simulations is worthy or a static simplification of the model would result in comparable and acceptable results.

In terms of IEQ performances, all solutions show comparable ranges with little spread. Being selected from the top performing Pareto-optima, all indeed achieve similar satisfactory IEQ results.
For this reason, the comparison is to focus on the relationship between permeability and energy demand, and identify the retrofit alternative providing for the best compromise between them.

Also, as the highest intrusiveness of the RV systems (described above) is met by comparable permeability limits and lower energy-saving potential as the WE and EV counterparts under all retrofit cases, the RV regime will be discarded as a potential optimal solution further in the analysis. The detailed results of the EV and WE regimes are then presented in Figures 63 and 64, respectively for insulated buildings and non-insulated buildings.

The results under the insulated and non-insulated scenarios reveal a clear parallel, leading into comparable retrofit recommendations.

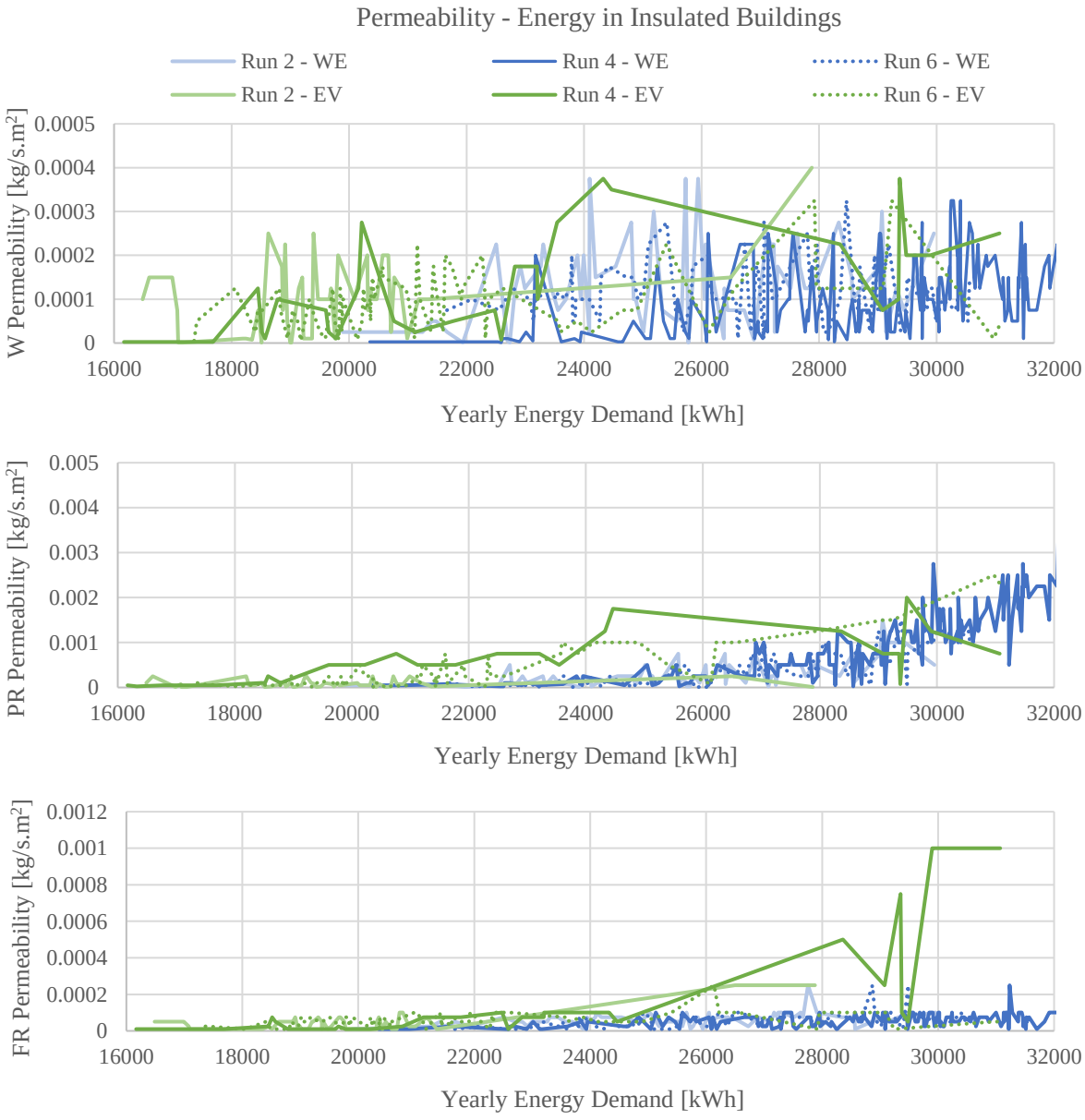

Figure 63: Permeability vs Energy - Insulated Buildings

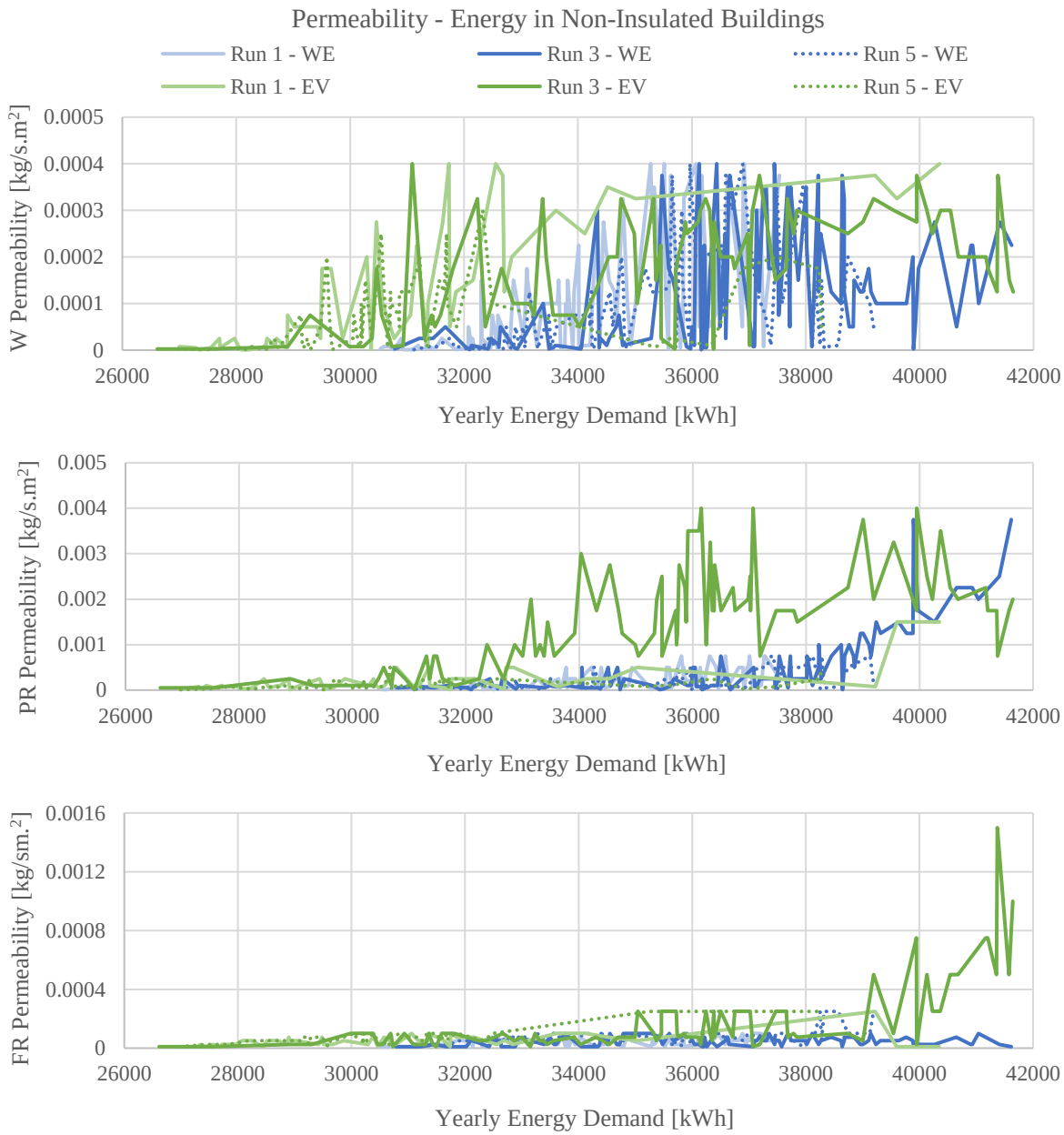

Figure 64: Permeability vs Energy - Non-insulated Buildings

For insulated buildings (shown in Figure 63), achieving an energy demand below 19000 kWh requires high airtightness of most surfaces.
With the CRC's energy demand falling at 27 197.0 kWh, a retrofit alternative with a demand anywhere between 20 000 kWh and 27 000 kWh would already be outperforming the CRC. This implies that over-sealing the surfaces in an attempt to reach less than 19 000 kWh of annual energy demand would be superfluous.

Targeting an energy demand in the range of 20 000 – 27 000 kWh, the WE regime generally fails to provide the same energy-savings as the EV regime without a stricter sealing of most surfaces. Additionally, at the exception of some peaks, the operation of the EV regime at higher fan flowrates (Run 4) clearly allows for higher permeability levels relative to its operation at the minimum ventilation flowrate (Run 2) and its equivalent static scenario (Run 6). The latter is of particular importance for walls (W) and the pitched roof (PR), as the flat roof (FR) might require some sealing under all scenarios.

The difference in the allowable permeability limit between the dynamic scenarios and their static counterpart is more distinguishable under Run 4 than Run 2, further supporting that higher fan flowrates are required to achieve a measurable IHR effect. Such results reiterate the significant potential of the IHR contribution to the building performance.

For non-insulated buildings (shown in Figure 64), achieving energy-savings of CRC standard, by reducing the energy demand to 27 000 kWh, is only possible through the tight sealing of most surfaces. This is the case for achieving energy demand anywhere below 31 000 kWh.
Situating the retrofit performance against the Non-insulated Conventional Retrofit Case (NCRC) with an energy demand is of 38 709.2 kWh, the target demand falls in the range of 31 000 – 38 000 kWh.

Applying the same rationale as in the insulated case, similar trends are observed. This includes:

- The higher sealing required for most surfaces to achieve the same energy-savings under the WE regime as in the EV regime
- The necessary sealing of the flat roof (FR) under all scenarios
- The clear permeability advantages of operating the EV regime at higher fan flowrates through a better exploitation of the IHR effect in the construction.
  Although, for energy demands within 35 500 – 38 000 kWh, the WE and EV regimes under all runs follow more of less the same wall permeability trends, the latter does not apply for the remaining surfaces.

Optimal Retrofit Strategy and Design Parameters Combinations

For both insulated and non-insulated buildings, the EV regime operating at higher fan flowrates – sized to accommodate an efficient IHR exploitation through the dynamic constructions – appears to deliver superior energy-savings while allowing the preservation of higher surface permeabilities.

Implementing the identified optimal strategy on the Case Study building, the various combinations of surface permeability levels, insulation thicknesses, and fan flowrates result in varying energy-saving levels illustrated in Figures 65 and 67 below, under the insulated and non-insulated cases respectively. All solutions, selected among the top-performing Pareto-optima, are considered to achieve comparable ranges of IEQ performance.

The optimal combinations of surface permeability, insulation thickness, and fan flowrate requirements are then selected among the solutions within the target energy-saving range, defined in the analysis above for insulated and non-insulated buildings. Such combinations aim for the highest possible surface permeabilities providing for a given performance in this range.
Accordingly, 5 and 8 solutions are respectively selected for the optimal retrofit of the building under insulated and non-insulated conditions, and presented in the Figures 66 and 68 below.

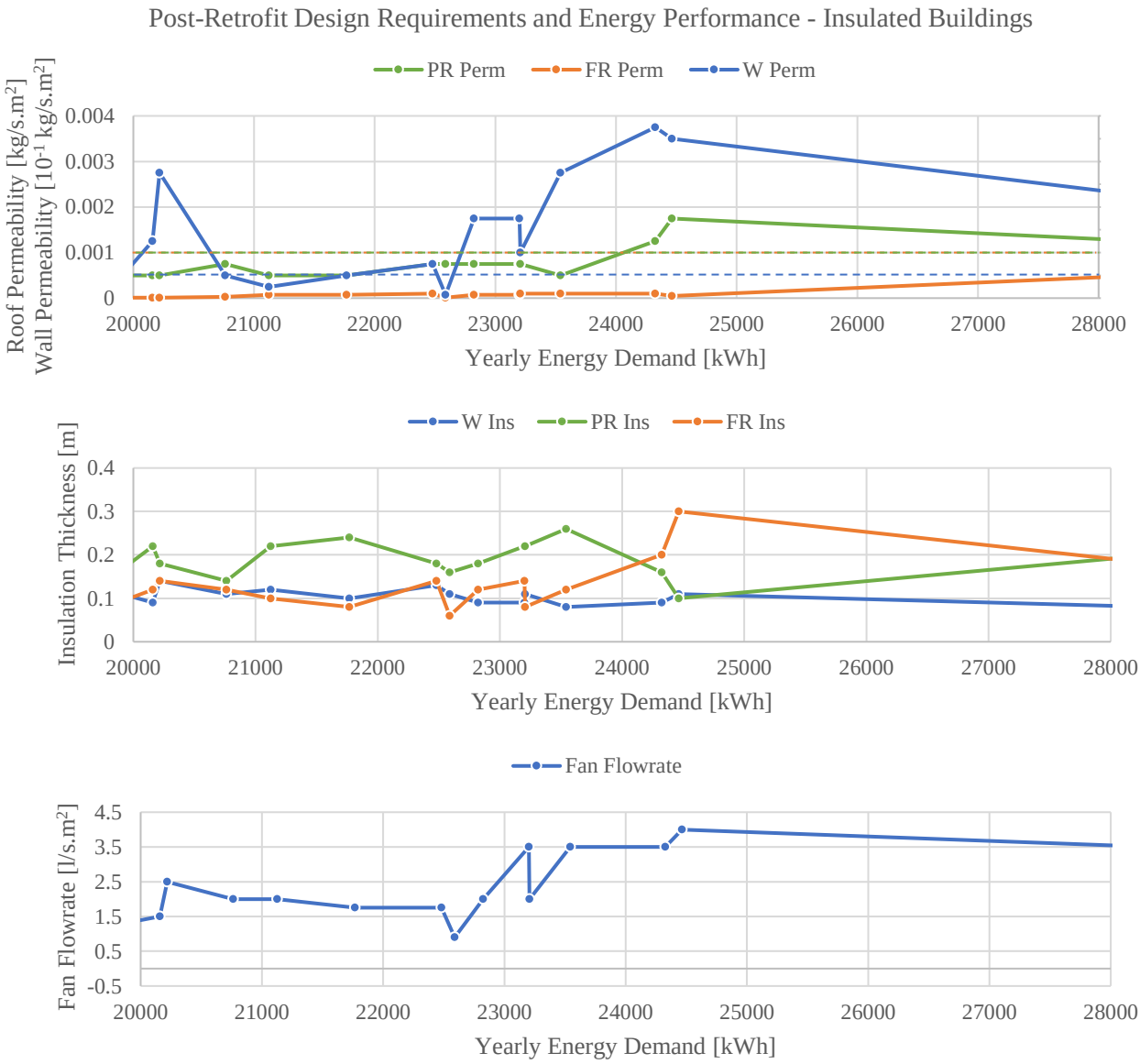

Figure 65: Post-Retrofit Design Requirements and Energy Performance - Insulated Case

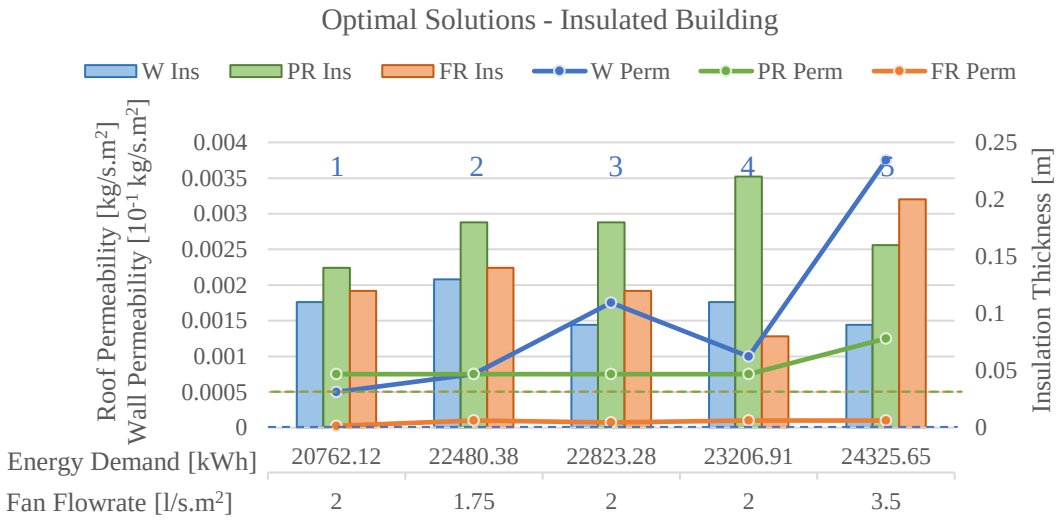

Figure 66: Optimal Solutions - Insulated Case

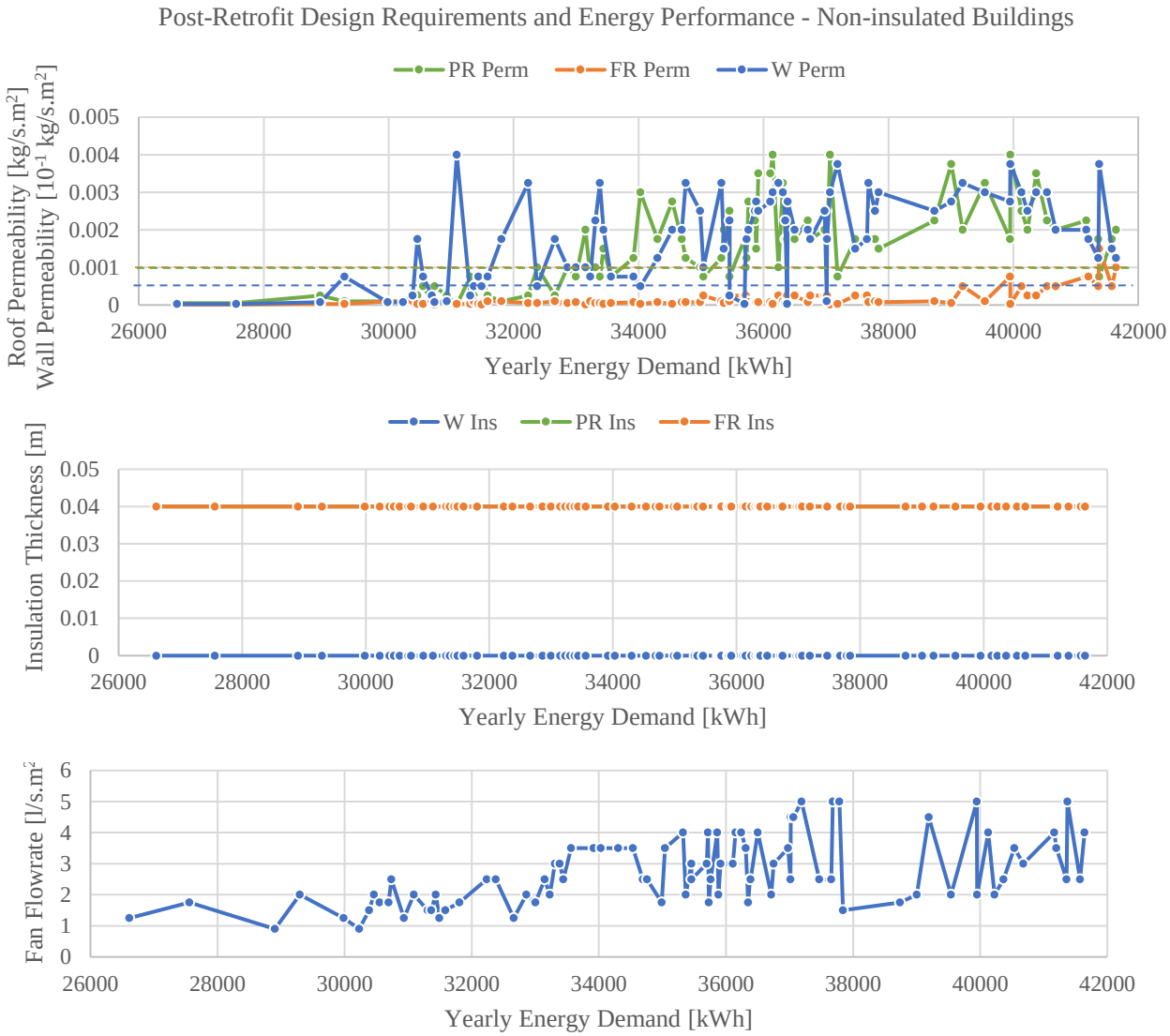

Figure 67: Post-Retrofit Design Requirements and Energy Performance - Non-insulated Case

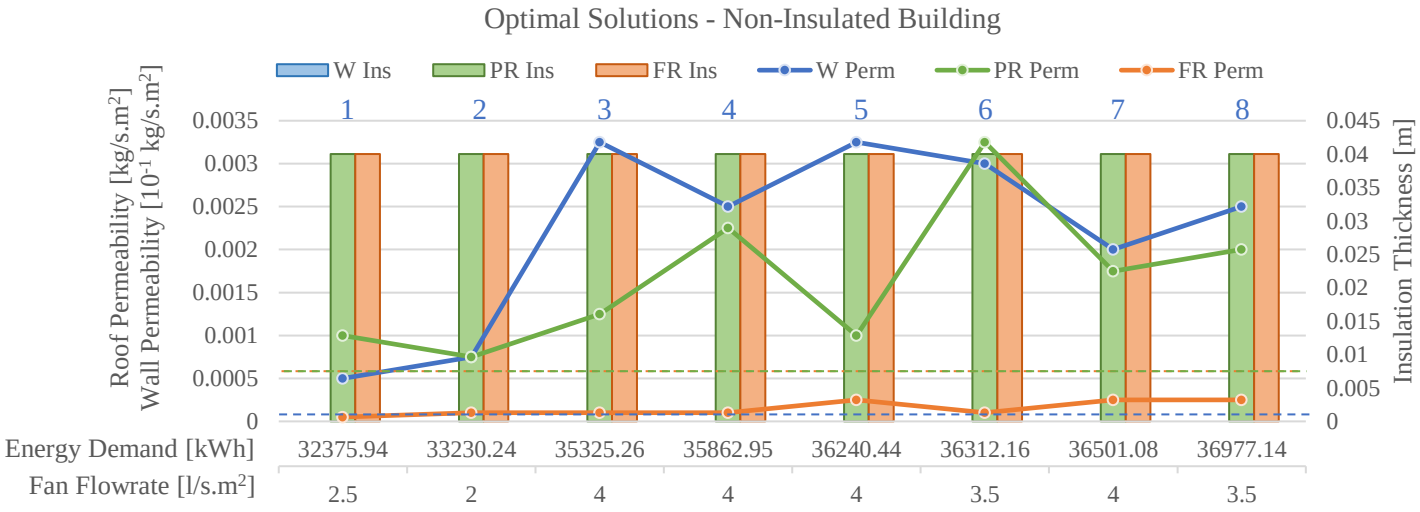

Figure 68: Optimal Solutions – Non-insulated Case

As per the calibrated air leakage model (Refer to Chapter 7.2), the Case Study building's surface permeability in the Base Case (BC) was defined at:

- Walls: 0.0000518 kg/s.m^2
- Pitched Roof: 0.001137 kg/s.m^2
- Flat Roof: 0.001137 kg/s.m^2

Comparing the Base Case (dashed lines) to the post-retrofit permeability of each envelope surface (Refer to Figures 66 and 68), the most suitable combination of airtightness, insulation, and fan flowrate for the Case Study building's retrofit that provides for minimal sealing of the existing air leakage considers the solution 5, in the insulated case, and solution 1, in the non-insulated case.

These solutions are preferred in the specific context of the Case Study building as they provide for the highest energy-savings while satisfying the following conditions:

- Outperforms the CRC
- Requires no sealing on either the walls or the pitched roof
- Requires only sealing on the flat roof, however needed in all solutions.

Proof of Concept

Due to the lack of added insulation in the non-insulated case, all energy-savings improvements may be attributed to changes in the surface permeabilities and fan flowrates, in other words, changes in the air leakage flow. The effectiveness of the IHR effect thus transpires when looking at certain sets of Pareto-optimal solutions, represented in the Figures 69 to 72.

The potential to achieve heating energy-savings by increasing air infiltration through the envelope (by higher permeability and/or higher fan flow rate) is in direct contradiction with the conventional approach to air leakage and presents as a proof of concept to the effectiveness of the retrofit strategy optimizing the design of traditional breathable construction to operate as dynamic insulations.

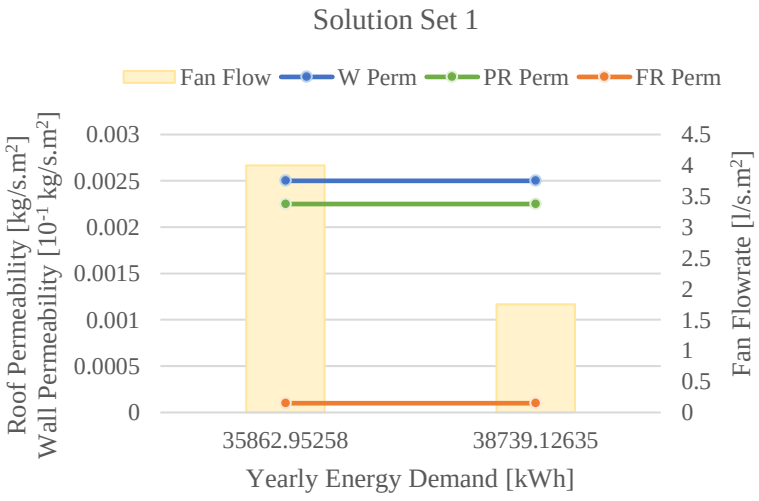

Figure 69: IHR Effect in Solution Set 1

- Maintaining the same envelope properties (permeability & insulation), the energy demand is significantly decreased by around 3000 kWh/year by increasing the exhaust fan flowrate from 1.75 to 4 l/s.m^2.

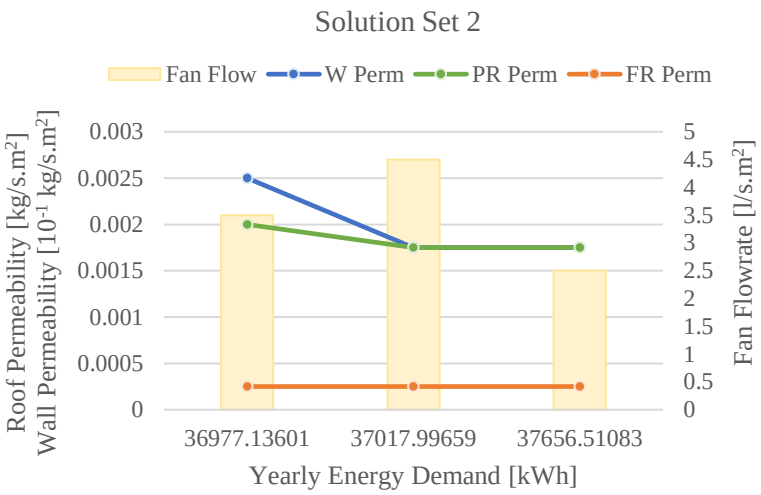

Figure 70: IHR Effect in Solution Set 2

- Maintaining the same envelope properties (permeability & insulation), the energy demand decreases by 640 kWh/year by increasing the exhaust fan flowrate from 2.5 to 4.5 l/s.m^2.
- Higher energy savings, down to 36977 kWh may be achieved at lower fan flowrates if the surface permeabilities of the walls (W) and pitched roof (PR) are also increased.

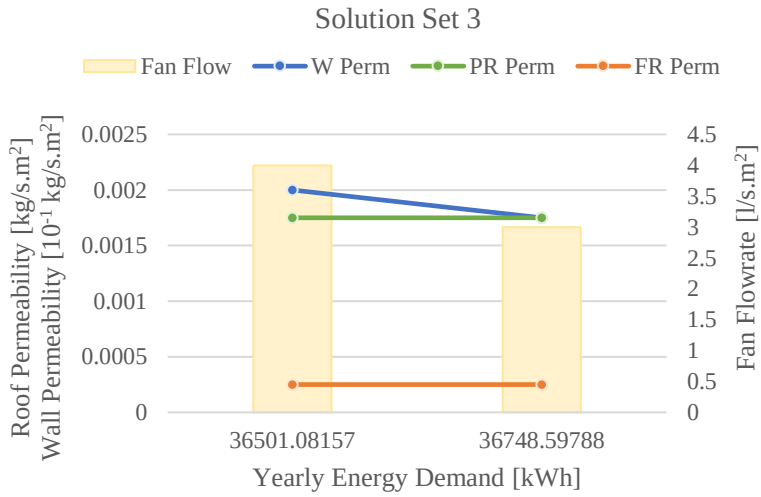

Figure 71: IHR Effect in Solution Set 3

- Increasing the wall (W) permeability only with an 1 l/s.m^2 increase in the fan flowrate entails a drop in the yearly energy demand from 36749 to 36501 kWh.

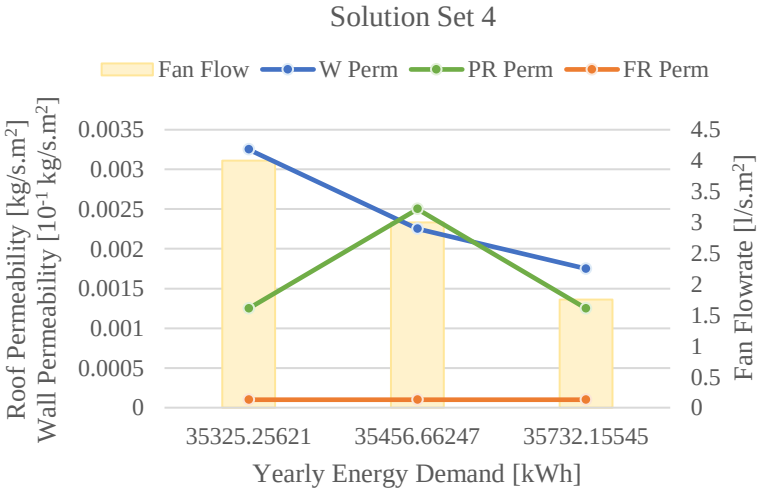

Figure 72: IHR Effect in Solution Set 4

- Reducing the energy demand from 35732 to 35457 kWh is possible by increasing both wall (W) and pitched roof (PR) permeabilities, along with an increase in of the flowrate from 1.75 l/s.m^2 to 3 l/s.m^2.
- Higher energy-savings, down to 35325 kWh, are possible through an increase of the permeability of the walls (W) only, however with higher fan flowrates of up to 4 l/s.m^2.

9.5. Conclusions

Building upon the outcomes of the evolutionary optimization and the subsequent analysis of its results, several conclusions are reached.

Per the significance of construction dynamicity and fan flowrates definition in building performance assessments, and the associated influence of the retrofit scenario on efficient IHR exploitation, the effective performance of buildings with dynamic constructions requires three factors:

1. An inherently well-insulating construction, designed as a composite masonry-insulation structure for higher IHR efficiency (lower U-values at lower airflow rates).
2. A mechanically-assisted depressurization of the building, sized beyond the ventilation requirements to accommodate a sufficient and reliable IHR exploitation.
3. An exhaust fan-based ventilation regime (EV) for efficient IHR utilization, and a reduced trade-off between energy-efficiency and IEQ performance.

Further expanding the above conclusions:

1. Achieving performances comparable to the fully-insulated conventional retrofit case (CRC) is feasible only through improved envelope insulation.
   - Non-insulated buildings may reach 80% of the equivalent CRC improvement when neither insulation nor IHR-based fan flowrates are applied, and would necessitate the sealing of the envelope.
   - Achieving higher performances, in exceedance of 85% of the CRC improvement, are possible without significant surface sealing when IHR-based fan flowrates are adopted. Although the IHR effect compensates some of the performance lost to the lack of envelope insulation, it is yet not sufficient to fully meet the CRC performance.
   - Still, non-insulated buildings may outperform the equivalent non-insulated conventional retrofit case (NCRC) while maintaining substantial surface permeability, if fan flowrates are sized for an efficient IHR utilization.

2. As suggested by the results of the Sensitivity Analysis (Refer to Chapter 8), the fan flowrates must be sized beyond those dictated by minimum ventilation requirements to accommodate for a reliable depressurization of the building, and the consequent effective IHR exploitation into the post-retrofit building performance.
   - In both insulated and non-insulated buildings, the construction dynamicity is not of significant importance when fan flowrates are sized to only meet ventilation demands. Such design resulting in performances comparable to the equivalent static construction case, the construction dynamicity could be neglected with only minimal deviations between simulated and actual building performance.
   - In contrast, when the fan flowrates are raised beyond the building's ventilation requirements, as to ensure a reliable under-pressure at virtually all envelope surfaces, the construction dynamicity becomes of critical importance. It results in noticeable impact on the performance outcomes, relative to the assumed-static construction case, and thus influences the retrofit decisions.

2
- While the exploitation of the IHR effect through fan-assisted building depressurization enhances building performance, it primarily elevates low-performing cases to well-performing cases (comparable or slightly better than the CRC) with minimal intrusion. However, the highest possible energy-savings still mostly necessitate the intrusive conventional sealing of the envelope.
- The effective exploitation of the IHR effect in retrofit design requires both the construction dynamicity and the IHR-based fan sizing to be considered in the Building Performance Simulation (BPS) analysis during the retrofit decision-making process.
  - This highlights the (currently unmet) need for BPS tools capable of effectively incorporating the dynamic behavior of building materials and their interaction with the dynamic airflows, in case the IHR is to be used in the efficient and non-intrusive retrofit of historic traditional buildings.

3
- Ventilation regime variants diverge in their ability to efficiently exploit the IHR effect into achieving a balanced overall building performance.
  - The EV delivers superior energy-savings while accommodating higher surface permeability, and thus efficiently exploits the IHR effect. The WE follows closely, but fails to meet the same energy-saving levels at high permeabilities.
  - The RV exhibits performances and requirements almost up to WE standards but with significantly greater implementation intrusiveness.
  - The NV, acceptable only in buildings with heritage-protected interiors, offers sub-optimal overall performance and relies on conventional surface sealing.

The recommended retrofit approach, addressing each aspect of the considered retrofit strategy variants (Refer to Chapter 4), for traditional historic dwellings both with heritage-protected and non-protected interior surfaces is determined based on:

1. An adopted Warm loft configuration for the conditioned zone boundary
2. The ability to achieve performances comparable to (or better than) the conventional retrofits
3. The ability to achieve such performances with minimal interventions on the building, prioritizing the preservation of existing air permeability into its post-retrofit design.

The resulting recommended retrofit approach, accordingly, appears consistent for all traditional historic dwellings, at the exception of one aspect; in buildings with heritage-protected interior surfaces, envelope insulation (both external and internal) is not an option and must thus be neglected as a potential and optimal retrofit variant.

The resulting recommended retrofit approach then considers:

- Dynamic Constructions – The dynamicity of the construction must be considered in the building performance simulation guiding the retrofit design decisions
- Insulated Constructions – All envelope surfaces must be insulated with air permeable and inherently-insulating materials, at the exception of heritage surfaces that are both internally- and externally-protected.
- IHR-based Sizing of Fan Flowrates – The fan flowrates must be sized beyond the ventilation requirements to provide reliable and sufficient building depressurization and, accordingly, accommodate an effective IHR exploitation.
- Local Exhaust Fans with All Year Operations – Local exhaust fans with heat recovery, installed in the wet rooms, must be operated all year to provide for the highest energy-savings while maintaining a good IEQ performance and, consequently, outperform the corresponding conventional retrofit.

Implementing the recommended retrofit strategy on the Case Study building reveals the optimal combinations of surface permeability, insulation thickness, and fan flowrate requirements that maximize the performance improvements at the highest possible surface permeabilities. Highest-performing design solutions are identified and presented in Figures 66 and 68 above, respectively for insulated and non-insulated conditions.
Considering the Case Study building's base case permeability and performance, the adopted optimal solutions (Refer to Table 29) are selected for:

- Outperforming the CRC.
- Requiring no sealing on either the walls or the pitched roof.
- Requiring only sealing on the flat roof, needed in all solutions.

Table 29: Optimal Retrofit Design - Case Study Building

 Heritage-protected Exterior Surfaces		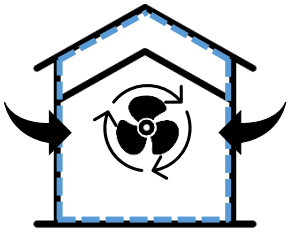 Heritage-protected Exterior & Interior Surfaces
	Conditioned Zone Boundary	
Warm Loft		Warm Loft
	Envelope Properties	
Permeability [kg/s.m^2] [0.000375] W [0.00125] PR [0.0001] FR Insulation Thickness [m] [0.09] W [0.16] PR [0.20] FR		Permeability [kg/s.m^2] W [0.00005] PR [0.001] FR [0.00005] Insulation Thickness [m] W [0] PR [0.04] FR [0.04]
	Ventilation Strategy	
Fan Flowrate [l/s.m^2] [3.5] Exhaust	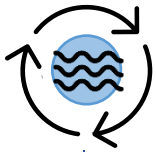	Fan Flowrate [l/s.m^2] Exhaust [2.5]
	Energy Demand	
Energy Demand [kWh] [24325.7] Annual		Energy Demand [kWh] Annual [32375.9]

10. Final Retrofit Recommendation

The final retrofit recommendation for traditional historic dwellings, characterized by a breathable solid wall construction, considers two cases: buildings with heritage-protected exterior surfaces, and buildings with protected exterior and interior surfaces.

At the exception of the insulation of their envelope, the optimal retrofit approaches for both heritage-protection scenarios are identical. The retrofit strategy is founded upon a **significant and well-spread diffuse leakage**, an **effective sealing of the concentrated leakage pathways**, mitigating the risks of draughts and by-passing the DI systems, and the implementation of **heat recovery on the exhaust air**. It considers the following aspects:

Table 30: Final Recommendation - Retrofit Strategy

Heritage-protected Exterior Surfaces		Heritage-protected Exterior & Interior Surfaces
	Conditioned Zone Boundary	
Warm Loft		Warm Loft
	Envelope Properties	
Dynamic Construction & Insulated Envelope		Dynamic Construction & Non-insulated Envelope
	Ventilation Strategy	
Exhaust Ventilation (All Year with Heat Recovery) & IHR-based fan flowrates	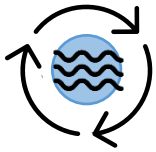	Exhaust Ventilation (All Year with Heat Recovery) & IHR-based fan flowrates

Although the Warm loft configuration was selected for this study, the Sensitivity Analysis results show that both the Warm and the Cold loft configurations present high potential for effective IHR exploitation under high-depressurization operations. The Cold loft configuration could thus still be investigated, as it may allow for comparable performances at slightly lower fan flowrates.

The corresponding combinations of airtightness, insulation thickness, and fan flowrates for the successful application of such retrofit strategies in the Case Study building are thus presented below. All combinations outperform the corresponding conventional retrofit case (CRC for insulated buildings and NCRC for non-insulated buildings). It is considered that the varying combinations provide for comparable IEQ performances, and only diverge by their energy-savings.

Table 31: Final Recommendation - Design Requirements & Performance

Heritage-protected
Exterior Surfaces

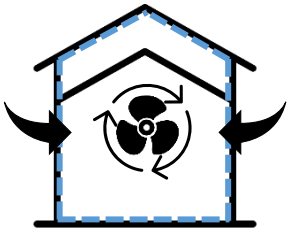

Heritage-protected
Exterior & Interior Surfaces

Conditioned Zone Boundary

Warm Loft

Warm Loft

Envelope Properties

Permeability [kg/s.m^2]
[0.00005 – 0.000375] W
[0.00075 – 0.00125] PR
[0.000025 – 0.0001] FR

Insulation Thickness [m]
[0.09 – 0.13] W
[0.14 – 0.22] PR
[0.08 – 0.20] FR

Permeability [kg/s.m^2]
W [0.00005 – 0.000325]
PR [0.00075 – 0.00325]
FR [0.00005 – 0.00025]

Insulation Thickness [m]
W [0]
PR [0.04]
FR [0.04]

Ventilation Strategy

Fan Flowrate [l/s.m^2]
[1.75 – 3.5] Exhaust

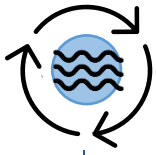

Fan Flowrate [l/s.m^2]
Exhaust [2.5 – 4]

Energy Demand

Energy Demand [kWh]
[20762 – 24326] Annual

Energy Demand [kWh]
Annual [32376 – 36977]

Optimal design requirements for insulated and non-insulated configurations fall within, more-or-less, comparable ranges. Nonetheless, non-insulated buildings tend to encourage higher roof permeability levels and, correspondingly, higher fan flowrates. This reflects their greater reliance on higher air leakage flows for a higher IHR effect, to compensate the construction's lower thermal resistance. The higher IHR effect may, however, not fully compensate the insulation's performance and only meets 75-85% of the fully-insulated buildings' energy-savings.

With reference to the Case Study building, the specific optimal combinations of surface permeability, insulation thickness, and fan flowrate are presented in more detail under the Chapters 9.4 and 9.5 above.

11. Final Summary and Discussion

This Chapter outlines the present research. It, first, it describes its main contributions (Chapter 11.1). Then, it comprehensively answers the research's main and sub-questions to present a more inclusive insight into the research contributions (Chapter 11.2).

11.1. Main Research Contributions

The retrofit of traditional historic buildings is often hindered by a lack of overarching guidelines to retrofit strategies tailored to their characteristic building properties and heritage preservation requirements. And the currently conventional retrofit approach, relying on the combined increase of the envelope's airtightness and insulation, fails to properly address these two decisive facets.

Limitations to the development of these needed retrofit strategies are, first, the focus of retrofit decisions on the buildings' energy performance and, second, the neglect of two factors affecting the relationship between the building's breathability and its overall performance: The Indoor Environment Quality (IEQ) as primary performance indicators, and the Infiltration Heat Recovery's (IHR) as complement to the energy performance.
Addressing these limitations is vital for efficiently achieving reliable optimal post-retrofit performances in buildings characterized by intricate dynamics and unique requirements.

The present research contributed with a recommendation for the retrofit of traditional historic dwellings that exploits the building's air leakage into achieving optimal building performance, in terms of Energy-Efficiency (EE) and Indoor Environment Quality (IEQ), while preserving the building's original character and behavior as practically-possible.

The main contributions of this research thus relate to the developed retrofit strategy, and may be summarized as follows:

- Proposing an innovative strategy mitigating the trade-off in the air leakage's influence on the building performance, which consists of treating the building's breathable construction as a dynamic insulation system with an optimizable design, to enhance the Infiltration Heat Recovery (IHR) and exploit the diffuse air leakage into the optimal post-retrofit performance.
- Providing a comprehensive analytical framework to make well-informed performance-based decisions over the design of tailored retrofit strategies for traditional breathable buildings. It considers the conflicting energy and IEQ performance parameters for the assessment of the building's post-retrofit performance, and investigates the retrofit variants of relevance in the optimization of the air leakage contribution to the building performance.
- Providing an evaluation tool with both an air leakage model and dynamic insulation model, to emulate the complex building physics of traditional buildings' breathable construction and achieve more reliable solutions in their building performance assessment and optimization.
- Establishing the significance of incorporating the dynamicity of the construction into the retrofit strategies for breathable buildings by evaluating the extent of its influence on building performance and identifying its contextual relevance.
- Proposing a targeted retrofit strategy recommendation and corresponding application framework for traditional historic buildings, with solid wall constructions, of varying levels of performance and heritage restriction.

11.2. Detailed Research Contributions

A deeper grasp of the research contributions is achieved by addressing the main research question and sub-questions.

MAIN

What airtightness and ventilation retrofit approaches could optimize the performance of traditional historic buildings, in terms of energy-efficiency and Indoor Environment Quality (IEQ), while accounting for their characteristic building physics principles and heritage preservation requirements?

For all breathable buildings, retrofit recommendations underscore the importance of considering the dynamicity of breathable constructions in performance assessments and retrofit design.
Optimal design and performance conditions may vary in traditional historic buildings based on the presence of heritage-protected interior surfaces. At the exception of the envelope insulation, the optimal retrofit approach for both heritage-protection scenarios are identical. They are founded on the significant and well-spread diffuse air leakage, the effective sealing of concentrated leakage pathways, and the implementation of heat recovery on the exhaust air.

The optimal dynamic insulation performance of the existing breathable construction then relies on: An inherently well-insulating construction with well-spread diffuse leakage pathways, and an all-year mechanical exhaust fan-assisted depressurization of the building, sized beyond the ventilation requirements for reliable IHR exploitation.
The warm loft configuration was adopted for its higher preservation potential of the surface permeability at various airflow rates, both with and without the exploitation of the IHR effect. However, the Cold Loft configuration still presents potential for further exploration under high IHR exploitation conditions.

This approach allows numerous combinations of air permeability levels, insulation thickness, and fan flowrates optimizing energy-efficiency and IEQ. Optimal design requirements are overall, more-or-less, comparable between insulated and non-insulated cases.
However, non-insulated buildings tend to encourage higher roof permeability levels and fan flowrates. This reflects the greater reliance on air leakage flows for a higher IHR effect, compensating for the lower construction thermal resistance.
Although non-insulated buildings can only meet 75-85% of the energy-savings achieved by fully-insulated buildings, both scenarios provide significant improvement from the base case.

The adopted optimal combination depends on the building's initial performance and permeability levels, its heritage protection restrictions, and the design priorities.
The application of the optimal retrofit approach on the Case Study building, its resulting allowable ranges and selected values for the design parameters may be referred to under Chapters 9.5. and 10.0.

Research Question Group 1

The theoretical background covered in Chapter 2 provides insight into the properties of building air leakage, its relation to the building performance, and the current strategies addressing its retrofit.

1 **What are: (1) the characteristics of building air leakage? (2) its different types? (3) their relationships with the building's performance, in terms of energy-efficiency and Indoor Environment Quality (IEQ)?**

Air leakage is the uncontrolled movement of air driven by the dynamic pressure gradient across the building's envelope. The accurate modeling of air leakage may thus only be done dynamically.
A building's air leakage owes to a wide and variable network of joints, gaps, and cracks in its envelope. The complexity of such network challenges reliable envelope airtightness, and supports the air leakage exploitation over its impractical sealing attempts.

Air leakage is categorized by direction (Infiltration and Exfiltration) and nature of its pathways (Concentrated and Diffuse). These distinctions are important for their associated differences in the leakage flow regime and heat loads, and their impact on the air leakage's trade-off between Energy and IEQ.
The air leakage's impact on the building energy and IEQ is well-documented. Conventionally depicted as an unnecessary and major source for heat loss, the air leakage's heat load has actually often been overestimated. Often neglected, the diffuse leakage's Infiltration Heat Recovery (IHR) phenomenon challenges the conventionally-linear relationship between air leakage flow and heat loss, either increasing or decreasing the leakage heat load.
Besides potentially enhancing the building's energy-efficiency, air leakage plays a crucial role in its IEQ: influencing the air change rates and contaminant removal, the hygrothermal balance, and the release of accumulated heat gains.

2 **How could the trade-off identified in the air leakage's relationship with the building's performance be improved?**

Optimizing the trade-off between energy-efficiency and Indoor Environmental Quality (IEQ) may consider intentionally integrating and enhancing the Infiltration Heat Recovery (IHR) effect in building designs, function that is found in the concept of Dynamic Insulations.

DI systems enhance the IHR phenomenon by introducing a running fluid into the static constructions, creating a heat exchanger within the envelope. Although purpose-designed DI structures are still limited in application, their concept addresses many of the limitations faced in the retrofit of breathable buildings.
Despite their similarities with DI systems, the limitation of existing breathable constructions lies in their original design, which was not tailored for them to efficiently exploit the IHR effect. The retrofit of such constructions to act as DI systems holds a potential solution to simultaneously providing for energy-efficiency and a satisfactory IEQ. Design considerations for optimal DI systems in heating-dominated temperate climates set the foundation for the retrofit's relevant design variants.

3 **With a particular focus on historic traditional buildings, what are: (1) the state-of-the-art airtightness and ventilation retrofit strategies? (2) their limitations? (3) the measures that have been conventionally used to address these limitations?**

Driven by current environmental goals and standards, the conventional approach to building airtightness emphasizes achieving energy-savings through airtight constructions. Uniformly relying on the same retrofit approaches across diverse contexts, this approach tends to overlook variations in climates and building characteristics, and their effects on performance.

Several limitations emerge, notably the neglect of crucial aspects in the relationship between air leakage and building performance. This misinforms retrofit decisions in two key ways:

- **Neglecting coupling of air leakage and conduction heat flows** – extends to the neglect of the IHR effect, and entails an overestimation of the leakage heat loads by 10-95%, thereby misjudging the energy-savings achieved by airtightness improvements.
- **Disregard of the IEQ as primary performance parameters** – results in indoor air contaminant build-up, increased humidity levels and moisture-related risks, and reduced heat removal in summer, causing discomfort and potential overheating.

Research Question Group 2

The identification of the relevant retrofit variants and definition of the comparative reference cases, addressed in Chapters 4 and 5, define the solution search space and provide the benchmarks to situate them in context.

4 **What are the airtightness and ventilation retrofit strategies that could present as potential solutions for traditional historic buildings?**

The retrofit variants navigate the intricate balance between energy-efficiency, IEQ, and heritage preservation by tackling various factors that influence the potential for Infiltration Heat Recovery (IHR) and the exploitation of air leakage in the optimal building performance.

An effective retrofit approach must provide the potential for optimal combinations of airtightness, insulation, and fan flowrate. This is achieved by selecting the most suitable variant from each of five explored retrofit aspects, addressing three critical building features:

- **Conditioned Zone Boundary** – considering the loft's warm or cold configuration
- **Envelope Properties** – considering the added insulation and construction dynamicity
- **Ventilation Strategy** – considering the ventilation regime and the mechanical ventilation's sizing factor

5 **What are the comparative references to the investigated strategies, namely: (1) the baseline properties and performance of a traditional historic buildings with reference to a case study in the Netherlands, and (2) their estimated properties and performance under an unrestricted conventional retrofit approach?**

The comparative references serve to contextualize the performance of explored retrofit alternatives within the research framework. Each alternative's performance is then gauged by its relative improvement of the building's overall performance (energy and IEQ) compared to the base case, with the conventional retrofit case serving as a benchmark.

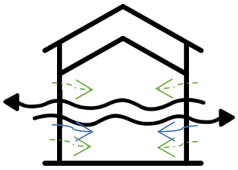
[BC]

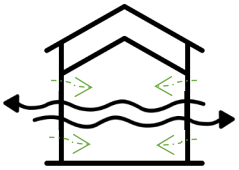
[BRC]


[CRC]


[NCRC]

The Base Cases consider the initial pre-retrofit conditions of the building.
The Base Case [BC] characteristics mirror the Case Study building – a 1750's monumental row dwelling – before its partial retrofits in the 1980s and 2020s. The air leakage model defines the envelope's permeability based on in-situ air leakage measurements.
These measurements provide insight into the building's total air leakage and its partitioning between concentrated and diffuse leakage pathways.
A variant of the Base Case with sealed openings [BRC] serves as the template for retrofit alternatives, emphasizing the mitigation of risks associated with concentrated leakage pathways – risks of draughts and by-passing of DI systems.

The conventional retrofit cases represent the implementation of the conventional retrofit approach, identified in literature, onto the base case building.
The Conventional Retrofit Case [CRC] considers a sealed, heavily insulated envelope with balanced Mechanical Ventilation with Heat Recovery (MVHR).
An alternative conventional retrofit case [NCRC] is developed for heritage buildings with protected interior surfaces, by omitting envelope insulation. It results in lower performance compared to the original conventional approach, and serves as a realistic reference for highly heritage-protected buildings.

Research Question Group 3

The evaluation framework and tool, developed in Chapters 6 and 7, provide the means for the retrofit performance assessment and the foundation for the resolution of the problem.

6 **What performance parameters and associated criteria are indicative of the building's overall post-retrofit performance, and could be used to evaluate a retrofit strategy's effectiveness?**

An effective retrofit strategy mitigates the trade-off between energy-efficiency and indoor health & comfort.
Energy efficiency is evaluated by the minimization of a single parameter – the end-use building energy demand – while indoor health & comfort addresses four key IEQ aspects: Winter Thermal Comfort, Summer Thermal Comfort, Ventilation and IAQ, and Indoor Humidity. These aspects are quantified as annual weighted IEQ scores based on hourly criteria satisfaction, following EN 16798 standards, and are set to be maximized.

The target retrofit strategy is identified by comparing the retrofit variants through a design optimization and analysis process. The goal is to uphold satisfactory IEQ levels, decrease the building's energy demand, and preserve the construction's breathability to safeguard the heritage building's unique character and behavior.

7 **How can the dynamic overall building performance be evaluated, in relation to the building's characteristic air leakage behavior and envelope properties?**

A holistic dynamic building performance simulation (BPS) model was developed for the reliable evaluation of the retrofit alternatives' performances. It integrates three sub-models:

- **BES model** – The BES model mirrors the case study building, a traditional brick masonry solid wall construction with a wooden roof structure. It comprises five zones—four occupied and one unoccupied—assumed to have uniform envelope and system features. Local dynamic weather data is employed for accurate context representation.

- **Air leakage model** – Through an Airflow Network (AFN), the air leakage model estimates multi-zone pressures, airflows, and associated heat loads. The air leakage path distribution is defined as a Crack Template, derived from the AIVC Guide 5 database, validated and calibrated against in-situ air leakage measurements. The Crack Template pertaining to the Blower Door Test conditions is then used as a foundation for the remaining variants' templates.
  The validation process highlights gaps and deficiencies in the data estimating roof leakage. These are addressed by refining roof leakage estimates based on in-situ results.
- **DI model** – The DI model considers the IHR effect through an airflow-dependent dynamic U-value (U_{dyn}), as per the analytical Taylor Model, that is custom-coded into the model via its Energy Management System (EMS).
  The custom DI model is validated against the original analytical Taylor Model through a comparative analysis. A validity limit is identified at an airflow of 0.008 $m^3/s.m^2$, comfortably surpassing the building model's maximum encountered airflow rate.
  An incompatibility of the EMS model with constructions containing "NoMass" materials, defined solely by their thermal resistance, is also revealed. This can be readily circumvented by conventionally defining all material layers.

Integration of these component models is facilitated by the EnergyPlus software tools, allowing multi-zone airflow and energy modeling, and potential custom-coded controls.

Research Question Group 4

The comprehensive analysis of the retrofit variants' performances and their contextualization relative to each other and the comparative references, as discussed in Chapters 8 and 9, supplies the requisite information for formulating retrofit recommendations tailored historic traditional dwellings.

8 **What is the recommended: (1) building loft insulation configuration and (2) ventilation regime, for the exploitation of traditional historic building's air leakage into their optimal building operations?**

The **Sensitivity Analysis** (SA) – by Morris Method – assessed the impact of envelope surface permeabilities on the building energy demand across various conditioned zone boundary configurations – warm loft and cold loft – and building depressurization – 2 Pa for ventilation requirements and 30 Pa for IHR-enhancing requirements. Key findings included:

- An efficient IHR utilization – increasing energy-efficiency in response to higher surface permeability – necessitates exhaust flowrates surpassing those dictated by ventilation requirements. It does not undermine exploring lower flowrates to achieve balance between space energy savings and system efficiency.
- Both Warm and Cold loft configurations show significant potential for the IHR exploitation under high depressurization conditions. However, even with limited IHR at low flowrates, the Warm Loft configuration still exhibits a potential for preserving wall permeabilities with minimal impact on energy-efficiency.

The Warm Loft configuration was selected for further analysis, including investigations into both ventilation-based and IHR-based fan flowrates.

The **Evolutionary Optimization** (EOpt) – by NSGA II method – and the following Multi-Criteria Decision Analysis (MCDA) – by TOPSIS method – identified optimal combinations of air permeability, insulation thickness, and fan flowrates that enhance the Energy-Efficiency and IEQ performance under each retrofit scenario, and situated them in context.
The results emphasized the importance of accounting for the dynamic nature of breathable constructions in performance assessments and retrofit design. While the IHR effect is limited at low airflow rates, it becomes crucial at higher rates and noticeably impacts the performance outcomes and retrofit decisions.
This highlights a (currently unmet) need for Building Performance Simulation (BPS) tools that effectively capture dynamic material behavior and airflow interactions.

The thorough analysis asserts the dependence of the optimal DI performance on: An inherently well-insulating construction, and an all-year mechanical exhaust fan-assisted depressurization of the building, sized beyond the ventilation requirements for reliable IHR exploitation. The recommended retrofit approach for traditional historic dwellings with or without heritage-protected interior surfaces then only diverges by the possibility for added insulation.

9 **What are the airtightness, insulation thickness, and fan flow rates associated to the successful application of the recommended retrofit approaches, for traditional historic buildings of varying levels of performance and heritage restrictions?**

The recommended retrofit approach provides numerous combinations of air permeability levels, insulation thickness, and fan flowrates optimizing energy-efficiency and IEQ with minimal intrusion on the monument. The identified optimal design parameter ranges may be referred to under Chapters 9.5 and 10.0.
Optimal design requirements are overall, more-or-less, comparable between the insulated and non-insulated cases. However, non-insulated buildings tend to encourage higher roof permeability levels and fan flowrates. This may be attributed to the greater reliance on high air leakage flows for a higher IHR effect, to compensate for the lower construction thermal resistance. Despite the adjustments, non-insulated buildings can only meet 75-85% of the energy savings achieved by the fully-insulated buildings.

The adopted optimal design depends on the building's initial permeability levels and performance, its heritage protection restrictions, and the designer's priorities.
Its application on the specific Case Study building is presented under the Chapters 9,5 and 10 above.

12. Conclusions and Recommendations

This Chapter concludes the research. First, it summarizes its key findings and main contributions (Chapter 12.1). Then, it presents research' relevance and recommendations for practice (Chapter 12.2) and future research (Chapter 12.3).

12.1. Conclusions

The present research aimed to contribute with a recommendation for the retrofit of traditional historic dwellings that optimizes their Energy-Efficiency (EE) and Indoor Environment Quality (IEQ), while preserving their characteristic building dynamics and heritage as practically-possible.

The proposed solution was to exploit the building's existing air leakage into its post-retrofit performance, rather than sealing it as conventional. This would avoid the disruption of their balanced breathable systems, preventing the degradation of their IEQ and providing the needed ventilation with minimal intrusion onto the building's heritage.

The investigation of the air leakage's behavior in breathable constructions revealed a phenomenon that is often neglected in building performance evaluations and that presents as a potential solution to the retrofit of traditional historic buildings: The Infiltration Heat Recovery (IHR) of diffuse leakage. The efficient exploitation of this effect creates construction elements, referred to as Dynamic Insulations (DI), in which the air leakage could act as heat exchanger, diffuse ventilation source, airborne contaminant filter, and diffusion barrier. The result thus appears to address many of the limitations faced in the retrofit of traditional historic buildings.
Despite their similarities with dynamic insulations, the existing breathable constructions' limitation resides in their original design and operations, which are not tailored to efficiently exploit the IHR effect.

The study thus particularly investigated the potential of retrofitting the building's existing breathable construction to act as an efficient Dynamic Insulation. In other words, it was to characterize the potential of exploiting the Infiltration Heat Recovery (IHR) of existing breathable constructions into achieving the desired performance improvements and, consequently, identify the specific retrofit strategy that enhances this potential.

The target building performance, in terms of Energy-Efficiency and Indoor Environment Quality, consisted in achieving improvements from the base case that are comparable to or better than the ones met by the conventional retrofit approach – relying on high airtightness and insulation combined with the implementation of balanced mechanical ventilation systems.

The results of the research, outlined in detail under Chapter 11, support that such performances are indeed achievable without any of the highly-intrusive conventional retrofit measures. The retrofit of the breathable construction as a Dynamic Insulation system allows the preservation of the walls' and pitched roof's surface permeabilities by the simple implementation of high exhaust fan flowrates, that are sized to provide for an efficient Infiltration Heat Recovery (IHR).

Such retrofit may or may not be associated with the insulation of the envelope, depending on the building's heritage restrictions. Although both solutions have comparable requisite levels of surface permeability and fan flowrates, and achieve satisfactory IEQ, the added insulation provides significantly larger energy-savings. The combination of the insulation with the IHR effect also allow to meet such energy-savings at lower insulation thicknesses relative to the conventional retrofit.

Nonetheless, both insulated and non-insulated retrofits provide for significant performance improvements – reducing the base case's energy demand at least by half and out-performing their equivalent insulated and non-insulated conventional retrofits.

The foundations of such retrofit approach are, however, the possibility for significant and well-spread diffuse leakage pathways across the envelope surfaces, the effective sealing of the concentrated leakages, and the implementation of heat recovery on the exhaust air.
The results also underscore the importance of accounting for the conventionally-neglected IHR effect in the retrofit of breathable buildings, as it affects their performance and retrofit design decisions.

Considering that the building fabric in retrofit projects is an existing pre-condition, the characterization of the building's air leakage types and distribution is necessary prior to any discussion about the implementation of this strategy.
The predominance of highly-diffuse leakages through the fabric is, however, more critical for buildings with heritage-protected exteriors and interiors than for buildings where the implementation of insulation is allowed. The addition of permeable internal insulation layers converts all leakages in the building envelope, concentrated or diffuse, into diffuse leakages and evades a major limitation of the developed retrofit strategy.

The specific requisite air permeability levels, insulation thickness, and fan flowrates providing for the optimal application of such performance depend on the building's original conditions, its heritage protection restrictions, and the design priorities.

12.2. Practical Relevance, Limitations, and Recommendations

The current study recommends an alternative retrofit strategy that outperforms the conventional methods, while maintaining the building's breathability and building dynamics, and preserving its heritage value. It thus underscores the value of conserving a building's intrinsic behavior and dynamics during post-retrofit endeavors, and emphasizes the substantial opportunities found in exploiting the understanding of the building's existing operations to strategically enhance its performance with minimal intrusion.

The identified approach not only enhances energy-efficiency while ensuring balanced and satisfactory IEQ performances, it minimizes the extent of the needed interventions and their associated heritage disruptions. Exploiting the air leakage for ventilation and reducing the insulation thickness requirements, it also potentially results in economic and financial advantages and improves the retrofit's carbon footprint: it limits the reduction of the usable floor area, and minimizes the system installations and material usage.

Although recommending the consideration of the above-defined retrofit approach and potential in future traditional historic building retrofits, one should be mindful of the compatibility of the retrofitted building with such interventions, and adapt the retrofit approach to the specific project. Particularly, it is to consider the compatibility of its original leakage types and behavior, its envelope surfaces and properties, and its exhaust ventilation potential.

Besides defining an optimal retrofit approach tailored to the characteristics of traditional historic buildings, the core of this research was to question: the standardization of designs and solutions, in general, and the growing trend in the building sector towards the complete isolation of the indoor environment from its dynamic outdoor environment, in particular.

On the one hand, simple interventions built upon the building's inherent characteristics and dynamics can prove as effective as invasive retrofits, that rely on by-passing the building's original operational mode and substituting it with purpose-designed systems to fulfil its needs.
On the other hand, standardizing retrofit approaches, with a sole focus on enhancing energy performance while disregarding the building's unique operational intricacies, can lead to detrimental outcomes. This is particularly pertinent in bioclimatic systems, which rely on their adaptability to the environment to maintain a holistic balance across its various performance aspects.

Understanding the assumptions on which the 'standard' strategies are built and what they entail in terms of overlooked potential in different buildings is at the foundation of their effective implementation and the prevention of their unintended consequences. The most optimal and efficient interventions may only be identified through an integration of the building's inherent properties and behaviors into their retrofit.

On a broader scale, the development of targeted retrofit guidelines for traditional historic buildings is essential to promote and enhance the renovation rate of this segment of the building stock. The latter, constituting of a majority of dwellings with poor energy performance, indeed play a significant role in achieving global environmental goals. But their retrofit has often been hindered by the lack of comprehensive guidelines tailored to their particular building physics and heritage preservation requirements.
The present retrofit strategy is presented as a start for overarching guidelines on the retrofit of buildings with varying properties and constructions. While it was developed based on a specific building, the latter can be assumed representative of the main characteristics of a broader section of the target building stock. Even if not perfectly replicable on all buildings, the recommendation provides a foundation for future designers to pay greater attention to often overlooked aspects of buildings and explore a wider range of unconventional alternative retrofit approaches.

12.3. Recommendations for Future Work

Future research direction may address three aspects of the developed retrofit recommendation:

1. **Its practical implementation**
   Obstacles to the practical implementation of the retrofit recommendation in regular industry projects considers, first, the severe lack of readily available Building Performance Simulation (BPS) tools that integrate the breathable constructions' complex building physics and air leakage dynamics and, second, the substantial computational cost of the simulations.

   This underscores the need for the development of building performance simulation tools capable of more effectively implementing the dynamic behavior of breathable constructions and their interaction with dynamic flows. Exploring further simplifications of the model that do not significantly affect its outcomes may also offer a solution to its computational costs.

2. **Its further development and improvement**
   Further improvements on the practical implementation of the presented retrofit strategy could investigate its potential under the alternative Cold Loft configuration. The sensitivity analysis indeed revealed comparable potential under both loft configurations for the exploitation of the infiltration heat recovery when fan flowrates are oversized beyond the ventilation demands. Not only is the Cold Loft often favored by building owners for technical and financial reasons, it may allow to achieve the desired depressurization of the building at lower and more practical fan flowrates by reducing the conditioned zone volume.

   An alternative avenue for advancing the recommended retrofit strategy considers exploring the feasibility and implications of replacing mechanical constant volume exhaust fans with variable fans, to avoid the system's operation beyond the building's actual needs.
   The variable fans could be mechanical fans actuated to provide the needed building depressurization under the varying environmental conditions and indoor environment requirements. This could avoid the over-sizing and operation of the fans at when it may not be necessary.

Or it could evolve further by investigating the potential of wind-driven exhaust fans, as self-regulating systems with the capacity to maintain the required airflow direct without the limitations of its mechanical alternative, such as the system's energy consumption and fixed flowrates. It holds the potential for the full preservation of the building's bioclimatic nature, while further enhancing the building's energy savings.

Further research prospects must also consider the validation of the retrofit's implementation in existing breathable buildings. Existing buildings are limited by their existing constructions and material properties, and present significant uncertainties as to their actual response to different interventions. One limitation, for instance, is that the dynamic U-value approach to the DI model assumes a relatively homogeneous spread of the diffuse air leakage and IHR effect over each surface, which may not be guaranteed in existing buildings. The validation of the recommendation requires its implementation in a real case-study building, with the ongoing monitoring of its performance both before and after the retrofit.

3 Its broadening to a wider building stock

The current retrofit strategy was tailored around the presumed layout, functions, loads, and other operational aspects of single-family row dwellings with solid wall masonry construction, yet presents an intriguing opportunity for expansion to encompass traditional historic buildings with diverse functions and heritage-protection requirements – e.g. offices, museums, public and governmental buildings, etc.

References

Alev, Ü., Eskola, L., Arumägi, E., Jokisalo, J., Donarelli, A., Siren, K., Broström, T., & Kalamees, T. (2014). Renovation alternatives to improve energy performance of historic rural houses in the Baltic Sea region. *Energy and Buildings*, *77*, 58–66. https://doi.org/10.1016/j.enbuild.2014.03.049

Alongi, A., Angelotti, A., & Mazzarella, L. (2017). Experimental investigation of the steady state behaviour of Breathing Walls by means of a novel laboratory apparatus. *Building and Environment*, *123*, 415–426. https://doi.org/10.1016/j.buildenv.2017.07.013

Alongi, A., Angelotti, A., & Mazzarella, L. (2020a). Experimental validation of a steady periodic analytical model for Breathing Walls. *Building and Environment*, *168*. https://doi.org/10.1016/j.buildenv.2019.106509

Alongi, A., Angelotti, A., & Mazzarella, L. (2020b). Measuring a Breathing Wall's effectiveness and dynamic behaviour. *Indoor and Built Environment*, *29*(6), 783–792. https://doi.org/10.1177/1420326X19836457

Alongi, A., Angelotti, A., & Mazzarella, L. (2021). A numerical model to simulate the dynamic performance of Breathing Walls. *Journal of Building Performance Simulation*, *14*(2), 155–180. https://doi.org/10.1080/19401493.2020.1868578

Alongi, A., Scoccia, R., Motta, M., & Mazzarella, L. (2015). Numerical investigation of the Castle of Zena energy needs and a feasibility study for the implementation of electric and gas driven heat pump. *Energy and Buildings*, *95*, 32–38. https://doi.org/10.1016/j.enbuild.2014.11.012

American Society of Heating, R. and A.-C. E. (2022). *ASHRAE Position Document on Indoor Carbon Dioxide*.

Architektenburo Bob C Van Beek bv. (1980). *Bestektekening II, Restauratie Herengracht 15, Leiden*.

Ascione, F., Bianco, N., De Stasio, C., Mauro, G. M., & Vanoli, G. P. (2015). Dynamic insulation of the building envelope: Numerical modeling under transient conditions and coupling with nocturnal free cooling. *Applied Thermal Engineering*, *84*, 1–14. https://doi.org/10.1016/j.applthermaleng.2015.03.039

Baharavand, M., Bin Ahmad, M. H., Safikhani, T., & Binti Abdul Majid, R. (2013). DesignBuilder Verification and Validation for Indoor Natural Ventilation. *Journal of Basic and Applied Scientific Research*, *3*(4), 182–189. https://www.textroad.com/pdf/JBASR/J.%20Basic.%20Appl.%20Sci.%20Res.,%203(4)182-189,%202013.pdf

Baker, P. H. (2003). The thermal performance of a prototype dynamically insulated wall. *Building Services Engineering Research and Technology*, *24*(1), 25–34. https://doi.org/10.1191/0143624403bt057oa

Bakowski, J. (2013, June). Refurbishment of a historical building - design issues. *Central Europe towards Sustainable Building CESB 13*. https://www.researchgate.net/publication/265964041_Refurbishment_of_a_historical_building_-_design_issueshttps://www.researchgate.net/publication/265964041_Refurbishment_of_a_historical_building_-_design_issues

Balesdent, M., Brevaul, L., Lacaze, S., Missoum, S., & Morio, J. (2016). Methods for high-dimensional and computationally intensive models. In *Estimation of Rare Event Probabilities in Complex Aerospace and Other Systems* (pp. 109–136). Elsevier. https://doi.org/10.1016/B978-0-08-100091-5.00008-3

Becchio, C., Corgnati, S. P., Vio, M., Crespi, G., Prendin, L., & Magagnini, M. (2017). HVAC solutions for energy retrofitted hotel in Mediterranean area. *Energy Procedia*, *133*, 145–157. https://doi.org/10.1016/j.egypro.2017.09.380

Berge, A. (2011). *Analysis of Methods to Calculate Air Infiltration for Use in Energy Calculations* [Master Thesis]. Chalmers University of Technology.

Blázquez, T., Ferrari, S., Suárez, R., & Sendra, J. J. (2019). Adaptive approach-based assessment of a heritage residential complex in southern Spain for improving comfort and energy efficiency through passive strategies: A study based on a monitored flat. *Energy*, *181*, 504–520. https://doi.org/10.1016/j.energy.2019.05.160

Blázquez, T., Suárez, R., Ferrari, S., & Sendra, J. J. (2023). Improving winter thermal comfort in Mediterranean buildings upgrading the envelope: An adaptive assessment based on a real survey. *Energy and Buildings*, *278*. https://doi.org/10.1016/j.enbuild.2022.112615

Bone, A., Murray, V., Myers, I., Dengel, A., & Crump, D. (2010). Will drivers for home energy efficiency harm occupant health? *Perspectives in Public Health*, *130*(5), 233–238. https://doi.org/10.1177/1757913910369092

Bouwbesluit Online 2012. (n.d.). Rijksoverheid. https://rijksoverheid.bouwbesluit.com/Inhoud/docs/wet/bb2012

Braam, M. (n.d.). *The Re-use of Brick from Dutch Post-war Housing (1945-1970) in the Circular Built Environment*. https://repository.tudelft.nl/islandora/object/uuid:7c7c7a99-892d-4326-9b89-50391f6fa0bd/datastream/OBJ1/download

Buchanan, C. R., & Sherman, M. H. (1998, September). CFD Simulation of Infiltration Heat Recovery. *19th AIVC Conference*. https://www.researchgate.net/publication/237621203_CFD_Simulation_of_Infiltration_Heat_Recovery

Buchanan, C. R., & Sherman, M. H. (2000, September). A Mathematical Model for Infiltration Heat Recovery. *Proceedings 21st AIVC Annual Conference, "Innovations in Ventilation Technology."* https://www.aivc.org/sites/default/files/members_area/medias/pdf/Conf/2000/paper45.pdf

Cabeza, L. F., de Gracia, A., & Pisello, A. L. (2018). Integration of renewable technologies in historical and heritage buildings: A review. *Energy and Buildings*, *177*, 96–111. https://doi.org/10.1016/j.enbuild.2018.07.058

Camarasa, C., Catenazzi, G., Goatman, D., Jakob, M., Meijer, A., Nägeli, C., Ostermeyer, Y., Palacios, A., Sainz de Baranda, E., Saraf, S., & Visscher, H. (2018). *Building Market Brief, the Netherlands* . https://mraduurzaam.nl/wp-content/themes/40-45/Rapporten%20en%20onderzoeken/181023-CK-BMB-BMB_NETHERLANDS-DEF-CIE-Edition.pdf

Cassar, M., Hawkings, Chris., University College, London. C. for S. Heritage., Engineering and Physical Sciences Research Council., UK Climate Impacts Programme., & English Heritage. (2007). *Engineering historic futures : stakeholders dissemination and scientific research report*. UCL Centre for Sustainable Heritage. https://discovery.ucl.ac.uk/id/eprint/2612/1/2612.pdf

Chen, R., & Tsay, Y.-S. (2021). An Integrated Sensitivity Analysis Method for Energy and Comfort Performance of an Office Building along the Chinese Coastline. *Buildings*, *11*(8), 371. https://doi.org/10.3390/buildings11080371

Chen, W., & Liu, W. (2004). Numerical analysis of heat transfer in a composite wall solar-collector system with a porous absorber. *Applied Energy*, *78*(2), 137–149. https://doi.org/10.1016/j.apenergy.2003.07.003

Craig, S., & Grinham, J. (2017). Breathing walls: The design of porous materials for heat exchange and decentralized ventilation. *Energy and Buildings*, *149*, 246–259. https://doi.org/10.1016/j.enbuild.2017.05.036

Craig, S., Halepaska, A., Ferguson, K., Rains, P., Elbrecht, J., Freear, A., Kennedy, D., & Moe, K. (2021). The Design of Mass Timber Panels as Heat-Exchangers (Dynamic Insulation). *Frontiers in Built Environment*, *6*. https://doi.org/10.3389/fbuil.2020.606258

D'Agostino, D., Zangheri, P., & Castellazzi, L. (2017). Towards Nearly Zero Energy Buildings in Europe: A Focus on Retrofit in Non-Residential Buildings. *Energies*, *10*(1), 117. https://doi.org/10.3390/en10010117

d'Ambrosio Alfano, F., Dell'Isola, M., Ficco, G., Palella, B., & Riccio, G. (2016). Experimental Air-Tightness Analysis in Mediterranean Buildings after Windows Retrofit. *Sustainability*, *8*(10), 991. https://doi.org/10.3390/su8100991

De Hoon, M. J. (2016). *Air Tightness Predicting the performance of a building envelope* [Master Thesis, Delft University of Technology]. http://repository.tudelft.nl/

Deb, K., Pratap, A., Agarwal, S., & Meyarivan, T. (2002). A fast and elitist multiobjective genetic algorithm: NSGA-II. *IEEE Transactions on Evolutionary Computation*, *6*(2), 182–197. https://doi.org/10.1109/4235.996017

Dimoudi, A., Androutsopoulos, A., & Lykoudis, S. (2004). Experimental work on a linked, dynamic and ventilated, wall component. *Energy and Buildings*, *36*(5), 443–453. https://doi.org/10.1016/j.enbuild.2004.01.048

Doran, S., Zapata, G., Tweed, C., Suffolk, C., Forman, T., & Gemmel, A. (2014). *Solid wall heat losses and the potential for energy saving Literature review Check-Phase I done Solid wall heat losses and the potential for savings-literature review Commercial in Confidence*. www.bre.co.ukhttp://www.bre.co.uk/swi

Elsarrag, E., Al-Horr, Y., & Imbabi, M. S.-E. (2012). Improving building fabric energy efficiency in hot-humid climates using dynamic insulation. *Building Simulation*, *5*(2), 127–134. https://doi.org/10.1007/s12273-012-0067-6

Emmerich, S. J., Ng, L. C., & Stuart Dols, W. (2019). Simulation Analysis of Potential Energy Savings from Air Sealing Retrofits of U.S. Commercial Buildings. In *Symposium on Whole Building Air Leakage: Testing and Building Performance Impacts* (pp. 61–70). ASTM International. https://doi.org/10.1520/STP161520180021

Energy performance of buildings directive. (n.d.). European Commission. https://energy.ec.europa.eu/topics/energy-efficiency/energy-efficient-buildings/energy-performance-buildings-directive_en

EnergyPlus. (n.d.). https://energyplus.net/

EnergyPlus Validation Reports. (n.d.). https://simulationresearch.lbl.gov/dirpubs/valid_ep.html

EPW Map. (n.d.). https://www.ladybug.tools/epwmap/#close

Etheridge, D. W., & Clare, A. D. (2001, September 11). Dynamic Insulation - Recent Experimental and Theoretical studies. *22ND ANNUAL AIVC CONFERENCE*. https://www.semanticscholar.org/paper/DYNAMIC-INSULATION-RECENT-EXPERIMENTAL-AND-STUDIES-Etheridge/ba642f554926e641de388d32f21173bce6b65d57

European Climate Law. (n.d.). European Commission. https://climate.ec.europa.eu/eu-action/european-green-deal/european-climate-law_en

European Committee for Standardization. (2019a). *Energy performance of buildings - Ventilation for buildings - Part 2: Interpretation of the requirements in EN 16798-1 - Indoor environmental input parameters for design and assessment of energy performance of buildings addressing indoor air quality, thermal environment, lighting and acoustics (Module M1- 6) (NPR-CEN/TR 16798-2)*.

European Committee for Standardization. (2019b). *Energy performance of buildings - Ventilation for buildings - Part 1: Indoor environmental input parameters for design and assessment of energy performance of buildings addressing indoor air quality, thermal environment, lighting and acoustics - Module M1-6 (EN 16798-1)*.

Factsheet - Energy Performance of Buildings. (2021, December 15). European Commission. https://ec.europa.eu/commission/presscorner/detail/en/fs_21_6691

Fathalian, A., & Kargarsharifabad, H. (2018). Actual validation of energy simulation and investigation of energy management strategies (Case Study: An office building in Semnan, Iran). *Case Studies in Thermal Engineering*, *12*, 510–516. https://doi.org/10.1016/j.csite.2018.06.007

Fawaier, M., & Bokor, B. (2022). Dynamic insulation systems of building envelopes: A review. In *Energy and Buildings* (Vol. 270). Elsevier Ltd. https://doi.org/10.1016/j.enbuild.2022.112268

Gan, G. (2000). Numerical evaluation of thermal comfort in rooms with dynamic insulation. *Building and Environment*, *35*(5), 445–453. https://doi.org/10.1016/S0360-1323(99)00034-7

Gillott, M. C., Loveday, D. L., White, J., Wood, C. J., Chmutina, K., & Vadodaria, K. (2016). Improving the airtightness in an existing UK dwelling: The challenges, the measures and their effectiveness. *Building and Environment*, *95*, 227–239. https://doi.org/10.1016/j.buildenv.2015.08.017

Goia, F., Chaudhary, G., & Fantucci, S. (2018). Modelling and experimental validation of an algorithm for simulation of hysteresis effects in phase change materials for building components. *Energy and Buildings*, *174*, 54–67. https://doi.org/10.1016/j.enbuild.2018.06.001

Guillén-Lambea, S., Rodríguez-Soria, B., & Marín, J. M. (2019). Air infiltrations and energy demand for residential low energy buildings in warm climates. *Renewable and Sustainable Energy Reviews*, *116*. https://doi.org/10.1016/j.rser.2019.109469

Hafez, A. H. (2016). *Integrating Building Functions into Massive External Walls* [PhD Thesis, Delft University of Technology]. https://doi.org/10.7480/abe.2016.9

Halliday, S. (2001). *Performance of Dynamic Insulation*. https://www.semanticscholar.org/paper/Performance-of-Dynamic-Insulation-Halliday/415df0cbc1bfa989082bfdd8337d53d5373fa397

Historisch metselwerk (URL 4003). (n.d.). ERM. https://www.stichtingerm.nl/kennis-richtlijnen/url4003

Historisch timmerwerk (URL 4001). (n.d.). ERM. https://www.stichtingerm.nl/kennis-richtlijnen/url4001

Holland, J. H. (1992). *Adaptation in Natural and Artificial Systems: An Introductory Analysis with Applications to Biology, Control, and Artificial Intelligence* (1st ed.). MIT Press Edition. https://books.google.nl/books?hl=nl&lr=&id=5EgGaBkwvWcC&oi=fnd&pg=PR7&ots=mJor5-Opph&sig=UvbGLDro78dca1haKRkNwjf-d6w&redir_esc=y#v=onepage&q&f=false

Homem, J. T. (2017). *Dynamic Insulation as a strategy for Net-Zero Energy Buildings* [Master Thesis, University of Lisbon]. https://repositorio.ul.pt/bitstream/10451/28285/1/ulfc121992_tm_Jo%C3%A3o_Alves_Homem.pdf

Imbabi, M., & Elsarrag, E. (n.d.). *Tuneable U-Values for Energy Efficient, Low Carbon Building Envelopes*. https://www.academia.edu/25038519/Tuneable_U_values_for_energy_efficient_low_carbon_building_envelopes

Imbabi, M. S.-E. (2006). Modular breathing panels for energy efficient, healthy building construction. *Renewable Energy*, *31*(5), 729–738. https://doi.org/10.1016/j.renene.2005.08.009

Imbabi, M. S.-E. (2012). A passive–active dynamic insulation system for all climates. *International Journal of Sustainable Built Environment*, *1*(2), 247–258. https://doi.org/10.1016/j.ijsbe.2013.03.002

International Organization for Standardization. (2005). *Ergonomics of the thermal environment Analytical determination and interpretation of thermal comfort using calculation of the PMV and PPD indices and local thermal comfort criteria (ISO Standard No. 7730:2005)*. https://www.iso.org/standard/39155.html

Iooss, B., & Lemaitre, P. (2015). A Review on Global Sensitivity Analysis Methods. In Springer (Ed.), *Uncertainty Management in Simulation-Optimization of Complex Systems. Operations Research/Computer Science Interfaces Series* (Vol. 59). https://doi.org/https://doi.org/10.1007/978-1-4899-7547-8_5

Jokisalo, J., Kurnitski, J., Korpi, M., Kalamees, T., & Vinha, J. (2009). Building leakage, infiltration, and energy performance analyses for Finnish detached houses. *Building and Environment*, *44*(2), 377–387. https://doi.org/10.1016/j.buildenv.2008.03.014

Jones, S. R. (1988). *Old Houses in Holland*. https://books.google.nl/books?hl=en&lr=&id=I-V1EAAAQBAJ&oi=fnd&pg=PT21&dq=traditional+external+wall+construction+netherlands+dutch+monuments&ots=8eYJI_byIG&sig=kHULeqMevhP9b7dG27el363LG_E&redir_esc=y#v=onepage&q&f=false

Kölsch, B., Tiddens, A., Estevam Schmiedt, J., Schiricke, B., & Hoffschmidt, B. (2019). Detection of Air Leakage in Building Envelopes Using Ultrasound Technology. In *Symposium on Whole Building Air Leakage: Testing and Building Performance Impacts* (pp. 160–183). ASTM International. https://doi.org/10.1520/STP161520180022

Krarti, M. (1994). Effect of Air Flow on Heat Transfer in Walls. *Journal of Solar Energy Engineering*, *116*(1), 35–42. https://doi.org/10.1115/1.2930063

Lara, R. A., Naboni, E., Pernigotto, G., Cappelletti, F., Zhang, Y., Barzon, F., Gasparella, A., & Romagnoni, P. (2017). Optimization Tools for Building Energy Model Calibration. *Energy Procedia*, *111*, 1060–1069. https://doi.org/10.1016/j.egypro.2017.03.269

Little, J., Ferraro, C., Arregi, B., & Eachdraidheil Alba, À. (2015). *Assessing risks in insulation retrofits using hygrothermal software tools Heat and moisture transport in internally insulated stone walls Historic Environment Scotland*. www.historic-scotland.gov.uk/technicalpapers

Long, L. D. (2023). An AI-driven model for predicting and optimizing energy-efficient building envelopes. *Alexandria Engineering Journal*, *79*, 480–501. https://doi.org/10.1016/j.aej.2023.08.041

Martínez-Molina, A., Tort-Ausina, I., Cho, S., & Vivancos, J. L. (2016). Energy efficiency and thermal comfort in historic buildings: A review. In *Renewable and Sustainable Energy Reviews* (Vol. 61, pp. 70–85). Elsevier Ltd. https://doi.org/10.1016/j.rser.2016.03.018

Mateus, N. M., Pinto, A., & Graça, G. C. da. (2014). Validation of EnergyPlus thermal simulation of a double skin naturally and mechanically ventilated test cell. *Energy and Buildings*, *75*, 511–522. https://doi.org/10.1016/j.enbuild.2014.02.043

Menberg, K., Heo, Y., & Choudhary, R. (2016). Sensitivity analysis methods for building energy models: Comparing computational costs and extractable information. *Energy and Buildings*, *133*, 433–445. https://doi.org/10.1016/j.enbuild.2016.10.005

Monumenten Verduurzamen. (n.d.). Monumenten.Nl. https://www.monumenten.nl/monumenten-verduurzamen/een-monument-verduurzamen-hoe-doet-u-dat

Murata, S., Tsukidate, T., Fukushima, A., Abuku, M., Watanabe, H., & Ogawa, A. (2015). Periodic Alternation between Intake and Exhaust of Air in Dynamic Insulation: Measurements of Heat and Moisture Recovery Efficiency. *Energy Procedia*, *78*, 531–536. https://doi.org/10.1016/j.egypro.2015.11.731

NAIMA Canada. (n.d.). *Airflow Principles*. Insulation and Air Sealing Manual. https://guides.co/g/insulation-manual-moisture-flow-principles/127621

Ng, L. C., Musser, A., Persily, A. K., & Emmerich, S. J. (2013). Multizone airflow models for calculating infiltration rates in commercial reference buildings. *Energy and Buildings*, *58*, 11–18. https://doi.org/10.1016/j.enbuild.2012.11.035

Orme, M., & Leksmono, N. (2002). *AIVC Guide 5 - Ventilation Modelling Data Guide*.

Orme, M., Liddament, M. W., & Wilson, A. (1998). *Numerical Data for Air Infiltration & Natural Ventilation Calculations*. https://www.aivc.org/sites/default/files/members_area/medias/pdf/Technotes/TN44%20NUMERICAL%20DATA%20FOR%20AIR%20INFILTRATION.PDF

Ortiz, M., & Bluyssen, P. M. (2022). Indoor environmental quality, energy efficiency and thermal comfort in the retrofitting of housing. In *Routledge Handbook of Resilient Thermal Comfort* (pp. 433–445). Routledge. https://doi.org/10.4324/9781003244929-32

Ozdenefe, M., Rezaei, M., & Atikol, U. (2016). Comparison Of Dynamic Thermal Simulation Results With Experimental Results: Trombe Wall Case Study For A Cyprus Test Building. *BSO Conference 2016: Third Conference of IBPSA-England*. https://publications.ibpsa.org/conference/paper/?id=bso2016_1132

Paleari, L., Movedi, E., Zoli, M., Burato, A., Cecconi, I., Errahouly, J., Pecollo, E., Sorvillo, C., & Confalonieri, R. (2021). Sensitivity analysis using Morris: Just screening or an effective ranking method? *Ecological Modelling*, *455*, 109648. https://doi.org/10.1016/j.ecolmodel.2021.109648

Paris Agreement. (n.d.). European Commission . https://climate.ec.europa.eu/eu-action/international-action-climate-change/climate-negotiations/paris-agreement_en

Park, K.-S., Kim, S.-W., & Yoon, S.-H. (2016). Application of Breathing Architectural Members to the Natural Ventilation of a Passive Solar House. *Energies*, *9*(3), 214. https://doi.org/10.3390/en9030214

Penna, P., Prada, A., Cappelletti, F., & Gasparella, A. (2015). Multi-objectives optimization of Energy Efficiency Measures in existing buildings. *Energy and Buildings*, *95*, 57–69. https://doi.org/10.1016/j.enbuild.2014.11.003

Prignon, M., Altomonte, S., Ossio, F., Dawans, A., & Van Moeseke, G. (2021). On the applicability of meta-analysis to evaluate airtightness performance of building components. *Building and Environment*, *194*, 107684. https://doi.org/10.1016/j.buildenv.2021.107684

Prignon, M., & Van Moeseke, G. (2017). Factors influencing airtightness and airtightness predictive models: A literature review. In *Energy and Buildings* (Vol. 146, pp. 87–97). Elsevier Ltd. https://doi.org/10.1016/j.enbuild.2017.04.062

Qiu, K., & Haghighat, F. (2007). Modeling the combined conduction—Air infiltration through diffusive building envelope. *Energy and Buildings*, *39*(11), 1140–1150. https://doi.org/10.1016/j.enbuild.2006.11.013

Renovation. (n.d.). In *Cambridge Dictionary*. https://dictionary.cambridge.org/dictionary/english/renovation

Renovation wave. (n.d.). European Commission. https://energy.ec.europa.eu/topics/energy-efficiency/energy-efficient-buildings/renovation-wave_en#:~:text=The%20Renovation%20Wave%20initiative%20builds,and%20climate%20plans%20(NECPs).

Ridley, I., Fox, J., Oreszczyn, T., & Hong, S. H. (2003). The Impact of Replacement Windows on Air Infiltration and Indoor Air Quality in Dwellings. *International Journal of Ventilation*, *1*(3), 209–218. https://doi.org/10.1080/14733315.2003.11683636

RVO. (n.d.). *All-in-one permit for renovating or demolishing protected monuments*. Business.Gov.Nl. https://business.gov.nl/regulation/all-in-one-permit-monuments/

Salehi, A., Torres, I., & Ramos, A. (2017). Assessment of ventilation effectiveness in exiting residential building in mediterranean countries: Case study, existing residential building in Portugal. *Sustainable Cities and Society*, *32*, 496–507. https://doi.org/10.1016/j.scs.2017.04.018

Saltelli, A., Ratto, M., Andres, T., Campolongo, F., Cariboni, J., Gatelli, D., Saisana, M., & Tarantola, S. (2008). *Global Sensitivity Analysis: The Primer*. John Wiley & Sons. https://books.google.nl/books?hl=en&lr=&id=wAssmt2vumgC&oi=fnd&pg=PR7&ots=VWBwVm5R64&sig=JIDCV6JIL3r1RS7IYgkDLoPB2zc&redir_esc=y#v=onepage&q&f=false

Samuel, A., Imbabi, M., Peacock, A., & Strachan, P. (2003, September). An engineering approach to modelling of dynamic insulation using ESP-r. *7th ASHRAE/CIBSE Conference*. https://www.researchgate.net/publication/270285485_An_engineering_approach_to_modelling_of_dynamic_insulation_using_ESP-r

Sherman, M. H., & Walker, I. S. (2001). *Heat Recovery in Building Envelopes*. https://www.semanticscholar.org/paper/Heat-recovery-in-building-envelopes-Walker-Sherman/ab97dafff3f521e2991e87d9b41bd8d3b744c233

Solupe, M., & Krarti, M. (2014). Assessment of infiltration heat recovery and its impact on energy consumption for residential buildings. *Energy Conversion and Management*, *78*, 316–323. https://doi.org/10.1016/j.enconman.2013.10.058

Stenvert, R. (2012). *Biografie van de Baksteen 1850-2000* (Wbooks). https://www.cultureelerfgoed.nl/publicaties/publicaties/2012/01/01/de-biografie-van-de-baksteen

Stephen, R. K. (1998). *Airtightness in UK Dwellings: BRE's test results and their significance*. www.bre.co.uk

Taylor, B., & Imbabi, M. (1998). The application of dynamic insulation in buildings. *Renewable Energy*, *15*(1–4), 377–382. https://doi.org/10.1016/S0960-1481(98)00190-6

Taylor, B. J., Cawthorne, D. A., & Imbabif, M. S. (1996). *Analytical Investigation of the Steady-State Behaviour of Dynamic and Diffusive Building Envelopes* (Vol. 31, Issue 6).

Taylor, B. J., & Imbabi, M. (2000). Environmental design using dynamic insulation. *ASHRAE Transactions*. https://www.semanticscholar.org/paper/Environmental-design-using-dynamic-insulation.-Taylor-Imbabi/bdf0580ada9a41c6762c9f07820cabbb13d4d799

Taylor, B. J., & Imbabi, M. S. (1997). The effect of air film thermal resistance on the behaviour of dynamic insulation. *Building and Environment*, *32*(5), 397–404. https://doi.org/10.1016/S0360-1323(97)00012-7

Taylor, B. J., Webster, R., & Imbabi, M. S. (1997). The use of dynamic and diffusive insulation for combined heat recovery and ventilation in buildings. *BEPAC/EPSRC Sustainable Building Conference*, 168–174. https://www.semanticscholar.org/paper/The-use-of-dynamic-and-diffusive-insulation-for-and-Taylor-Webster/f215e68256cc6f4052c0b97a3841790ddb826be5#cited-papers

Taylor, B. J., Webster, R., & Imbabi, M. S. (1998). The building envelope as an air filter. *Building and Environment*, *34*(3), 353–361. https://doi.org/10.1016/S0360-1323(98)00017-1

Thamban, A. (2020). *Analysis of infiltration in buildings using LES and airflow network models* [Master Thesis, Delft University of Technology]. http://repository.tudelft.nl/

The Parameters. (2020). JEPlus.Org. http://www.jeplus.org/wiki/doku.php?id=docs:jeplus:v21:params

Tian, W. (2013). A review of sensitivity analysis methods in building energy analysis. *Renewable and Sustainable Energy Reviews*, *20*, 411–419. https://doi.org/10.1016/j.rser.2012.12.014

Toolkit Duurzaam Erfgoed. (n.d.). Duurzaam Erfgoed. https://www.duurzaamerfgoed.nl/partnervoorbeelden/toolkit-duurzaam-erfgoed

U.S. Department of Energy. (2022). *Application Guide for EMS*.

U.S. Department of Energy. (2023). *Engineering Reference*. https://energyplus.net/assets/nrel_custom/pdfs/pdfs_v23.2.0/EngineeringReference.pdf

Verbeke, S., & Audenaert, A. (2020). A prospective Study on the Evolution of Airtightness in 41 low energy Dwellings. *E3S Web of Conferences*, *172*, 05005. https://doi.org/10.1051/e3sconf/202017205005

Walker, I. S., & Wilson, D. J. (1998). Field Validation of Algebraic Equations for Stack and Wind Driven Air Infiltration Calculations. In *HVAC & Research* (2nd ed., Vol. 1, Issue 2, pp. 119–139). https://www.aivc.org/sites/default/files/airbase_11869.pdf

Walker, I. S., Wilson, D. J., & Sherman, M. H. (1998). A comparison of the power law to quadratic formulations for air infiltration calculations. *Energy and Buildings*, *27*(3), 293–299. https://doi.org/10.1016/S0378-7788(97)00047-9

Wang, Z., & Ierapetritou, M. (2018). *Global sensitivity, feasibility, and flexibility analysis of continuous pharmaceutical manufacturing processes* (pp. 189–213). https://doi.org/10.1016/B978-0-444-63963-9.00008-7

Wang, Z., & Rangaiah, G. P. (2017). Application and Analysis of Methods for Selecting an Optimal Solution from the Pareto-Optimal Front obtained by Multiobjective Optimization. *Industrial & Engineering Chemistry Research*, *56*(2), 560–574. https://doi.org/10.1021/acs.iecr.6b03453

Whitear, H., & Duxbury, T. (n.d.). *Understanding Traditional Buildings*. https://www.tywicentre.org.uk/media/1051/tywileaflet2-eng-final.pdf

Wong, J. M., Glasser, F. P., & Imbabi, M. S. (2007). Evaluation of thermal conductivity in air permeable concrete for dynamic breathing wall construction. *Cement and Concrete Composites*, *29*(9), 647–655. https://doi.org/10.1016/j.cemconcomp.2007.04.008

Wurtz, A., Schalbart, P., & Peuportier, B. (2021, September). Application of optimisation, building energy simulation and life cycle assessment to the design of an urban project. *Building Simulation 2021 Conference*. https://hal.science/hal-03379987/document

Younes, C., Shdid, C. A., & Bitsuamlak, G. (2012). Air infiltration through building envelopes: A review. *Journal of Building Physics*, *35*(3), 267–302. https://doi.org/10.1177/1744259111423085

Zagorskas, J., Paliulis, G. M., Burinskienė, M., & Venckauskaitė, J. (2013). Energetic Refurbishment of Historic Brick Buildings: Problems and Opportunities. *Scientific Journal of Riga Technical University. Environmental and Climate Technologies*, *12*(1), 20–27. https://doi.org/10.2478/rtuect-2013-0012

Zesdelig stappenplan verduurzaming. (n.d.). Duurzaam Erfgoed. https://www.duurzaamerfgoed.nl/partnervoorbeelden/zes-stappen-naar-een-duurzaam-monument

Zhang, C., & Wang, J. (2021). Determining the critical insulation thickness of breathing wall: Analytical model, key parameters, and design. *Case Studies in Thermal Engineering*, *27*. https://doi.org/10.1016/j.csite.2021.101326

Zmeureanu, R. (2000). Cost-Effectiveness of Increasing Airtightness of Houses. *Journal of Architectural Engineering*, *6*(3).

Appendices

Appendix A – Case Study Building Plans

The Case Study building, at Herengracht 15 in Leiden, is a historic traditional single-family dwelling, of solid wall brick masonry construction with a pitched clay-tiled roof. Built in 1750, it is registered as a National Monument and is thus subject to the associated monumental restrictions on its renovation works.

It harbors characteristics representative of the buildings of the residential buildings of that time, although it could be considered on high-end of that segment of the building stock. It underwent two partial renovations, in the 1980's and 2020's, and was maintained in fairly good condition.

The building elevations, sections, and floor plans are provided in Figures 73 and 74 below, from the 1980's renovation drawings (Architektenburo Bob C Van Beek bv., 1980)

Figure 73: Case Study Building - Facade Drawing

Figure 74: Case Study Building - Plans

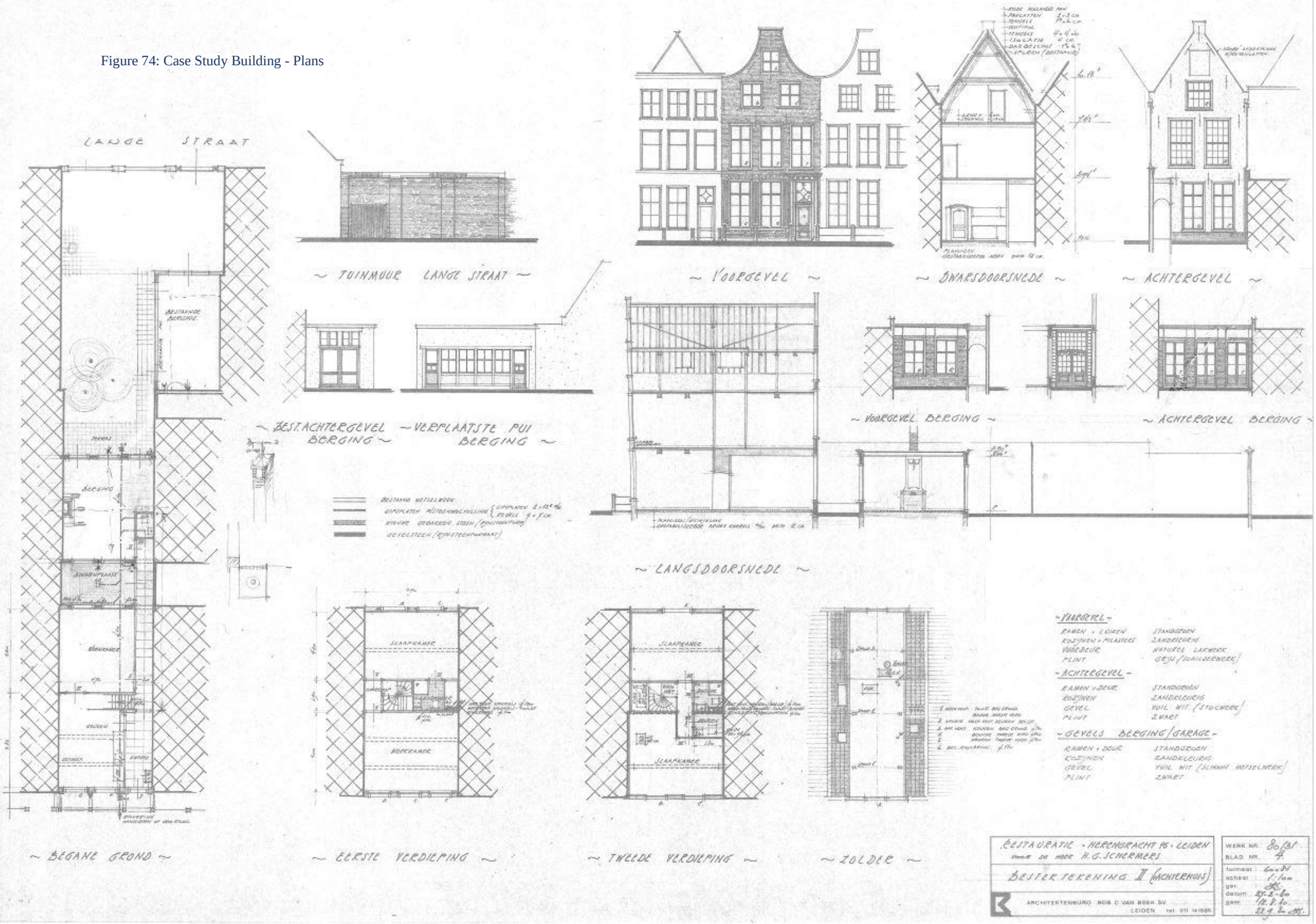

Appendix B – Building Air Leakage Characterization

The fan pressurization results consider a set of paired leakage flow and pressure gradient measurements for pressure differences varying between 10 Pa and 50 Pa, under both pressurization and depressurization conditions. The corrected measurements are presented in the Tables 32, 34, and 36 for the Rounds 1, 2, and 3 respectively.

The corrected measurements are then fitted into a power law equation (Refer to Figures 75, 77, and 79), and the resulting air leakage flow at the characteristic pressures of 10 Pa and 50 Pa are deduced. The building's characteristic air leakage data is then taken as the average of the pressurization and depressurization results (Refer to Tables 33, 35, and 37).

The power law equation characterizing the building's behavior under each of the Rounds 1, 2, and 3 is then fitted (Refer to Figures 76, 78, and 80). The final results are summarized and compared under Chapter 5.3.

Round 1 Measurements

Table 32: Fan-pressurization's Round 1 Measurement Results

Under-Pressure								
Induced Pressure	[Pa]	-45.3	-44.3	-36.6	-29.1	-25.5	-18	-13.9
Corrected Flow	[l/s]	1389.7	1358.4	1246.8	1066.9	980.06	806.6	680.14
Error	[%]	-0.2	-1.1	-1.8	-0.1	-0.5	-1.0	-0.7
Over-Pressure								
Induced Pressure	[Pa]	48.9	47	40.2	35.4	28.6	23	16.8
Corrected Flow	[l/s]	1541.4	1494	1355.5	1244.8	1082.3	936.52	723.02
Error	[%]	-0.6	-1.1	0.1	0.5	1.2	1.9	-2.0

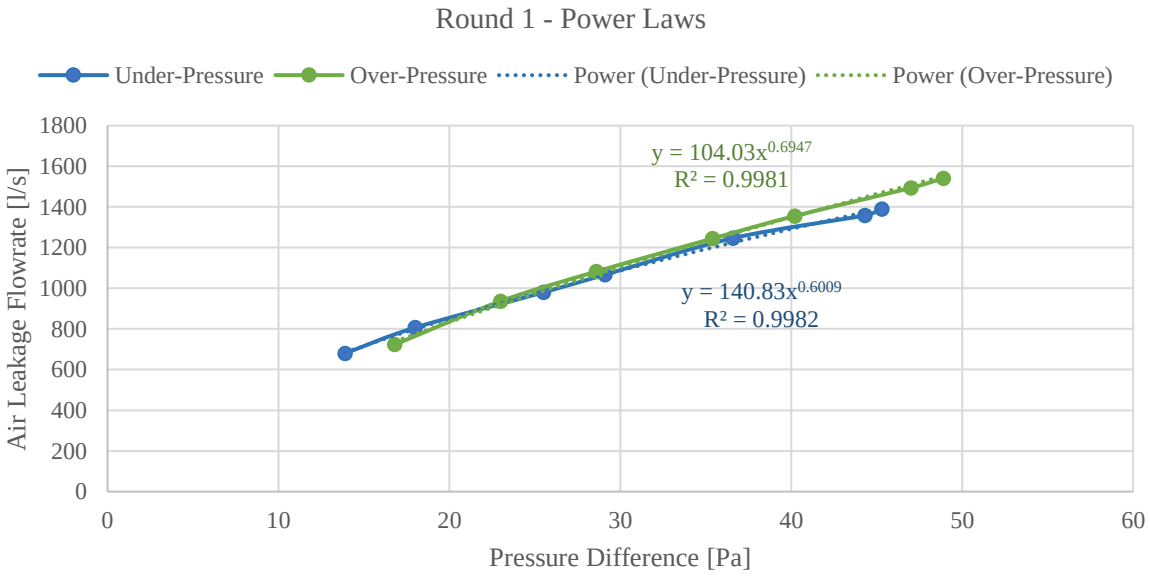

Figure 75: Round 1 Under-Pressure and Over-Pressure Power Law Equations

Table 33: Round 1 Characteristic Building Air Leakage Data

Power Law									
Pressure [Pa]	50	45	40	35	30	25	20	15	10
Flow [l/s]									
Under-Pressure	1477.8	1387.1	1292.3	1192.7	1087.2	974.4	852.1	716.8	561.82
Over-Pressure	1575.6	1464.4	1349.3	1229.8	1104.9	973.4	833.7	682.6	515.1
Average	1526.7	1425.7	1320.8	1211.2	1096.0	842.9	699.7	538.4	538.4

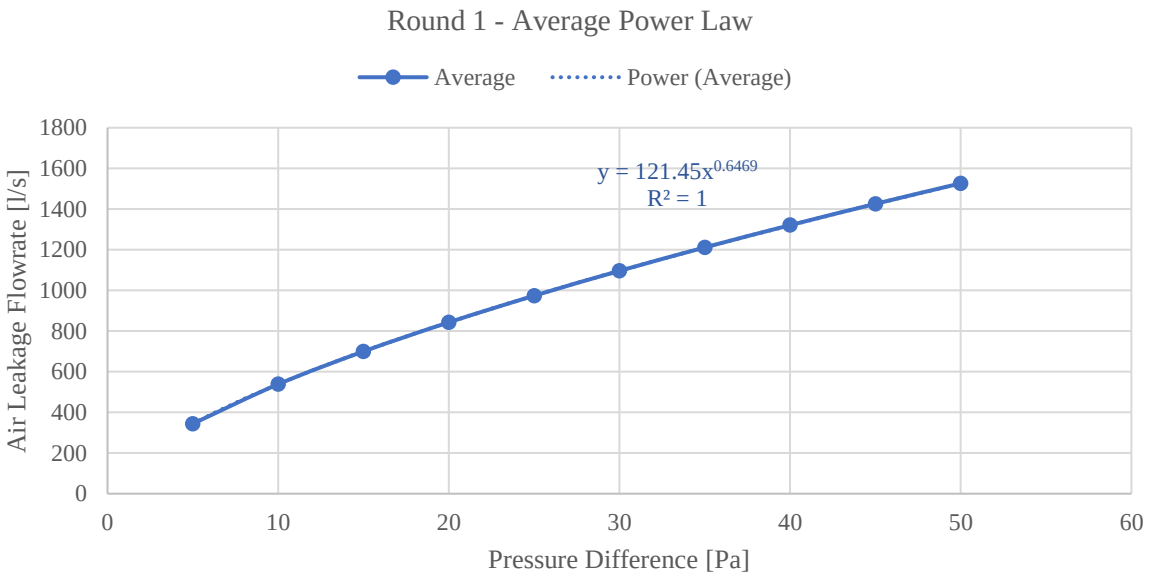

Figure 76: Round 1 Average Power Law Equation

Round 2 Measurements

Table 34: Fan-pressurization's Round 2 Measurement Results

Under-Pressure									
Induced Pressure	[Pa]	-56.6	-54.8	-50.1	-42.9	-36.1	-29.8	-24	-19.2
Corrected Flow	[l/s]	1400	1384.8	1316.3	1201.7	1073.2	955.46	839.01	727.12
Error	[%]	-0.9	-0.0	0.4	0.7	-0.1	0.0	0.3	-0.4
Over-Pressure									
Induced Pressure	[Pa]	56.5	56.6	52	45	39.1	31.9	26.8	20.3
Corrected Flow	[l/s]	1562.3	1546.9	1458.7	1316.2	1166.5	1056.1	935.48	825.83
Error	[%]	2.1	1.1	0.6	-0.6	-3.6	-0.7	-1.9	3.3

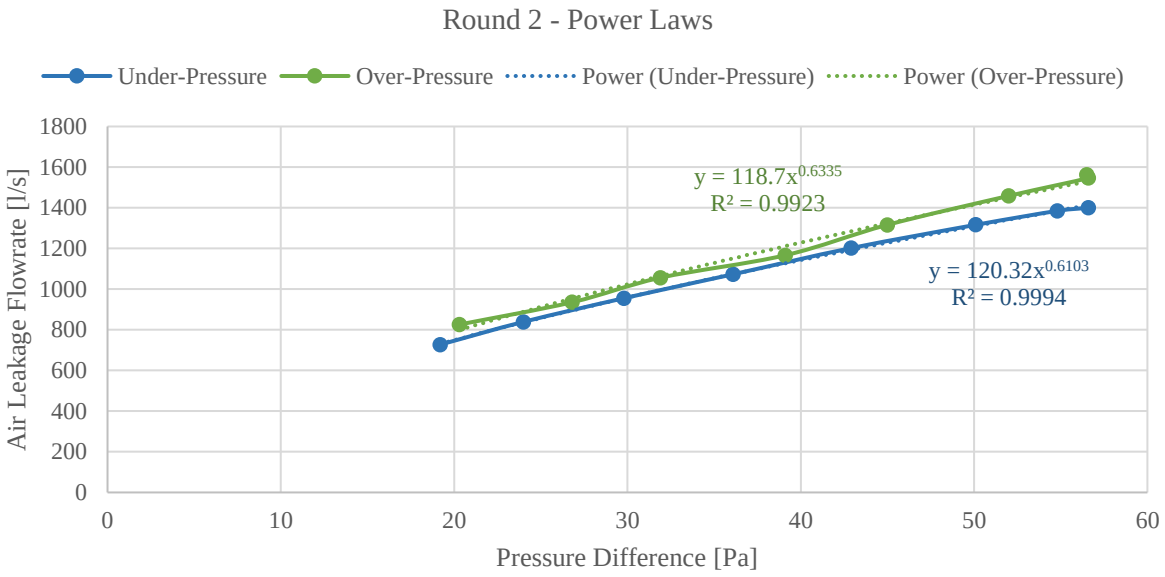

Figure 77: Round 2 Under-Pressure and Over-Pressure Power Law Equations

Table 35: Round 2 Characteristic Building Air Leakage Data

	Power Law								
Pressure [Pa]	50	45	40	35	30	25	20	15	10
Flow [l/s]									
Under-Pressure	1309.8	1228.3	1143.1	1053.6	959.0	858.0	748.8	628.2	490.3
Over-Pressure	1415.0	1323.6	1228.4	1128.8	1023.8	912.1	791.9	660.0	510.4
Average	1362.4	1276.0	1185.8	1091.2	991.4	885.1	770.3	644.1	500.5

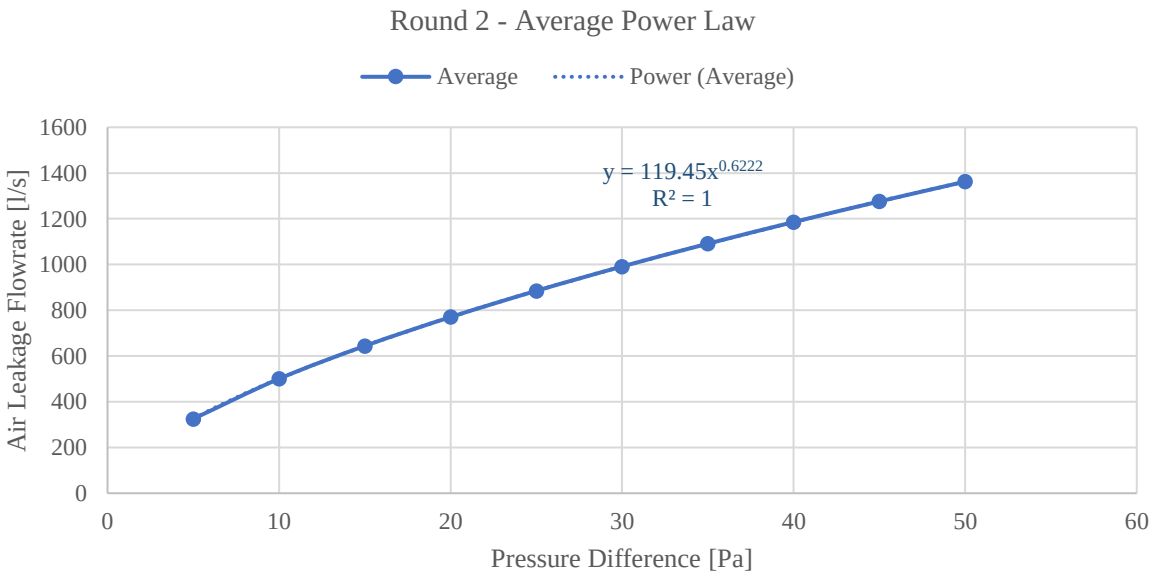

Figure 78: Round 2 Average Power Law Equation

Round 3 Measurements

Table 36: Fan-pressurization's Round 3 Measurement Results

Under-Pressure									
Induced Pressure	[Pa]	-60.2	-59.2	-52.1	-44	-36.2	-28.4	-21.1	-14.7
Corrected Flow	[l/s]	1467.7	1456.7	1327.2	1189.7	1060.1	914.4	765.53	656.75
Error	[%]	1.6	1.8	-0.1	-1.1	-1.3	-2.0	-2.3	3.6
Over-Pressure									
Induced Pressure	[Pa]	57.5	57.8	52.3	46.4	39.3	30.8	22.6	15
Corrected Flow	[l/s]	1521.6	1533.7	1458.4	1352.9	1206.8	1026.1	809	692.18
Error	[%]	-0.3	0.2	1.4	1.2	0.1	-1.1	-5.3	4.1

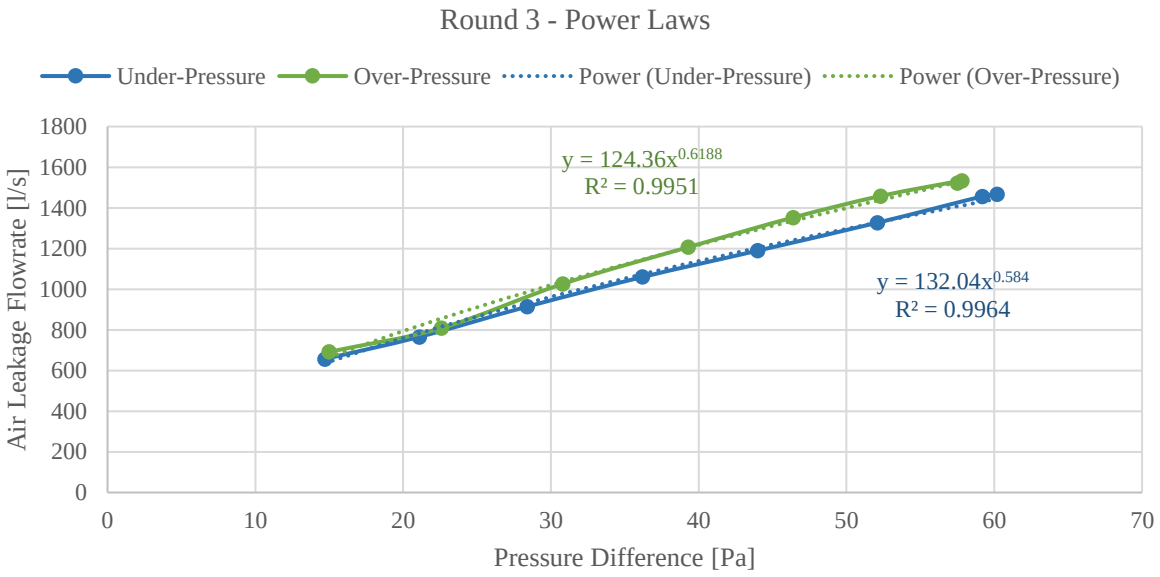

Figure 79: Round 3 Under-Pressure and Over-Pressure Power Law Equations

Table 37: Round 3 Characteristic Building Air Leakage Data

Power Law									
Pressure [Pa]	50	45	40	35	30	25	20	15	10
Flow [l/s]									
Under-Pressure	1296.9	1219.5	1138.4	1053.0	962.4	865.2	759.5	642.0	506.6
Over-Pressure	1399.6	1311.3	1219.1	1122.4	1020.3	911.4	793.9	664.4	517.0
Average	1265.4	1178.8	1087.7	991.3	888.3	776.7	653.2	511.8	337.3

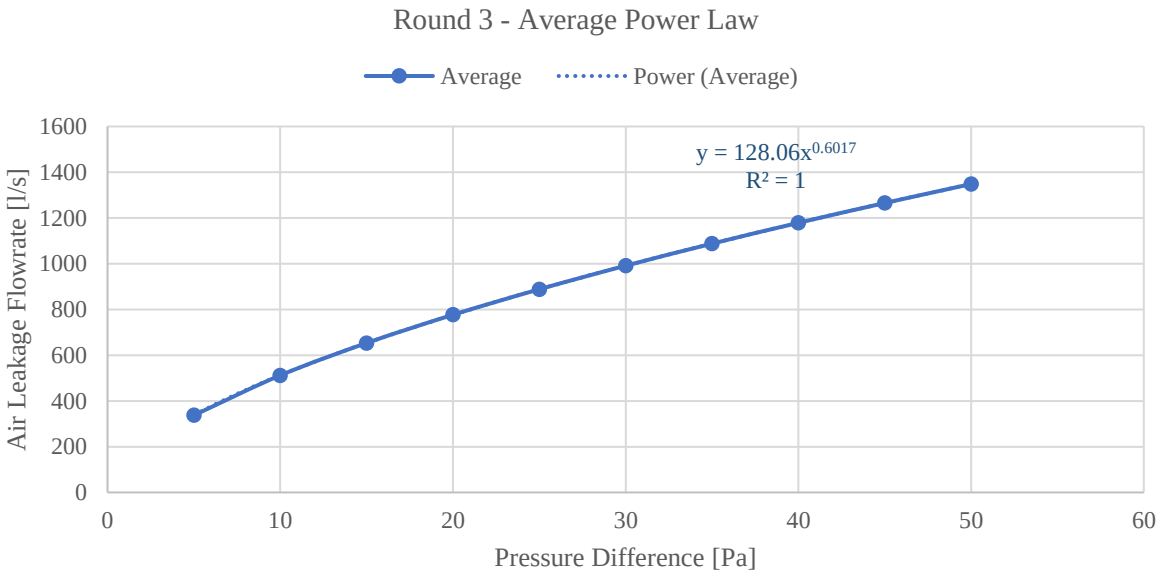

Figure 80: Round 3 Average Power Law Equation

Appendix C – Component Air Leakage Characterization

The reductive sealing method helps quantify the contribution of air leakage pathways to the building's total leakage, up to the measurement apparatus' precision. A sealed component's air leakage is then estimated as the difference in the measured air leakage flows between consecutive reductive sealing rounds.

The conducted reductive sealing accordingly provide information about the contribution of openings (windows and doors) as the difference between Rounds 1 and 2, and the living room's plenum hatch as the difference between Rounds 2 and 3, and the envelope surfaces (walls and roof) as the remaining leakage when all other concentrated leakage is subtracted.

The leakage flow contributions are presented in the Tables 38, 40, and 41 for the openings, living room's plenum hatch, and envelope surfaces respectively.
The calculated component contributions are then fitted into a power law equation (Refer to Figures 81, 82, and 83), and normalized by the components' length or area.

The final partitioning of the building's total air leakage into its components is summarized in the form of their total leakage and normalized leakage under Chapter 5.4.

Openings Contribution

Table 38: Sealed Openings' Leakage Flow Contribution Results

Sealed Openings Contribution: Round 1 – Round 2

Pressure	[Pa]	50	45	40	35	30	25	20	15	10
Flow	[l/s]	164.25	149.79	135.06	120.02	104.63	88.83	72.54	55.65	37.97

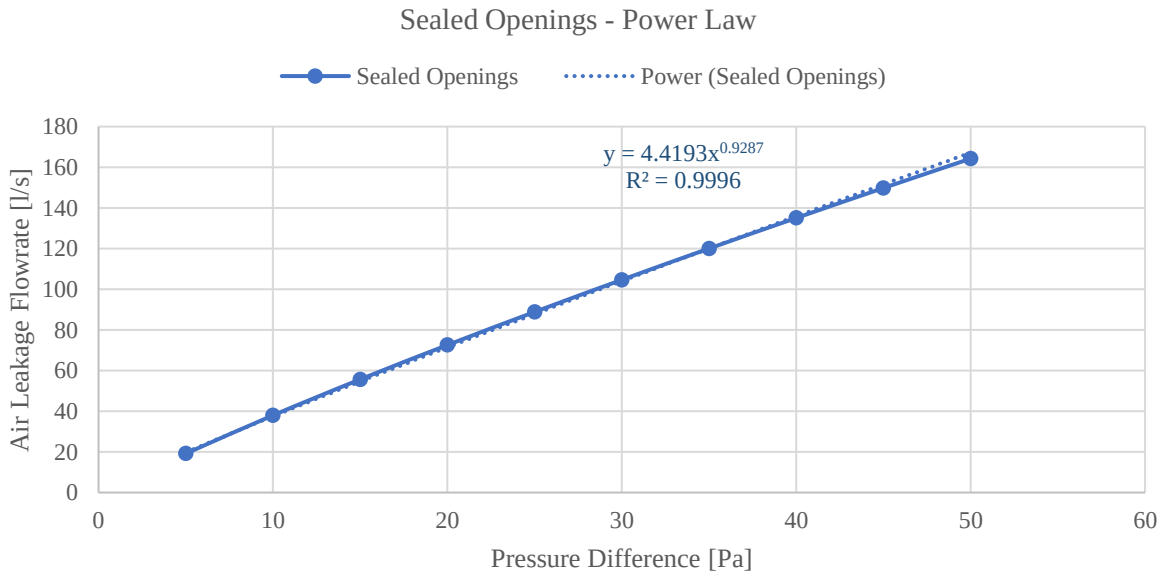

Figure 81: Openings' Fitted Power Law Equation

Relative to the Round 1, the Round 2 considers the sealing of all windows and doors, at the exception of the skylight windows and the main entrance door, where the blower door fan was located.
The corresponding power law coefficient (C) is then normalized against the total opening perimeter, considering the sealed openings only.

Opening Perimeter Length = 151.456 [m]
without skylights and main entrance door

- Power Law Equation
  - $Q = 4.4193 \times \Delta P^{0.9287}$ [l/s]
- Normalized Power Law Equation
  - $Q = 0.029 \times \Delta P^{0.9287}$ [l/s.m]
  - $Q = 0.0000351 \times \Delta P^{0.9287}$ [kg/s.m]

For the purpose of this analysis, all windows are assumed to have the same contribution. The resulting normalized power law equation is thus considered to be representative of all openings.

The openings' total leakage is estimated using the openings' normalized power law equation, identified above, and the openings' total perimeter length:

Opening Perimeter Length = 175.376 [m]
with skylights and main entrance door

- Normalized Power Law Equation
  - $Q = 0.029 \times \Delta P^{0.9287}$ [l/s.m]
- Power Law Equation
  - $Q = 5.086 \times \Delta P^{0.9287}$ [l/s]

Table 39: All Openings' Leakage Flow Contribution

All Openings Contribution

Pressure	[Pa]	50	45	40	35	30	25	20	15	10
Flow	[l/s]	192.40	174.46	156.39	138.15	119.72	101.07	82.15	62.89	43.16

Living Room's Plenum Hatch

Table 40: Living Room Plenum Hatch's Leakage Flow Contribution Results

Living Room's Plenum Hatch Contribution: Round 2 – Round 3

Pressure	[Pa]	50	45	40	35	30	25	20	15	10
Flow	[l/s]	14.16	10.56	7.00	3.49	0.07	-3.24	-6.35	-9.14	-11.34

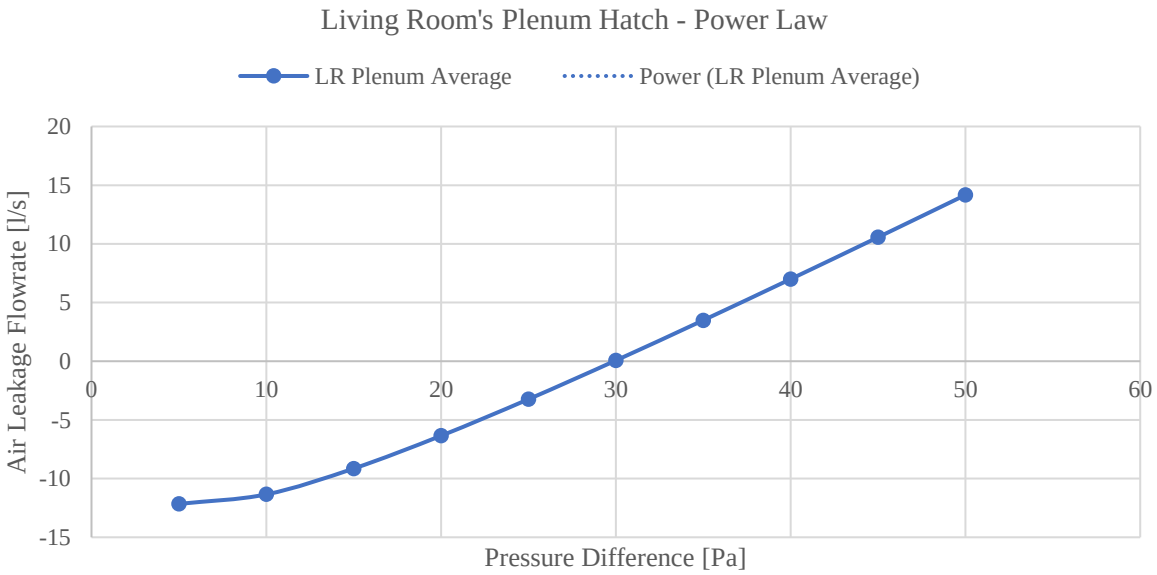

Figure 82: Living Room Plenum Hatch's Fitted Power Law Equation

The air leakage into the building shows practically the same behavior before and after the sealing of the living room's plenum hatch. Its contribution is thus assumed to be negligible and will be, accordingly, not considered.

Envelope Surfaces

Considering the case study building's previous renovation works, measurable treatment to concentrated leakage pathways has been done. This is put forward by the IR thermal images; practically all potential locations for concentrated air leakage are limited to around the openings' frames. Other locations could consider the living room's plenum hatch and the chimney's flue. No joint leakage locations between the walls and other surfaces are worthy of mention.

The living room's plenum hatch's leakage was found to be, by far, the most significant air leakage source, based on both the IR imagery and the sensed draught in-situ. With this leakage identified as negligible to the fan pressurization apparatus' resolution, the other concentrated leakage locations observed may be assumed to be too small to be captured into the measurements.

Accordingly, the building's total leakage is assumed to be divided between the concentrated leakage of the openings (doors and windows) and the diffuse leakage of the envelope surfaces (roof and walls).

The contribution of the envelope surfaces may thus be defined as the difference between the building's total measured leakage (Round 1) and the air leaking from all openings.

Table 41: Envelope Surfaces' Leakage Flow Contribution Results

Envelope Surfaces' Contribution: Round 1 – All Openings Contribution

Pressure	[Pa]	50	45	40	35	30	25	20	15	10
Flow	[l/s]	1334.26	1251.27	1164.42	1073.08	976.30	872.82	760.71	636.83	495.28

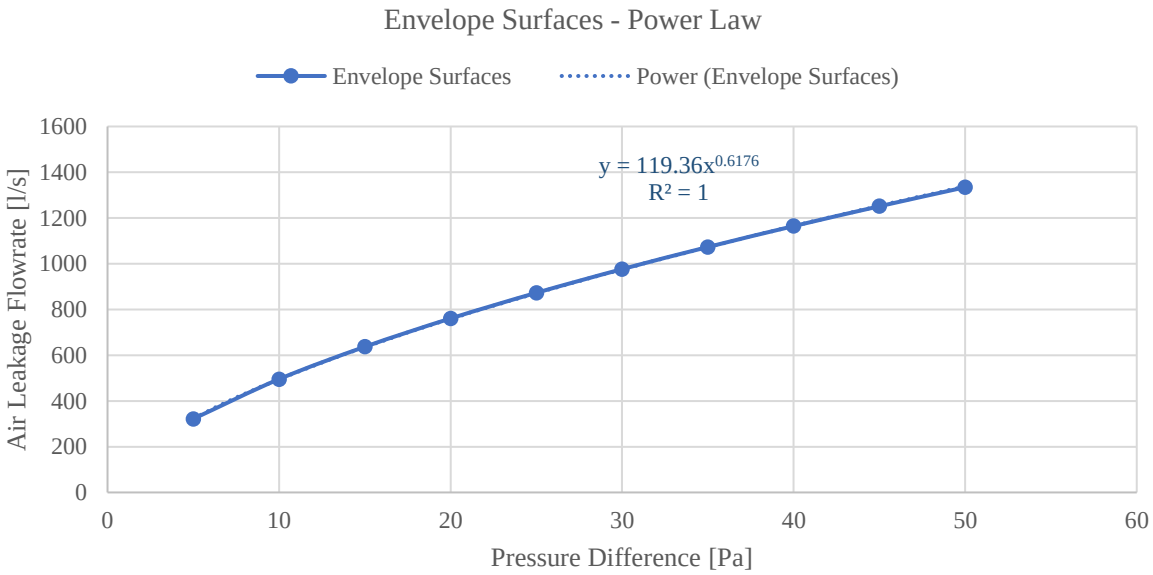

Figure 83: Envelope Surfaces' Fitted Power Law Equation

The envelope surfaces consider all external walls, the pitched roof of the main building, and the flat roof of the living room extension. The corresponding power law coefficient (C) is then normalized against the total envelope surface area.

Envelope Surface Area = 254.582 [m^2]
without walls, pitched roof, and flat roof

- Power Law Equation
  - $Q = 119.36 \times \Delta P^{0.6176}$ [l/s]
- Normalized Power Law Equation
  - $Q = 0.469 \times \Delta P^{0.6176}$ [l/s. m^2]
  - $Q = 0.000565 \times \Delta P^{0.6176}$ [kg/s. m^2]

Appendix D – Air Leakage Model Calibration

The air leakage model considers the definition of Crack Templates, that characterize the building's air leakage path distribution by defining the power law equations of the different building components. A Crack Template is first developed to reflect the Blower Door Test conditions. And the latter is then used as a foundation for the development of Crack Templates for all reference scenarios.

The detailed Crack Templates consider the standardized coefficients and exponents defined in the AIVC Guide 5 for Ventilation Modeling Data (Orme & Leksmono, 2002), then calibrated and validated against the in-situ air leakage measurements (Under Chapters 5.3 and 5.4).
The AIVC guide compiles component air leakage data from both published and unpublished sources, summarized by Orme *et al.* (1998). The compiled database aids in estimating the building's leakage behavior and potential retrofit improvements.

Such data are primarily based on in-situ pressurization tests, and supported by laboratory test data when needed. Some components (e.g. windows) have ample in-situ and laboratory measurements, enabling a detailed understanding and differentiation of component types and characteristics.
While the specific types and treatments for walls, windows, and doors may be accounted for in the estimates, roofing data only distinguishes between three types of roofs (tiles, shingles, and metal) with small sample sizes (9, 3, and 6 respectively). No further distinction is thus possible, regarding the types of surface treatments, presence of vapor membranes, or level of sealing and insulation.

The AIVC power law coefficients and exponents that underpin these estimations are outlined under the Appendix E, for reference.

Blower Door Test Crack Template

A primary estimate of the building's air leakage under the measurements' Round 1 and Round 2 conditions, and of the corresponding contribution of the openings and envelope surfaces is produced and compared to the equivalent measurement results (Refer to Table 42 and Figure 84 and 85)

Table 42: Measurements and AIVC Estimates of Building & Component Air Leakage

Building Air Leakage

			Round 1				Round 2			
Pressure [Pa]			50		10		50		10	
Flow [l/s]	Measured		1526.66	ε [%]	538.44	ε [%]	1362.41	ε [%]	500.47	ε [%]
	AIVC	Q1	2557.16	67.5	981.52	82.3	2430.55	78.4	933.31	86.5
		Median	2862.15	87.5	1112.70	106.7	2581.42	89.5	1005.82	101.0
		Q2	4585.56	200.4	1858.25	245.1	4028.06	195.7	1645.99	228.9

Component Air Leakage

			Openings (Windows + Doors)				Envelope Surfaces (Walls + Roof)			
Pressure [Pa]			50		10		50		10	
Flow [l/s]	Measured		192.40	ε [%]	43.16	ε [%]	1334.26	ε [%]	495.28	ε [%]
	AIVC	Q1	141.92	-26.2	54.04	25.2	2415.24	81	927.48	87.3
		Median	304.23	58.1	115.83	168.4	2557.92	91.7	996.87	101.3
		Q2	632.34	228.1	240.75	457.8	3953.22	196.3	1617.50	226.6

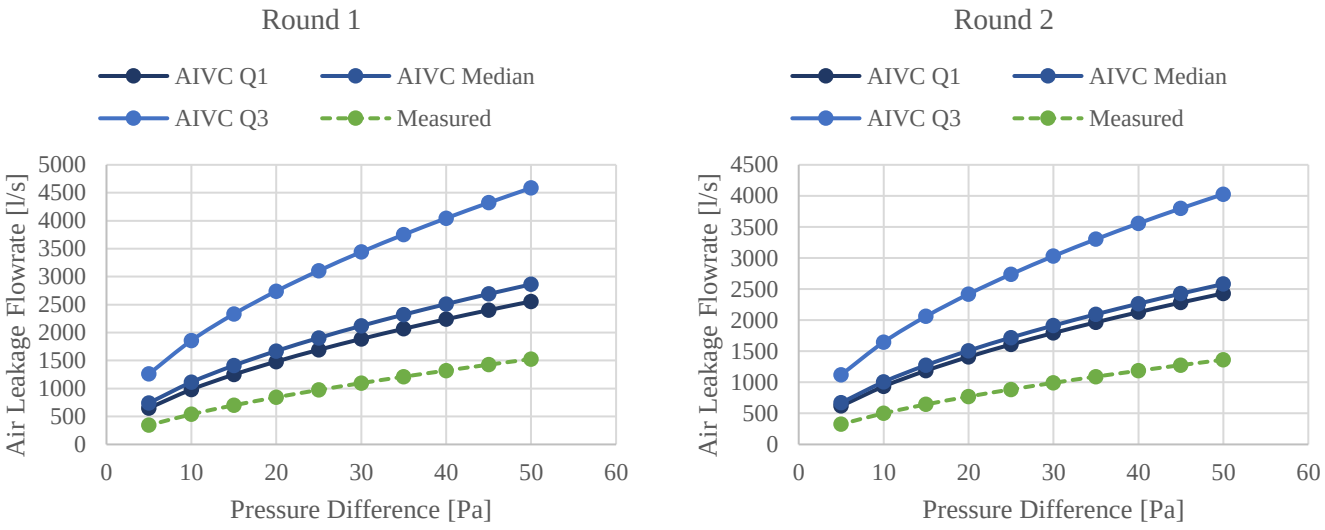

Figure 84: Measurements and AIVC Estimates of Building Air Leakage

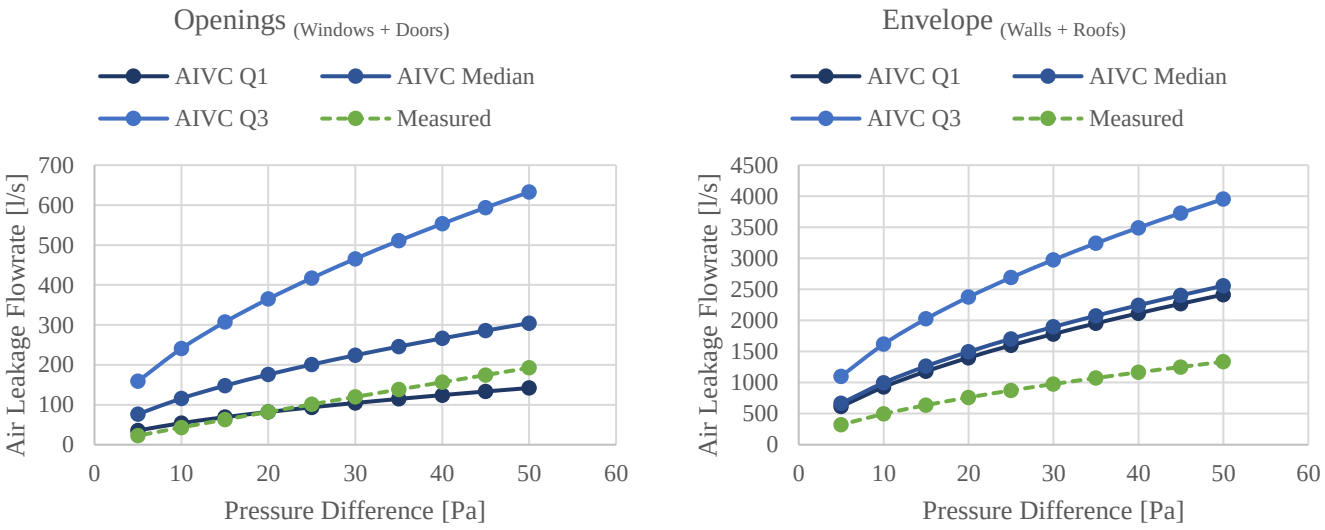

Figure 85: Measurements and AIVC Estimates of Component Air Leakage

The comparison of the measured and calculated building data (Refer to Table 42 and Figure 84) reveals a notable discrepancy between the assumed AIVC power law coefficients and the actual building air leakage; the AIVC-computed leakage flowrates are approximately twice as large as the measured values.

The consistent magnitude of the overestimation between the Round 1 and Round 2 implies that the calculated leakage contribution of the openings aligns with the measured values. In other words, the AIVC-based openings' air leakage accurately represents the measurements, while the source of the overestimation may be attributed to the Envelope surface leakage.

These findings find validation in the data pertaining to the components' air leakage (Refer to Table 42 and Figure 85).

- The openings' measured leakage varies around the AIVC's lower quartile values, which may be considered a reasonable estimate. The relatively "Good" level of airtightness of the openings may be justified by the building already undergoing a series of minor renovation works targeting its openings.
- The AIVC values for the envelope surfaces' leakage are, however, almost twice their measured counter-part. Further analysis of the AIVC values and comparison with the results of the meta-analysis on building components' airtightness (Prignon et al., 2021) highlight the source of the results discrepancies.

Envelope Surface: Brick Walls

AIVC estimates for Brick Walls detail the type and level of surface treatments and finishing.

The AIVC's power law equations for Bare Walls generate results that are consistent with the leakage results found in the Meta-analysis for Masonry with pointing of joints, representative of the Case Study' conditions.

The visual inspection of the Case Study building reckons relatively good construction and maintenance conditions. As per the guidelines of Orme *et al* (1998), the walls are thus assigned the median of the corresponding data

Envelope Surface: Tiled Roof

AIVC estimates for Tiled Roofs do not provide any detailing with regard to the type and finishing, which greatly affects the airtightness performance of the roof's wooden construction.

Little data is found in the literature on the air leakage through pitched tiled roofs with timber constructions.
The meta-analysis considers 1 study on pitched tiled roofs with no sealing of any kind, the results of which are perfectly consistent with the AIVC's estimates.

Although the Case Study building's roof is responsible for measurable leakage, as exhibited by the IR thermal images, it is lined with a weather-proofing "Ventifol" layer, suggesting an above-average airtightness performance.

The Case Study building's roof conditions is not compatible with the unsealed roofs represented in the AIVC and Meta-analysis data, and may therefore be attributed, with enough confidence, the source of the overestimation of the leakage.

Accordingly, the Base Case Crack Template attributes:

- The AIVC's lower quartile (Q1) power law coefficients and exponents for windows, doors, and skylights.
- The AIVC's median power law coefficients and exponents for walls.
- Fitted power law coefficients and exponents for the roof air leakage, estimated as the remaining leakage at each pressure gradient.

$$Q_{roof} = Q_{T_{measured}} - (Q_{windows} + Q_{doors} + Q_{walls})_{AIVC}$$

Q_{roof} – roof leakage flow [l/s]
$Q_{T_{measured}}$ – building's total measured leakage [l/s]
$Q_{i_{AIVC}}$- component i's AIVC estimated leakage [l/s]

The Blower Door Test Crack Template is thus:

Table 43: Crack Template - Blower Door Test (BDT) Conditions

Crack Template – Blower Door Test (BDT)

Surface Component	Coefficient		Exponent	Area
	C [l/s.m^2]	C [kg/s.m^2]	n [-]	A [m^2]
Walls				
Bare	0.0430	0.0000518	0.84	36.45
Plastered	0.0180	0.0000217	0.86	67.24
Roof				
Pitched	0.944	0.001137	0.64	111.89
Attic Floor	0.150	0.000181	0.74	36.05

Linear Component	Coefficient		Exponent	Perimeter
	C [l/s.m]	C [kg/s.m]	n [-]	P [m]
Windows				
Hinged – Skylights	0.086	0.000104	0.6	16.96
Sliding – Windows	0.0793	0.0000955	0.6	120.20
Doors				
Hinged	0.082	0.0000987	0.6	38.22

Base Case Crack Template

The Base Case Crack Template examines pre-retrofit leakage and insulation conditions. For the purpose of this study, it is assumed that all walls are still bare (no wet plaster was applied) and the flat roof was not sealed for the implementation of the green roof. The resulting Crack Template is thus corrected to:

Table 44: Crack Template - Base Case (BC) Conditions

Crack Template – Base Case (BC)

Surface Component	Coefficient		Exponent	Area
	C [l/s.m^2]	C [kg/s.m^2]	n [-]	A [m^2]
Walls				
Bare	0.0430	0.0000518	0.84	103.69
Roof				
Pitched	0.944	0.001137	0.64	111.89
Flat	0.944	0.001137	0.64	39
Attic Floor	0.150	0.000181	0.74	36.05

Linear Component	Coefficient		Exponent	Perimeter
	C [l/s.m]	C [kg/s.m]	n [-]	P [m]
Windows				
Hinged – Skylights	0.086	0.000104	0.6	16.96
Sliding – Windows	0.0793	0.0000955	0.6	120.20
Doors				
Hinged	0.082	0.0000987	0.6	38.22

Base Retrofit Crack Template

The Retrofit Crack Template considers the leakage conditions under the retrofit scenarios.

A distinction is made between the effects of concentrated and diffuse air leaks on both the heating energy demand and the indoor thermal comfort (Refer to Chapter 2.2): Unlike diffuse air leakage, concentrated leaks have no significant infiltration heat recovery effect and often cause uncomfortable draughts.
Moreover, the construction's effective performance as DI system hinges upon the mitigation of the risks associated to the air flows by-passing it through the concentrated leakage pathways (Refer to Chapter 2.4.2). Consequently, the proper sealing of the concentrated leaks around openings is imperative.

The studied retrofit strategy thus explores the potential of exploiting the building's diffuse air leakage into achieving the best trade-off between energy-efficiency and IEQ, in the absence of measurable concentrated leakage.

For this purpose, the Base Retrofit Crack Template is defined as follows:

Table 45: Crack Template - Base Retrofit Case (BRC) Conditions

Crack Template – Base Retrofit Case (BRC)

Surface Component	Coefficient		Exponent	Area
	C [l/s.m^2]	C [kg/s.m^2]	n [-]	A [m^2]
Walls				
Bare	0.0430	0.0000518	0.84	103.69
Roof				
Pitched	0.944	0.001137	0.64	111.89
Flat	0.944	0.001137	0.64	39
Attic Floor	0.150	0.000181	0.74	36.05

Linear Component	Coefficient		Exponent	Perimeter
	C [l/s.m]	C [kg/s.m]	n [-]	P [m]
Windows				
Hinged – Skylights	0.0332	0.00004	0.65	16.96
Sliding – Windows	0.0332	0.00004	0.65	120.20
Doors				
Hinged	0.0332	0.00004	0.65	38.22

The highlighted air leakage coefficients are the reference values; these will be modified with the retrofit scenarios, as described in Chapter 4.

Conventional Retrofit Crack Template

The Conventional Retrofit approach is built upon the "build tight-ventilate right" concept, whereby the construction is made as airtight as practically possible and all ventilation needs are met through purpose-provided openings and systems.

The Airtight Crack Template thus assumes high airtightness of all building components, based on the air leakage data compiled in the AIVC guide 5 (Orme & Leksmono, 2002)and the meta-analysis on building components' airtightness Click or tap here to enter text.(Prignon et al., 2021), and is defined in Table 46.

Table 46: Crack Template - Conventional Retrofit Case (CRC) Conditions

Crack Template – Conventional Retrofit Case (CRC)

Surface Component	Coefficient		Exponent	Area
	C [l/s.m^2]	C [kg/s.m^2]	n [-]	A [m^2]
Walls				
Wet Plastered	0.00208	0.0000025	0.84	103.69
Roof				
Pitched	0.0208	0.000025	0.64	111.89
Flat	0.0208	0.000025	0.64	39
Attic Floor	0.150	0.000181	0.74	36.05

Linear Component	Coefficient		Exponent	Perimeter
	C [l/s.m]	C [kg/s.m]	n [-]	P [m]
Windows				
Hinged – Skylights	0.0332	0.00004	0.65	16.96
Sliding – Windows	0.0332	0.00004	0.65	120.20
Doors				
Hinged	0.0332	0.00004	0.65	38.22

Crack Templates Overview and Validation

The building's overall air leakage behavior resulting from the crack templates defined for each reference scenario are compared and presented in conjunction with the actual measured air leakage results (Refer to Figure 86).

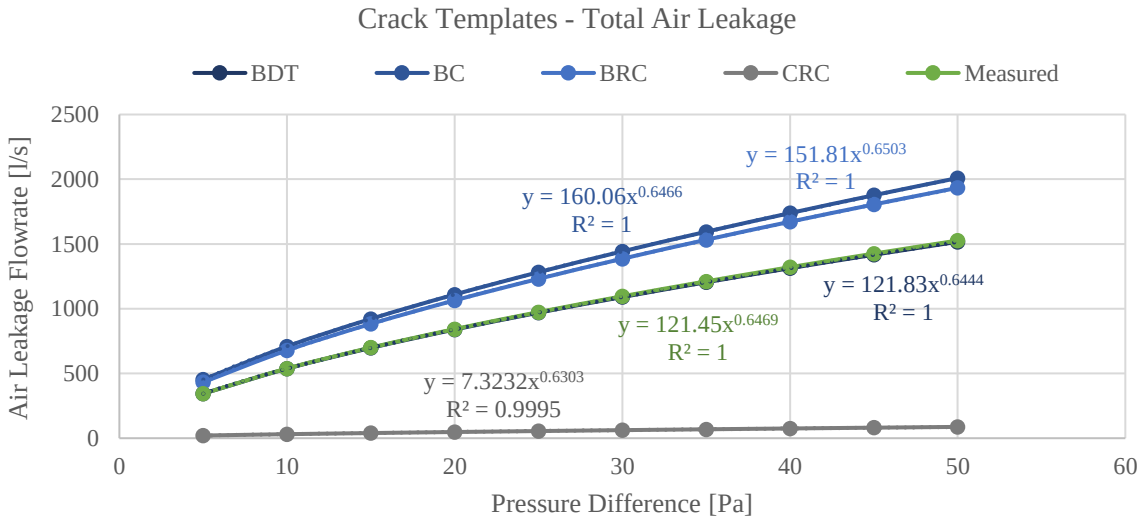

Figure 86: Building's Air Leakage Behavior - Measurements vs Crack Templates

The Base Case's Blower Door Test (BDT) crack template shows a virtually perfect overlapping with the measured air leakage values, thus validating the air leakage model's accurate representation of the case study's air leakage behavior.

The simulated building model under the different scenarios, however, takes the form of variations of the existing situation. Correspondingly, the adopted crack templates deviate from the representative BDT model in their properties, as well as in their corresponding building air leakage behavior. The comparison of each reference case and its relative air leakage behavior are described below.

The Base Case (BC) considers a pre-retrofits scenario of the case study building, namely prior to sealing some of the envelope surfaces	〉 Significantly increases the building's total air leakage relative to the measured case
The Base Retrofit Case (BRC) seals the concentrated leakage pathways around the openings, preventing their associated faults	〉 Slightly decreases the building's total air leakage relative to BC, as the openings' contribution is much less significant than the breathable envelope's contribution, as shown under Chapter 5.4
The Conventional Retrofit Case (CRC) exemplifies an airtight scenario, meticulously sealing all surfaces as practically possible	〉 Substantially diminishes the building's total air leakage, reducing its magnitude by several orders so that it is close to null.

Appendix E – Air Leakage Model's AIVC Reference

The Crack Templates, characterizing the building's leakage pathway distribution and flow, are defined using the AIVC Guide 5 (Orme & Leksmono, 2002) power law coefficients and exponents. Such data are primarily based on global in-situ fan-pressurization tests, and supported by laboratory test data when needed.
Depending on the extent of available data, it provides for a distinction of the estimates for a specific component depending on its types and some of its characteristics. The estimates for each studied item are also categorized into lower quartile (Q1), median, and upper quartile (Q3) estimates, accounting for the range of air leakage results for each component.

The power law coefficients and exponents that underpin the estimates for this study's air leakage model are presented in the Table 47 and 48 below, for openings and envelope surfaces respectively. The AIVC normalized coefficients are multiplied by the corresponding perimeter or area.
The components shown are relevant for the estimates equivalent to the Round 1 and/or Round 2 of the measurements, according to the following color legend.

Round	Color
1	
2	
1 & 2	

Table 47: AIVC coefficients and exponents - Openings

Windows

	Hinged Windows							
			C [l/s.m]			C [l/s]		
	Perimeter	n	Q1	Median	Q3	Q1	Median	Q3
Weather-stripped Windows	16.960	0.6	0.086	0.13	0.41	1.459	2.205	6.954
	Sliding Windows							
			C [l/s.m]			C [l/s]		
	Perimeter	n	Q1	Median	Q3	Q1	Median	Q3
	120.196	0.6	0.079	0.15	0.21	9.495	18.029	25.241

Doors

	External Hinged Doors							
			C [l/s.m]			C [l/s]		
	Perimeter	n	Q1	Median	Q3	Q1	Median	Q3
Weather-stripped Doors	31.26	0.6	0.082	0.27	0.84	2.56332	8.4402	26.2584

Wall/Window - Wall/Door Frame Joints

	Caulked Joints							
			C [l/s.m]			C [l/s]		
	Perimeter	n	Q1	Median	Q3	Q1	Median	Q3
Doors	31.260	0.6	0.0003	0.0025	0.012	0.0103	0.078	0.375
Windows	137.156	0.6	0.0003	0.0025	0.012	0.0453	0.343	1.646
	16.960	0.6	0.0003	0.0025	0.012	0.0056	0.042	0.204

Table 48: AIVC Coefficients and Exponents - Envelope Surfaces

Walls, Ceiling, and Floors

	Bare Wall									
		n			C [l/s.m2]			C [l/s]		
	Area	Q1	Median	Q3	Q1	Median	Q3	Q1	Median	Q3
Brick Wall	36.450	0.84	0.8	0.76	0.022	0.043	0.094	0.802	1.567	3.426
	Plastered Wall									
		n			C [l/s.m2]			C [l/s]		
	Area	Q1	Median	Q3	Q1	Median	Q3	Q1	Median	Q3
	67.242	0.86	0.85	0.84	0.016	0.018	0.021	1.076	1.210	1.412

Roofs

	Tiles									
		n			C [l/s.m2]			C [l/s]		
	Area	Q1	Median	Q3	Q1	Median	Q3	Q1	Median	Q3
Pitched Roof	111.891	0.59	0.58	0.55	2.1	2.3	4	234.971	257.349	447.563

The resulting power law equations are used to estimate the air leakage flow at varying pressures under the conditions of the Round 1 and Round 2 of measurements, as well as the contribution of the openings – doors and windows – and the envelope surfaces – walls and roofs under the base conditions.
The AIVC results – accounting for three levels of performance depicted by the Q1, Median, and Q3 estimates – are then put against the corresponding in-situ fan-pressurization results. The comparison of the values allows to pinpoint similarities and discrepancies and, accordingly, calibrate the model to be representative of the Case Study building.

The compiled results are presented in the Tables 49 and 50, for the Round 1 and Round 2 estimates, and in Tables 51 and 52, for the estimated leakage contributions of openings and envelope surface.

Table 49: AIVC Estimates and In-situ Measurements - Round 1

Round 1

AIVC Estimates											
Pressure [Pa]		**50**	45	40	35	30	25	20	15	**10**	5
Flow [l/s]	**Q1**	**2557.159**	2401.555	2238.826	2067.679	1886.363	1692.386	1481.988	1248.963	**981.519**	650.347
	Median	**2862.151**	2690.222	2510.264	2320.814	2119.882	1904.640	1670.810	1411.320	**1112.702**	741.376
	Q3	**4585.560**	4321.796	4044.932	3752.532	3441.276	3106.423	2740.777	2332.370	**1858.251**	1260.582

Measurements										
Pressure [Pa]	**50**	45	40	35	30	25	20	15	**10**	5
Flow [l/s]	**1526.661**	1425.73	1320.816	1211.226	1096.024	973.8958	842.869	699.7266	**538.4392**	344.3271

Table 50: AIVC Estimates and In-situ Measurements - Round 2

Round 2

AIVC Estimates											
Pressure [Pa]		**50**	45	40	35	30	25	20	15	**10**	5
Flow [l/s]	**Q1**	**2430.545**	2282.697	2128.078	1965.458	1793.172	1608.852	1408.922	1187.481	**933.313**	618.543
	Median	**2581.416**	2426.684	2264.708	2094.164	1913.255	1719.424	1508.803	1274.997	**1005.817**	670.859
	Q3	**4028.057**	3798.446	3557.290	3302.435	3030.941	2738.608	2419.053	2061.650	**1645.993**	1120.544

Measurements										
Pressure [Pa]	**50**	45	40	35	30	25	20	15	**10**	5
Flow [l/s]	**1362.408**	1275.941	1185.76	1091.209	991.3974	885.0666	770.3263	644.0761	**500.4729**	325.173

Table 51: AIVC Estimates and In-situ Measurements - Openings

Openings (Doors + Windows)

AIVC Estimates											
Pressure [Pa]		**50**	45	40	35	30	25	20	15	**10**	5
Flow [l/s]	**Q1**	**141.924**	133.230	124.139	114.581	104.459	93.635	81.901	68.917	**54.035**	35.650
	Median	**304.233**	285.596	266.109	245.621	223.922	200.719	175.567	147.733	**115.831**	76.420
	Q3	**632.341**	593.604	553.102	510.517	465.417	417.189	364.911	307.060	**240.752**	158.837

Measurements										
Pressure [Pa]	**50**	45	40	35	30	25	20	15	**10**	5
Flow [l/s]	**192.398**	174.464	156.387	138.148	119.721	101.073	82.155	62.893	**43.159**	22.673

Table 52: AIVC Estimates and In-situ Measurements - Envelope Surfaces

Envelope (Walls + Roofs)

AIVC Estimates											
Pressure [Pa]		**50**	45	40	35	30	25	20	15	**10**	5
Flow [l/s]	**Q1**	**2415.236**	2268.326	2114.687	1953.098	1781.904	1598.751	1400.087	1180.046	**927.484**	614.697
	Median	**2557.918**	2404.626	2244.155	2075.194	1895.960	1703.921	1495.243	1263.586	**996.871**	664.957
	Q3	**3953.219**	3728.193	3491.831	3242.016	2975.859	2689.234	2375.866	2025.310	**1617.500**	1101.746

Measurements										
Pressure [Pa]	**50**	45	40	35	30	25	20	15	**10**	5
Flow [l/s]	**1334.263**	1251.266	1164.429	1073.078	976.3036	872.823	760.7141	636.8335	**495.2806**	321.6545

Appendix F – DI Model Validation

The Taylor model, by itself, is a validated model (Alongi et al., 2017). Its implementation into EnergyPlus' EMS is, however, not. It was thus important to ensure that the EMS-integrated BES tool was functioning properly and generating the correct results.

The validation of the EMS script was thus established against the existing steady-state analytical Taylor Model:

The script's accuracy is verified through the juxtaposition of the dynamic U-values it computes with those derived from the analytical model, for each breathable material layer within the construction

The validity of the EMS-integrated building energy model is substantiated by comparing the heat flux through the dynamically-insulated construction's outside surface at pseudo-steady-state conditions, as computed by the BES tool, to the heat flux calculated by the analytical model.

For this purpose, a shoebox test model was thus built, considering a simple 3 x 3 x 5 m room with no openings. All surfaces, but one, are adiabatic.

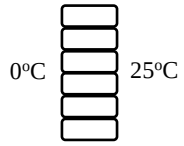

The non-adiabatic wall has a single-layered porous brick masonry construction, with its thermal conductivity dynamically controlled by the EMS code described above.

The indoor temperature was stabilized at 25ºC, and the outdoor conditions were defined by a custom-made weather file with :

- Constant outdoor temperature of 0ºC
- Constant outdoor relative humidity of 80%
- Constant pressure
- No sun
- No rain

The temperature gradient of 25ºC across the envelope is large enough to prompt measurable heat conduction. The outdoor and indoor surface convection and radiation coefficients follow the DOE-2 and TARP estimates, respectively, as customary in EnergyPlus.
An exhaust fan is used to put the room under-pressure and control the leakage flow through the wall. The outdoor dynamic solar and wind effects were eliminated, to reach pseudo-static conditions.

The construction's dynamic U-value and associated outgoing heat flux at 12 different leakage flowrates through the wall were then estimated using both methods and compared. The results, displayed in the Figures 87 and 88, show almost perfect coincidence, validating the EMS script and the model's proper functioning for single-layered breathable constructions.

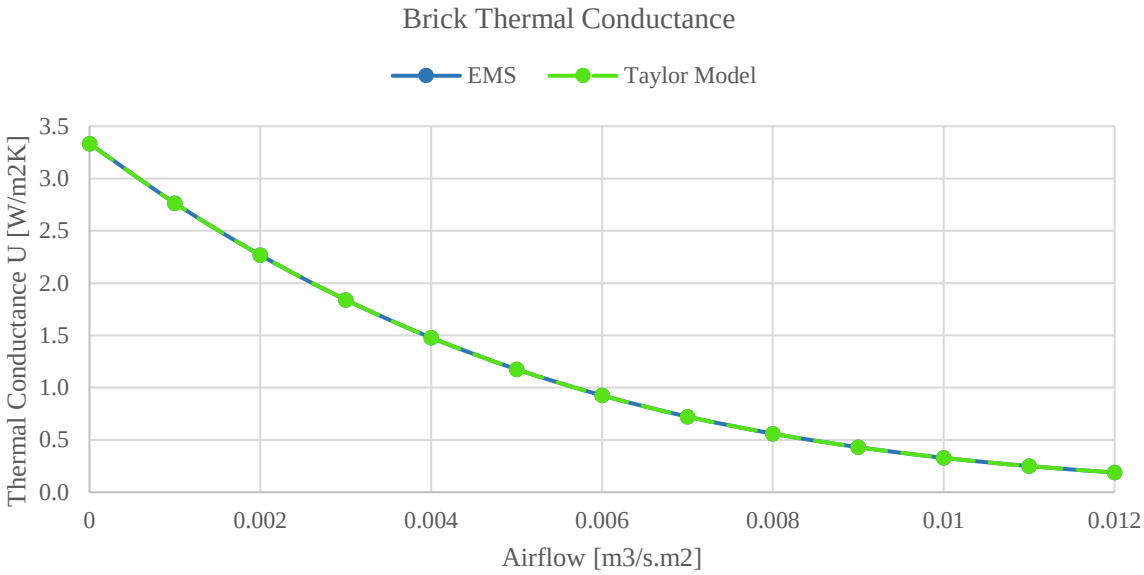

Figure 87: Single-layered Construction's Brick U-value - EMS vs. Taylor Model

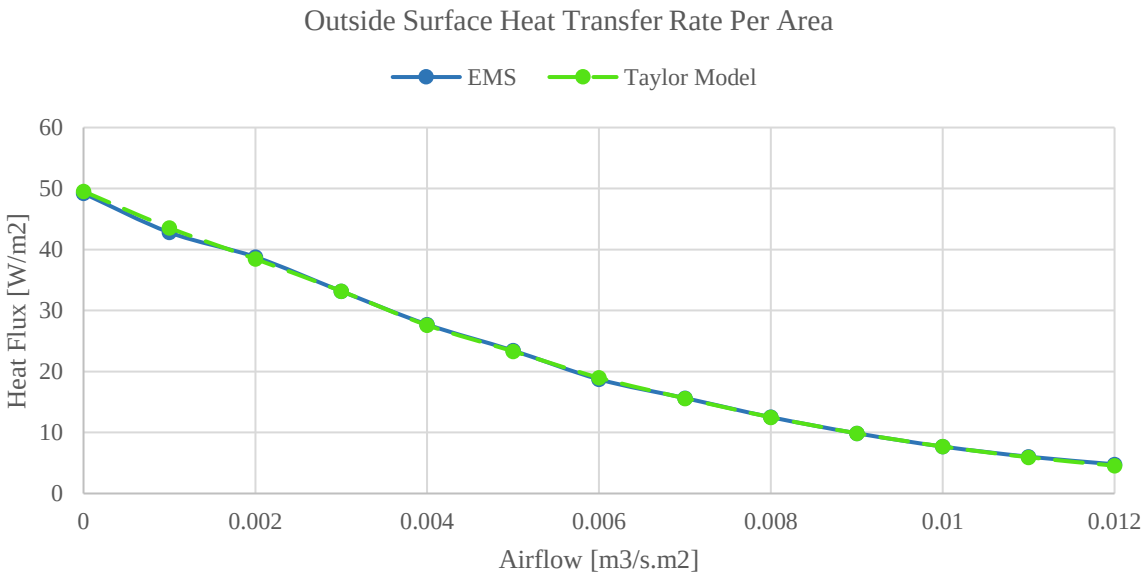

Figure 88: Single-layered Construction's Outward Heat Flux - EMS vs. Taylor Model

The building's constructions are, however, often multi-layered. Three multi-layered construction variants were thus substituted into the shoebox model's dynamically-insulated wall.

Multi-layered Construction 1

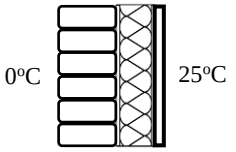

- Three layers with no air-gap
  - Porous brick masonry and rockwool insulation layers, with their thermal conductivity controlled by the EMS.
  - A plasterboard layer with static thermal conductivity.

Multi-layered Construction 2

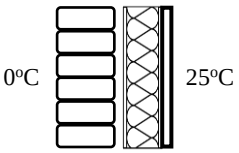

- Three layers with air-gap as "NoMass" material
  - Porous brick masonry and rockwool insulation layers, with their thermal conductivity controlled by the EMS.
  - A plasterboard layer with static thermal conductivity.
  - An air gap layer defined as a "NoMass" material, with only an R-value.

Multi-layered Construction 3

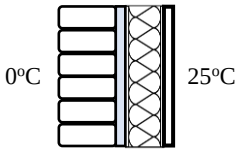

- Three layers with air-gap as conventional material
  - Porous brick masonry and rockwool insulation layers, with their thermal conductivity controlled by the EMS.
  - A plasterboard layer with static thermal conductivity.
  - An air gap layer defined as a conventional material, with a static thermal conductivity.

The outgoing heat flux through the multi-layered construction, and the associated dynamic U-values of the dynamic brick and insulation layers, are similarly compared for the two methods. The detailed results are displayed in Appendix G.

The dynamic U-value (U_{dyn}) of the breathable brick and insulation layers are compared for all three multi-layered constructions. All scenarios result in the same distribution of the materials' U_{dyn} against the airflow rate through the wall (Refer to Figures 89 and 90) and show perfect coincidence with the values derived directly from the analytical Taylor model, indicating no errors in the EMS code.

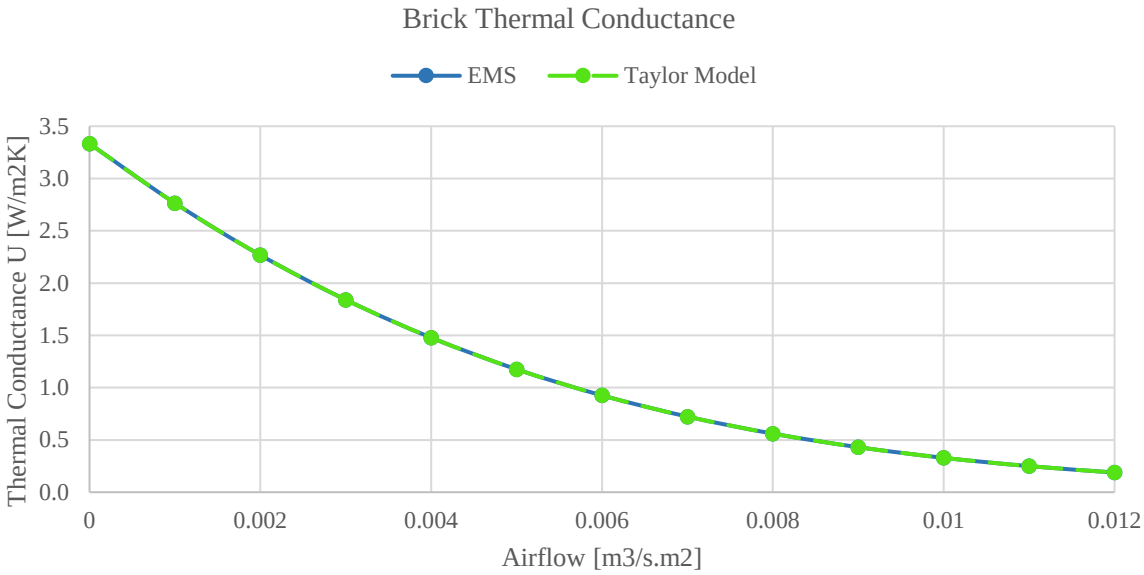

Figure 89: Multi-layered Constructions' Brick U-value - EMS vs. Taylor Model

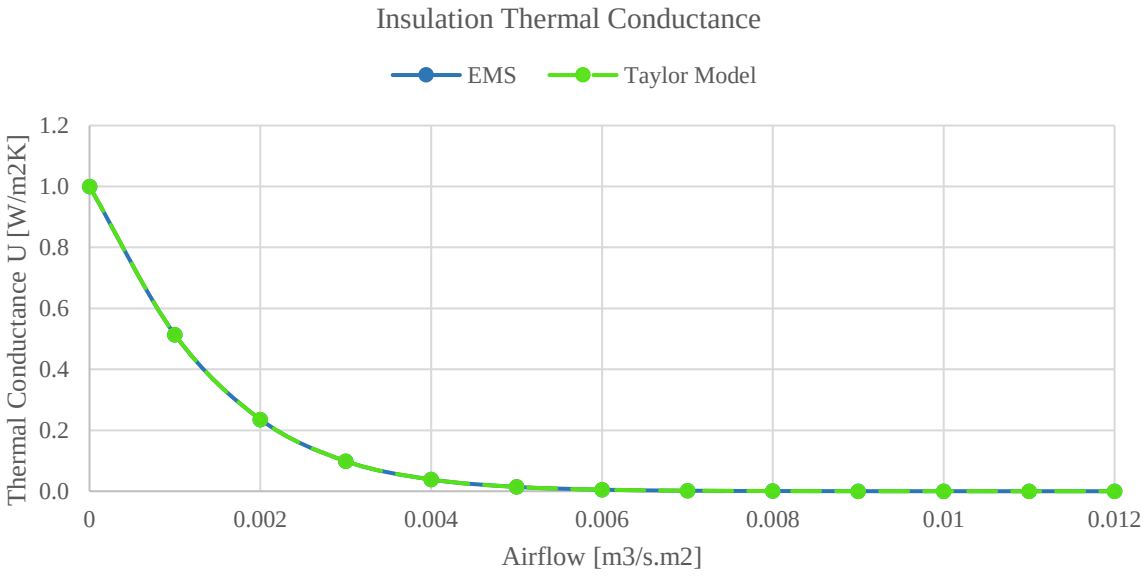

Figure 90: Multi-layered Constructions' Insulation U-value - EMS vs. Taylor Model

However, accounting for the integration of the EMS code into the BES model for multi-layered constructions, disparities and limitations are identified.

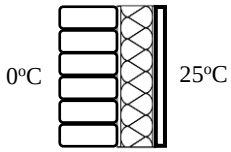

Multi-Layered Construction 1
In case of multi-layered constructions with no air gaps, the outward heat flux obtained in the EMS-integrated BES model shows good coincidence with the values derived from the analytical model up to an airflow of around 0.008 $m^3/s.m^2$. Beyond that airflow, the BES model overestimates the conductive heat losses relative to the Taylor model.
Simulating the Case Study building's annual air leakage flowrate under both natural and exhaust fan scenarios, the leakage rate does not exceed 0.003 $m^3/s.m^2$, falling significantly lower than the model's validity limit of 0.008 $m^3/s.m^2$.

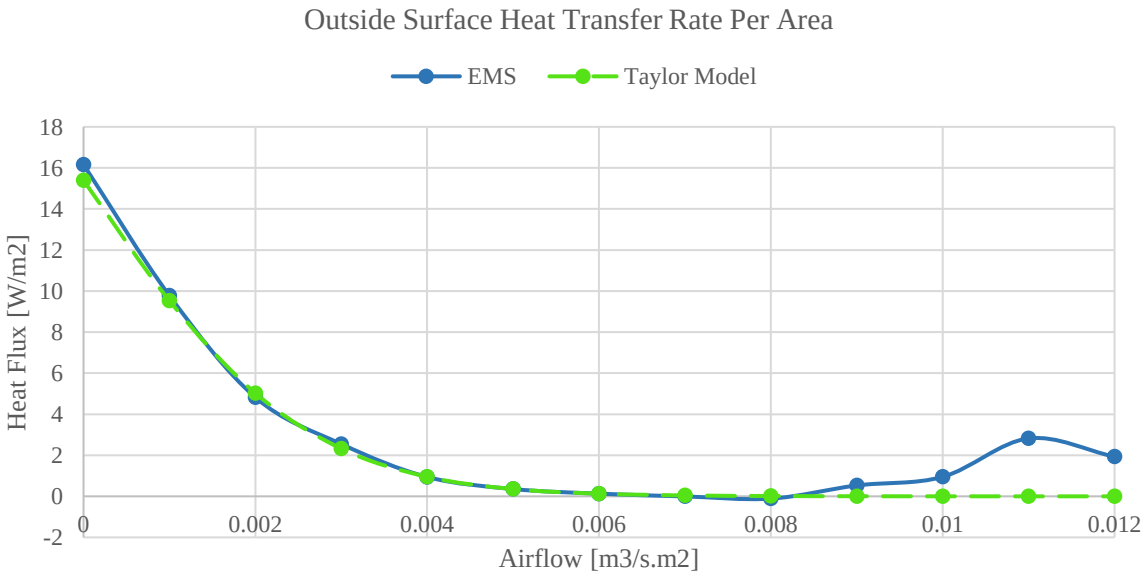

Figure 91: Multi-layered Construction 1's Outward Heat Flux - EMS vs. Taylor Model

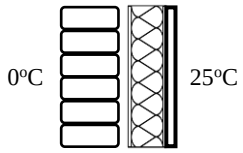

Multi-Layered Construction 2
When an air gap is introduced into the construction and defined as a "NoMass" material with only its thermal resistance (R-value) specified, as conventional in EnergyPlus, unexpected results are obtained.
The construction's outside face conduction heat flux drops to the vicinity of 0 starting from flowrates as low as 0 $m^3/s.m^2$, despite the material's defined U-value being correct. Beyond the 0.008 $m^3/s.m^2$ limit, the construction exhibits a similar erroneous behavior as in the Multi-layered construction 1 above.
This highlights on a malfunction of the EnergyPlus software tool, unveiling an incompatibility of the EMS thermal conductivity actuator with material layers within the same construction as "NoMass" material layers.

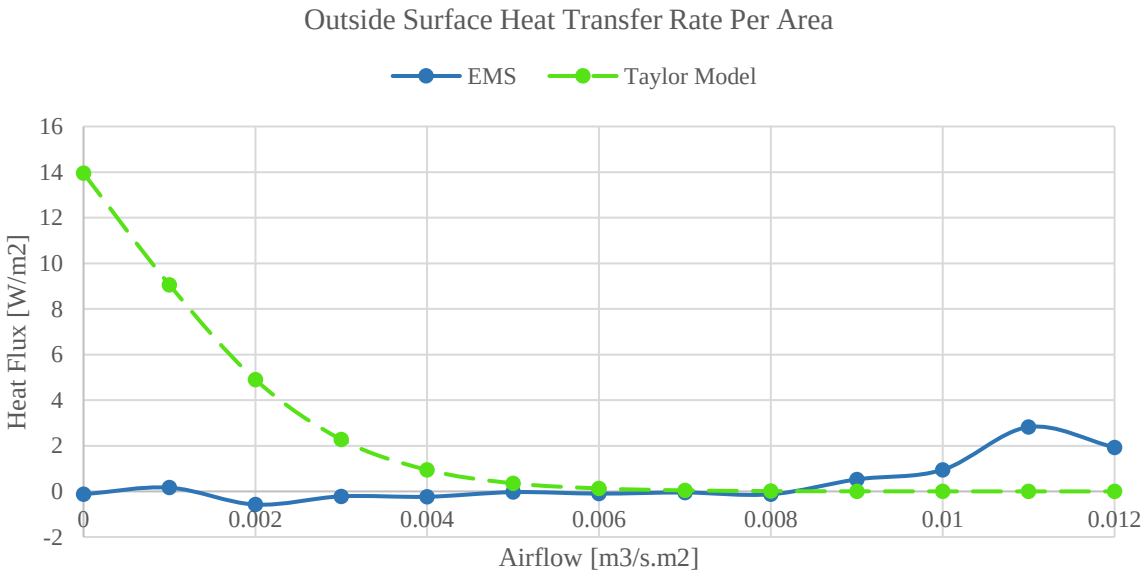

Figure 92: Multi-layered Construction 2's Outward Heat Flux - EMS vs. Taylor Model

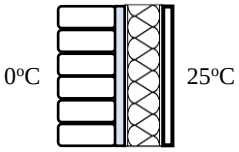

Multi-Layered Construction 3

To ensure reliability of the results, the detected anomaly within the BES tool was circumvented by substituting the "NoMass" material layers with conventionally-defined equivalents; meaning, the air gaps are defined as materials with a thermal conductivity, density, and specific heat capacity. This adjustment yielded acceptable results falling within the established 0.008 $m^3/s.m^2$ treshold.

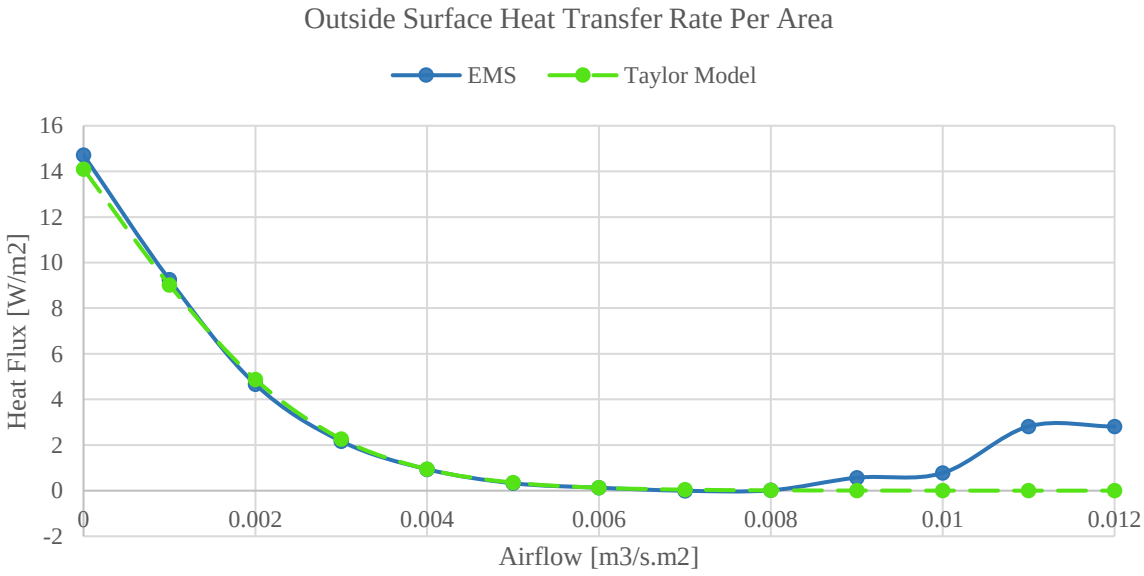

Figure 93: Multi-layered Construction 3's Outward Heat Flux - EMS vs. Taylor Model

The model was thus found valid for the present application. The detailed tabulated results of the EMS validation runs are found under Appendix G.

Appendix G – DI Model Detailed Validation Results

The detailed tabulated results from the DI Model's validation process are presented in the following tables, for each of the studied constructions.

Table 53: DI Model Validation Results - Run 1

			EMS Model			Taylor Model		
Target Flow **v**	Surface Outside Face Temperature **Tso**	Surface Inside Face Temperature **Tsi**	Surface Outside Face Conduction Heat Transfer Rate per Area **qco**	Brick Thermal Conductance **U(br)**	Insulation Thermal Conductance **U(ins)**	Surface Outside Face Conduction Heat Transfer Rate per Area **qco**	Brick Thermal Conductance **U(br)**	Insulation Thermal Conductance **U(ins)**
[m/s]	[C]	[C]	[W/m2]	[W/m2.K]	[W/m2.K]	[W/m2]	[W/m2.K]	[W/m2.K]
0	2.04817	16.91094	49.20722	3.33333	[-]	49.54258	3.33333	[-]
0.001	1.91089	17.66597	42.80420	2.76432	[-]	43.55204	2.76432	[-]
0.002	1.49811	18.45473	38.77257	2.26762	[-]	38.44981	2.26754	[-]
0.003	1.20329	19.23663	33.16719	1.84023	[-]	33.18547	1.84023	[-]
0.004	1.34597	20.01415	27.70631	1.47802	[-]	27.59225	1.47804	[-]
0.005	0.87874	20.71475	23.43606	1.17532	[-]	23.31537	1.17541	[-]
0.006	0.87768	21.38013	18.72158	0.92600	[-]	18.98527	0.92600	[-]
0.007	0.36424	21.94533	15.64888	0.72312	[-]	15.60566	0.72312	[-]
0.008	0.12555	22.45914	12.51466	0.56008	[-]	12.50864	0.56008	[-]
0.009	-0.01053	22.92051	9.87480	0.43054	[-]	9.87275	0.43054	[-]
0.01	-0.12117	23.31790	7.69407	0.32868	[-]	7.70387	0.32868	[-]
0.011	-0.19811	23.61969	6.03257	0.24933	[-]	5.93853	0.24933	[-]
0.012	-0.30779	23.95172	4.79106	0.18806	[-]	4.56216	0.18806	[-]

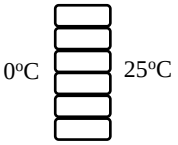

Table 54: DI Model Validation Results - Run 2

Target Flow **v**	Surface Outside Face Temperature **Tso**	Surface Inside Face Temperature **Tsi**	EMS Model: Surface Outside Face Conduction Heat Transfer Rate per Area **qco**	EMS Model: Brick Thermal Conductance **U(br)**	EMS Model: Insulation Thermal Conductance **U(ins)**	Taylor Model: Surface Outside Face Conduction Heat Transfer Rate per Area **qco**	Taylor Model: Brick Thermal Conductance **U(br)**	Taylor Model: Insulation Thermal Conductance **U(ins)**
[m/s]	[C]	[C]	[W/m2]	[W/m2.K]	[W/m2.K]	[W/m2]	[W/m2.K]	[W/m2.K]
0	0.31410	21.86478	16.16073	3.33333	1.00000	15.39334	3.33333	1.00000
0.001	-0.01600	22.93400	9.77826	2.76432	0.51376	9.52991	2.76432	0.51375
0.002	-0.24453	23.79285	4.82194	2.26754	0.23580	5.02671	2.26754	0.23580
0.003	-0.69409	24.36376	2.54827	1.84016	0.09859	2.32338	1.84023	0.09860
0.004	-0.80448	24.66718	0.94350	1.47799	0.03842	0.95037	1.47804	0.03842
0.005	-0.49542	24.83315	0.35521	1.17533	0.01422	0.35551	1.17541	0.01423
0.006	-0.80512	24.90114	0.13038	0.92594	0.00507	0.12971	0.92600	0.00508
0.007	-0.66089	24.92046	-0.00338	0.72312	0.00176	0.04498	0.72312	0.00176
0.008	-0.49106	24.93367	-0.11186	0.56008	0.00060	0.01524	0.56008	0.00060
0.009	-0.55095	24.93219	0.53058	0.43054	0.00020	0.00512	0.43054	0.00020
0.01	-0.52654	24.94083	0.94870	0.32868	0.00007	0.00169	0.32868	0.00007
0.011	-0.43453	24.94339	2.82110	0.24933	0.00002	0.00055	0.24933	0.00002
0.012	-0.52327	24.93863	1.92902	0.18806	0.00001	0.00018	0.18806	0.00001

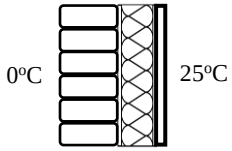

Table 55: DI Model Validation Results - Run 3

Target Flow **v**	Surface Outside Face Temperature **Tso**	Surface Inside Face Temperature **Tsi**	EMS Model: Surface Outside Face Conduction Heat Transfer Rate per Area **qco**	EMS Model: Brick Thermal Conductance **U(br)**	EMS Model: Insulation Thermal Conductance **U(ins)**	Taylor Model: Surface Outside Face Conduction Heat Transfer Rate per Area **qco**	Taylor Model: Brick Thermal Conductance **U(br)**	Taylor Model: Insulation Thermal Conductance **U(ins)**
[m/s]	[C]	[C]	[W/m2]	[W/m2.K]	[W/m2.K]	[W/m2]	[W/m2.K]	[W/m2.K]
0	-0.52739	21.09469	-0.12508	3.33333	1.00000	13.94973	3.33333	1
0.001	-0.57231	22.60320	0.16487	2.76432	0.51376	9.05928	2.76432	0.51375
0.002	-0.49933	23.68664	-0.57699	2.26754	0.23580	4.90396	2.26754	0.23580
0.003	-0.55537	24.34060	-0.21624	1.84023	0.09860	2.27670	1.84023	0.09860
0.004	-0.73325	24.66522	-0.23531	1.47804	0.03842	0.94236	1.47804	0.03842
0.005	-0.52071	24.83225	-0.03179	1.17536	0.01422	0.35510	1.17541	0.01423
0.006	-1.01328	24.89978	-0.09750	0.92600	0.00508	0.13065	0.92600	0.00508
0.007	-0.66387	24.92042	-0.04823	0.72312	0.00176	0.04497	0.72312	0.00176
0.008	-0.49178	24.93366	-0.12669	0.56008	0.00060	0.01524	0.56008	0.00060
0.009	-0.55119	24.93219	0.52641	0.43054	0.00020	0.00512	0.43054	0.00020
0.01	-0.52660	24.94083	0.94752	0.32868	0.00007	0.00169	0.32868	0.00007
0.011	-0.43454	24.94339	2.82095	0.24933	0.00002	0.00055	0.24933	0.00002
0.012	-0.52328	24.93863	1.92896	0.18806	0.00001	0.00018	0.18806	0.00001

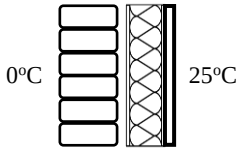

Table 56: DI Model Validation Results - Run 4

			EMS Model			Taylor Model		
Target Flow **v**	Surface Outside Face Temperature **Tso**	Surface Inside Face Temperature **Tsi**	Surface Outside Face Conduction Heat Transfer Rate per Area **qco**	Brick Thermal Conductance **U(br)**	Insulation Thermal Conductance **U(ins)**	Surface Outside Face Conduction Heat Transfer Rate per Area **qco**	Brick Thermal Conductance **U(br)**	Insulation Thermal Conductance **U(ins)**
[m/s]	[C]	[C]	[W/m2]	[W/m2.K]	[W/m2.K]	[W/m2]	[W/m2.K]	[W/m2.K]
0	-0.52739	21.09469	-0.12508	3.33333	1.00000	13.94973	3.33333	1
0.001	-0.57231	22.60320	0.16487	2.76432	0.51376	9.05928	2.76432	0.51375
0.002	-0.49933	23.68664	-0.57699	2.26754	0.23580	4.90396	2.26754	0.23580
0.003	-0.55537	24.34060	-0.21624	1.84023	0.09860	2.27670	1.84023	0.09860
0.004	-0.73325	24.66522	-0.23531	1.47804	0.03842	0.94236	1.47804	0.03842
0.005	-0.52071	24.83225	-0.03179	1.17536	0.01422	0.35510	1.17541	0.01423
0.006	-1.01328	24.89978	-0.09750	0.92600	0.00508	0.13065	0.92600	0.00508
0.007	-0.66387	24.92042	-0.04823	0.72312	0.00176	0.04497	0.72312	0.00176
0.008	-0.49178	24.93366	-0.12669	0.56008	0.00060	0.01524	0.56008	0.00060
0.009	-0.55119	24.93219	0.52641	0.43054	0.00020	0.00512	0.43054	0.00020
0.01	-0.52660	24.94083	0.94752	0.32868	0.00007	0.00169	0.32868	0.00007
0.011	-0.43454	24.94339	2.82095	0.24933	0.00002	0.00055	0.24933	0.00002
0.012	-0.52328	24.93863	1.92896	0.18806	0.00001	0.00018	0.18806	0.00001

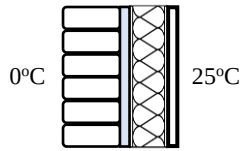

Appendix H – TOPSIS Analysis Results

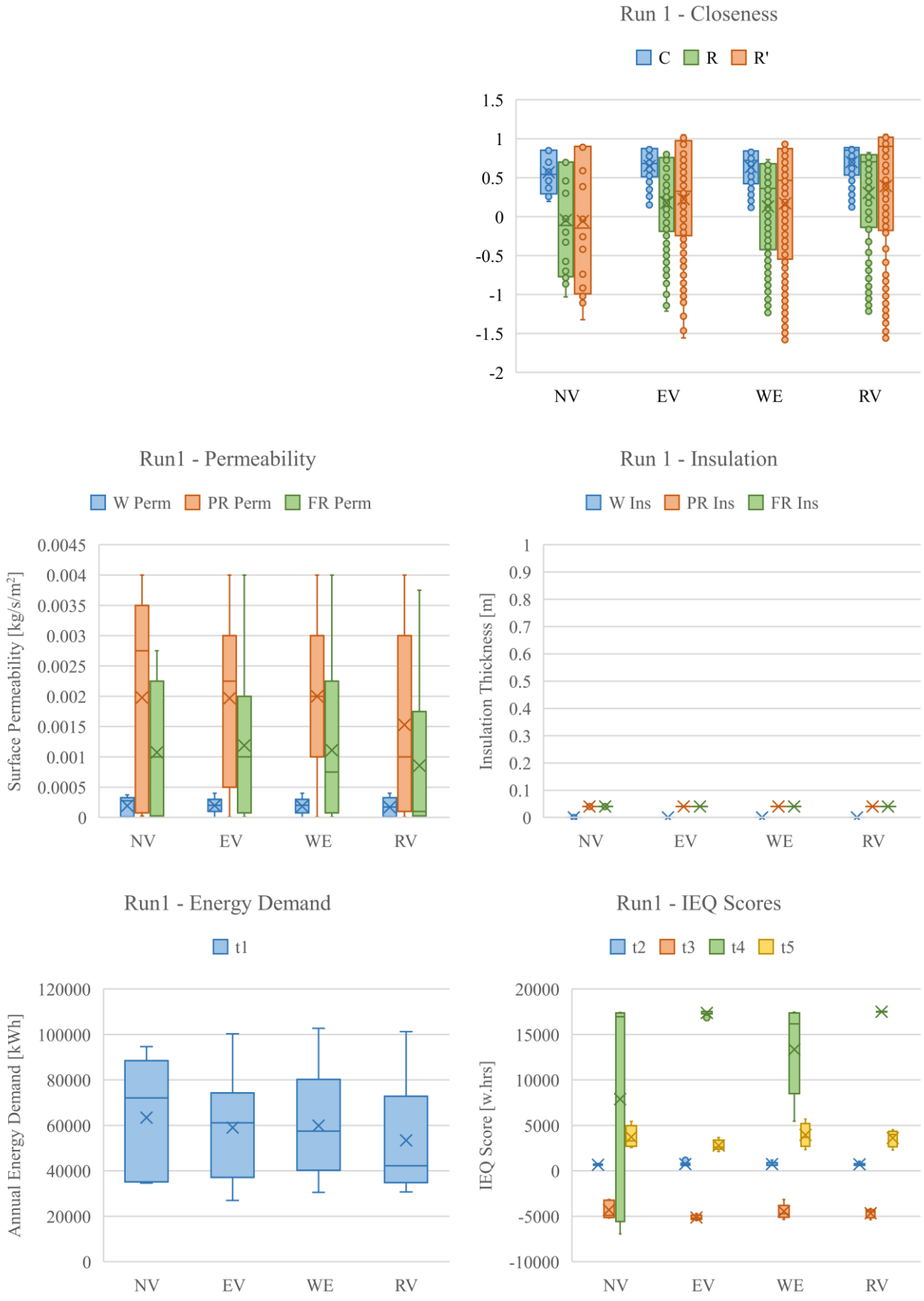

Figure 94: Design and Performance Parameters - Run 1

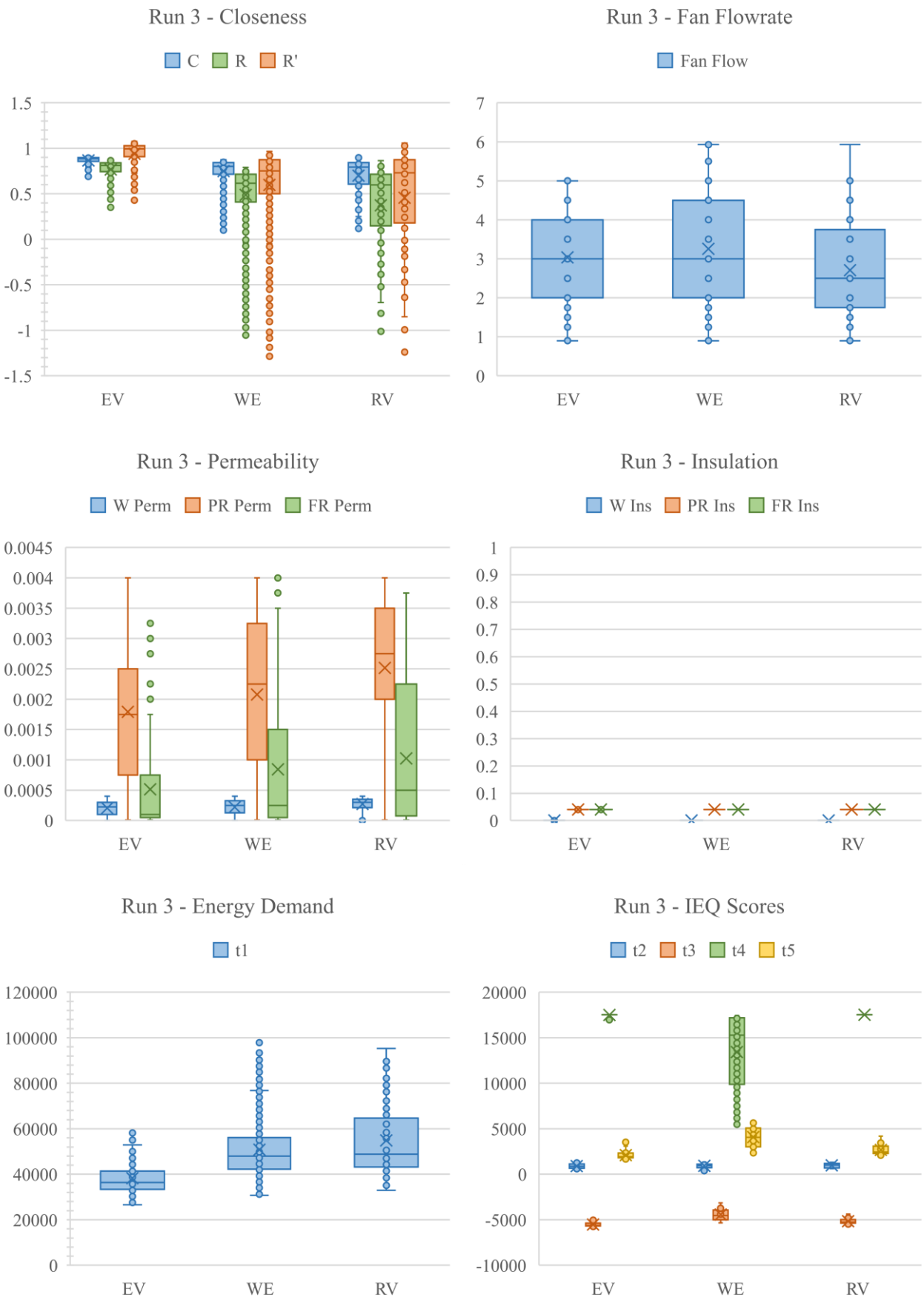

Figure 95: Design and Performance Parameters - Run 3

Figure 96: Design and Performance Parameters - Run 5

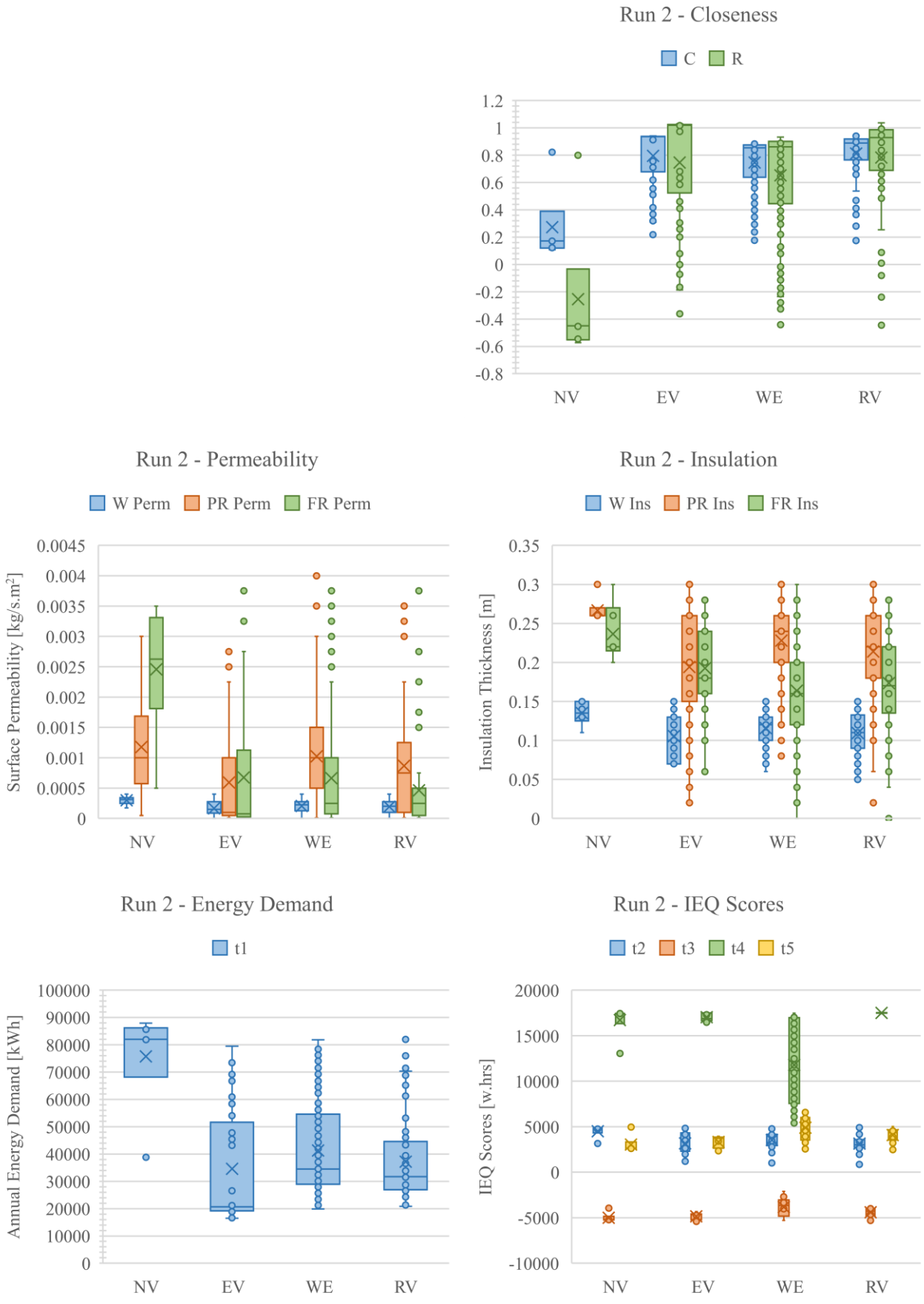

Figure 97: Design and Performance Parameters - Run 2

Figure 98: Design and Performance Parameters - Run 4

Figure 99: Design and Performance Parameters - Run 6